



**Technische Universität München
Fakultät für Medizin**

Effects of *Ccn2* loss during hematopoietic stress

Sandra Romero Marquez

Vollständiger Abdruck der von der Fakultät für Medizin der Technischen Universität München zur Erlangung einer

Doktorin der Naturwissenschaften (Dr. rer. nat.)

genehmigten Dissertation.

Vorsitz: Prof. Dr. Heiko Lickert

Prüfende der Dissertation:

1. apl. Prof. Dr. Robert Oostendorp
2. Prof. Angelika Schnieke, Ph.D.

Die Dissertation wurde am 17.11.2022 bei der Technischen Universität München eingereicht und durch die Fakultät für Medizin am 21.03.2023 angenommen.

Table of contents

1	Introduction	1
1.1	Hematopoiesis	1
1.1.1	Hematopoietic hierarchy	1
1.1.2	Hematopoietic stem cell characteristics and regulation of behavior	3
1.2	Niche cells in the bone marrow supporting hematopoietic stem cells	5
1.2.1	Bone marrow niche	5
1.3	Signaling pathways involved in HSC regulation	13
1.3.1	Wnt/beta-catenin signaling	13
1.3.2	Gp130/JAK/STAT signaling	14
1.3.3	NF- κ B signaling	16
1.3.4	TGF beta signaling	18
1.4	Hematopoietic stress and HSC regulation by the niche	19
1.4.1	5-Fluorouracil treatment	19
1.4.2	Lipopolysaccharide treatment	19
1.4.3	Total body irradiation	21
1.5	Cellular communication network factors	25
1.5.1	Cellular communication network factor 2 (CCN2)	27
1.6	Aim of the thesis	33
2	Material and methods	35
2.1	Material	35
2.1.1	Consumption-utensils	35
2.1.2	Machines and equipment	36
2.1.3	Softwares	38
2.1.4	Chemicals	39
2.1.5	Biological reagents	40
2.1.6	Buffer, Medium and Solution	41

2.1.7	Kits	43
2.1.8	Primary and Secondary Antibodies.....	44
2.1.9	Primer.....	49
2.1.10	Vectors	49
2.1.11	Cell lines.....	50
2.1.12	Mice strains	50
2.2	Methods	52
2.2.1	Molecular Biological Methods	52
2.2.2	Protein Biochemical Methods.....	56
2.2.3	Cell Biological Methods.....	57
2.2.4	Animal Experimental Techniques.....	63
2.2.5	Statistical Analysis	66
3	Results	67
3.1	Establishment of a new single stem cell culture method using conditioned medium of mouse embryonic fibroblasts	67
3.2	Ccn2 during steady state and stress condition	75
3.2.1	Verification of an efficient Ccn2 knockout	75
3.2.2	Function of Ccn2 during single-cell culture stress.....	76
3.2.3	Ccn2 during steady state conditions	79
3.2.4	Ccn2 during in vivo stress conditions.....	86
4	Discussion.....	148
4.1	Function of Ccn2 during steady state and stress conditions.....	148
4.1.1	Single HSCs in culture with stromal MEF-CM and Ccn2 ^{ΔA} -MEF-CM	148
4.1.2	The function of Ccn2 expression during different stress conditions.....	148
5	Summary.....	159
6	Zusammenfassung	162

7 Appendices.....	164
7.1 List of Figures	164
7.2 List of Tables.....	167
8 Publications.....	169
9 Acknowledgments	169
10 References.....	169

List of Abbreviations

AB	antibody
AGM	aorta-gonad-mesonephros
ALCAM	activated leukocyte cell adhesion molecule
ALL	acute lymphoblastic leukemia
AML	acute myeloid leukemia
ANGPT1	angiopoietin
As(2)O(3)	arsenic trioxide
BM	bone marrow
BMP	bone morphogenic protein
BSA	bovine serum albumine
CAR	C-X-C motif chemokine ligand abundant reticular cells
CBA	Cytometry bead array
Cbfa1	core binding factor 1
CCN	Cellular communication network factor
CCN2	cellular communication network factor 2
cDNA	complementary desoxyribonucleic acid
CFU-F	colony forming fibroblast
cKIT	CD117
CLP	common lymphoid progenitors
CMP	common myeloid progenitors
CNTF	ciliary neurotrophic factor
CT	cardiotrophin
CTCK	carboxyl-terminal cystine knot
CTGF	connective tissue growth factor
CYR61	cysteine-rich angiogenic inducer 61
CXCL-12	C-X-C motif chemokine ligand 12

CXCR4	CXC chemokine receptor 4
DEL	developmental endothelial locus
DDR	DNA damage response
DKK-1	Dickkopf-related protein
DMSO	Dimethylsulfoxide
DSB	double strand breaks
DTR	diphtheria toxin receptor
DVL	disheveled
E	embryonic day
EBF-2+	immature early B-cell factor 2+
EC	endothelial cell
ECM	ECM
EGF	epidermal growth factor
FACS	fluorescence-activated cell sorting
FCS	fetal calf serum
FITC	Fluoresceinisothiocyanat
FGF	fibroblast growth factor
FL	fetal liver
FLK-2/FLT-3	fetal liver kinase 2/Fms-like tyrosine kinase3 positive
FS	forward scatter
G-CSF	granulocyte colony-stimulating factor
gDNA	genomic desoxyribonucleic acid
GP-130	glycoprotein 130
GMP	granulocyte/monocyte progenitors
GSK3 β	glycogen synthase kinase-3 β
HBSS	Hank's buffered salt solution
HF	high fidelity

HSC	hematopoietic stem cells
HUVEC	human umbilical vascular endothelial cells
Id1	inhibitor of differentiation 1
IEO	early B-cell factor ²⁺ (EBF-2 ⁺) osteoblasts
IF	immunofluorescence
IFN- γ	interferon gamma
IGF	insulin growth factor
IGFBP	insulin-like growth factor binding protein
IKK	I κ B kinase
IL	interleukin
IL6R	type 1 cytokine α -receptor subunit
IR	irradiation
JAK	Januskinase
KO	knockout
LEP-R	leptin receptor
LIF	leukemia inhibitory factor
LIN	lineage
LPS	lipopolysaccharide
LRP6	LDL receptor-related protein 6
LSK	lineage ⁻ Sca1 ⁺ Kit ⁺
LT	long-term
LT-HSCs	long-term repopulating hematopoietic stem cells
Ly-6A/E	Lymphocyte antigen 6A-2/6E-1
MCP-1	monocyte chemotactic protein 1
MEP	megakaryocyte/erythrocyte progenitors
MK	megakaryocytes
MMP	matrix metalloproteinase

MP	multipotent cells
MPP	multipotent progenitor cells
MSC	mesenchymal stem cell
NHEJ	non-homologous end joining
NFκB	nuclear factor 'kappa-light-chain-enhancer' of activated B-cells
OBC	osteoblast cell
OPN	osteopontin
OSN	oncostatin M
Osx	osterix
PAS	para-aortic-splanchnopleura
PB	peripheral blood
PCR	polymerase chain reaction
PDGF	platelet-derived growth factor
PECAM	platelet endothelial cell adhesion molecule
PenStrep	Penicillin/Streptomycin
PI	propidium iodide
PPAR-γ	Peroxisome proliferator-activated receptor gamma
PTEN	Phosphatase and Tensin homolog
PTN	pleiotrophin
PW	pulse width
RT-qPCR	quantitative real time PCR
RelA	transcription factor p65
RIBE	radiation-induced bystander effects
ROS	reactive oxygen species
RT	room temperature
SAHF	senescence-associated heterochromatin foci
SASP	senescence-associated secretory phenotype

Sca1 ⁺	stem cell antigen 1
SCF	stem cell factor
SDF-1	stroma derived factor 1
SEC	sinusoidal endothelial cell
SEM	standard error of the mean
SFRP	secreted-frizzled-related protein 1
SNO	spindle-shaped N-cadherin ⁺ CD45 ⁻ osteoblasts
STAT3/5	signal transducer and activator of transcription 3/5
ST	short term
ST-HSCs	short-term repopulating hematopoietic stem cells
SS	sideways scatter
TAM	tamoxifen
TBI	total body irradiation
TCF/LEF	T cellfactor/lymphoid enhancer factor
TGF- β	transforming growth factor β
TH	T-helper
TPO	thrombopoietin
TNF- α	tumor necrosis factor α
TSP-1	thrombospondin type I
VCAM	vascular adhesion molecule
VEGF	vascular endothelial growth factor
VWFC	von Willebrand factor type C module
WISP	Wnt induced secreted proteins
Wnt	Wingless-type MMTV integration site family member
WT	wild-type
x-gal	5-bromo-4-chloro-3-indoyl- β -d-galactopyranoside
ZPF	Zentrum für präklinische Forschung

β -ME	β -mercaptoethanol
CD48	SLAMF-2

1 Introduction

1.1 Hematopoiesis

1.1.1 Hematopoietic hierarchy

To ensure multiple functions of the blood system (tissue remodeling, defense of pathogens or the supply with oxygen) mature blood cells separate into functionally distinct red- (erythrocytes) white blood cells (myeloid and lymphoid cells) and platelets. As these mature blood cells have an average half live time of only six to eight hours, over 10^{12} blood cells have to be generated every day (Rufer et al., 1999; Summers et al., 2010). These newly produced cells form from single hematopoietic stem cells (HSCs) in the bone marrow (BM) to populate different hematopoietic organs such as the spleen, liver, lymph nodes or thymus, and the blood (Summers et al., 2010). Ter119⁺ erythrocytes are the dominant circulating blood cell type. The white blood cells (leukocytes) form a much smaller population in the circulation and can be divided into the lymphoid B- and T- cells, positive for the surface marker B220 or CD3e, respectively (Doutlatov et al., 2012), myeloid Gr1⁺CD11b⁺ granulocytes (neutrophils, eosinophils, mast cells and basophils) and Gr1^{med}CD11b⁺ monocytes (Doutlatov et al., 2012).

These specialized mature hematopoietic cells emerge from lineage-restricted progenitor cells in a hierarchically organized process: collectively called hematopoiesis. The most immature cells of the hierarchy lack the expression of lineage (LIN⁻) markers (B220, CD3e, CD11b, Gr1), and they express the cytokine receptor CD117 (cKIT) (Akashi et al., 2000; Kondo et al., 1997). However, further expression of different cell surface markers distinguishes different cell types. The origin of lymphoid cells is common lymphoid progenitors (CLPs) that are distinguishable as Lymphocyte antigen 6A-2/6E-1 lo (Ly-6A/E⁻, SCA1^{lo}), fetal liver kinase 2/Fms-like tyrosine kinase3 positive (FLK-2/FLT-3⁺) and IL7-R⁺ (Shizuru et al., 2005; Weissman et al., 2001; Renström et al., 2010). Myeloid cell types emerge from two different progenitors the SCA1⁻ CD16/34^{hi} CD34^{hi} granulocyte-monocyte progenitors (GMPs) or SCA1⁻ CD16/34^{lo} CD34^{lo} megakaryocyte-erythroid progenitors (MEPs) (Doutlatov et al., 2012; Shizuru et al., 2005; Weissman et al., 2001). Both GMPs as well as MEPs share the same origin the SCA1⁻ CD16/34^{lo} CD34^{int} common myeloid progenitor cells (CMPs). Interestingly, CLPs and CMPs emerge from the same cell type the multipotent cells (MPs) that are CD34⁺CD150⁻ and FLK-2/FLT-3⁺ (Seita and Weissman, 2010; Shizuru et al., 2005; Weissman et al., 2001). MPs however, still lack the self-renewal and multipotent characteristics of stem cells but gain their ability for lineage commitment (Adolfsson et al., 2001; Morrison et al., 1997; Seita and Weissman, 2010).

Upstream of the MPs are multipotent progenitor cells (MPPs), as well as the cells able to replenish the whole blood cell system by engraftment in the BM, differentiation, proliferation, and self-renewal: the HSCs (Orkin and Zon, 2008). These HSCs are a rare population with a frequency of only 0.05% of all BM cells (Uchida and Weissman, 1992). The HSCs were first defined as part of a heterogenic population of LIN⁻ cKIT⁺ SCA1⁺ or LSK cells (Ikuta and Weissman, 1992; Spangrude et al., 1988). The LSK HSCs separate into cells with a life cycle of only eight till twelve weeks, - the so called the short-term- (ST) HSCs, which express CD34, and FLK-2/FLT-3 (= CD135), and the long-term- (LT) HSCs which lack the expression of CD34, CD135, or the CD48 (SLAMF-2) antigen, but express CD150 and the EPC-receptor (Benveniste et al., 2010; Kent et al., 2009; Kiel et al., 2005; Osawa et al., 1996; Schreck et al., 2014). Within the LT-HSC population Morita and colleagues showed in 2010, that only the CD150^{high} expressing cells reconstituted multilineage hematopoiesis in secondary mice, whereas the CD150^{med/low} lack this secondary repopulation potential (Morita et al., 2010).

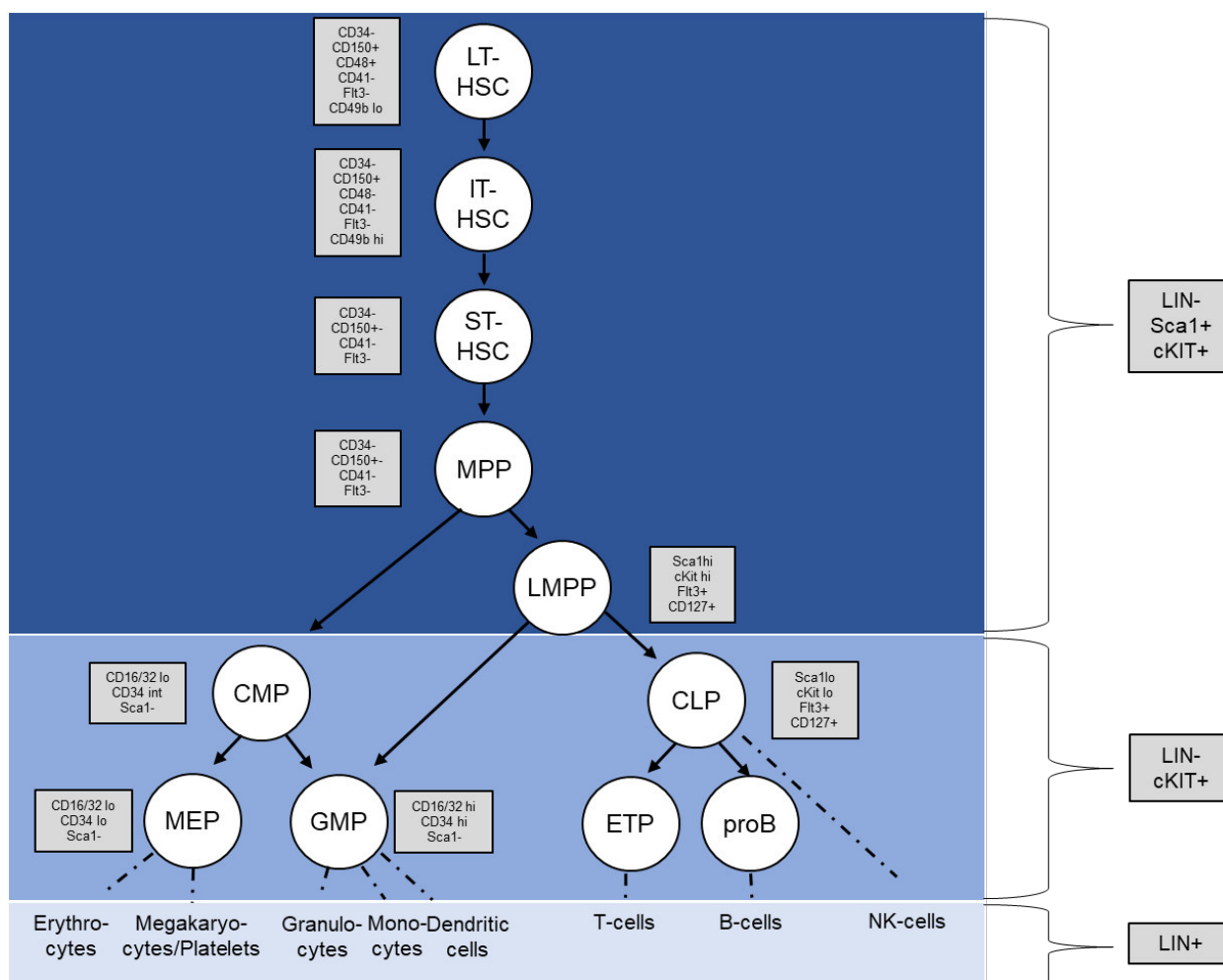


Figure 1. Mouse hematopoietic hierarchy model. On top of the hematopoietic system are long-term HSCs (LT-HSCs) that downstream give rise to intermediate-term-HSCs (IT-HSCs) that further differentiate into short-term-HSCs (ST-HSCs). ST-HSCs produce multipotent progenitors (MPPs). MPPs further give rise to common myeloid progenitors (CMPs) and lymphoid primed multipotent progenitors (LMPPs). Through further differentiation the mature hematopoietic cells are formed at the end. Different surface marker expression of cells from the hematopoietic hierarchy allows the analyzation by flow cytometry methods (scheme modified based on Doulatov et al., 2012).

1.1.2 Hematopoietic stem cell characteristics and regulation of behavior

HSCs are multipotent somatic cells that give rise to different cells of the hematopoietic lineage. Additionally, stem cells are defined as cells able to home to their appropriate habitat and remain to harbor the ability to self-renew – the ability for stem cells to build an identically daughter cell (Inaba and Yamashita, 2012). Self-renewal either takes place through symmetrically-, resulting in two identical cells (increasing the stem cell number), or asymmetrically cell division, in which one identical twin and one differentiated cell is generated (maintaining the stem cell number; Inaba and Yamashita, 2012; Molofsky et al., 2004).

Besides self-renewal HSCs also differentiate symmetrically (resulting in a reduced stem cell number, Molofsky et al., 2004). Therefore, self-renewal is thought to prevent the HSC exhaustion (Boulais and Frenette, 2015; Schreck et al., 2014).

Another way to prevent the exhaustion is the ability of HSCs to restrain in a non-dividing cell cycle state (G0) the quiescent or dormant state. During hematopoietic homeostasis most of the HSCs with about 75% persist in this dormant state. Interestingly, it was discovered, that 99% of the most primitive HSCs (long term (LT) HSCs) enter the cell cycle on average every 57 days and afterward return to quiescence (Bradford et al, 1997; Cheshier et al., 1999; Wilson et al., 2008). The quiescent phenotype is maintained by decreased expression of genes known to progress the cell cycle, DNA replication or mitochondrial function (Cabezas-Wallscheid et al., 2017; Cheung and Rando, 2013; Fukushima et al., 2019; Schönberger et al., 2022). Additionally, the presence of cell cycle inhibitors, such as Cyclin D Kinase inhibitors (p21Cip1, p27, p57, p53) or the presence of H3K27 methyltransferase EZH2 or PB family maintain the G0 state of quiescent cells (Cheung and Rando, 2013, Cheng et al., 2000). Other important molecules regulating the maintenance of quiescence are members of the Foxo family by reducing the reactive oxygen species (ROS) accumulation in quiescent HSCs during environmental stress (Tothova et al., 2007).

In the case of telomere shortening (due to excessive cell cycling) or irreparable DNA damage (cycling, irradiation eg.) the cells may enter another non-dividing cell behavior – the senescent state. Cellular senescent cells do not respond to hematopoietic stress but remain their metabolism and stay alive (Chotinantakul and Leeanansaksiri, 2012; Krizhanovsky et al., 2008). Senescent cells additionally fulfill several characteristics such as up-regulation of p53 and p16^{Ink4a} (product of the *Cdkn2a* gene) as well as the condensation of chromatin into senescence-associated heterochromatin foci (SAHF), down regulation of Laminin B, or the up-regulation of senescence-associated secretory phenotype (SASP; van Deursen 2014). The SASPs include molecules involved in different biological processes such as the insulin growth factor (IGF), IGF-binding proteins (IGFBPs), interleukin 6 (IL-6), the cysteine-rich angiogenic inducer 61 (CYR61) or WNT16B which are biologically active and secreted to influence their microenvironment (Coppé et al., 2010; Jun and Lau, 2010; van Deursen, 2014).

However, HSC behavior such as self-renewal and differentiation are regulated by their microenvironmental cells (Schreck et al., 2014; Wilson and Trumpp, 2006) and will be discussed in further detail in the next chapters.

1.2 Niche cells in the bone marrow supporting hematopoietic stem cells

1.2.1 Bone marrow niche

The BM niche is a heterogeneous composition of different hematopoietic and non-hematopoietic types of cells. Recent analyses of different single cell RNA-seq studies (Baryawno et al., 2019; Tikhonova et al., 2019; Baccin et al., 2020; Zhong et al., 2020) revealed 14 different non-hematopoietic cell clusters and their frequency in the BM niche. The most frequent cells with 32% are endothelial cells (ECs, sinusoidal, arterial, arteriolar), followed by 27% mesenchymal stem cells (MSCs) and adipogenic as well as osteogenic progenitor cells, 18% fibroblasts, 16% chondrocytes, 5% osteoblastic cells (OBCs), 1% pericytes 0.3% Schwann cells and 0.1% smooth muscle cells (Dolgalev and Tikhonova, 2021). All these different cell types communicate with each other through regulatory molecules such as growth factors and cytokines. This communication may be caused through autocrine or paracrine signaling pathways as well as through direct cell contact using adhesion molecules (Boulais and Frenette 2015; Chamberlain et al., 2007; Scheck et al., 2014; Fröbel et al., 2021).

The first idea of a stable microenvironment, extrinsically regulating HSCs self-renewal was proposed by Schofield, which he termed the “niche” (Schofield 1978). The following decades, studies on the niche revealed an exclusive role in the maintenance of HSC homeostasis, through the regulation of its activation, return to dormancy, reducing the accumulation of ROS, as well as its decision between differentiation and renewal capacities or the survival of the cells (Crippa and Bernardo, 2018; Morrison and Spradling, 2008; Fuchs et al., 2004; Renström et al., 2009, Wilson et al., 2008).

Today two functionally and anatomical distinct niches can be separated: the inner BM which is called the central niche, and the side close to the bone surface, the endosteal niche (Massalha and Ferrer 2022).

1.2.1.1 Central niche

The area proximally to the arteriolar and sinusoid endothelia was found to harbor the majority of lymphoid cells as well as hematopoietic progenitor and stem cells in the BM (Kiel et al., 2005; Sipkins et al., 2005; Winkler et al., 2010).

Generally, most of the anatomical compartment of HSCs localizes close to the vasculature. The original idea was that this localization ensures a fast entrance in the blood stream after hematopoietic stress. Therefore, it was assumed that stem cells in this niche are more active compared to the bone lining area (Kiel and Morrison, 2008). In accordance with this is the finding that deletion of E-selectin exclusively expressed by vascular endothelial cells, leads to an enhanced number of dormant HSCs (Kiel et al., 2007; 2009, Winkler et al., 2012).

However, this original hypothesis has developed as Li and colleagues discovered that transplantation of liver or brain isolated microvascular ECs expressing CD31, increase the recovery of host lethally irradiated HSCs (Li et al., 2010) indicating a role for ECs in the maintenance of LT-HSCs. Additionally, it was described that ECs regulate the renewal capacities of activated HSCs through paracrine signaling (Butler et al., 2010; Sugiyama et al., 2006). Besides ECs the perivascular CXCL12-abundant reticular cells (CAR) were found to maintain the dormancy of HSCs (Butler et al., 2010; Sugiyama et al., 2006). Besides the CAR cells also leptin receptor (LEP-R⁺) and Nestin expressing MSCs secrete factors named stroma derived factor 1 (SDF-1) or CXCL12 known to be essential for HSC homeostasis (Ding et al., 2012; Frenette et al., 2013; Schreck et al., 2014; Sugiyama et al., 2006; Yamazaki et al., 2011). However, another secreted factor the stem cell factor (SCF) revealed the importance of ECs and LEP-R⁺ cells in the maintenance of HSCs as its deletion in these cell types reduced the number of HSCs, whereas its deletion in Nestin⁺, OBCs and hematopoietic cells did not alter the frequency of HSCs (Ding et al., 2012; Visnjic et al., 2004). Adjacent to sinusoid endothelial cells are megakaryocytes which were shown to co-regulate HSC quiescence through the secretion of different factors such as platelet factor-4, thrombopoietin and transforming growth factor- β (Nakamura-Ishizu et al., 2014; Bruns et al., 2014).

1.2.1.2 Endosteal niche

The endosteal niche is the area between the marrow space and bone and is mainly composed of bone lining osteoblastic cells (Calvi et al., 2003; Schreck et al., 2014; Zhang et al., 2003; Wang and Wagers, 2011). In comparison to the arteriolar and sinusoid endothelia area the endosteal niche is thought to be a hypoxic area harboring most of the dormant HSCs (Schreck et al., 2014; Winkler et al., 2012).

Already in the year 1975 Lord and colleagues analyzed the trabecular bones and found HSCs next to the endosteal cells (Lord et al., 1975). This niche was discovered to be highly chemoattractive for HSCs as the real-time imaging showed HSCs close to osteoblastic cells shortly after BM transplantation (Lo Celso et al., 2009, Xie et al., 2009). Besides osteoblastic cells the endosteal niche also harbors MSCs (Mendez-Ferrer et al., 2010).

Mesenchymal stem cells

MSCs are multipotent cells located in the BM niche. MSCs have the capacity to differentiate into fibroblasts, chondrocytes osteoblasts and adipocytes (Friedenstein et al., 1976; Mendez-Ferrer et al., 2010; Oswald et al., 2004; Wang et al., 2006). Besides their differentiation capacity MSCs are defined as cells expressing specific surface markers, show plastic adherence and a characteristic spindle-shaped growth in culture (Friedenstein et al., 1974,

1987; Pittenger et al., 1999). Different surface markers were found to define different MSC populations maintaining HSCs in the endosteal niche. For example, besides the Nestin⁺ MSCs, Nakamura et al., postulated that CD31⁻, TER119⁻, CD45⁻, ALCAM⁻, SCA-1⁺ MSCs in the endosteal niche increase the expression of cytokines and homing genes in HSCs that are associated with the reconstitution of the HSC LT-status (Nakamura et al., 2010). Interestingly, Mende et al., discovered a strong interaction between MSCs and HSCs through extracellular matrix proteins such as Itgβ1 and Tenascin-C and substantiates the importance for MSCs in the regulation of HSCs (Mende et al., 2019).

Osteoblastic cells

As mentioned earlier osteoblastic cells build the majority of cells in the endosteal niche and are defined as CD45⁻CD31⁻Ter119⁻ALCAM⁺SCA-1⁻ cells (Caplan, 1991; Prockop, 1997; Nakamura et al., 2010). The osteoblastic lineage is derived from MSCs and its primary role is bone formation (Caplan, 1991; Prockop, 1997). Formation of the endosteal niche is thought to require endochondral ossification, a process of bone formation, and therefore the presence of osteoblastic cells and other stromal cells such as reticular cells, fibroblasts, and adipocytes (Chan et al., 2009). The differentiation of MSCs into osteoblastic lineage is a stepwise process resulting in osteoblastic precursors that give rise to mature osteoblastic cells able to mineralize their microenvironment and secrete matrix proteins such as osteocalcin, and type I collagen (Askmyr et al., 2009; Maes et al., 2010). The maturation is regulated through the expression of *Runx2* also known as *core binding factor 1 (Cbfa1)* that downstream activates *Osterix* which is essential for the progression of osteogenesis (Komori et al., 1997; Nakashima et al., 2002). Different osteoblastic cell types were found in the endosteal niche including CD31⁻ TER119⁻ CD45⁻ ALCAM⁺ SCA-1⁻ OBCs, immature early B-cell factor 2⁺ (EBF-2⁺) osteoblasts (IEO) or Spindle-shaped N-cadherin⁺ CD45⁻ osteoblasts (SNO) (Kieslinger et al., 2010; Nakamura et al., 2010; Zhang et al., 2003).

A first evidence for the importance of osteoblasts in the regulation of HSCs was published already in the year 1994 by Taichman and Emerson that revealed that the HSC regulating cytokine granulocyte colony-stimulating factor (G-CSF) was secreted from human osteoblasts (Taichman and Emerson, 1994). Furthermore, studies on the involvement of osteoblastic cells in HSC regulation discovered a correlation between the OBCs and HSCs number (Calvi et al., 2003; Taichman et al., 1996). For CD31⁻ TER119⁻ CD45⁻ ALCAM⁺ SCA-1⁻ OBCs an influence on the behavior of HSCs through adhesion in the endosteal niche could be investigated (Nakamura et al., 2010). Additionally, IEO and SNO were found to secrete high levels CXCL12, explaining the chemoattractive capacity of the endosteal niche (Schreck et al., 2014), suggesting these cells are the same as the CAR cells (Sugiyama et al., 2006).

However, another study in which the gene for CXCL12 was deleted in osteoblastic cells could not show alterations in the behavior or number of HSCs (Greenbaum et al., 2013; Kiel and Morrison, 2008). Additionally, deletion of N-Cadherin, which is known to be expressed exclusively on cells of the endosteal surface, did not change the hematopoietic composition or HSCs (Kiel et al., 2007). In another study, Ma and colleagues deleted osteoblastic cells in mice and analyzed the HSC behavior. Interestingly they did not find changes in the cell cycle state of LT-HSCs nor in their functionality (Ma et al., 2009).

These publications clearly show that the precise role of osteoblastic cells in the maintenance of HSCs is still unclear and suggests that the osteoblastic differentiation state may be relevant in HSC regulation. Observations that mature osteoblastic cells were less potent in the maintenance of HSCs than their precursor cells support this view (Ding and Morrison, 2013; Ding et al., 2012; Greenbaum et al., 2013; Raaijmakers et al., 2010).

Besides the positive contribution of the niche on HSCs, more and more studies reveal that alterations in the niche composition or the release of signaling molecules result in a varied HSC actions (Birbrair and Frenette, 2016; Ho and Méndez-Ferrer, 2020; Raaijmakers et al., 2010) underlining the importance of an intact microenvironment and the understanding of this interaction.

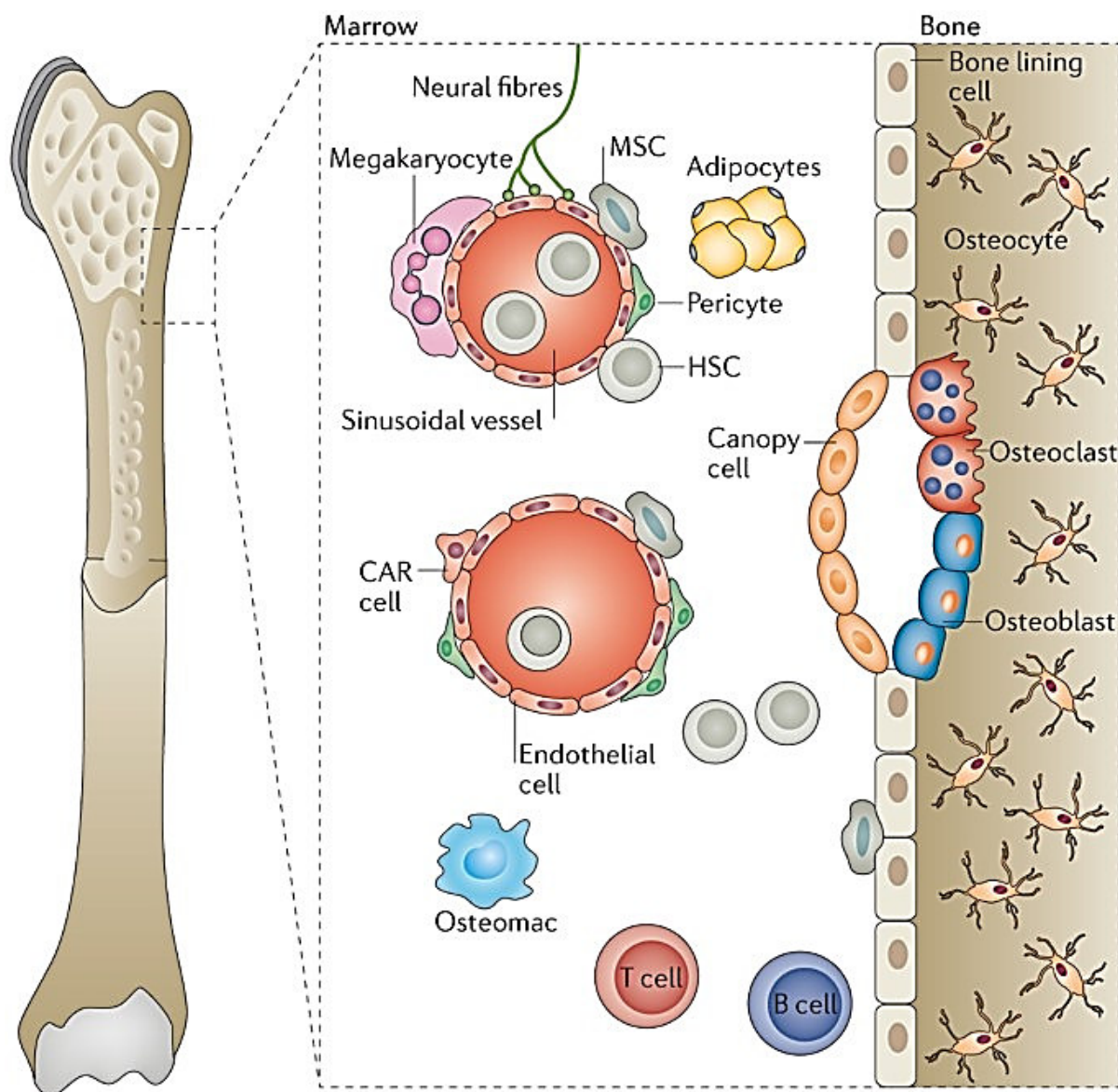


Figure 2. The central niche and the endosteal niche. The niche is a composition of various types of hematopoietic and non-hematopoietic cells. The area on the inner side of the bone marrow is an oxygen enriched area with arteriolar and sinusoid endothelia cells but also CAR-cells and megakaryocytes. The area next to the bone is hypoxic and harbors osteoblasts and osteoclasts as well as mesenchymal stem cells and is called the endosteal niche (Reagan and Rosen et al., 2015).

1.2.1.3 Extrinsic molecules influencing HSCs

Many decades on the study of HSCs revealed different mechanisms of how the cells are extrinsically regulated by their microenvironment. Besides direct physical interaction through binding of adhesion molecules between cells and/or cells and their extracellular matrix, it is known that cells interact with each other through the secretion of proteins such as growth factors, chemokines, cytokines, or hormones (Jeong et al., 2009). Additionally, the field of

extracellular vesicles or the importance of miRNAs was recently discovered to be involved in cell-cell communication (O'Connell et al., 2010; Raposo et al., 2019; Grabher et al., 2011).

1.2.1.3.1 Cell-adhesion molecules

There are many different adhesion molecules known to have an impact on HSC behavior. One of the main cellular regulations in which the cell-adhesion is considered to be important is their influence in the cell cycling. Cell-adhesion, however, might have a positive as well as negative impact on HSC proliferation and number. For the binding of HSCs on Osteospondin (OPN) a reduced proliferation of HSCs was discovered (Nilsson et al., 2005; Stier et al., 2005). OPN is mainly expressed by osteoblasts in the endosteal niche (Haylock and Nilsson, 2006). In OPN knockout mice as well as in an extrinsic transplantation model in which wild type HSCs were regenerated in an OPN deficient niche, increased HSC numbers were detected (Nilsson et al., 2005; Stier et al., 2005), demonstrating the negative impact of OPN on HSC cycling in the BM. N-cadherin however, was shown to have a positive impact on the HSC number resulting in increased HSCs in the BM (Wilson et al., 2004; Zhang et al., 2003). Spindle shaped N-cadherin⁺ Osteoblasts (SNO) represent on their surface the receptor N-Cadherin. A direct correlation between SNO and LT-HSCs was found as the enhanced number of SNO additionally resulted in enhanced LT-HSCs (Zhang et al., 2003). The expression of N-Cadherin was reported to be regulated by Tie-2 and myc both products of HSCs (Arai et al., 2004; Wilson et al., 2004). The secretion of Angiopoietin-1 by osteoblasts results in the binding to its receptor Tie-2 which then enhances the adhesion of HSCs through N-cadherin and also β 1-integrin (Arai et al., 2004). However, the Myc inactivation or loss in HSCs leads to overexpression of N-cadherin and integrins resulting in a proliferation and detachment failure of HSCs (Wilson et al., 2004).

Another important cell-adhesion molecule is VCAM-1. VCAM-1 is expressed by endothelial cells and binds VLA-4 which was found on the surface of HSCs (Chan and Watt, 2001; Oostendorp and Dörmer, 1997). An impaired VLA-4/VCAM-1 pathway results in an enhanced mobilization of HSCs shown by studies using anti-VLA-4 and anti-VCAM-1 antibodies or the inhibition using an VLA-4 inhibitor (Papayannopoulou et al., 1995; Papayannopoulou and Nakamoto, 1993; Ramirez et al., 2009).

1.2.1.3.2 Secreted proteins

Different niche cells were found to produce various types of secreted proteins regulating HSCs in a paracrine manner. Endothelial cells secrete jagged-1, stem cell factor (SCF) and developmental endothelial locus (DEL)-1, mesenchymal stem cells produce interleukin 6 and

11, CCL-2, CXCL-12, SCF growth and granulocyte colony-stimulating factor (G-CSF) (Audet et al., 2002; Baccin et al., 2020; Ding et al., 2012; Negahdaripour, Nezafat and Ghasemi, 2016; Paul et al., 1990; Rafii et al., 1997; Yang et al., 2020) and osteoblastic cells were found to secrete thrombopoietin (TPO), osteopontin (OPN), angiopoietin 1 (ANGPT1) but also CXCL-12 (Arai et al., 2004; Mosteo et al., 2021).

CXCL-12 is the ligand of the CXC chemokine receptor 4 (CXCR4) which was found to be expressed on the surface of HSCs (Sugiyama et al., 2006). Together with VLA-4/VCAM-1 the combination of CXCL-12 with CXCR4 is thought to guide HSCs to their prospective niche (Lapidot and Kollet, 2002; Mazo et al., 2011; Nagasawa et al., 1996). The knockout of either CXCR4 or its ligand CXCL-12 is embryonic lethal (Ma et al., 1998; Tachibana et al., 1998; Zou et al., 1998). However, the transplantation of CXCR4 knockout HSCs isolated from the fetal liver did not reveal an engraftment failure in lethally irradiated recipient mice but showed an impaired potential for LT myeloid reconstitution (Kawabata et al., 1999; Ma et al., 1998). The conditional deletion of CXCR4 in adult mice by activation of Cre recombinase which was under the control of an Mx promoter led to decreased HSC numbers (Sugiyama et al., 2006). Further investigations showed that the loss of CXCL-12 in osterix expressing cells had no effects on the maintenance of HSCs, however the concentration of blood circulating HSCs increased (Greenbaum et al., 2013; Wang and Wagers, 2011). Although, no changes in the HSCs could be found in mice when CXCL-12 was removed from osteoblasts housing in the endosteal niche using Col-2.3-Cre, decreased mature lymphoid hematopoietic cell numbers were detected (Ding and Morrison, 2013; Wang and Wagers, 2011).

During injury, different proinflammatory cytokines such as CCL2, Tumor necrosis factor- α (TNF- α) and interleukin-6 (IL-6) are secreted and extrinsically regulate hematopoietic mature but also stem cells (Aggarwal et al., 2003; Bernard et al., 1994; Ishibashi et al., 1989; Kimura and Kishimoto, 2010; Moxey-Mims et al., 1991; Pearl-Yafe et al., 2010; Serbina and Pamer et al., 2006; Si et al., 2010; Tsou et al., 2007).

CCL2 also known as monocyte chemoattractant protein-1 (MCP-1) is a strong chemoattractant that guides mature monocytes into the circulation and to the side of wounding through a CCL2/CCR2 signaling (Serbina and Pamer et al., 2006; Tsou et al., 2007). However, CCL2 is not only secreted by hematopoietic cells such as myeloid cells or T cells but also from endothelial cells, smooth muscle cells, epithelial cells, fibroblasts, astrocytes, and mesangial cells (Brown et al., 1992; Cushing et al., 1990; Strieter et al., 1989; Standiford et al., 1991). Interestingly, MSCs were found to produce 10-fold more CCL-2 when stimulated with an inflammatory cytokine such as TNF- α (Ren et al., 2012).

However, besides monocytes, HSCs and progenitor cells were also found to express CCR2 and be attracted through CCL2/CCR2 axis to the side of injury (Si et al., 2010).

TNF- α binds to different membrane bound receptors TNF-R1 and TNF-R2 and induces intracellular signaling (Aggarwal et al., 2003). TNF- α modulates the up-regulation of many other cytokines, including IL-3, IL-6 and GM-CSF (Bonavida, 1991; Brouckaert et al., 1993; Caux et al., 1990).

Furthermore, TNF- α attracts neutrophils to the side of inflammation. It additionally enhances neutrophil cytotoxicity and phagocytic activity (Moxey-Mims et al., 1991).

The effect of TNF- α signaling on HSC was demonstrated when TNF- α receptor- HSC were transplanted into wild-type mice. These mice showed defects at the early stage of engraftment and failure of lasting hematopoietic contribution upon host hematopoietic recovery (Pearl-Yafe et al., 2010).

IL-6 is a cytokine secreted by monocytes but also endothelial cells and adipocytes as a response to tissue injuries or infections (Rattazi et al., 2003; Tanaka et al., 2018). IL-6 mainly binds type 1 cytokine, α -receptor subunit (IL6R) to fulfil its action on acute-phase hematopoiesis but also immune responses (Akira et al., 1992; Tanaka et al., 2018; Kishimoto, 1989). Further IL-6 signaling is explained downstream at chapter GP130/STAT3 signaling (1.3.2).

Besides megakaryocyte maturation, IL-6 promotes differentiation of B-cells and naïve CD4⁺ T-cells. In combination with TGF- β it is essential for T-helper (Th) 17 cell differentiation while at the same time, it inhibits regulatory-T cell (T-reg) differentiation (Ishibashi et al., 1989; Kimura and Kishimoto, 2010).

Already in 1989, Ishibashi and colleagues discovered that IL-6 stimulates the differentiation of hematopoietic stem cells (Ishibashi et al., 1989).

IL-6 in combination with IL-3, shorten the G0 period of HSCs and stimulate colony formation (Leary et al., 1988). *In vivo* cultivation of bone marrow cells together with IL-6 and stem cell factor (SCF) increases the survival of bone marrow transplanted mice (Luskey et al., 1992).

In accordance with that, the loss of IL-6 resulted in defective proliferation and self-renewal capacity of HSCs (Bernard et al., 1994).

Another important secreted or membrane-bound molecule from the niche is SCF. SCF binding to its receptor Kit tyrosine kinase on the surface of HSCs was found to maintain the renewal capacity of HSCs and therefore protects from HSC exhaustion (Lyman and Jacobsen 1998). The importance of SCF/KIT binding in HSC regulation was demonstrated in SCF as well as KIT deficient mice. While the loss of the ligand SCF resulted in an impaired maintenance the

mice harboring a deficient KIT receptor showed significantly decreased HSC numbers and function (Waskow et al., 2002; Waskow et al., 2009).

Interestingly, both the LepR⁺ cells perivascular and endothelial cells seem to be an essential source for SCF from the niche as its deletion in these cells resulted in a significant reduction of HSCs in the BM (Zhao and Li 2015; Ding et al., 2012).

Furthermore, the niche is known to secrete molecules involved in different signaling pathways important for HSC regulation. As so cellular communication network factor 2 (CCN2) was shown to be secreted by the niche and activates the transforming growth factor β (TGF- β) signaling in HSCs (Istvánffy et al., 2015). Further the niche secretes molecules involved in the Wnt signaling as for example Dickkopf-related protein 1 (DKK1), Wntless-type MMTV integration site family members (Wnt) 5a or classical Wnt inhibitors such as Secreted frizzled-related proteins (SFRP) 1 and 2 (Fleming et al., 2008; Renström et al., 2009; Ruf et al., 2016, Baksh et al., 2007; Sesler and Zayzafoon, 2013), which were shown to have an impact on steady state as well as stress induced hematopoiesis.

These extrinsic molecules activate different intrinsic signaling pathways which will be discussed in the next chapter.

1.3 Signaling pathways involved in HSC regulation

Here we will focus on Wnt/ β -catenin, Gp130/JAK/STAT, NF- κ B and TGF- β signaling as these pathways are known to be important for HSC regulation (Austin et al., 1997; Blank and Karlsson, 2015; Heinrich et al., 1998; Holyoake et al., 1996; Miller et al., 1997; Reya et al., 2003; Renström et al., 2009; Yamane et al., 2001; Yamazaki et al., 2011; Yonemura et al., 1997; Zhao et al., 2012; 2014).

1.3.1 Wnt/beta-catenin signaling

Besides its fundamental role during development several publications have proofed that the Wnt/ β -catenin signaling is essential for hematopoietic homeostasis at steady state as well as during different stress conditions (Austin et al., 1997; Reya et al., 2003; Renström et al., 2009; Yamane et al., 2001).

Wnt/ β -catenin signaling is activated by the binding of WNT proteins on LRPs that downstream disrupts the multiprotein destruction complex which then further is not able to phosphorylate β -catenin for ubiquitination and degradation. This leads to an accumulation of β -CATENIN in the nucleus that further binds TCF and therefore leads to the expression of the target genes.

However, in the regulation of hematopoiesis Wnt/ β -catenin signaling was found to be controlled by both intrinsic as well as extrinsic mechanisms (Reya et al., 2003; Renström et al., 2009). Although conditional deletion of β -catenin and the double deletion of β -catenin and gamma-catenin did not affect the behavior of HSCs (Cobas et al., 2004; Jeannet et al., 2008), other studies revealed the importance of β -catenin regulation in the HSCs. For example, an expansion of HSCs and hematopoietic progenitor cells *in vivo* was detected when the activated form of β -catenin was overexpressed (Reya et al., 2013). In accordance with that Wnt3a deficient embryos showed reduced numbers of HSCs and hematopoietic progenitor cells (Luis et al., 2009). The importance of extrinsic regulation of the β -catenin amount in the HSCs was demonstrated by our group by using an extrinsic transplantation model which showed a reduced maintenance and self-renewal potential of the HSCs regenerated in a Sfrp1 deficient microenvironment (Renström et al., 2009).

1.3.2 Gp130/JAK/STAT signaling

Another important pathway during regeneration and inflammation is the GP130/JAK/STAT. Interestingly, there are different cytokines binding to the receptor subunit gp130 which all share a similar structural four- α -helix-bundle. This structural similarity defines the IL-6-type cytokine family and includes the cardiotrophin (CT)-1, ciliary neurotrophic factor (CNTF), interleukin (IL)-6 and -11 as well as leukemia inhibitory factor (LIF) and oncostatin M (OSM) (Heinrich et al., 1998). However, each IL-6 type cytokine binds to its specific receptors which trigger either a gp130-homodimerization or a gp130-LIFR or gp130-OSMR heterodimerization upon ligand binding (Heinrich et al., 1998). Dimerization then leads to the phosphorylation and activation of the gp130 associated janus kinase (JAK) which further phosphorylates gp130 at the cytoplasmic site of the receptor. The phosphorylated sites then serve as a docking site for different types of STAT proteins (Heinrich et al., 1998; Silver and Hunter, 2010), which enables JAK to phosphorylate STAT leading to homo- or heterologous dimerization and translocation to the nucleus. The STAT dimers then serve as transcription factors (Heinrich et al., 1998) targeting genes involved in cell division, cell-death, and proliferation (Hirano et al., 2000). In accordance with the biological role of the gp130/JAK/STAT signaling it was found to be involved in the regulation of the cell cycle status of hematopoietic primitive cells.

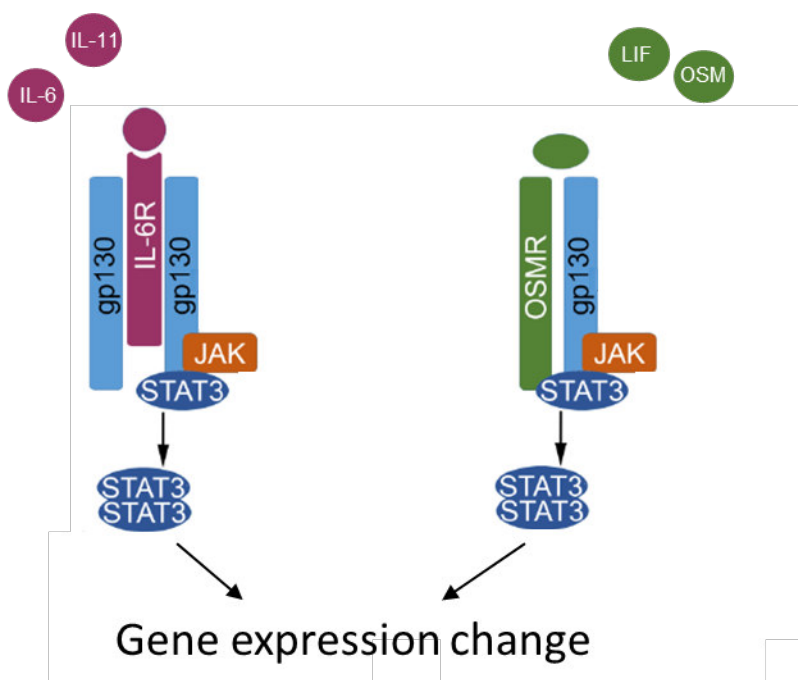


Figure 3. Gp130/JAK/STAT signaling. Binding of IL-6, IL-11, LIF or OSM, to their specific receptors leads to gp130 activation. Gp130 activation leads to STAT3 phosphorylation by JAK and its dimerization. Dimerized STAT3, promotes gene transcription (scheme modified based on Junk et al., 2014).

First evidence for gp130 in regulating hematopoietic stem cells was discovered when knockout mice for gp130 showed fewer early hematopoietic cells than control mice (Yoshida et al., 1996). Additionally, IL-11 which is one ligand of gp130 is important for *in vitro* expansion of hematopoietic stem cells (Heinrich et al., 1998; Holyoake et al., 1996; Miller et al., 1997, Yonemura et al., 1997). Audet et al., discovered that *in vitro* cultivation of HSCs required beside steel factor and flt3-ligand which stimulate stem cell proliferation, the activation of gp130 for the retention of stem cell activity (Audet et al., 2001). Mice overexpressing IL-6 and soluble ligand-binding alpha subunit (sIL-6R α) or LIF alone showed splenomegaly and thrombocytosis (Shen et al., 1994; Peters et al., 1997). Furthermore, the hyperactivation of STAT1/3 using a knock-in mutation of gp-130 results in severe hematopoietic abnormalities such as lymphadenopathy, thrombocytosis and splenomegaly (Jenkins et al., 2005). Additionally, these mice show expanded numbers of immature as well as committed hematopoietic progenitor cells in the spleen and bone marrow (Jenkins et al., 2005). The altered hematopoiesis in the spleen and bone marrow, as well as splenomegaly and thrombocytosis could be rescued when the knock-in mutation of gp130 was generated in mice heterozygous for STAT3, indicating that the altered STAT3 signaling rather than STAT1 is the cause for the hematopoietic defects in the gp130 hyperactivated signaling (Jenkins et al., 2005).

The transplantation of *Stat3* knockout BM cells resulted in an engraftment failure with myeloid-skewed hematopoiesis in the BM and accumulation of myeloid cells in the peripheral blood (Zhang et al., 2018). Additionally, the loss of *Stat3* in endothelial cells and hematopoietic cells revealed an additional impact of the STAT3 signaling during the regulation of HSC homeostasis as these mice revealed fewer LT-HSCs (CD34⁺LSK cells) and more LSK cells in G1 phase of cell cycle with concomitant more gamma H2AX staining (Zhang et al., 2018), indicating the importance of a correct gp130/JAK/STAT signaling in the regulation of hematopoiesis. Interestingly STAT3 was found to have an anti-inflammatory activity in mature myeloid cells which could be linked to a repression of *Ube2n* gene transcription resulting in reduced proinflammatory enzyme Ubc13 (Zhang et al., 2014; Deng et al., 2000). The double knockout of *Stat3* and *Ube2n* rescued the phenotype of *Stat3* mice supporting the idea of an excessive inflammation caused by enhanced Ubc13 signaling (Zhang et al., 2018).

1.3.3 NF- κ B signaling

The NF- κ B signaling plays an important role during the inflammatory response of the hematopoietic system. Inflammatory cytokines and genes involved in the NF- κ B signaling can be detected during regeneration for example after injury or irradiation, but especially as a result of an infection (Sun, 2017). The application of lipopolysaccharide (LPS), or elevated levels of IL-1 β or TNF- α leads to a binding on their specific receptors and downstream to the activation of the canonical NF- κ B pathway whereas CD40L, BAFF, TGF β and lymphotoxin- β heterotrimers (LTs) stimulate the non-canonical NF- κ B pathway (Wu et al., 2015; Iwai et al., 2012; Yamashita et al., 2008).

Canonical activation through IL-1 β or TNF- α and their specific membrane bound receptors differ in further signaling but downstream both lead to phosphorylation of I κ B components (β , ϵ , or γ (NEMO)) by I κ B kinase (IKK). Subsequently Lys48 is ubiquitinated and I κ B degraded (Wu et al., 2015). The NF- κ B factors (dimerized from combinations of Nfkb1 (p50), Nfkb2 (p52), (c) Rel, RelA (p65), or RelB) are then freed and translocate from the cytoplasm to the nucleus to stimulate target gene expression (Hoesel and Schmid 2013).

Activation of the non-canonical pathway downstream leads to p52/RelB (NF- κ B) or JNK, p38 or additional TAK1 activation (Wu et al., 2015; Yamashita et al., 2008).

Interestingly, both canonical and non-canonical NF- κ B signaling involve Ubc13-dependent ubiquitination that then leads to NF- κ B activation or in the case of TNF α either NF- κ B activation or activation of apoptosis (Hodge et al., 2016).

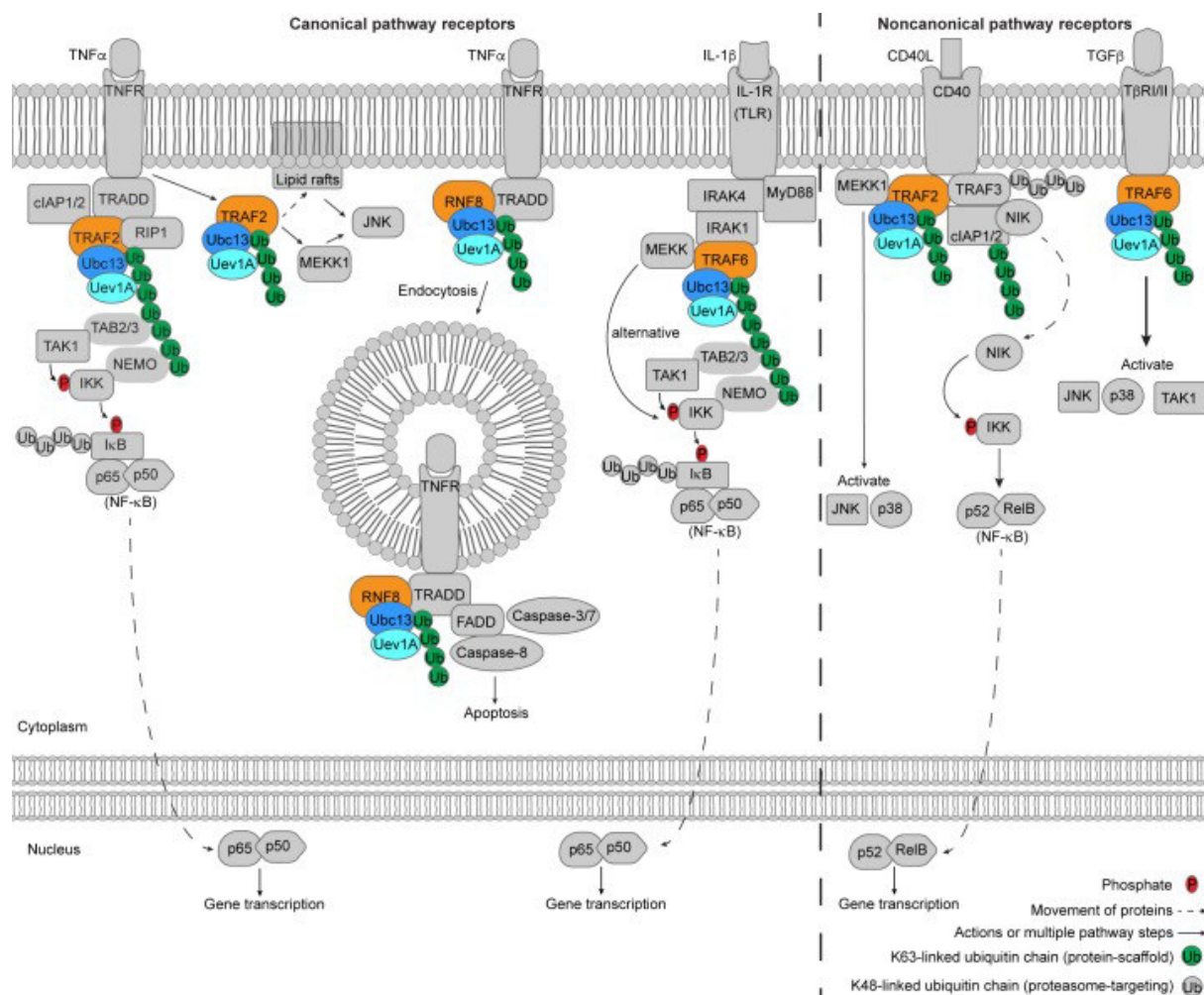


Figure 4. Canonical and noncanonical NF- κ B. IL-1 β or TNF- α bind specific receptors and activate the canonical pathway through phosphorylation of I κ B components (β , ϵ , or γ (NEMO)) by I κ B kinase (IKK). Subsequent I κ B degradation and release of p65/p50 complex takes place that further stimulate gene transcription. CD40L, BAFF, TGF β and lymphotoxin- β heterotrimers (LTs) bind specific receptors and activate non-canonical signaling that activate p52/RelB (NF- κ B), JNK, p38 or additional TAK1. Canonical and non-canonical NF- κ B signaling involve Ubc13-dependent ubiquitination that then further leads to NF- κ B activation (Hodge et al., 2016).

The importance of Ubc13 in hematopoiesis was demonstrated as conditional *Ubc13* knockout mice die within days after deletion with concomitant loss of multilineage blood cells including B-cells and myeloid cells and hematopoietic progenitor cells in the BM. In this study however, the effect of Ubc13 loss was linked to an aberrant Wnt signaling with a role for Ubc13 as a negative regulator for Wnt, rather than an impaired NF- κ B signaling (Wu et al., 2009).

However, in knockout mouse models of RelA, RelB, or p50/NF- κ B2 it was demonstrated that the canonical as well as the non-canonical NF- κ B pathway is necessary for the differentiation of lymphoid, myeloid as well as dendritic and osteoclast cells (Beg et al., 1995; Burkly et al., 1995; Weih et al., 1995; Franzoso et al., 1997; Horwitz et al., 1997; Iotsova et al., 1997).

Moreover, in RelB/NF- κ B2 double knockout mice it was shown that the non-canonical NF- κ B signaling is essential for HSC self-renewal capacity with resulting impaired engraftment potential (Zhao et al., 2012). Loss of niche NF- κ B signaling resulted in a transient but potent phenotype of wild-type (WT) transplanted HSCs with enhanced cycling and altered differentiation (Zhao et al., 2012). The stromal compartment of the RelB/NF- κ B2 double knockout mice was impaired with a reduced number of stromal cells, CFU-F forming cells as well as an enhanced osteogenic differentiation. Furthermore, bone lining cells demonstrated an impaired niche expression of Cxcl-12, Thpo, SCF, and OPN but increased inflammatory cytokines such as G-CSF, GM-CSF and IL-6 (Zhao et al., 2012).

Inhibition of NF- κ B signaling in endothelial cells using *Tie2::I κ B-SS* mice resulted in enhanced HSC self-renewal, activity and recovery after myelosuppression (Poulos et al., 2016). These mice revealed a protective BM microenvironment in terms of stress such as chemotherapeutics or irradiation which may support HSC recovery. Moreover, I κ B-SS BMEC transplantation protects BM cells from myeloablative irradiation as discovered by enhanced monocytes, macrophages neutrophils, and eosinophils in the BM with increased cellularity in the BM and Spleen 10 days after irradiation (Poulos et al., 2016).

Another study demonstrated the importance for the NF- κ B pathway in the formation of the bone as *Rela*^{-/-} mice developed osteopenia caused by an impaired bone formation (Mise-Omata et al., 2014). Moreover, this impaired bone formation was linked to reduced numbers of F4/80⁺ macrophages in NF- κ B *Rela*^{-/-} mice as the transplantation of wild-type F4/80⁺ macrophages were able to rescue the impaired bone (Mise-Omata et al., 2014).

Interestingly, constitutive active NF- κ B signaling using a conditional mouse model in which I κ B β (IKK2) is expressed as an active form in HSCs showed decreased LT-HSC numbers, with an impaired ability to engraft successfully into lethally irradiated mice. Furthermore, the numbers of HSCs in the dormancy state were reduced with concomitant increased proliferative active HSCs (Nakagawa et al., 2018). This study indicates the importance of a correctly regulated NF- κ B signaling especially in the HSCs.

1.3.4 TGF beta signaling

The TGF- β signaling is another important signaling pathway involved in the regulation of hematopoiesis. Two main factors including to this superfamily were shown to have a major effect on HSCs, the bone morphogenetic proteins (BMPs) and TGF- β . While the action of BMPs, especially BMP4 was mainly documented during embryonical development in the hemangioblast, the role of TGF- β especially TGF- β 1 was mainly found in *in vitro* cell culture (Capron et al., 2010; Marshall et al., 2000; Johansson and Wiles 1995). In general, TGF- β binds the TGF- β type II receptor resulting in a dimerization of the heterotetrametric complex of TGF-

β type I and type II receptor and the phosphorylation of the TGF- β type I receptor. Further downstream in the canonical TGF- β pathway Smad2 and 3 are phosphorylated, build a heterodimer together with Smad4, translocate from the cytoplasm into the nucleus where they at the end regulate gene expression (Fabregat and Caballero-Díaz et al, 2018). Interestingly, different *in vitro* studies showed that this active signaling pathway reduces the transcription of c-Myc and Cdk4 and increase the amount of cell cycle inhibitors such as p57^{Kip2} and p21^{Cip1} (Kim and Letterio, 2003; Ewen et al., 1993; Keller et al., 1991; Ohta et al., 1987; Scandura et al., 2004). Interestingly, two different cell types known to be present in the BM were found to be a source for TGF- β . Yamazaki and colleagues revealed the TGF- β secreted by non-myelinating Schwann cells is important for the induction of HSC G0 state of the cell cycle (Yamazaki et al., 2011). In accordance with that the loss of TGF- β 1 in Megakaryocytes lead to an entrance of the HSCs into the cell cycle, demonstrating the role for TGF- β in the maintenance of HSCs (Zhao et al., 2014; Blank and Karlsson, 2015)

1.4 Hematopoietic stress and HSC regulation by the niche

HSC activation especially takes place during wounding (blood loss, irradiation, 5-FU) or the application of arsenic trioxide (As(2)O(3)), G-CSF and IFN alpha, resulting in accumulation of reversible gH2AX-dependent DNA damage response (DDR) (Essers et al., 2009; Essers and Trumpp 2010; Trumpp et al., 2010).

1.4.1 5-Fluorouracil treatment

The chemotherapeutic compound 5-Fluorouracil (5-FU) is known to be intercalated into the DNA during S-phase instead of thymidine and therefore disrupts the RNA synthesis with the result of the apoptosis (Longley et al., 2003). As 5-FU acts during the S-phase, only cells with an active cell cycle are disrupted by this metabolite. This especially concerns hematopoietic progenitor and mature cells resulting in an imbalanced homeostasis of hematopoietic cells. As a result, dormant HSCs get activated and enter the cell cycle to restore the whole hematopoietic system. Besides HSC activation 5-FU enhances the frequency of hematopoietic niche cells such as AdipoCAR cells and *Col16a1*⁺*Tnn*⁺ osteoblasts (Tikhonova et al., 2019; Wolock et al., 2019)

1.4.2 Lipopolysaccharide treatment

Bacterial lipopolysaccharide (LPS) is the major outer surface membrane components present in almost all gram-negative bacteria. LPS acts as a strong stimulator of innate or natural immunity in mammals (Sweet et al., 1996). Interestingly, LPS was found to mimic different inflammatory effects such as induced by IL-6, TNF- α , or IL-1 β (Wright et al., 1999; Poltorak et

al., 1998; Qureshi et al., 1999). LPS binds the TLR4 receptor at the outer membrane of a cell, starts a signaling cascade through MyD88, IRAK, TRAF-6, as well as NADPH oxidase (Nox) to finally activate NF- κ B which further induces the gene expression of pro-inflammatory cytokines (Akira et al., 2001; 2003; Park et al., 2004).

In hematopoiesis, LPS treatment rapidly activates dormant HSCs into the cycling through the binding of LPS on TLR4 receptor on the surface of HSCs (Nagai et al., 2006; Takizawa et al., 2017). It was documented that Flk2⁻ as well as IL7R⁻ LSK cells start to proliferate and differentiate into myeloid lineage (Nagai et al., 2006). Furthermore, a chronic treatment with a daily injection of 6 μ g LPS for four till six weeks lead to increased cycling and HSC expansion with the result of a myeloid skewing and impaired self-renewal capacity of HSCs (Esplin et al., 2011). These results were in accordance to that of Zhao et al., who treated the mice every day with 1 μ g LPS for a duration of 30 days. Additionally, to that, he found an association of enhanced protein levels of the inhibitor of differentiation 1 (Id1). Loss of Id1 in HSCs was shown to reduce the effects of chronic LPS treatment in HSC behavior (Zhao et al., 2013).

However, the effect of LPS on HSC behavior might be dependent on the dosage and/or duration (Schuettpelez and Link, 2013) as other studies revealed a decreased proliferation (Rodriguez et al., 2009) or enhanced ability of HSCs for multilineage repopulation (Takizawa et al., 2011).

Interestingly, beside the known proliferative action of HSCs during LPS treatment and a depart of neutrophils from the BM, Vandoorne and colleges found a remodeling of the sinusoidal vasculature (Vandoorne et al., 2018). Also, BM mesenchymal stem cells express the TLR4 receptor and TLR4 activation results in an altered proliferation, differentiation, migration, survival and secretion of pro-inflammatory cytokines (Fiedler et al., 2013; Liotta et al., 2008; Raicevic et al., 2010; 2012). Upon LPS treatment MSCs enhance their proliferation through activated signaling of TLR4 and PI3K/Akt and Wnt signaling through Wnt3a and Wnt5a (He et al., 2016; Wang et al., 2009).

LPS treatment in mice activated a pro-inflammatory signature in CAR cells up-regulating IL-6, CXCL10 and CCL5 as well as in sinusoidal endothelial cells increasing CCN1 as well as CCN2, CCL2/7 and IL-15 (Helbling et al., 2019).

An indirect effect of LPS treatment was found when nestin-GFP⁺ stromal cells as well as CAR cells were shown to enhance their CCL2 expression after LPS treatment (Shi et al., 2011). Interestingly, as described earlier in the chapter secreted proteins (1.2.1.3.2), not only monocytes were found to express CCR2 (which is the receptor for CCL2) also HSCs express

CCR2 and were discovered to migrate to sites of inflammation in a CCR2 dependent manner as discovered in *Ccr2*^{-/-} mice (Si et al., 2010).

1.4.3 Total body irradiation

Myeloablation using total body irradiation (TBI) and subsequent BM transplantation is a powerful method to treat leukemia (Barriga, 2012). Besides myeloablation, irradiation causes severe injury not only in the hematopoietic compartment but also in organs, different tissues and the hematopoietic microenvironment (Costa and Reagan, 2019). Therefore, a detailed knowledge about the effects of irradiation on cell behavior is necessary to increase the life span and survival of TBI BM transplanted patients (Li et al., 2021).

In cases of DNA damage caused by irradiation the intrinsic apoptosis pathway is activated through binding of BH-3 only proteins to proteins of the Bcl-2 family which downstream activates Bax and Bak that further at the end lead to the activation of the apoptosome (Czabotar et al., 2014).

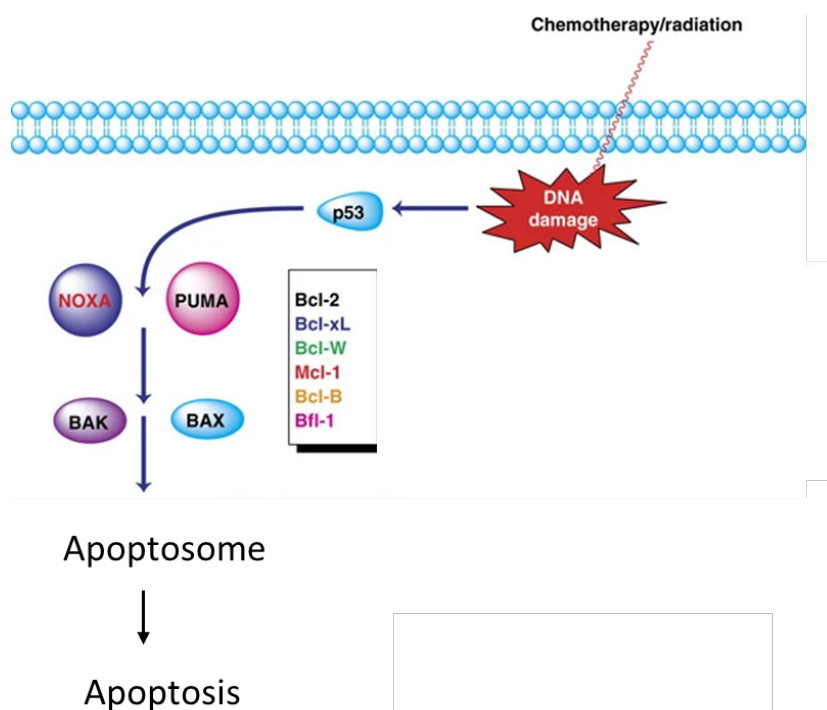


Figure 5. DNA damage induced apoptosis. DNA damage leads to activation of p53 and the Bcl-2 family members. Bcl-2 family members stimulate Bax and Bak regulating the apoptosome, which further lead to cell apoptosis (Placzek et al., 2010).

Irradiated HSCs show reduced LT repopulation with decreased self-renewal and myeloid skewing (Shao et al., 2014). Already a few days after irradiation apoptosis of the hematopoietic progenitor cells causes acute BM suppression (Mohrin et al., 2010). HSC

radiosensitivity is highly dependent on irradiation dosage with a drop of colony formation potential in methylcellulose already at an irradiation dose of 4Gy (Mohrin et al., 2010). In addition, while HSCs displayed a high radioresistance at 2Gy irradiation, MMPs (CMP and GMPs) lost their colony-forming ability to almost 50%. Interestingly, in case of radiation induced double strand breaks (DSB) of the DNA, the resistance of HSCs through different DNA repair mechanisms was observed. While quiescent HSCs induce the non-homologous end joining (NHEJ), active HSCs use the high-fidelity (HR) pathway to repair the DNA (Mohrin et al., 2010). NHEJ DNA reparation mechanism includes genomic rearrangements which may result in DNA abnormalities (Mohrin et al., 2010). Additionally, Mohrin discovered enhanced levels of antiapoptotic Bcl-2 proteins (Bcl-xL, and Mcl-1) with concomitant decreased levels proapoptotic proteins such as Bax, Bak, Bid and Noxa (Mohrin et al., 2010). In this study the Bcl-2 overexpression, however, did not lead to a protection from irradiation-induced apoptosis of CMPs or GMPs (Mohrin et al., 2010). This is in contrast to other investigations were overexpressed Bcl-2 in mice protect hematopoietic subtypes including HSCs (Domen et al., 1998; Ogilvy et al., 1999; Orelia et al., 2004).

In another study it was shown that already a low dosage of 20 mGy irradiation impairs the ability of HSC reconstitution while their differentiation potential was uneffaced (Henry et al., 2021). Low dosage irradiation (20 mGy) was not shown to induce DSB of the DNA but increases ROS levels with activation of the p38 MAPK pathway (Henry et al., 2021).

Furthermore, low-dose irradiation does not affect HSC cell numbers or their apoptosis. But, an HSCs from low-dose TBI mice show increased senescence with no detectable changes in telomeres but enhanced ROS, SA- β -gal, p16 and Arf (Shao et al., 2014). Interestingly, HSC senescence caused by TBI seems to be independent of p16 and/or Arf expression as their deletion did not show significant differences compared to WT HSCs after TBI (Shao et al., 2014). Long term effects of sublethal irradiation (5Gy) resulted in an excessive loss of functional hematopoietic progenitor and stem cells resulting in impaired leukemogenesis 15 weeks post TBI (Batey et al., 2022). Additionally, 62 weeks after TBI an impaired LSK, MPP, MP, CLP and CD45R B cell recovery was detectable. Furthermore, the BM cells from mice, 49 weeks post TBI, were transplanted into lethally irradiated mice which underlined their inability of HSCs for stem and progenitor cell recovery as well as CD45R B cells (Batey et al., 2022).

Besides, the effects on the hematopoiesis, TBI dramatically changes the bone structure with reduced osteoblasts and increased adipocytes (Green et al., 2014). Already ten days after sublethal (5Gy) as well as lethal (12Gy) TBI, mice enhanced adipocytes in the marrow. It was assumed that MSCs after irradiation favorably differentiate into the adipogenic instead of

osteogenic lineage, leading to an impaired bone formation with impaired bone homeostasis (Green et al., 2014).

Additionally, to that Dominici et al., discovered besides the typical hematopoietic depletion a strong disruption of the niche cells after high-dose (1125 cGy) TBI of eight weak old mice (Dominici et al., 2009). Already 48 hrs after irradiation the endosteal niche, mainly of the trabecular bone, showed an excessive expansion of osteoblastic cells resulting in multiple cell layers as confirmed by osteocalcin and collagen I staining and RT-PCR (Dominici et al., 2009). Interestingly, osteoblasts increase their SDF-1 expression after irradiation (Dominici et al., 2009; Ponomaryov et al., 2000). SDF-1 promotes megakaryocytes of homing and survival (Hodohara et al., 2000; Hamada et al., 1998). Additionally, osteoblasts secrete thrombopoietin which is another factor known to induce megakaryocyte migration (Olson et al., 2013). This together with the findings that megakaryocytes are radioresistant up to 7-10 days after irradiation (Tanum 1984; Ebbe et al., 1986) may explain the major number of megakaryocytes 48 hrs after irradiation on the site of endosteal niche of the trabecular bone (Dominici et al., 2009). Furthermore, irradiated megakaryocytes increase their expression of basic fibroblast growth factor (bFGF) and platelet-derived growth factor (PDGF- β), both factors known to enhance the proliferation of N-cadherin-/osteopontin-positive osteoblasts (Dominici et al., 2009; Olson et al., 2013). After the hematopoietic homeostasis has been restored, also the niche cells revert their expanded numbers to homeostasis (Dominici et al., 2009).

However, MSCs were reported to show radioresistance as a result of decreased ROS and reduced DNA damage (Chen et al., 2006). As HSCs, MSCs are able to repair DSB of DNA by homologous as well as NHEJ DNA repair mechanisms after irradiation (Chen et al., 2006).

A *in vivo* study documented a radiosensitivity of MSCs with an immense impact on survival even at the non-irradiated neighboring site (Cao et al., 2011). Local 4Gy irradiation of the left distal femur resulted in decreased numbers of osteoclasts, osteoblasts with increased adipogenesis one and four weeks after irradiation when compared to the left non-irradiated proximal femora (Cao et al., 2011). Interestingly, no CFU-F formation was detectable from BM MSCs isolated from the left distal irradiated as well as from the left proximal non-irradiated femur one week after irradiation, whereas the non-irradiated right femur showed CFU-F and CFU-OB formation. After four weeks MSC numbers were enhanced in the left proximal femur with additional CFU-Fs and CFU-OB formation (Cao et al., 2011). One and four weeks after irradiation MSCs were detected in the peripheral blood (doubled after one week, fourfold after four weeks), indicating the mobilization of MSCs into the circulation after injury (irradiation). Increased levels of free radicals were detected in the irradiated distal femur one and four weeks and in the proximal femur one week after irradiation. Cao assumed that MSC survival was

affected by these free radicals diffusing ipsilaterally through the bone medullary canal from the irradiated site of the bone into the non-irradiated femora (Cao et al., 2011).

Contrary to these studies, stromal cells were documented to show typical irradiation effects as they enhance the expression of p16^{INK4a}/p19^{ARF} as well as SA- β -gal. Moreover, the reduced stromal cell number in BM aspirates eight weeks after irradiation was correlated with the Ink^{4a}/Arf-signaling and indicates long term effects on the behavior of the stromal cells (Carbonneau et al., 2012). Additionally, 2 Gy irradiated MSCs displayed a delayed stromal cell proliferation with reduced CFU as well as differentiation potential in culture (Iwasa et al., 2021). These MSCs did not lack their ability to support hematopoietic stem and progenitor expansion or their differentiation into CD11b⁺ myeloid cells. Irradiation however affects IL-7 and CXCL12 expression resulting in impaired CD19⁺ B cell numbers (Iwasa et al., 2021).

The importance of healthy MSCs in the relation to HSC recovery after irradiation was discovered as the transplantation of MSCs into sublethal irradiated (6 Gy) mice resulted in an enhanced proliferation of the hematopoietic cells and recovery of myeloid as well as lymphoid cells in the peripheral blood (Kim et al., 2018). *In vitro* studies furthermore revealed that irradiated HSCs cultured on MSCs showed reduced apoptosis and DNA damage indicating a potential of MSCs to protect HSC damage caused by irradiation. Kim et al.,

found that this effect was caused by secreted Jagged1 from MSCs which activated the Notch2 signaling in HSCs and prevented them from cytotoxicity (Kim et al., 2018). Additionally, it was shown that an irradiation induced impaired niche increases radiation-induced bystander effects (RIBE) on transplanted human HSCs indicating a major role of the irradiated niche on the recovery of healthy HSCs (Hu et al., 2021). Human HSCs were transplanted in non-irradiated and irradiated murine recipients. Likewise, murine HSCs also human HSCs showed a reduced ability to engraft in the irradiated microenvironment compared to the non-irradiated control (Hu et al., 2021). Hu and colleagues found an enhanced oxidative stress of the HSCs and hematopoietic progenitor recovered in an IR-niche. This oxidative stress resulted in elevated DNA damage response, p53-dependent apoptosis, and cell cycle arrest (Hu et al., 2021).

Nevertheless, stromal cells were also reported to enhance HSCs during irradiation recovery by expressing different molecules (Dominici et al., 2009; Himburg et al., 2017). Osterix (Osx) expressing mesenchymal progenitor cells express enhanced dickkopf-1 (Dkk1) protein levels during HSC regeneration (Himburg et al., 2017). The cultivation of irradiated HSCs in culture media containing Dkk1 enhanced the recovery of both LT-HSCs as well as progenitor cells. Extrinsic Dkk1 further was found to decrease reactive oxygen species (ROS) in the mitochondria as well as HSC senescence. Besides the direct role for Dkk1 in the HSC recovery an additional indirect role could be discovered as Dkk1 enhanced epidermal growth factor

(EGF) secretion of the BM endothelial cells and its deletion reduced HSC recovery (Himburg et al., 2017). EGF was increased after sublethal (750cGy) TBI in the BM serum of *Tie2-Cre; Bak1^{-/-}; Bax^{dox/-}* mice. TBI of these mice resulted in 100% survival and radioprotection of HSCs (Doan et al., 2013) supporting the importance of EC secreted EGF. Another study underlines the importance of EC after TBI induced hematopoietic recovery as VEGFR2 conditional knockout mice showed sinusoidal endothelial cell (SEC) regression with the result of an impaired HSC engraftment (Hooper et al., 2009). Recently a single cell RNAseq analysis from irradiated mice discovered a high sensitivity of stromal cells with the result of a strong reduction in stromal cell numbers (Severe et al., 2019). Among these cells were AdipoCAR cells and osteoblastic cells which are known to support HSCs (Severe et al., 2019). In this study CD73⁺NGFR⁺ chondrocytic cells showed radioresistance and CD73^{-/-} mice displayed that CD73⁺ cells are important for hematopoietic stress response by expressing different cytokines known to support hematopoietic cells such as CXCL12, IL7, KITL, SPP1, and TGF- β (Severe et al., 2019).

Beside the regulation of HSCs by the niche it was also discovered that HSCs regulate their microenvironment after irradiation. Together with LepR⁺ stromal cells, hematopoietic stem and progenitor cells express *Angiopoietin-1* which was shown to be necessary for hematopoietic recovery as well as the vascular recovery after irradiation (Zhou et al., 2015).

However, irradiation stress was found to increase the expression of the CCN2, a molecule known to be important for the regulation of stromal cell as well as hematopoietic cell behavior during stress (Zhang et al., 2015; Leask and Abraham, 2006, Ivkovic et al., 2003, Battula et al., 2013; 2017; Cheung et al., 2014; Istvanffy et al., 2015).

1.5 Cellular communication network factors

The family of cellular communication network factor (CCN) proteins contains six cysteine-rich members sharing a similar modular structure (Moussad and Brigstock 2000). These matricellular proteins include the founding members CCN1/CYR61, CCN2/CTGF, CCN3/NOV which were all described between 1990 and 1992 (Bradham et al., 1991; Joliot et al., 1992; O'Brien et al., 1990), and the Wnt induced secreted proteins (WISP), CCN4/WISP1, CCN5/WISP2, and CCN6/WISP3 (Pennica et al., 1998).

All six known family members contain N-terminal and C-terminal fragments that are connected through a cleavable hinge region (Perbal, 2004). In the N-terminal fragment, the CCN proteins share a signaling module necessary for secretion. Additionally, the N-terminal site harbors two

highly conserved domains, the insulin-like growth factor (IGFBP)-binding module and a von Willebrand factor type C (VWFC)-binding domain. The C-terminal fragment is composed of a thrombospondin type I (TSP-1)-binding module and a carboxyl-terminal cystine knot motif (Bork, 1993; Perbal, 2004). This cysteine knot motif is lacking in CCN5/WISP2, but present in the other five CCNs (Bork, 1993; Chen and Lau, 2009).

Beside their cleavable hinge region, the four different modules of the CCNs also contain additional proteolytic cleavage sites (Holbourn et al., 2008). Furthermore, CCN isoforms were found in different tissues and are (beside of the proteolytically cleaving) the result of alternative splice variants or post-translational processing (Perbal, 2004).

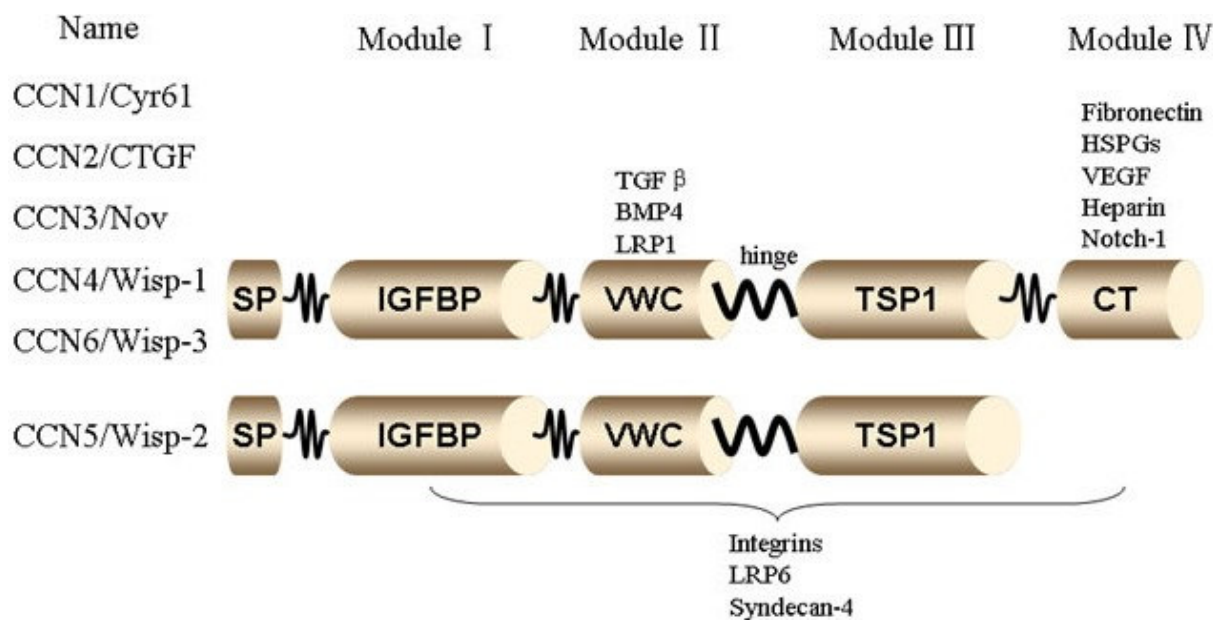


Figure 6. CCN family members. CCN family members with CCN1/Cyr61, CCN2/CTGF, CCN3/Nov, CCN4/Wisp-1 and CCN6/Wisp-3 sharing the same structural domains I (with signal peptide (Sp) and IGF binding domain (IGFBP)), II (von Willebrand type C domain (VWC)), III (thrombospondin-1 domain (TSP1)), and IV (cystine knot domain (CT)). CCN5/Wisp-2 sharing same structural modules I, II and III but lacks module IV. Domain II and III are linked with a hinge region (Jia et al., 2016).

Although the CCN proteins share highly similar structure and are mainly found in the extracellular microenvironment, the interplay between the different modules account for their diverse biological functions (Perbal and Takigawa, 2005). Moreover, an inhibitory effect of CCN3/NOV on the action of CCN2/CTGF was found in rat mesangial cells as well as in human dermal fibroblasts (Riser et al., 2009; Peidl et al., 2019).

1.5.1 Cellular communication network factor 2 (CCN2)

CCN2 is the most investigated member of all CCNs and specifically located in the extracellular matrix (Leask and Abraham, 2006; Moussad and Brigstock, 2000). This heparin binding pleiotropic growth factor is also known as Ctgf, Fist12, Hcs24 and Ecogenin (Leask and Abraham, 2006; Planque and Perbal, 2003). CCN2 was first described in a study identifying immediate early genes in the response to serum-stimulated NIH3T3 cells (Almendral et al., 1988). In further studies CCN2 was isolated from supernatant of human umbilical vascular endothelial cells (HUVECs) and found to be a protein with chemotactic as well as mitogenic characteristics (Bradham et al., 1991). Total deletion of *Ccn2* gene in mice resulted in severe skeletal and vascular malformations indicating a major role for CCN2 in cell differentiation and vascularization (Ivkovic et al., 2003).

Furthermore, CCN2 was found to be up-regulated after irradiation (Zhang et al., 2015), important for normal stromal cell behavior (Battula et al., 2013; 2017; Ivkovic et al., 2003; Safadi et al., 2003; Schutze et al., 2005; Wang et al., 2009), as well as involved in hematopoietic homeostasis (Cheung et al., 2014; Istvanffy et al., 2015). In this thesis, the molecular mechanisms of CCN2 and its mediators in stress responses of HSCs and niche cells will be studied in more detail.

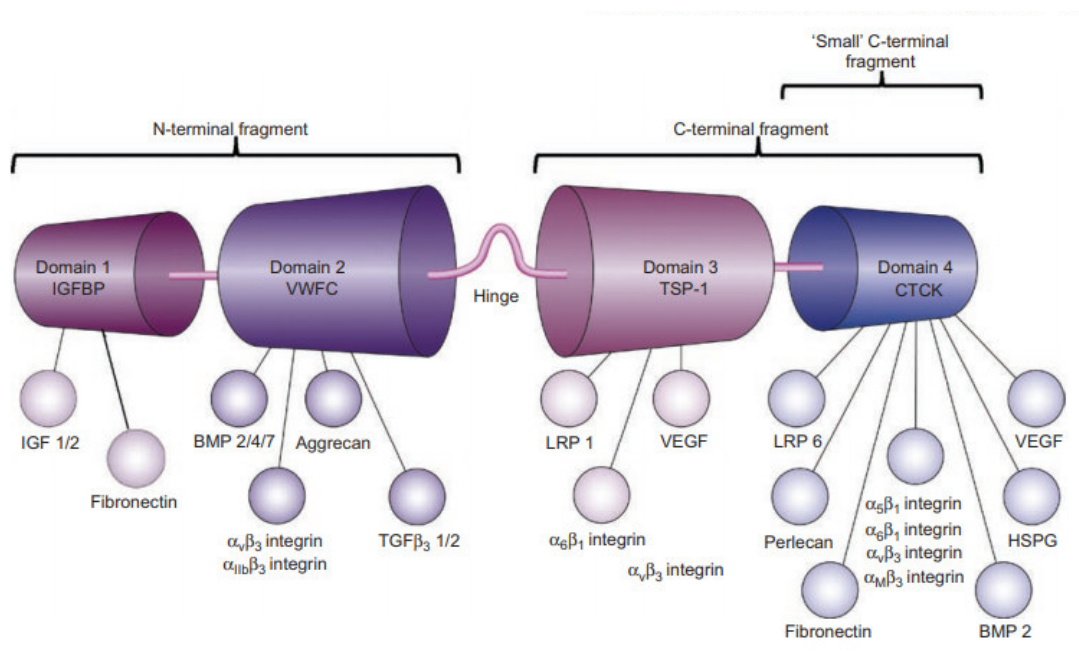


Figure 7. CCN2 and its binding partners. CCN2 protein contains four different domains. The N-terminal fragment includes an insulin-like growth factor-binding (IGFBP) domain and the von Willebrand factor type C (VWFC) domain. The C-terminal fragment contains a thrombospondin type I (TSP-1) domain and the carboxyl-terminal cystine knot (CTCK) domain. The N-terminal and the C-terminal

fragment are connected by a protease cleavable hinge region. Every CCN2 domain binds with different ligands and favors or minors their actions resulting in different cellular responses (Dendooven et al., 2011).

The *Ccn2* gene is located at Chromosome 6 with 1 splice variant in human (Ensembl: ENSG00000118523) and on Chromosome 10 with three different splice variants in mice (Ensembl: ENSMUSG00000019997). The *Ccn2* gene contains five exons encoding for a 38-40 kDa protein (Planque and Perbal, 2003). Different binding partners were found to bind to the four different domains of CCN2 described above. The IGFBP domain binds mainly to IGF1/2, the VWFC binds several cytokines, including BMP2/4/7 as well as TGF- β 1 and 2. Furthermore, the TSP-1-module was found to attach to LRP1, VEGF and integrins and the cysteine knot motif binds to LRP6, Integrin, Fibronectin, BMP2, HSPG and VEGF (Dendooven et al., 2011).

With this variety of binding partners, CCN2 is involved in various biological functions and cellular processes of possible importance in hematopoiesis and the BM niche, such as the formation of bone and cartilage during development, the synthesis of ECM, wound healing, angiogenesis as well as the survival, adhesion, migration, proliferation, and differentiation of different cell types (Igarashi et al., 1993; Takigawa, 2018). Therefore, CCN2 action is not only dependent on the cell type but also on their belonging microenvironment (Cicha and Goppelt-Struebe 2009).

1.5.1.1 *Ccn2* regulation

While during embryonal development *Ccn2* was reported to be expressed by various cell types in the bone (Ivkovic et al., 2003), its expression after birth reduces with age and was found to be highly expressed at the age of four-weeks in the trabecular bone (Wang et al., 2015).

However, *Ccn2* promotor contains specific response elements such as: Hypoxia inducible factor-1, Smad, basal control element-1; transcription enhancer factor; specificity protein 1, cis-acting element of structure-anchored repression (Leask et al., 2009). Through these elements, *Ccn2* gene expression is induced/regulated by various factors such as growth factors (TGF- β or endothelin1) and hormones, but also coagulation factors, bioactive lipids, mechanical stretch or hypoxia (Bai et al., 2013, Chambers et al., 2000, Chowdhury and Chaqour, 2004, Grotendorst et al., 1996; Gu et al., 2012, Guo et al., 2011, Holmes et al., 2001, 2003; Honjo et al., 2012, Valley-Tenney et al., 2020). Beside this, the application of lethal TBI induces *Ccn2* expression in multiple organs including hematopoietic organs such as kidney, liver and the spleen (Zhang et al., 2015). Also, during wound healing *Ccn2* expression is induced and is related to proliferation of fibroblasts, their migration and the production of ECM (Kapoor et al., 2008; Shi-Wen et al., 2008).

Gene expression of *Ccn2* is mainly regulated by a TGF- β response as well as SMAD-binding elements (Grotendorst, 1997, Arnott et al., 2008). Increased CCN2 is essential for the progression in many different fibrotic diseases including kidney, lung, liver, skin and heart (Abdel-Wahab et al., 2002; Ahmed et al., 2004; Charrier and Brigstock, 2010; Igarashi et al., 1993; 1996; Lasky et al., 1998; Liu et al., 2011; Murphy et al., 1999; Paradis et al., 1999). During fibrotic diseases, TGF- β is thought to be necessary to initiate the fibrotic response while *Ccn2* is important to maintain this response (Mori et al., 1999). Interestingly, radiation induces tissue fibrosis through the initiation of the TGF- β /CCN2 axis and the ECM molecule deposition. Irradiation of NIH-3T3 as well as mouse embryonic fibroblast cells increased the expression of *Ccn2*. Treatment of irradiated cells with TGF- β inhibitor as well as overexpression of the microRNA miR-26a reduced *Ccn2* expression after irradiation and implies a novel role for *Ccn2* regulation (Yano et al., 2021).

CCN2 does also regulate TGF- β action as it binds to TGF- β with its VWFC domain and increase TGF- β activity (Abreu et al., 2002).

Another factor observed in *Ccn2* regulation is LPS, which significantly up-regulates *Ccn2* mRNA expression in cultured human bronchial epithelial cells, through interaction with NF κ B (Nishioka et al., 2010). NF κ B was also found to be involved in the regulation of *Ccn2*, as it can either activate the expression of the *Ccn2* gene or be activated by CCN2 (Blom, Goldschmeding, and Leask, 2002; Hall-Glenn et al., 2013). The *Ccn2* promotor contains a NF κ B responsive element, that activates *Ccn2* expression either through tumor necrosis factor- α (TNF- α) or through VEGF signaling (Hall-Glenn et al., 2013). CCN2 itself activates NF κ B through phosphorylation and degradation of the inhibitor I κ B α , which in turn leads to translocation of NF κ B into the nucleus. There, NF κ B promotes survival of hepatic stellate cells, by preventing apoptosis (Gao and Brigstock, 2005).

Interestingly, *Ccn2* appears to regulate itself through a positive feedback loop using an, as yet, undiscovered mechanism, by auto-inducing its own expression (Riser et al., 2000; Shimo et al., 2001).

However, *Ccn2* mRNA has been reported to be posttranscriptional as well as posttranslational regulated by different factors including microRNAs (Charrier et al., 2014; Che et al., 2020; Chen et al., 2019), as well as different cytokines (interferon gamma (IFN- γ), TNF- α), hypoxia and VEGF (Kondo et al., 2002 and 2006; Cooker et al., 2007; Laug et al., 2012).

1.5.1.2 CCN2 signaling

As mentioned earlier, due to its broad spectrum of binding partners, CCN2 binds to different surface receptors (TGF- β receptor, IGF2 receptor, LRP6, and the integrins ITGAV; Istvanffy et al., 2015), which are involved in many different signaling pathways. It is of note, that CCN2

signaling is not only elicited by full-length CCN2, but also by truncated protein, like N-terminal or C-terminal fragments or even splice variants (Abd El Kader et al., 2014; Brigstock et al., 1997; Holbourn et al., 2009; Kaasbøll et al., 2018; Welch et al., 2015;). Therefore, CCN2 does not act as a typical growth factor with one particular receptor. Moreover, CCN2 was reported to regulate several different biological processes in different ways: through direct binding on receptor or co-receptors and activating cell signaling, or its binding on growth factors that inhibits or enhances their actions. Furthermore, CCN2 is defined as a matricellular protein, which modifies the extracellular matrix (ECM) and its turnover through direct binding to aggrecan, fibronectin, heparin, perlecan, etc. (Aoyama et al., 2009; Bork 1993; Chen and Lau 2009; Frazier et al., 1996; Hoshijima et al., 2006, Istvanffy et al., 2015, Nishida et al., 2003; Pi et al., 2008). Besides its extrinsic role, CCN2 was reported to act intrinsically by its endocytic uptake and might affect gene transcription (Escolar et al., 2008; Kawata et al., 2006; 2012; Sumiyoshi et al., 2010).

Ccn2 plays a role in different signaling pathways. For example, in *Xenopus* embryos CCN2 was associated with the Wnt pathway, according to its ability to bind to the Wnt co-receptor LDL receptor-related protein 6 (LRP6) (Mercurio et al., 2004). In mesangial cells, CCN2 was observed to stimulate the phosphorylation of LRP6 and GSK-3 β , which results in an accumulation and nuclear localization of β -catenin, TCF/LEF activity and expression of Wnt targets (Rooney et al., 2011). Inhibition of DKK-1 and LRP6, proteins that are also involved in hematopoietic regeneration, can reverse those effects (Himburg et al., 2017; Rooney et al., 2011). Additionally, a connection between CCN2, BMP-4 and TGF- β was identified. CCN2 was found to bind both molecules through its VWTC domain and exerts an activating effect on TGF- β , while it inhibits BMP-4 activity (Abreu et al., 2002). Both TGF-beta and BMP-4 regulate HSC maintenance (Blank and Karlsson 2015; Goldman et al., 2009).

Downstream of CCN2, an increase in EGF, PDGF and FGF, all factors known to be involved in the regulation of hematopoiesis or BM stromal cells, was observable in fibroblasts (Doan et al., 2013; Luft, 2008; Pinho and Frenette, 2019; Zhao et al., 2012; Xue et al., 2012).

1.5.1.2.1 Ccn2 signaling in hematopoiesis

That Ccn2 might play a role during hematopoiesis first became into the focus of researchers when an increased expression of CCN2 was detected in childhood and adult patients of acute lymphoblastic leukemia (ALL) (Sala-Torra et al., 2007; Vorwerk et al., 2000). By separating different types of ALL and analyzing CCN2 mRNA expression Boag and colleagues revealed that the overexpression of CCN2 in ALL is exclusively for B-lineage ALL (pediatric and adult)

and high expression was associated with a poor outcome of the disease (Boag et al., 2007; Kang et al., 2010, Sala-Torra et al., 2007; Vorwerk et al., 2000).

The role of CCN2 during normal hematopoiesis still needs to be elucidated. As the *Ccn2* knockout mice die within the first minutes after birth due to a respiratory failure, which is the result of an impaired skeletal development (Ivkovic et al., 2003), the study of *Ccn2* during adult hematopoiesis was difficult. Cheung and colleagues analyzed the impact of *Ccn2* during embryogenesis and found a reduced percentage of B-cells in the *Ccn2*-deficient embryos. Furthermore, *in vitro* experiments showed that recombinant human CTGF/CCN2 together with IL-7 enhanced B-cell proliferation and increased the B-cell maturation as increased pro-B to pre-B differentiation was detectable (Cheung et al., 2014).

Cheung and colleagues transplanted *Ccn2*^{-/-} HSCs into the fetal liver of neonatal mice and found no differences compared to WT HSCs (Cheung et al., 2014). Consistent to that no *Ccn2* expression was detectable in the hematopoietic cells of the BM. However, Cheung found a strong expression in stromal cells (MSCs, CAR cells, ECs and VCAM-1⁺ cells) with the highest expression in CAR cells. This together with the results that the addition of rhCTGF/CCN2 *in vitro* showed an impact on B-cell maturation led to the postulation that, extrinsic CCN2, mostly secreted by stromal cells, affects hematopoiesis more strongly than intrinsically generated CCN2 (Cheung et al., 2014).

Our own group showed previously, that *Ccn2* is strongly upregulated in both LSK cells and in UG26-1B6 stromal cells during 24 hour-co-cultures. Further studies using co-culture experiments on *shCcn2* and control pLKO.1 stromal cells, revealed that extrinsic CCN2 regulates the progression of the cell cycle of the earliest HSCs from G0 to G1 by regulating WNT and TGF- β signaling. In accordance to that, a decline in donor engraftment of WT HSCs cultured on *shCtgf* compared with pLKO.1 was noted at week 10 and 16 post-transplant (Istvánffy et al., 2015). This decline was caused by reduced regeneration of donor MPs and LSK cells as well as reduced myeloid and B-cells in mice receiving HSC co-cultured on *shCtgf* stroma (Istvánffy et al., 2015). In single cell cultures, addition of recombinant CCN2 restored HSC proliferation, showing a direct effect of extrinsic CCN2 on HSC proliferation (Istvánffy et al., 2015).

1.5.1.2.2 CCN2 signaling in niche cells

Besides the direct role of *CCN2* on the hematopoietic cells, the loss of *Ccn2* might result in an altered hematopoietic niche function, which might impair its ability to maintain HSCs. Indeed, increased levels of *Ccn2* were detectable in MSCs from acute myeloid leukemia (AML)-bearing mice when compared their controls (Battula et al., 2017). However, extrinsic CCN2 was reported to favor or as well as reduce the engraftment of AML in murine hosts, showing the exact role of CCN2 is unclear (Battula et al., 2017; Battula et al., 2013).

Nevertheless, *Ccn2* was shown to have a major impact on endothelial cells as well as endosteal niche cells (Arnott et al., 2011; Battula et al., 2013; 2017; Cheung et al., 2014; Cicha and Goppelt-Struebe, 2009; Luo et al., 2004; Inoki et al., 2002; Ivkovic et al., 2003; Muehlich et al., 2004; Xu et al., 2000). For instance, *Ccn2* expression is required in BM skeletal stromal cells, since *Ccn2*^{-/-} mice exhibit several developmental skeletal defects, including a lethal malformation of the ribcage (Ivkovic et al., 2003). Ivkovic and colleagues found evidence that this malformation is due to altered chondrogenic differentiation. In addition, the *Ccn2*^{-/-} mice showed decreased vascular endothelial growth factor (VEGF) expression and an enlarged hypertrophic zone, probably impairing endochondral ossification (Ivkovic et al., 2003).

The consequences of the decreased VEGF expression in *Ccn2*^{-/-} mice is not entirely clear. Indeed, it was reported that CCN2 exerts an anti-angiogenic effect *in vitro* as well as *in vivo*. Here, CCN2 inhibited the action of VEGF by preventing its binding to endothelial cells and therefore blocking the activation of angiogenesis (Inoki et al., 2002). Thus, the role of CCN2 during angiogenesis remains controversial, and has been attributed to developmental stage, the type of cells and the CCN2-binding receptors they express (Arnott et al., 2011; Cicha and Goppelt-Struebe, 2009).

In most cell types, steady state levels of *Ccn2* are rather low. But, as an early stress response, such as in wound healing, CCN2 is upregulated, and it serves a pro-reparative role (Alfaro et al., 2013). An increased *Ccn2* mRNA expression was also detectable *in vitro* when endothelial cells were cultured with sphingosine-1-phosphate, lysophosphatidic acid or platelets (Muehlich et al., 2004). Additionally, high expression of *Ccn2* was detectable during development in different BM stromal cells such as Sca-1⁺PDGFR α ⁺ MSCs, VCAM-1⁺ reticular cells with the highest expression in CAR cells. In the *Ccn2*^{-/-} mice, however, the endothelial and CAR cell number and proportions were unchanged compared to controls (Cheung et al., 2014).

Additionally, *Ccn2* was shown to be increased in MSCs during new bone formation and promotes bone and cartilage regeneration (Abd El Kader et al., 2014; Arnott et al., 2011; Kikuch et al., 2008). Recently, an *in vitro* study revealed the role for *Ccn2* in different events

necessary for bone regeneration such as migration, osteogenesis, and vascularization (Fahmy-Garcia et al., 2021). In a Boyden chamber assay, CCN2 was shown to be chemoattractive for MSCs and ECs and the treatment with CCN2 on HUVEC cells resulted in increased tube formations in Matrigel indicating a role of CCN2 in angiogenesis (Fahmy-Garcia et al., 2021). In contrast to other studies, this study did not reveal any alteration of osteogenic differentiation when MSCs and SV-HFO cells were treated with CCN2 (Fahmy-Garcia et al., 2021).

How these results can be reconciled with *in vitro* loss of *Ccn2* is unclear. Here, *CCN2* loss resulted in decreased proliferation rate with concomitant decreased S-phase cells of human MSCs (Battula et al., 2013). Also, the *in vitro* experiments point to a decisive effect on the balance between osteo- and adipogenesis, where the loss of *CCN2* increases adipogenesis with simultaneously reduction of osteogenesis (Battula et al., 2013). In line with this finding, a decreased *CCN2* mRNA level was additionally found in MSCs gaining adipogenic lineage (Schutze et al., 2005). In accordance to that, overexpression of *CCN2* in human MSCs lead to increased osteoblasts (Wang et al., 2009). Interestingly, MSCs showed an excessive *Ccn2* expression, during BMP and Wnt3a induced osteogenic differentiation. The role for *CCN2* during osteogenesis appears only to play a role in the early stages of osteogenic differentiation, as increased expression was observed in pre-osteoblasts but not in committed osteoblasts (Luo et al., 2004; Xu et al., 2000). Interestingly, the expression of *Ccn2* correlated with the confluence of the osteoblastic cells: the higher the confluence, the lower *Ccn2* mRNA levels (Safadi et al., 2003). In addition to differentiation osteoblastic cells increased their proliferative and mineralization behavior when cultured with rCCN2 (Safadi et al., 2003).

1.6 Aim of the thesis

Ccn2 is known as an early response gene to stress (Alfaro et al., 2013; Almendral et al., 1988; Cicha and Goppelt-Struebe, 2009) and is involved in different regenerative processes in a variety of cell types and contexts (Leask and Abraham, 2006; Kapoor et al., 2008; Shi-Wen et al., 2008). Previously our group showed in *in vitro* experiments that extrinsic *CCN2* is essential for the progression of cell cycling in HSCs by reducing senescence, pSMAD2/3, and CDKN1B while enhancing Cyclin D1 (Istvánffy et al., 2015). Furthermore, the introduction states that *Ccn2* is important not only for hematopoietic cells (Istvánffy et al., 2015; Cheung et al., 2014), but also for cells of the hematopoietic microenvironment (Abd El Kader et al., 2014; Arnott et al., 2011; Fahmy-Garcia et al., 2021; Kikuch et al., 2008; Luo et al., 2004; Safadi et al., 2003; Schutze et al., 2005; Xu et al., 2000). The studies reveal *Ccn2* to be involved in a variety of signaling pathways known to be necessary for hematopoietic and/or stromal cell behavior

(Inoki et al., 2002; Istvánffy et al., 2015; Luo et al., 2004; Xu et al., 2000). While *Ccn2* levels are low during steady state conditions in adult mice (Wang et al., 2015), high *Ccn2* levels are reported during stress conditions in cells of the stromal compartment (Muehlich et al., 2004; Battula et al., 2013; 2017; Fahmy-Garcia et al., 2021).

Therefore, we expected that *Ccn2* expressed by stromal cells is involved in regulating HSCs and progenitor cells *in vivo* during hematopoietic stress conditions in adult mice.

Aim of this thesis was to reveal a possible role of *Ccn2* during steady state conditions in adult hematopoietic and/or stromal cells and to shed light on how *Ccn2* loss will affect stress induced hematopoiesis during different stress conditions.

For this purpose, we decided to use an inducible conditional *Ccn2* knockout model in which *Ccn2* is deleted in adult mice in the hematopoietic as well as in the stromal compartment. After *Ccn2* deletion, hematopoietic and stromal composition were investigated under steady state conditions and compared to different hematopoietic stress conditions such as 5-FU, LPS, bone marrow transplantation and irradiation studies. Moreover, we used apoptosis and BrDU studies, as well as immunofluorescence stainings to reveal possible altered intracellular signaling pathways and to shed light on the *Ccn2* involvement in stress induced regulation of HSCs.

2 Material and methods

2.1 Material

2.1.1 Consumption-utensils

Utensils	Manufacturers
Cell Culture Dish, 10 cm, growth-enhanced treated	TPP Techno Plastic Products AG (Trasadlingen, CH)
Cell Culture Plates Cellstar 6, 12, 24, 48 well	Greiner Bio-One GmbH (Frickenhausen, DE)
Cryogenic vial, 2 mL	Corning Inc. (Corning, USA)
Disposable bags	Carl Roth (Karlsruhe, DE)
Filter Vacuum driven disposable bottle top filter Steritop	Millipore Co. (Billerica, USA)
Filter 22 µm, 30 µm, 45 µm	BD™ Filcon, BD Bioscience (Heidelberg, DE)
Filter tips TipOne 1-10 µL, 20 - 200 µL, 200 - 1000 µL	Starlab (Hamburg, DE)
Freezing container	Mr Frosty™ – Thermo Fisher Scientific Cool Cell® - Bio Cision
Hamilton Needle: 6/pk	Hamilton (Bonaduz, CH)
MACS LS cell separation columns	Miltenyi Biotec (Bergisch Gladbach, DE)
MicroAmp® Fast 96-Well Reaction Plate	Applied Biosystems (Foster City, U.S.A.)
Microcentrifuge safe-lock tubes, 1.5, 2 mL	Eppendorf AG (Hamburg, DE)
Monoject, blunt cannula needles	Kendall Healthcare (Mansfield, USA)
Mortale	Thermo Fisher Scientific Inc. (Waltham, USA)
Needles, 100 Sterican, 27 Gauge	B. Braun Melsungen AG (Melsungen, DE)

Pestle	Thermo Fisher Scientific Inc. (Waltham, USA)
Polylysine® Slides	Thermo Fisher Scientific Inc. (Waltham, USA)
Polypropylene centrifuge tubes 15, 50 mL	Greiner Bio-One GmbH (Frickenhausen, DE)
Round-bottom 96 well plate	Nunc A/S (Roskilde, DK)
Serological Pipettes, 2, 5, 10, 25, 50 mL	Greiner Bio-One GmbH (Frickenhausen, DE)
S-Monovette Blood Collection System	Sarstedt AG & Co. (Nümbrecht, DE)
Superfrost Plus™ Adhesion Microscope Slides	Thermo Fisher Scientific Inc. (Waltham, USA)
Super PAP PEN	Thermo Fisher Scientific Inc. (Waltham, USA)
Syringes, U-40 Insulin, Omnifix, 1 mL	B. Braun Meslungen AG (Melsungen, DE)
Syringes single-use Omnifix 3/5/10 mL	B. Braun Meslungen AG (Melsungen, DE)

Table 1. List of used consumption-utensils

2.1.2 Machines and equipment

Machines and equipment	Name	Manufacturers
Animal Blood Counter	Counter Scil Vet Abc™	Scil vet academy (Viernheim, DE)
Incubator	Hera Cell 240	Heraeus Instruments (Hanau, DE)
Cell sorter	MoFlo High Speed Astrios S1 ARIA Illu	Beckman (Coulter, US) Beckman (Coulter, US) BD Bioscience (New Jersey, U.S.)
Centrifuges	Megafuge 3.0RS, Multifuge 3S	Heraeus Instruments (Hanau, DE)

	Biofuge fresco Sigma 1-14	Heraeus Instruments (Hanau, D) Heraeus Instruments (Hanau, DE) Sigma Laborzentrifugen GmbH (Osterode am Harz, D)
Counting chamber	Neubauer-improved	Paul Marienfeld GmbH (Lauda Königshofen, DE)
ELISA Reader	Multiscan FC	Thermo Fisher Scientific Inc. (Waltham, USA)
Flouresence Microscope	Leica DM RBE	Leica, Wetzlar, Germany
Flow cytometer	CyAn ADP LxP8	Beckman (Coulter, US)
Ice machine	S.-No:061244	Ziegra Eismaschinen (Isernhagen, DE)
Laminar flow hood	ANTAES 48/72	BIOHIT (Rosbach, DE)
Linear accelerator	Mevatron KD2	Siemens (Erlangen, DE)
Microscope	CKX41	Olympus Corporation (Tokyo, J)
NanoDrop	ND-1000 UV/Vis spectrophotometer	NanoDrop Technologies (Wilmington, U.S.A.)
Precision scales	PLJ 2100-2M	Kern & Sohn GmbH (Balingen, DE)
QuadroMACS Separator	MACS	Miltenyi Biotec (Bergisch Gladbach, DE)
Radiation Unit (Typ RS225)	Gulmay	Gulmay (Suwanee, U.S.A)
Radiation Unit (Typ OB29/902-1)	Buchler	Buchler GmbH (Braunschweig, Germany)

Real-Time PCR System	StepOne	Applied Biosystems (Foster City, U.S.A.)
Thermal Cycler	PTC 100 Peltier	Bio-Rad (Philadelphia, USA)
Thermomixer	comfort	Eppendorf AG (Hamburg, DE)
UV-light Gel-Doc	XR Imaging System	R&D Systems (Wiesbaden, DE)
Vortex	IKA MS1 minishaker	Werke & Co. (Staufen im Breisgau, DE)

Table 2. List of used machines and equipment's

2.1.3 Softwares

Software	Company
AxioVision	Carl Zeiss MicroImaging GmbH
FlowJo, Version 8.8.6.	TreeStar Inc. FlowJo™ Software (for Mac), Ashland, OR: Becton, Dickinson and Company; 2019.
GraphPad Prism, Version 7.0e	Graphpad Software Inc.
Image J, Version: 2.0.0-rc-43/1.50e	Rasband, W.S., ImageJ, U. S. National Institutes of Health, Bethesda, Maryland, USA, https://imagej.nih.gov/ij/ , 1997-2018.
Microsoft Exel, Version 2010	Microsoft Inc.
Microsoft Power Point, Version 2010	Microsoft Inc.
Microsoft Word, Version 2010	Microsoft Inc.
Photoshop, Version CS5 Extended 12.0x32	Adobe Inc.
Step One Software, Version v.2.3	Thermo Fisher Scientific/ Applied Biosystems

Table 3. List of used Software's

2.1.4 Chemicals

Chemicals	Company
Agarose Neo Ultra-Qualität	Carl Roth (Karlsruhe, DE)
Alizarin Red S	Sigma-Aldrich (Taufkirchen, DE)
Dimethyl sulfoxide (DMSO)	SERVA Electrophoresis GmbH (Heidelberg, DE)
Diphtheria toxin	Merck Group (Darmstadt, DE)
Ethanol, 99.8%	AppliChem (Darmstadt, DE)
Ethidium bromide, 1% solution	Carl Roth (Karlsruhe, DE)
Ethylendiamintetraessigsäure (EDTA)	Carl Roth (Karlsruhe, DE)
Glycerol	Sigma-Aldrich (Taufkirchen, DE)
Hygromycin B	Clontech (Saint-Germain-en-Laye, France)
Isofluran 100%	CP-Pharma Handelsgesellschaft mbH (Burgdorf, DE)
Isopropanol	Sigma-Aldrich (Taufkirchen, DE)
Methanol	Sigma-Aldrich (Taufkirchen, DE)
Oil Red O	Sigma-Aldrich (Taufkirchen, DE)
Paraformaldehyde (PFA), neutral buffered, 10%	Sigma-Aldrich (Taufkirchen, DE)
Polybrene	Sigma-Aldrich (Taufkirchen, DE)
Propidium-Jodid (PI)	Invitrogen (Darmstadt, DE)
SlowFade Gold Antifade Reagent with DAPI	Invitrogen (Darmstadt, DE)
Sodium tetraborate derahydrate	Sigma-Aldrich (Taufkirchen, DE)
SuperSignal® West Pico/Dura/Femto Extended Duration Substrate	Pierce Biotechnology (IL, USA)
Trypan blue	Invitrogen (Darmstadt, DE)
Tween 20	Carl Roth (Karlsruhe, DE)
UltraPure Dnase/Rnase-Free Distilled Water	Invitrogen (Darmstadt, DE)
β-mercaptoethanol	Invitrogen (Darmstadt, DE)

Table 4. List of used chemicals

2.1.5 Biological reagents

Biological reagents	Company
Adipogenic Supplement	R&D Systems (Wiesbaden, DE)
Albumin Fraction V, ≥98 %, bovine (BSA)	Carl Roth (Karlsruhe, DE)
Cell Adhere™ Type I Collagene	Stemcell Technologies (Köln, DE)
Collagenase Type 1	Worthington Biochemical (Corp, U.S.A)
DNase I	Sigma-Aldrich (Taufkirchen, DE)
Fetal calf serum (FCS)	PAA (Cölbe, DE)
Gelatin from bovine skin	Sigma-Aldrich (Taufkirchen, DE)
Horse serum (HS)	BioWhittaker (Vallensbaek, DK)
Human LDL	Stemcell Technologies (Köln, DE)
Lipofectamine®2000	Invitrogen (Darmstadt, DE)
Lipopolysaccharides (LPS) from Escherichia Coli 055:B5	Sigma-Aldrich (Taufkirchen, DE)
mIL-11	R&D Systems (Wiesbaden, DE)
mSCF	R&D Systems (Wiesbaden, DE)
NGF	R&D Systems (Wiesbaden, DE)
Osteogenic Supplement	R&D Systems (Wiesbaden, DE)
Penicillin/Streptomycin	Invitrogen (Darmstadt, DE)
PRI724-Inhibitor	Selleckchem (Houston, US)
Proteinase K	Thermo Fisher Scientific Inc. (Waltham, USA)
Puromycin	Invitrogen (Darmstadt, DE)
SMAD 2/3-Inhibitor	Selleckchem (Houston, US)
Trypsin 10x	Invitrogen (Darmstadt, DE)

Table 5. List of used biological reagents

2.1.6 Buffer, Medium and Solution

2.1.6.1 Ordered buffer, medium and solution

Ordered buffer, medium and solution	Company
Adipogenic/Osteogenic Base medium	R&D Systems (Wiesbaden, DE)
ACK Lysing Buffer	Thermo Fisher Scientific Inc. (Waltham, USA)
BIT 9500 Serum Substitute	Stemcell Technologies (Köln, DE)
α -MEM plus GlutaMAX	Invitrogen (Darmstadt, DE)
DMEM	Invitrogen (Darmstadt, DE)
Dulbecco's PBS (DPBS)	PAA (Cölbe, DE)
IMDM	Thermo Fisher Scientific Inc. (Waltham, USA)
Minimum Essential Medium Eagle	Sigma-Aldrich (Taufkirchen, DE)
MethoCult M3434	Stemcell Technologies (Köln, DE)
OptiMEM	Invitrogen (Darmstadt, DE)
0.5% Trypsin-EDTA (10x)	Invitrogen (Darmstadt, DE)

Table 6. List of ordered buffers, medium and solution

2.1.6.2 Self-made buffer, medium and solution

Self-made buffer, medium and solution	Composition
Alizarin Red solution	<ul style="list-style-type: none"> • 1 mg/mL in deionized H₂O
Blocking buffer (IF)	<ul style="list-style-type: none"> • 10% FCS • 0.1% Triton-X • 89.9% PBS
Destain solution	<ul style="list-style-type: none"> • 10% Cetylpyridiumchloride • 10mM Sodiumphosphate • → at pH 7.0
EDTA solution	<ul style="list-style-type: none"> • 0.5 M in deionized H₂O (pH=8.0)

FACS buffer (500 mL)	<ul style="list-style-type: none"> • 500 mL PBS • 0.5% BSA
Gelatin solution (1%, 500 mL)	<ul style="list-style-type: none"> • 5 g Gelatin powder • 500 mL deionized H₂O
HF2+ buffer (1 l)	<ul style="list-style-type: none"> • 10% HBSS (10x) • 2% FCS hi • 0.1% mL HEPES • 100 U/mL penicillin • 100 mg/mL streptomycin • 86% deionized H₂O
NaB buffer	<ul style="list-style-type: none"> • 0.01 M disodium tetraborate • deionized H₂O
MEF and NIH medium (500 mL)	<ul style="list-style-type: none"> • 445 mL DMEM (+L-glutamine) • 10% FCS hi • 100 U/mL penicillin • 100 mg/mL streptomycin
MSC medium (500 mL)	<ul style="list-style-type: none"> • α-MEM plus GlutaMAX • 10% FCS hi • 100 U/mL penicillin • 100 mg/mL streptomycin • 10 mM β-Mercaptoethanol
Oil Red O Stock solution	<ul style="list-style-type: none"> • 0.5 g Oil Red O • 100 mL Isopropanol
Stroma medium (500 mL)	<ul style="list-style-type: none"> • α-MEM plus GlutaMAX • 15% FCS hi • 5% HS hi • 100 U/mL penicillin • 100 mg/mL streptomycin • 10 mM β-Mercaptoethanol

Collagenase digestion	<ul style="list-style-type: none"> • 2 ml DMEM with 10% FCS • 200 µl HBSS (10x) • 20 µl Collagenase Type II • 6 µl Dnase I (5mg/mL)
Freezing medium	<ul style="list-style-type: none"> • 10% DMSO • FCS

Table 7. List of self-made buffers, medium and solution

2.1.7 Kits

Kits	Company
Annexin V Kit	BD Pharming (San Diego, U.S.A)
APC/FITC BrdU Flow Kit	BD Pharming (San Diego, U.S.A)
CBA Kit	BD Pharming (San Diego, U.S.A)
Comet Assay Kit	BD Pharming (San Diego, U.S.A)
Lineage cell depletion Kit (mouse)	Miltenyi Biotec (Bergisch Gladbach, DE)
Power SYBR Green PCR Master Mix	Applied Biosystems (Foster City, USA)
Quanti Tect Reverse Transcription Kit	Quiagen Inc. (Hilden, DE)
VWR Red Taq DNA Polymerase Master Mix	VWR life science (Pennsylvania, U.S)
RNeasy Micro Kit	Quiagen Inc. (Hilden, DE)
RNeasy Mini Kit	Quiagen Inc. (Hilden, DE)
Senescence Cells Histochemical Staining Kit	Cell Signaling Technology (Danvers, U.S)
Wizard® Genomic DNA Purification Kit	Promega (Medison, U.S.)

Table 8. List of used kits

2.1.8 Primary and Secondary Antibodies

2.1.8.1 Primary Antibodies

2.1.8.1.1 Primary Antibodies for flow cytometry

Antigens	Clone	Flouorochrome	Volume/1*10 ⁶ cells	Company
Anti-mouse CD3e	145-2C11	PE-Cy5.5	0.1 µL	ebioscience (San Diego, CA, USA)
Anti-mouse CD4	30-F11	PE-Cy5.5	0.1 µL	ebioscience (San Diego, CA, USA)
Anti-mouse CD8a	53-6.7	PE-Cy5.5	0.1 µL	ebioscience (San Diego, CA, USA)
Anti-mouse CD11b	M1/70	APC, APC- eFluor®780	0.1 µL	ebioscience (San Diego, CA, USA)
Anti-mouse CD31 (PECAM-1)	390	APC	0.1 µL	ebioscience (San Diego, CA, USA)
Anti-mouse CD34	RAM34	FITC	0.1 µL	ebioscience (San Diego, CA, USA)
Anti-mouse CD45	30-F11	FITC, PE, PE- Cy5.5. PE- Cy7, eFluor®450, APC, APC- eFluor®780	0.1 µL	ebioscience (San Diego, CA, USA)
Anti-mouse CD45R (B220)	RA3-6B2	PE-Cy7, PE- Cy5.5	0.1 µL	ebioscience (San Diego, CA, USA)
Anti-mouse CD117 (KIT)	2B8	APC, PE	0.1 µL	ebioscience (San Diego, CA, USA)
Anti-mouse CD150	9D1	APC, PE	0.1 µL	ebioscience (San Diego, CA, USA)
Anti-mouse CD166	eBioALC48	PE	0.1 µL	ebioscience (San Diego, CA, USA)

Anti-mouse Gr-1 (Ly-6G)	RB6-8C5	eFlour450®	0.1 µL	ebioscience (San Diego, CA, USA)
Anti-mouse SCA-1	D7	PE, PE-Cy7	0.1 µL	ebioscience (San Diego, CA, USA)
Anti-mouse TER119	TER119	PE, eFlour450®	0.1 µL	ebioscience (San Diego, CA, USA)
Biotinylated anti-mouse CD3e	145-2C11		0.1 µL	ebioscience (San Diego, CA, USA)
Biotinylated anti-mouse CD11b	M1/70		0.1 µL	ebioscience (San Diego, CA, USA)
Biotinylated anti-mouse CD48	HM48-1		0.1 µL	ebioscience (San Diego, CA, USA)
Biotinylated anti-mouse B220	RA3-6B2		0.1 µL	ebioscience (San Diego, CA, USA)
Biotinylated anti-mouse Gr1 (Ly-6G)	RB6-8C5		0.1 µL	ebioscience (San Diego, CA, USA)
Biotinylated anti-mouse TER-119	TER-119		0.1 µL	ebioscience (San Diego, CA, USA)

Table 9. List of used primary antibodies for flow cytometry

2.1.8.1.2 Primary Antibodies for Immunofluorescence

Antigens	Catalog Nr.	Antibody species	Conc.	Company
53BP1	NB100-305	rabbit	1:50	Novus Biologicals (Wiesbaden, DE)
Acetyl-p53	2570	rabbit	1:50	Cell Signaling Techn. (U.S)
AKT	9272s	rabbit	1:100	Cell Signaling Techn. (U.S)

Beta catenin (L54E2)	2677s	mouse	1:100	Cell Signaling Techn. (U.S)
BrdU [Bu1/75 (ICR1)]	ab6326	rat	1:100	Abcam (U.S)
CBP	7389	rabbit	1:50	Cell Signaling Techn. (U.S)
CDC42	07-1466	rabbit	1:100	Upstate/Millipore (U.S)
CDC42-GTP	26905	mouse	1:200	New East (DE)
CDKN1B	610242	mouse	1:100	BD Transduct. Laborat. (U.S)
C/EBPalpha	22959	rabbit	1:50	Cell Signaling Techn. (U.S)
Cyclin D1	2978	rabbit	1:25	Cell Signaling Techn. (U.S)
E2F1 [EPR3818(3)]	ab179445	rabbit	1:100	Abcam (U.S)
ERK1	sc-94	rabbit	1:50	Santa Cruz Biotechnology (U.S)
gamma H2AX	05-636	mouse	1:50	Upstate/Millipore (U.S)
GP-130	Sc-655	mouse	1:100	Santa Cruz Biotechnology (U.S)
GSK-3beta	9315	rabbit	1:100	Cell Signaling Techn. (U.S)
hTGF-beta1	MAB240	mouse	1:100	RnD Systems
Ikk alpha + Ikk beta	ab178870	rabbit	1:100	Abcam (U.S)
Jak2	3230	rabbit	1:100	Cell Signaling Techn. (U.S)
p16INK4a	TA336585	rabbit	1:100	OriGene (U.S)
p27 [Kip1]	610242	rabbit	1:100	BD Pharmingen
p300 CT	05-257	mouse	1:100	Upstate/Millipore (U.S)
p53	2524S	mouse	1:50	Cell Signaling Techn. (U.S)

p53 AC (K379)	2570	rabbit	1:50	Cell Signaling Techn. (U.S)
P-AKT (S473)	4060	rabbit	1:100	Cell Signaling Techn. (U.S)
P-AKT (Thr308)	2965	rabbit	1:100	Cell Signaling Techn. (U.S)
p-Beta Catenin (S33/37/T41)	9561s	rabbit	1:50	Cell Signaling Techn. (U.S)
p-ERK	4377	rabbit	1:100	Cell Signaling Techn. (U.S)
p-GSK-3beta (S9)	5558	rabbit	1:100	Cell Signaling Techn. (U.S)
p-LRP6	2568	rabbit	1:100	Cell Signaling Techn. (U.S)
P-SMAD2 (S465/467)/ PSMAD3 (S423/425)	9510	rabbit	1:100	Cell Signaling Techn. (U.S)
p-STAT3	sc-8059	mouse	1:100	Santa Cruz Biotechnology (U.S)
p-STAT5 (Y694)	9359	rabbit	1:100	Cell Signaling Techn. (U.S)
PTEN	9559	rabbit	1:100	Cell Signaling Techn. (U.S)
RelA	8242T	mouse	1:100	Cell Signaling Techn. (U.S)
RelB	10544S	rabbit	1:100	Cell Signaling Techn. (U.S)
SIRT	ab110304	rabbit	1:100	Abcam (U.S)
STAT3	119352	mouse	1:100	Abcam (U.S)
STAT5	9363	rabbit	1:100	Cell Signaling Techn. (U.S)

TAL-1	12831S	rabbit	1:100	Cell Signaling Techn. (U.S)
TGFBR1/ALK-5	AP0145 7PU-N	rabbit	1:100	OriGene (U.S)
TGF-β Receptor II (D3A1)	11888	rabbit	1:100	Cell Signaling Techn. (U.S)
Ubc13	ab25885	rabbit	1:100	Abcam (U.S)

Table 10. List of used primary antibodies for immunofluorescence

2.1.8.2 Secondary Antibodies

2.1.8.2.1 Secondary Antibodies for flow cytometry

Reagents	Conjugate	Volume/1*10 ⁶ cells	Company
Streptavidin	eFluor450®	0.1 μ L	Invitrogen (Darmstadt, DE)

Table 11. List of used secondary antibodies for FACS

2.1.8.2.2 Secondary Antibodies for Immunofluorescence

Antigens	Catalog Nr.	Antibody species	Flouorochrom	Conc.	Company
Mouse	A10036	Donkey	Alexa-Fluor 546	1:500	Thermo Fisher Scientific Inc. (U.S)
Rabbit	A11010	Goat	Alexa-Fluor 546	1:500	Thermo Fisher Scientific Inc. (U.S)
Mouse	A11001	Goat	Alexa-Fluor 488	1:500	Thermo Fisher Scientific Inc. (U.S)
Rabbit	A32731	Goat	Alexa-Fluor 488	1:500	Thermo Fisher Scientific Inc. (U.S)

Table 12. List of used secondary antibodies for immunofluorescence

2.1.9 Primer

2.1.9.1 PCR Primer

Name	Sequence 5' → 3'
Cre transgen Forward	ATC CGA AAA GAA AAC GT
Cre transgen Reverse	ATC CAG GTT ACG GAT ATA GT
Ccn2 Forward	AAT ACC AAT GCA CTT GCC TGG ATG G
Ccn2 Reverse	GAA ACA GCA ATT ACT ACA ACG GGA GTG G
WT Forward	AAA GTC GCT CTG AGT TTG TAT
WT Reverse	GGA GCG GGA GAA ATG GAT ATG
ROSA Reverse	CCT GAT CCT GGC AAT TTC G

Table 13. List of PCR primers

2.1.9.2 RT-PCR Primer

Name	Sequence 5' → 3'
Ccn2 Forward	GCGAGAGCTGAGCATGTGTCCCTCC
Ccn2 Reverse	ACTTGCCACAAGCTGTCCCT
Gorasp2 Forward	CACTGGGTTCCCTGTACCAC
Gorasp2 Reverse	GATGCGACTCACAGAGACCA
Rpl39 Forward	ATTCCTCCGCCATCGTGCGCG
Rpl39 Reverse	TCCGGATCCACTGAGGAATAGGGCG

Table 14. List of RT-PCR primers

2.1.10 Vectors

Name	Factory
pLKO.1	Open Biosystems, Huntsville, AL, USA
pMD2.G	Open Biosystems, Huntsville, AL, USA
psPax2	Open Biosystems, Huntsville, AL, USA

shCcn2	Open Biosystems, Huntsville, AL, USA
---------------	--------------------------------------

Table 15. List of used vectors

2.1.11 Cell lines

Name	Factory
NIH/3T3	Littlefield, J.W., NIH 3T3 cell line. Science, 1982.
Phoenix™ ecotropic helper-free retroviral producer cells	G Nolan, Stanford, USA
UG26-1B6 pLKO.1	Oostendorp et al. 2002; Renström et al. 2009
UG26-1B6 shCcn2	Istvánffy et al., 2015
UG26-1B6 shSfrp1	Renström et al. 2009

Table 16. List of used cell lines

2.1.12 Mice strains

Name	Factory
C57BL/6.J	Harlan Laboratories, Rossdorf, Germany
BL/6/SJL (Ly5.1)	Taconic Europe, Ry, Denmark
129S2/SvHsd	Harlan Laboratories, Rossdorf, Germany
129xBL/6	Breeding in ZPF: 129S2/SvHsd x C57BL6.J
129xLy5.1	Breeding in ZPF: 129S2/SvHsd x B6/SJL (Ly5.1)
129B6 Sfrp1^{-/-}	Laboratory of Akihiko Shimono (Sato et al. 2006), Breeding in ZPF
C57BL/6.J Sfrp1^{lox/lox}	Breeding in ZPF
B6.Cg-Tg(Sp7-tTA,tetO-EGFP/cre)1Amc/J	Breeding in ZPF
C57BL/6.J Sfrp1^{Δ+}	Breeding in ZPF
C57BL/6.J Sfrp1^{ΔΔ}	Breeding in ZPF

ROSA26-CreER^{T2}	Laboratory of Anton Berns (Hameyer D, et al., 2007) Breeding in ZPF
Ccn2^{fl/fl}	Laboratory of Andrew Leask (Liu S et al., 2013) Breeding in ZPF
ROSA26-CreER^{T2}/Ccn2^{fl/fl}	Laboratory of Yokoi (Toda et al., 2017) Breeding in ZPF

Table 17. List of used mice strains

2.2 Methods

2.2.1 Molecular Biological Methods

2.2.1.1 Genomic DNA Isolation

Genomic DNA (gDNA) isolation was performed using Wizard® Genomic DNA Purification Kit (Table 8). Therefore, tissues were digested in 300 μ L Nuclei Lysis Solution containing Proteinase K (200 μ g/mL, Table 5) and 60 μ L of a 0.5 M Ethylenediaminetetraacetic acid (EDTA, Table 4) solution (pH 8.0) at 55°C with gentle shaking. On the next day, proteins were isolated by adding 300 μ L of Protein Precipitation Solution, following an incubation step on ice for 5 minutes and a centrifugation at 13,000 x *g* for 10 minutes. The supernatant containing deoxyribonucleic acid (DNA) was transferred into a fresh 1.5 mL microcentrifuge tube containing 600 μ L isopropanol, inverted and centrifuged at 13,000 x *g* for 5 minutes. The isopropanol was discarded, and pellets were washed with 600 μ L 70% ethanol and centrifuged at 13,000 x *g* for 5 minutes. Ethanol was carefully aspirated, and the pellets were air-dried for 60 minutes. The DNA was ready to use, after rehydration with 100 μ L DNA Rehydration Solution and an incubation at 65°C for 1 hr.

2.2.1.2 Genotyping Polymerase-Chain-Reactions for *Ccn2* Conditional Mice

For genotyping on the basis of Polymerase-Chain-Reactions (PCR) we used VWR Red Taq DNA Polymerase Master Mix (1.1x Master Mix, 2.2 mM MgCl, Table 8) containing dNTPs, DNA Tag polymerase dimethyl sulfoxide (DMSO) and a loading buffer. The primers used for all PCRs are listed in the Table 13.

Two different PCRs (*Ccn2*, Cre) were performed to determine the genotype of the mice. With the *Ccn2* PCR we distinguished between a floxed and a WT gene. The Cre PCR was used to confirm the harboring of ROSA26-CreER^{T2}. PCRs were prepared according to the following scheme:

	Control (<i>Ccn2</i>^{wt/wt}); <i>Ccn2</i>^{fl/fl}	Cre
Master Mix	18 μ L	18 μ L
Each Primer-F and Primer-R	1 μ L	1 μ L
gDNA	1 μ L	1 μ L
Total volume	20 μ L	20 μ L

Table 18. Content PCR scheme

The PCR was adapted to the annealing temperatures of each primer pair and executed in a PTC 100 Peltier Thermal Cycler (Table 2) with following programs:

	Control (<i>Ccn2</i>^{wt/wt}) and <i>Ccn2</i>^{fl/fl}	Cre
Denaturation	95°C for 5 minutes 94°C for 30 sec	95°C for 7 minutes 94°C for 30 sec
Annealing	65°C for 30 sec	58°C for 45 sec
Extension	72°C for 2 minutes 72°C for 8 minutes	72°C for 1 minutes 72°C for 8 minutes
Hold	4°C forever	4°C forever
Cycles (from step 2-4)	35 x	35 x

Table 19. PCR programs

2.2.1.3 Agarose Gel Reaction

The separation of the PCR product was performed on a 1.5% agarose gel (NaB buffer based) containing ethidium bromide (0.5 µg/mL) in an electrophoresis chamber with NaB buffer (0.01 M disodium tetraborate). Gel electrophoresis was performed at 180V for 45 - 60 minutes. The separated PCR products were then visualized under UV-light on BioRad Gel-Doc XR Imaging System (Table 2).

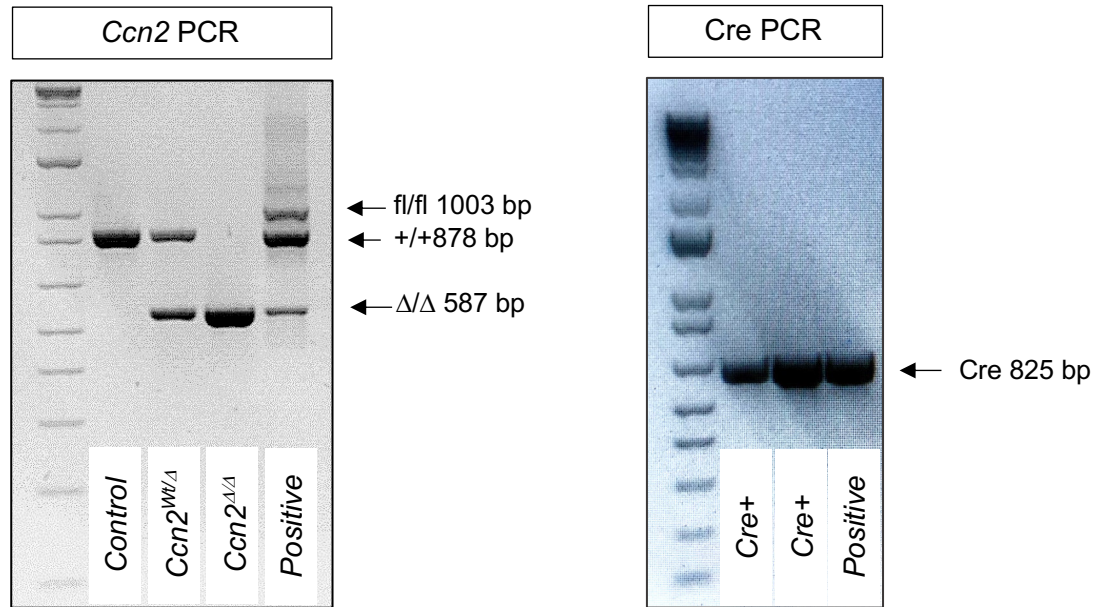


Figure 8. Representative picture for the genotyping of *Ccn2* conditional mice. On the left side the *Ccn2* PCR products with the 878-base pair (bp) DNA fragment of the Control mice, the 878 bp and 587 bp containing DNA fragments of the *Ccn2*^{Wt/Δ} and the deleted DNA fragment with 587 bp from the *Ccn2*^{Δ/Δ} mice. The positive control shows all three amplified DNA fragments, the floxed DNA fragment (*Ccn2*^{fl/fl} without tamoxifen) with 1003 bp, the wildtype (WT) fragments with 878 bp and the deleted *Ccn2* with 587bp. On the right side the Cre PCR product with (825) bp for RosaCre positive mice is shown.

2.2.1.4 Gene Expression Analysis

For the analysis of possible differences in gene expression, a quantitative real time PCR (RT-PCR) was executed. Ribonucleic acid (RNA) isolation was performed depending on the cell number with the RNeasy Mini Kit (Table 8) for cell numbers $> 5 \times 10^5$ and for cell numbers $< 5 \times 10^5$ with the RNeasy Micro Kit (Table 8). The lysis of cells and nuclei membrane was executed by resuspension of the cell pellet in RLT (Mini Kit) or RLT+ buffer (Micro Kit) containing 1% β -mercaptoethanol (Table 4) to reduce RNase activity. Cells were vortexed and furthermore homogenized by a QIAshredder spin column. Binding of the RNA to the silica-based membrane in the RNeasy spin column (Mini Kit) or RNeasy MinElute spin column (Micro Kit) was enhanced by the addition of one volume 70% ethanol (Table 4). Then the column was washed once with 700 μ L RW1 and either two times with 500 μ L RPE buffer (Mini Kit) or one time with 500 μ L RPE buffer and afterwards with 500 μ L 80% ethanol (Micro Kit) to remove contaminations. Total RNA was eluted using either 30 μ L (Mini Kit) or 14 μ L (Micro Kit) nuclease free water. The isolated total RNA using the RNeasy Mini Kit was measured using the NanoDrop (Table 2). The total RNA isolated with the Micro Kit was directly used for reverse transcription.

The RNA was then reverse transcribed into copy DNA (cDNA) following the manufacturer descriptions of the Quanti Tect Reverse Transcription Kit (Table 7).

Genomic DNA (gDNA) elimination:

- 1 μ L gDNA Wipeout Buffer (7x)
 - 1 μ g RNA sample
 - Variable RNase free water
-

14 μ l total volume

Reverse-transcription:

- 1 μ L Quantiscript Reverse Transcriptase
 - 4 μ L Quantiscript RT Buffer (5x)
 - 1 μ L RT Primer Mix
-

6 μ l total volume

Table 20. Genomic DNA elimination and reverse-transcription master mix preparation

To remove gDNA and reverse-transcribe the total RNA into cDNA a master mix was prepared as shown in Table 20.

The gDNA elimination master mix was added to the total RNA and incubated for 2 minutes at 42°C. Then the reverse-transcription master mix was added to each sample and incubated for 15 minutes at 42°C, following an incubation step for 3 minutes at 95°C to inactivate the Quantiscript Reverse Transcriptase.

To quantify the cDNA in order to analyze the expression of a specific gene we used the Power SYBR Green PCR Master Mix (Table 7). The primers used for target genes as well as housekeeping genes are listed in Table 14. Components that were used for RT-PCR are shown in Table 22.

RT-PCR components:

-
- 10 μ L SYBR Green
 - 0.03 ROX (1:50)
 - 0.1 μ L Primer-F
 - 0.1 μ L Primer-R
 - 1 μ L DNA
 - 8.77 μ L H₂O
 - 20 μ l total volume
-

Table 21. RT-PCR pipette scheme

Normalization was performed according to the specific housekeeping gene of different cell populations. For hematopoietic cells we used *Gorasp* and for stromal cells *Rpl39* as housekeeping gene. To compare different RT-PCR plates, we normalized the results to the universal mRNA.

2.2.1.5 Single Cell Gel Electrophoresis Assay (SCGE)/Comet Assay

For the analyzation of possible differences in DNA damage after irradiation of the control and *Ccn2^{Δ/Δ}* mice a Comet Assay was executed as described by the manufacturer instructions of the OxiSelect™ Comet Assay Kit (Table 8).

As a first step the Lysis Buffer, Electrophoresis Running Solution and Alkaline Solution was prepared, the OxiSelect™ Comet Agarose was heated to 90 - 95°C for 20 minutes in a water bath and was cooled down for 20 minutes in a 37°C water bath. Then 75 µL of the Comet Agarose were added on the OxiSelect™ Comet Slide before it was stored horizontally at 4°C for 15 minutes. Freshly sorted 1000 LSK (Lin⁻Sca1⁺Kit⁺) cells were prepared as they were centrifuged for 5 minutes at 500 x *g*, washed with ice - cold 1x PBS and centrifuged again.. The cells, resuspended in 8 µL ice – cold 1x PBS, were then mixed with 72 µL of Comet Agarose, transferred on the top of the earlier prepared Comet Agarose Base Layer and stored horizontally at 4°C for 15 minutes in the dark. Then, the slide was incubated in a basin prefilled with pre-chilled Lysis Buffer for 30 to 60 minutes at 4°C in the dark, before replacing the Lysis Buffer with the Alkaline Solution and storing the slide again for 30 minutes at 4°C in the dark. Alkaline Electrophoresis was performed by prefilling a gel electrophoresis chamber with ice – cold Alkaline Solution, positioning the slide horizontally into the chamber and starting the electrophoresis at 15 V for 15 to 30 min. Afterwards, the slides were three times immersed horizontally into a basin prefilled with deionized (DI) H₂O for 2 minutes. Then the slides were transferred in cold 70% ethanol for a duration of 5 minutes. Before the slides were incubated with 100µL/well Vista Green DNA Dye (1:10,000 diluted in TE buffer), the slide was air - dried to get rid of the remaining ethanol. The visualization of the comet tails (DNA damage) were performed using constant settings on a Leica DM RBE fluorescent microscope (Table 2) with an AxioVision software (Carl Zeiss, Table 3).

2.2.2 Protein Biochemical Methods

2.2.2.1 Immunofluorescence Staining

The fixed and dried stored cells (sorted cells and adherent grown cells) were reactivated by the incubation of 1x PBS for 15 minutes at room temperature (RT). Then, the non-specific binding sites were blocked by 1 hr incubation using blocking buffer (Table 7) followed by the

incubation of the primary antibody (Table 10) diluted in blocking buffer over night at 4°C. On the next day, the slides were washed three times with blocking buffer for 10 minutes at RT and incubated again over night at 4°C with the secondary antibody (Table 10) which was additionally diluted in blocking buffer. Afterwards, the slides were washed two times with blocking buffer and one time with 1x PBS for 10 minutes before the cells were counterstained with SlowFade Gold Antifade Reagent with DAPI (Table 4) and covered with a cover slide (Table 1). 30-40 cells were recorded at 100-fold magnification on a Leica DM RBE fluorescent microscope using an AxioVision software (Carl Zeiss). Then the protein content was analyzed as previously described (Schreck et al., 2017).

2.2.2.2 Cytometric Bead Array (CBA) Assay

For the detection of possible differences in the expression of inflammatory cytokines such as Interleukin-6 (IL-6), Interleukin-10 (IL-10), Monocyte Chemoattractant Protein-1 (MCP-1), Interferon- γ (IFN- γ), Tumor Necrosis Factor (TNF), and Interleukin-12p70 (IL-12p70), we used the BD™ Cytometric Bead Array (CBA) Mouse Inflammation Kit (Table 8). For this assay the mouse inflammation standard was diluted from 1:2 to 1:256. Then, for each single tube (standards and sample tubes) a master mix was prepared containing 3 μ L of each capture bead. The serum samples were thawed on ice and 50 μ L were then added to each sample tube. As a next step, 18 μ L of the PE detection and master mix of the capture beads were added to the sample tubes, following by an incubation at 4°C over night. On the next day, 300 μ L Wash Buffer were added and the samples were centrifuged at 500 x g for 5 minutes. Afterwards, the supernatant was removed by aspiration and the cytokine/bead pellet was resuspended in 300 μ L Wash Buffer. The labeled cytokines were measured using flow cytometry on CyAn ADP Lx P8.

2.2.3 Cell Biological Methods

2.2.3.1 Cell Culture of Adherent Cells

Culturing of adherent cells was performed on 0.1% gelatin - coated cell culture dishes except for mouse embryonic fibroblasts (MEFs). Therefore, the cell culture dishes were covered with 0.1% gelatin and cultured for 30 minutes at 37°C with 5% CO₂. Cells were then cultured on these culture dishes in the appropriated cell culture media at 37°C (except for UG26-1B6 which was cultured at 33°C) with 5% CO₂ until they reached 80% confluence. Then the culture media was removed, and the cells were washed two times with 1x PBS. In a next step, 1x Trypsin was added for 5 to 10 minutes and the trypsin reaction was stopped by 2 volumes of culture media containing fetal calf serum (FCS). The cells were centrifuged for 5 minutes at 500 x g to remove the trypsin/culture media mixture and used for further studies.

2.2.3.1.1 Culture of Cell Lines

Culturing of the cell lines was performed by using the UG26-1B6 (urogenital ridge-derived) cell line between passage 4 to 16 (Table 16) and the NIH/3T3 cell line between passage (Table 16). The deep - frozen cryogenic vials containing cells were thawed for 10 seconds in 37°C water bath. Immediately after the 10 seconds the cells were covered with 5 mL Stroma medium (Table 7) for the UG26-1B6 cell line and with NIH medium (Table 7) for the NIH/3T3 cells to reduce the cell toxic DMSO. Afterwards, the cells were centrifuged for 5 minutes at 500 x g. The cell lines were cultured in appropriated cell culture media (UG26 – Stroma medium Table 7, NIH/3T3 – NIH medium Table 7) with a starting density of 30-40% at 37°C with 5% CO₂.

2.2.3.1.2 Culture of Primary Cells

The isolated mouse embryonic fibroblasts (MEFs; E11.5, E13.5 or E14.5) were isolated and cultured in passage 0 (p0) as described in 2.2.4.2.1. MEF cells were then passaged on a 10 cm² culture dish when visible colonies were grown (4 to 5 days). Then the cells were either live frozen in FCS with 10% DMSO (freezing medium, Table 7) or passaged every 4 to 5 days until they reached passage 3. Afterwards the cells were counted and used for further analysis.

Mesenchymal stem cells (MSCs) were isolated from the bone chips as previously described by Zhu et al., in the year 2010. The culture medium from the cultured bone chips (2.2.4.2.1) was changed three days after culture to remove non - adherent cells. Then, the cells were passaged every 3 to 4 days at 80% confluency. At passage 1, half of the cells were live frozen in freezing medium and the other half was cultured till passage 3. Afterwards, the cells were trypsinized, pelleted by centrifugation, counted and used for further analysis.

2.2.3.1.3 Adherence Assay

To test whether the cells show differences in their ability to adhere to plastic, 1000 MSCs (2.2.3.1.2) were cultured for 1 hr at 37°C with 5% CO₂ on 0.1% gelatin-coated superfrost slide (Table 1). Then the slide was washed three times with 1x PBS and the remaining cells were fixed with 4% paraformaldehyde (PFA) for 10 minutes. The nuclei of the cells were stained using SlowFade Gold Antifade Reagent with DAPI (Table 2) and covered with a cover slide. The number of adherent cells was measured by counting the blue fluorescent nuclei on the Leica DM RBE fluorescent microscope with an AxioVision software (Carl Zeiss).

2.2.3.1.4 Colony-Forming-Unit-Fibroblasts (CFU-Fs)

The ability of MSCs to form CFU-F's was determined by culturing 500 (2.2.3.1.2) cells in one well of a 6 - well plate covered by 2 mL MSC medium.

Three days later, the colonies were fixed using 70% ethanol. 15 min later the ethanol was discarded and the fixed CFU-F's air dried. Then the wells were stained using 0,1% crystal violet solution for a duration of 45-60 min. After washing with distilled water (3x) numbers of colonies were determined under the microscope (Table 1).

2.2.3.1.5 Growth Curve (GC)

For the analyzation of possible differences in cell growth, we cultured 10,000 MSCs (2.2.3.1.2) in a 0.1% gelatin-coated well (6-well plate) with 2 mL MSC medium (Tale 7) at 37°C with 5% CO₂. Every 3 to 4 days when one well of the experiment reached 80 to 90% confluence all cells were detached using 1x Trypsin (Table 4). Cells were counted and again 10,000 cells were cultured. In the case, that the cell numbers was < 10,000 cells per well all the remaining cells were cultured. The growth curve was finished when there were no cells of one genotype left to culture.

2.2.3.1.6 Differentiation Assay

The potential of multipotent lineage differentiation is one of the main characteristics of MSCs. Differentiation into the osteogenic and adipogenic lineage *in vitro* happened either spontaneously or induced by the usage of the Stem Vivo Osteogenic/Adipogenic Base Medium with supplements (Table 6).

2.2.3.1.6.1 Spontaneous differentiation

For the spontaneous differentiation of the MSCs into mature lineages, 1×10^5 were cultured in a 6-well plate with 2 mL MSC medium (Table 7) at 37°C with 5% CO₂. The cells were cultured without passaging until the differentiation was visible. Then the cells were stained for adipogenic and osteogenic differentiation.

2.2.3.1.6.2 Induced Adipogenic differentiation and staining

For induced adipogenic differentiation 10,000 MSCs (2.2.3.1.2) were cultured in a 24-well plate with 1 mL MSC medium at 37°C with 5% CO₂. On the next day the cells were washed three times with 1x PBS and cultured with the Stem Vivo Osteogenic/Adipogenic Base Medium containing supplemented the Adipogenic supplement 1:100 (Table 8) until lipid drops were visible (4 to 7 days).

Oil red staining

Spontaneously adipogenic differentiated cells as well as induced adipogenic differentiated cells were washed with 1x PBS and fixed with 10% PFA at RT for 15 minutes, when multiple lipid vesicles were visible (4 to 7 days after induction). The lipid drops were stained with the liposoluble staining solution Oil Red O (Table 4). Therefore, 0.5 g of Oil Red O was diluted in 100 mL isopropanol and heated at 56°C for 60 minutes. This stock solution was then diluted 3:2 in distilled water and passed through a 45 µm filter (Table 1). The fixed cells were washed two times with 1x PBS and covered with the 60% Oil Red O for 10 minutes at RT. Subsequently, the cells were washed three times with 1x PBS following by microscopically examination of the red stained vesicles. After representative pictures were made, the Oil red O extraction was performed by adding 100 µL 100% isopropanol and measured at 520 nm OD in a multiplate reader (Table 2).

2.2.3.1.6.3 Induced Osteogenic differentiation and staining

Osteogenic spontaneous differentiation was performed by For osteogenic differentiation 7,000 MSCs p3 (2.2.3.1.2) were cultured in a 24-well plate with 1 mL MSC medium at 37°C with 5% CO₂. On the next day, the cells were washed three times with 1x PBS and cultured with the Stem Vivo Osteogenic/Adipogenic Base Medium containing supplemented the Osteogenic supplement 1:20 (Table 8) until a osteogenic differentiation was visible (between two and three weeks).

Alizarin red staining

The osteogenic differentiation was fixed two weeks after induction. Therefore, the cells were washed with 1x PBS and fixed with 10% PFA at RT for 30 minutes. Induced osteogenic differentiated and spontaneously differentiated cells were then washed three times with 1x PBS. The calcium deposition of the cuboidal formic osteogenic differentiated cells was stained covering the cells with 40 mM Alizarin Red (pH=4.2, Table 4) as it binds through a chelation process to Ca²⁺. Staining was performed at RT for 10 minutes with gentle agitation. Subsequently, the cells were washed with 1x PBS, pictures were taken, and the Alizarin Red was destained using 100 µL Destain Solution (Table 7).

2.2.3.1.7 Scratch Assay

The scratch assay was performed by seeding 100,000 MSCs (2.2.3.1.2) per well in a 6-well plate. On the next day a crosswise scratch was generated using a pipette tip. Representative pictures were taken from the artificial cross at the starting point (0 hr) and after 6, 12 and 24

hrs using a microscope. The migration of the cells was then measured via ImageJ software (Table 3).

2.2.3.1.8 Senescence Assay

The analyzation of cellular aging was performed using the Senescence Cell Histochemical Staining Kit (Table 8). Here, we cultured 1×10^4 cells without medium change in a 12-well plate at 37°C with 5% CO₂. After one week the cells were washed three times with 1x PBS before they were fixed for 6 to 7 minutes at RT using the 1x Fixation Buffer. Then the cells were covered with 500 µL staining mixture and incubated overnight at 37°C without CO₂ to ensure a permanent pH = 6. Measurement was performed by taking 10 representative pictures from each well and by counting senescence (blue stained) and non-senescence (not stained) cells.

2.2.3.1.9 Colony-Forming-Unit Assay

The colony-forming-unit assay was executed using the methylcellulose medium supplemented with growth factors (Table 6) as described in the manufacturer's instructions. For the MEF project, the clones grown from the single cell cultures (1/2 plate – 30 wells) were collected and cultured for 10 days at 37°C with 5% CO₂. After the culture the different colony types and numbers were evaluated. Additionally, the cells were harvested with HF2+ buffer and stained for surface markers for flow cytometry analyzation on CyAn ADP Lx P8.

2.2.3.2 Single-Cell Culture

2.2.3.2.1 Generating Conditioned Serum Free Medium

To generate conditioned medium for single-cell cultures, we used the hematopoietic stem cell supportive stromal UG26-1B6 cell line (Oostendorp et al., 2002) or primary MEF cells (Romero Marquez and Hettler et al., 2020).

Therefore, passage 4 of cultured MEF- and passage 12 to 16 of UG26-1B6 cells were immortalized with 30 Gy irradiation (Table 2) at 90% confluence. Then the MEF- and UG26-1B6 cells were washed twice with 1x PBS and covered with 12 mL of the serum free culture medium (BIT 9500 Serum Substitute, Table 6) containing 100 U/mL penicillin, 100 mg/mL streptomycin and 10 mM β-mercaptoethanol. In some experiments 40 µg/mL of low-density lipoprotein (LDL, Table 5) was added to the medium. The MEF cells were incubated at 37°C and the UG26-1B6 at 33°C with 5% CO₂. After three days the conditioned medium was collected and deep frozen in 6 mL aliquots in 15 mL tubes at -20°C until further use.

2.2.3.2.2 Single-Cell Sort and Culture

For single-cell culture we used a 96-well round-bottom plate that was prepared as previously described by (Istvanffy et al. 2015). In brief, single CD34⁻ SLAM cells were sorted into the inner 60 wells containing 100 μ L of the 0.25 nm filtered serum free medium (SFM), either conditioned or freshly used, supplemented with 100 ng/mL mSCF (stem cell factor) and 20 ng/mL IL-11 (Table 5), and in some experiments additionally supplemented with 250 ng/mL NGF (nerve growth factor) and 300 μ g/mL Collagen 1 (Table 5). To prevent a dry out of the CM the surrounding wells were filled with 100 μ L nuclease free water. Immediately after the sort the plate was centrifuged for one second at 300 x g and visually inspected for cells. For the next 5 to 7 days the number of cells was microscopically determined every 24 hrs. Additionally, to the cell numbers, the proliferation and differentiation was studied after 5 to 7 days by a Colony-Forming-Unit Assay (M3434, 2.2.3.1.9) or flow cytometry analysis. In some experiments the self-renewal potential was studied by transplantation of 20 cells/mouse into lethally irradiated mice.

2.2.3.3 Flow Cytometry Analyzation

2.2.3.3.1 Preparation for Cell Sort – Lineage Depletion

Lineage depletion from the flushed bone marrow (BM) was performed according to the manufacturer's recommendations of Lineage cell depletion Kit (Table 8). The separation of mature and primitive hematopoietic cell populations is based on a biotinylated monoclonal antibody cocktail binding the mature cell population (lineage positive cell population). Therefore, the BM cells were incubated with the Biotin-Antibody-Cocktail for 10 minutes at 4°C. Then, the lineage positive cells were secondary labeled with an anti-biotin magnetic antibody (MicroBeads) for 10 minutes at 4°C. Separation was performed using a MACS Separator (Table 1). Therefore, a MACS Column was placed in the MACS Separator that produces a magnetic field in which the non-labeled lineage negative cell population could pass through the column. In order to obtain the labeled lineage positive cell population, the cells have to be outside the magnetic field.

2.2.3.3.2 Flow Cytometry Staining

For fluorescence associated cell sorting (FACS) analysis the cell surface markers were stained in 100 μ L HF2+ buffer containing fluorescence associated antibodies (Table 9). The study of hematopoietic cells was performed in the peripheral blood (PB), bone marrow (BM) and spleen (SP). The composition of the hematopoietic mature cells was analyzed in the BM and SP using 2×10^6 and for the more primitive cell populations we stained 5×10^6 cells. The

whole cell pellet from the PB as well as lineage depleted BM or stromal cells were used for analyzations. Staining of the cells was performed on ice for 1 hr. Afterwards, the cells were washed with 2 mL HF2+ buffer and centrifuged at 500 x g for 5 minutes. The cell pellet was resuspended in 500 µL of HF2+ buffer with 1 µg/mL Propidium-Jodid (PI) and studied on a CyAn ADP Lx P8.

2.2.3.3.3 Apoptosis Assay

The study of potential differences in cell death due to extrinsic cell conditions was determined by the apoptosis assay. Therefore, 3000 sorted LSK cells were cultured in control medium (UG26-1B6 pLKO.1 or SFM 4GF) and conditioned medium from UG26-1B6 (sh*Ccn2*) or from MEF cells (2GF or 4GF) in a 12-well plate at 37°C with 5% CO₂. After 48 hrs the cells were harvested and the wells were washed three times with 2 mL HF2+ buffer following a centrifugation step for 5 minutes at 500 x g. Staining of the samples was performed by adding 500 µL Annexin Buffer (Table 8) with 0.1 µg/mL PI and 2 µL AnnexinV-FITC for 15 minutes at 4°C following the analyzation by flow cytometry on a CyAn ADP Lx P8.

2.2.4 Animal Experimental Techniques

2.2.4.1 *In vivo* Techniques

2.2.4.1.1 Mice Strains

The *in vivo* experiments were performed with ROSA26-ERT2CRE/flox*Ccn2* mice (*Ccn2*^{Wt/Δ}, and *Ccn2*^{Δ/Δ}). As controls we used age- and sex- matched ROSA26-ERT2CRE positive (*Ccn2*^{Wt/Wt} or Control) littermates in all experiments. Adult mice (eight to ten weeks) were injected intraperitoneally (i.p.) for 3 to 4 days with 0.2 mg/g body weight (BW) tamoxifen (in ethanol and diluted in peanut oil, Sigma Aldrich Table 4) to generate ROSA26-ERT2CRE/*Ccn2* mice (*Ccn2*^{Wt/Wt} or control, *Ccn2*^{Wt/Δ}, and *Ccn2*^{Δ/Δ}).

In the transplantation experiments, the F1 crosses of 129S2/SvPasCrl (129; CD45.2) and either B6.SJL-Ptprca Pepcb/BoyJCrI (Ly5.1; CD45.1) or C57BL/B6.JCrI (B6; CD45.2) were used as donor or recipients in extrinsic or intrinsic transplantation assays. All these mice were received from Charles River Laboratories. All animal studies were approved by the section Consumer Protection, Veterinary Services, and Food Hygiene of the Government of Upper Bavaria (Regierung Oberbayern, Munich, Germany). Before the experiments, the mice were housed for at least a week in micro-isolators under specific pathogen-free conditions at the Centre of Preclinical Research (TranslaTUM, Munich), according to the Federation of Laboratory Animal Science Associations and institutional recommendations.

For the generation of mouse embryonic fibroblast (MEFs) C57Bl/6J CR and ROSA26-ERT2CRE/flox*Ccn2* (*Ccn2*^{Wt/Wt} or control *Ccn2*^{Δ/Δ} littermates; Toda et al., 2013) mice were used.

2.2.4.1.2 *In vivo* Transplantation Assay

The transplantation assay, also called repopulation assay, was performed *in vivo* using a competitive transplantation of fresh and cultured (single cell culture) CD34⁺SLAM or LSK cells into lethally irradiated recipient mice. For the transplantation assays, we used the CD45 congenic system (CD45.1 and CD45.2) in order to differ between donor and recipient cells as previously described (Renström and Istvánffy et al., 2009; Schreck et al., 2017).

For the transplantation of fresh and cultured donor cells, we either sorted 300 CD34⁺SLAM (LT-HSCs) cells 1500 LSKs or 250,000 whole BM cells. In the single cell culture experiments we transplanted 20 clones/mouse after 5 days of culture. The donor cells were pelleted and resuspended in 100 μL HF2+ buffer together with 100.000 BM and 500.000 Spleen cells/mouse as helper cells of 129xB6 mice. We used eight to ten-week-old lethally irradiated recipient mice (8.5 Gy) for transplantation of donor cells via intravenous injection in the tail vein (i.v.). Via subcutaneous (s.c) injection the transplanted mice received 8 mg/kg bodyweight of the antibiotic Convenia® (80 mg/ml, Zoetis). Additionally, they received 1 mg/ml Borgal® solution (24%, Virbac) for a duration of three weeks in the drinking water.

At 5 and 10 weeks after transplantation the PB was collected in a EDTA coated tube from the facial vein and analyzed for the efficiency of the engraftment by flow cytometry. 16 weeks after transplantation the mice were sacrificed and the BM, SP and PB hematopoietic cells were collected for the analysis by flow cytometry. An efficient engraftment was detected at ≥ 1% lymphoid and ≥ 1% myeloid donor cell engraftment in the PB.

2.2.4.1.3 *In vivo* Irradiation Assay

The study of possible differences in cell regeneration without *Ccn2* were executed using a general deletion of hematopoietic and stromal cells upon sublethal irradiation (4.5 Gy, Table 2). At the age of eight-till twelve-weeks control and *Ccn2*^{Δ/Δ} mice were irradiated using g-irradiation (4.5 Gy). Depending on the experiment, the mice were sacrificed 2, 5, or 14 days after irradiation to analyze the effect of *Ccn2* in hematopoietic and stromal cells during irradiation stress and regenerative stress response. The hematopoietic organs and stromal cells were isolated as described earlier in 2.2.5.

2.2.4.1.4 *In vivo* Lipopolysachharide (LPS) Assay

To analyze the reaction of the hematopoietic cells in their ability to defense against pathogens the *in vivo* lipopolysachharide (LPS, Table 5) assay was executed. Eight- till twelve-weeks old control and *Ccn2*^{Δ/Δ} mice were intraperitoneal (i.p) injected with 1 μg LPS. 24 hrs after injection the PB, BM, SP and stromal niche cells were isolated and prepared for flow cytometry staining as described in 2.2.5.

2.2.4.1.5 BrdU Incorporation Assay

Cell cycle analyzation of the hematopoietic cells was performed using the BrdU Bromodeoxyuridine (5-bromo-2'-deoxyuridine, Table 8) incorporation assay. Therefore, the mice were sublethal irradiated (4.5 Gy) and 4 days later intraperitoneally (i.p.) injected with 1 mg BrdU diluted in HF2+ buffer. One day later the BM cells were flushed from the femur and tibia. Staining of the appropriate surface markers was executed prior to BrdU staining. The labeling of BrdU with an anti-BrdU antibody was performed following the manufacturer instructions before the cells were analyzed by flow cytometry.

2.2.4.2 *Ex vivo* Techniques

2.2.4.2.1 Preparation of Tissue Samples

To analyze the impact of *Ccn2* in hematopoiesis and stromal cells we isolated the mouse embryonic fibroblast (MEFs), peripheral blood (PB), spleen (Sp), bone marrow (BM) and stromal niche cells.

For the generation of MEF cells adult mice were mated in the late afternoon. The embryonic day 0 (E0) was determined when a vaginal plug was visible at the female mice in the early morning.

Depending on the project, the female mice were sacrificed with isoflurane and cervical dislocation 11.5 and 13.5 (MEF project) or 14.5 (*Ccn2* project) days after appearance of the vaginal plug. The uteri were isolated and washed in HF2+ buffer (Table 7). Then the embryos were separated from the uteri and dissection needles were used to separate the head from the body. The red organs (AGM region, heart and liver) were removed and the remaining embryo was chopped up with dissection needles and plated in a 10 cm² cell culture dish covered in 12 mL MEF culture medium (table 7) and cultured at 37°C with 5% CO₂.

Eight till twelve-week-old mice were sacrificed with isoflurane (isolation of PB) following a cervical dislocation (when no PB was collected).

The PB was either collected from the facial vein or directly from the heart with Hamilton Syringe (Table 1) and stored in EDTA-coated vials (Table 1). Analyzation of the PB cell composition was performed using the animal blood counter Counter Scil Vet Abc™ (Table 2). In some experiments the blood serum was isolated by a centrifugation step for 10 minutes at 2000 x *g* at 4°C. The supernatant, containing the serum, was collected into 1.5 mL tube. The serum was immediately stored at -80°C until further use. The remaining cells were treated with 5 mL Ammonium-Chloride-Potassium (ACK) lysing buffer (Table 6) for 15 minutes on ice to get rid of the erythrocytes. Samples were washed with 5 mL HF2+ buffer and centrifuged at 500 x *g* at 4°C. Cell pellet was resuspended in HF2+ buffer following the staining of the surface markers and analyzation by fluorescence-activated cell sorting (FACS).

For the analyzation of the SP cell composition, the SP was isolated and placed in a sterile 100 µm cell strainer and squeezed. Then the cell strainer was washed with 10 mL HF2+ buffer in order to gain the number of cells. The cell suspension was homogenized by resuspension. Cells were then filtered through a 30 µm filter and used for analysis.

The BM cells were obtained from the femurs and tibias of the hind legs by flushing out with HF2+ buffer. BM flush out was resuspended to homogenize the suspension and passed through a 30 µm filter, centrifuged at 500 x *g* for 5 minutes and used for analysis.

Stromal niche cells were isolated as previously described by Zhu et al., in the year 2010. Therefore, the flushed bones were crushed with mortar and pestle and the bone chips were incubated with 2 mL collagenase digestion medium (Table 7) for 1.5 hrs at 37°C. After the endosteal stromal cells were released from the bone chips the medium was aspirated, the bones were washed several times with HF2+ buffer and the suspension were passed through a 30 µm filter. Afterwards, the endosteal cells were centrifuged at 500 x *g* for 5 minutes and stained with appropriate surface marker antibodies for flow cytometry or sort analysis. The remaining bone chips were washed with HF2+ buffer and cultured with MSC medium at 37°C with 5% CO₂.

2.2.5 Statistical Analysis

Statistical analysis was executed using Mann-Whitney U test or unpaired and paired Student's t-test (Prism, GraphPad Software, Table 3). The *p* value ≤ 0.05 was set as the level significance. All data are presented as the mean ± standard deviation.

3 Results

3.1 Establishment of a new single stem cell culture method using conditioned medium of mouse embryonic fibroblasts

The study of hematopoietic stem cells (HSCs) at clonal resolution is a prerequisite for allowing statements of stem cells. Clonal serum-free cultures of human HSCs had been described previously (Zandstra et al., 1997). Cultures with murine HSCs were not as efficient, and a large proportion of dead cells could be noted at relatively low Kitl levels (Nakauchi et al., 2001, Lecault et al., 2011). It was also shown that the urogenital ridge-derived (UG) 26-1B6 cell clone supports the maintenance of repopulating HSCs, not only in cocultures for four weeks (Oostendorp 2002a, 2002b), but also under non-contact conditions (Oostendorp et al., 2005, Buckley et al., 2011). Wohrer and coworkers combined these findings to show that serum-free conditioned medium (CM) of UG26-1B6 cells highly efficiently supports repopulating HSCs together with low levels of Kit and IL-11 (Wohrer et al., 2014). They also described that the addition of two other cytokines: nerve growth factor (NGF), and collagen 1 (Col1) could substitute for the CM of UG26-1B6 in the capability of maintaining the stem cell status and survival of the cells *in vitro* (Wohrer et al., 2014).

Since UG26-1B6 cells are not transformed completely and change over time (Oostendorp et al., 2002b), we searched for alternative sources of CM to support HSC maintenance in stroma-free cultures. We here describe a single-cell culture assay with new conditions in which we used the CM of mouse embryonic fibroblasts (MEFs), which can be isolated freshly from embryos. To determine the potential of the MEF-CM to maintain HSCs we decided to test MEF-CM with either 2GF (SCF and IL-11) or 4GF (additionally NGF and Col1).

First, we performed single-cell culture assays with CD34⁻ SLAM cells (CD34⁻CD48⁻CD150⁺Lineage⁻SCA1⁺KIT⁺) from 129xLy5.1 mice in the serum-free (SFM 2GF and 4GF) or serum-free conditioned media from MEFs conditions (MEF-CM 2GF, and MEF-CM 4GF). The clone size of each well and each condition was monitored each day for a duration of five days. Then, the clones (>2cells/well) were harvested and differentiation, HSC maintenance as well as self-renewal potential of the clones was analyzed using different assays such as flow cytometry, colony forming unit assay (M3434) or transplantation assays (Figure 9A).

Similar to our previous study (Wohrer et al., 2014), we found that the addition of NGF and Col1 to SFM with 2GF increased the number of wells with dividing cells compared to the culture with 2GF alone (84% vs. 67%; Supplementary Figure 1A). However, in comparison to Wohrer et al., a lower survival was detectable (Supplementary Figure 1A, Wohrer et al., 2014). From this

result, we hypothesized that under different culture conditions, NGF and Col1 may not completely substitute for UG26-CM 2GFs and additional stromal factors may contribute or synergize in the survival and cell cycle recruitment of HSCs. Thus, there is a need to further define stromal cell factors substituting CM in HSC cultures. Since additional sources of CM will be needed to optimally define factors maintaining HSC self-renewal, we chose to study a robust, non-transformed source of mid-gestation embryonic stromal cells: mouse embryonic fibroblasts (MEFs).

In order to find the best culture condition to maintain HSCs with MEF-CM *in vitro* we first tested a series of different culture conditions with different methods of isolating and storing the MEF cells as well as different culture supplements. In general, MEF cells are isolated for experimental analysis at gestation day E13.5. However, as the UG26-1B6 cell lines were generated from gestational day E11.5 we also tested CM from MEFs isolated at gestation day E11.5. Interestingly, the CM from MEFs E13.5 showed similar numbers in dividing clones in comparison to the CM from E11.5 MEFs (Supplementary Figure 1A.). As E13-14 embryos are generally used for the support of embryonic stem cells (McElroy et al., 2008) and the isolation of MEFs from E13.5 results in a higher yield of cells than E11.5, we decided to use the MEF-CM at gestation day E13.5 for analyses of the HSCs and optimizations of the single-cell culture assay. The aim of the next experiment was to assess the robustness of different individual MEF-CM in their potential to maintain HSCs. For this purpose, we generated MEF-CM from seven individual embryos at gestation day E13.5 and compared the individual variation with the variation among single cell cultures with SFM and 4GF (Supplementary Figure 1B). After 4 and 5 days of culture we found no gross growth kinetics among the individual generated MEF-CM with 4GF (Supplementary Figure 1B). Furthermore, we aimed to study the possibility to freeze the MEF cells prior to generate the MEF-CM, eliminating the need to always work with freshly isolated MEF-CM. For this purpose, we generated E13.5 MEFs and froze one half of the cells at p1 and used the other half at p4 for fresh MEF-CM. Then the CM from the previously frozen MEFs (same animal) at p4 was prepared. A single-cell culture assay was performed with the fresh and frozen MEF-CM. Comparing both conditions, we did not find any differences in the potential to stimulate cell cycle recruitment or proliferation when the p4 MEF cells were frozen or used fresh (Supplementary Figure 2A). We also tested whether the CD34⁺SLAM cells from different mouse strains frequently used in the lab behave similar in our experiments. Therefore, we used the HSCs from B16 mice and compared them with HSCs isolated from 129xLy5.1 mice and found no differences in cell division, proliferation, or survival of these cells (Supplementary Figure 2B).

In experiments designed to compare single cell cultures in either MEF-CM or -4GF with serum-free conditions, we found a significant increased mean clone size in the MEF-CM (both 2GF and 4GF) compared to the SFM with 4GF which indicate an increased potential of the MEF-CM to stimulate the cell-cycle and survival. In order to test this further, we analyzed the recruitment of cells into cell cycle by investigating the number of wells with more than two cells at each time point. Indeed, in the SFM with 4GF compared to the MEF-CM (2 and 4GF) the cells revealed a longer time to first cell division as shown by the wells with >2 cells (Figure 9E) and by the calculation of the time to first cell division (Figure 9F). Unexpectedly, there were no differences found in the clone size or the enter in the cell cycle between MEF-CM with 2 or 4GF (Figure 9E, F, G).

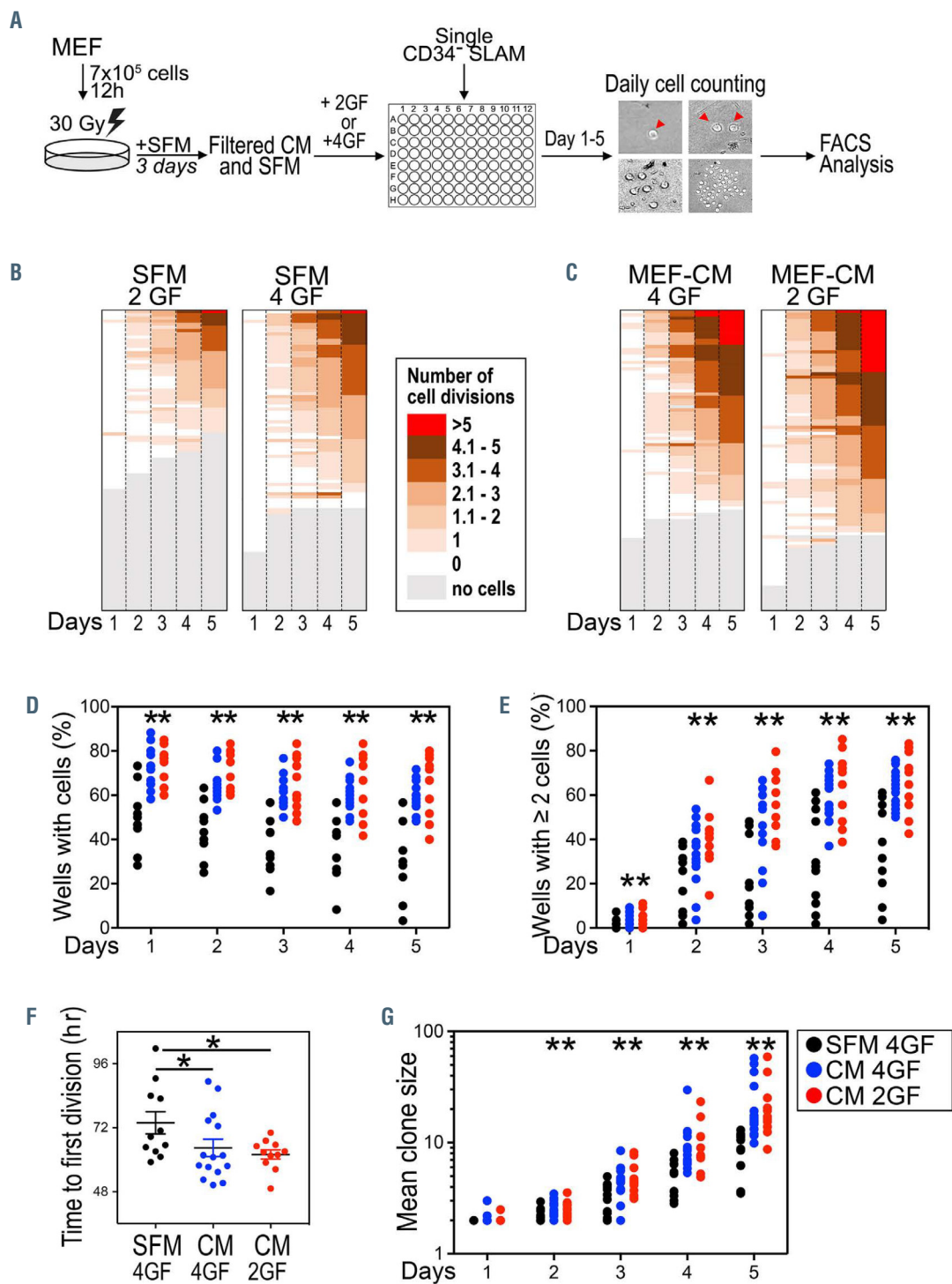


Figure 9. Single-cell cultures in SFM and MEF conditioned medium with 2GF and 4GF. (A) Experimental design: Generation of conditioned medium by irradiation of $7 \times 10^5 / 10 \text{ cm}^2$ MEF cells and incubating the SFM for three days. 96-round-bottomed plates were pre-filled with SFM and MEF-CM, containing either mSCF and IL-11 alone (2GFs) or additional NGF and Col1 (4GFs). Single CD34-SLAM cells of 129xLy5.1 mice were sorted into each well and microscopically inspected for the presence of cells. For a duration of five days the colony size was counted every 24 hrs. After five days the clones

(≥ 2 cells/well) were harvested and either analyzed per flow cytometry or transplanted into 129xB16 mice. (B) Representative heat maps for the number of cell divisions for each CD34⁻ SLAM cell at each day of culture (first heat map culture in SFM with 2GF, second heat map shows the culture in SFM with 4GF). (C) Representative heat maps for the number of cell divisions for each CD34⁻ SLAM cell at each day of culture (first heat map culture in MEF-CM with 4GF, second heat map shows the culture in MEF-CM with 2GF). (D) Wells with cells over five days. Each dot represents the mean of the wells with cells of a 96-well plate with different conditions. (E) Wells with ≥ 2 cells in percentage for each day. Each dot represents the mean of divided cells of a 96-well plate with different conditions (SFM with 4GFs, MEF-CM 4GFs and MEF-CM 2GFs). (F) Calculated time to first division of cells cultured in SFM with 4GF, MEF-CM with 4 and 2GF. (G) Counted mean of clone size over 5 days. Each dot represents the mean clone size of a 96-well plate with different conditions (SFM with 4GFs, MEF-CM 4GFs and MEF-CM 2GFs). B and C show a representative example of two 96-well plates for each condition. D, E, F and G show SFM in black dots, MEF-CM with 4GF in blue dots and MEF-CM with 2GF in red dots. D, E, F and G show SFM in black dots, MEF-CM with 4GF in blue dots and MEF-CM with 2GF in red dots. Figures D, E, F and G show five independently performed experiments with different donor mice: $n = 11$ for SFM 4GFs, $n = 15$ for MEF-CM 4GFs, and $n = 11$ for MEF-CM 2GFs; * p -value ≤ 0.05 show significance in the comparison of SFM and MEF-CM (2GF and 4GF) using the Mann-Whitney U-test (Romero Marquez and Hettler et al., 2020).

The cause of the difference in the cell number/well or time to first cell division between SFM with 4GF and MEF-CM (2 and 4GF) is not entirely clear. We only monitor cell number, which relies on the balance between cell death (loss of cells) and proliferation (increase in cell number). Thus, reduced cell numbers are not necessarily caused by reduced proliferation but could also be caused by increased cell death. This hypothesis is supported by the decreased numbers of wells with cells between SFM with 4GF and the MEF-CM (2 and 4GF). As for the cell numbers, both MEF-CM with 2 or 4GF supported increases in cell number in a similar manner (Figure 9G). To test the rates of cell death between the different culture conditions, Lineage⁻SCA1⁺KIT⁺(LSK) cells were cultured for 48 hours and survival was determined using an apoptosis assay (Annexin V staining). The flow cytometric analysis of cell survival using the apoptosis assay showed a reduced potential of SFM with 4GF to maintain the survival of LSK cells in culture compared to MEF-CM with 2GF but not with 4GF (Figure 10A).

Besides the survival and cell cycle progression of the cells cultured in the different conditioned media, it was of interest whether the different conditions may increase the self-renewal or the differentiation potential of the HSCs into the different lineages. To answer these questions, we performed different analyses. For all further experiment's wells with cells of ≥ 2 were harvested on day five. The flow cytometric study of differentiation potential or LSK retention revealed no gross differences of all three media in the potential of cells to differentiate into Gr1⁺CD11b⁺

and Gr1^{med}CD11b⁺ cells (Figure 10D). Interestingly, only the MEF-CM with 2GF maintained the LSK phenotype significantly compared to the SFM with 4GF and additionally to the MEF-CM with 4GF as shown in Figure 10F. As expected, the increased LSK numbers of cells cultured in MEF-CM with 2GF resulted in a significantly increased potential of cells to form myeloid colonies in a semi-solid medium (Figure 10G). The increased numbers of LSK cells and the potential to form more colonies in the semi-solid medium from the cells cultured in MEF-CM with 2GF, indicates that this culture condition is appropriate in the maintenance of the progenitor function and the stem cell phenotype *in vitro*.

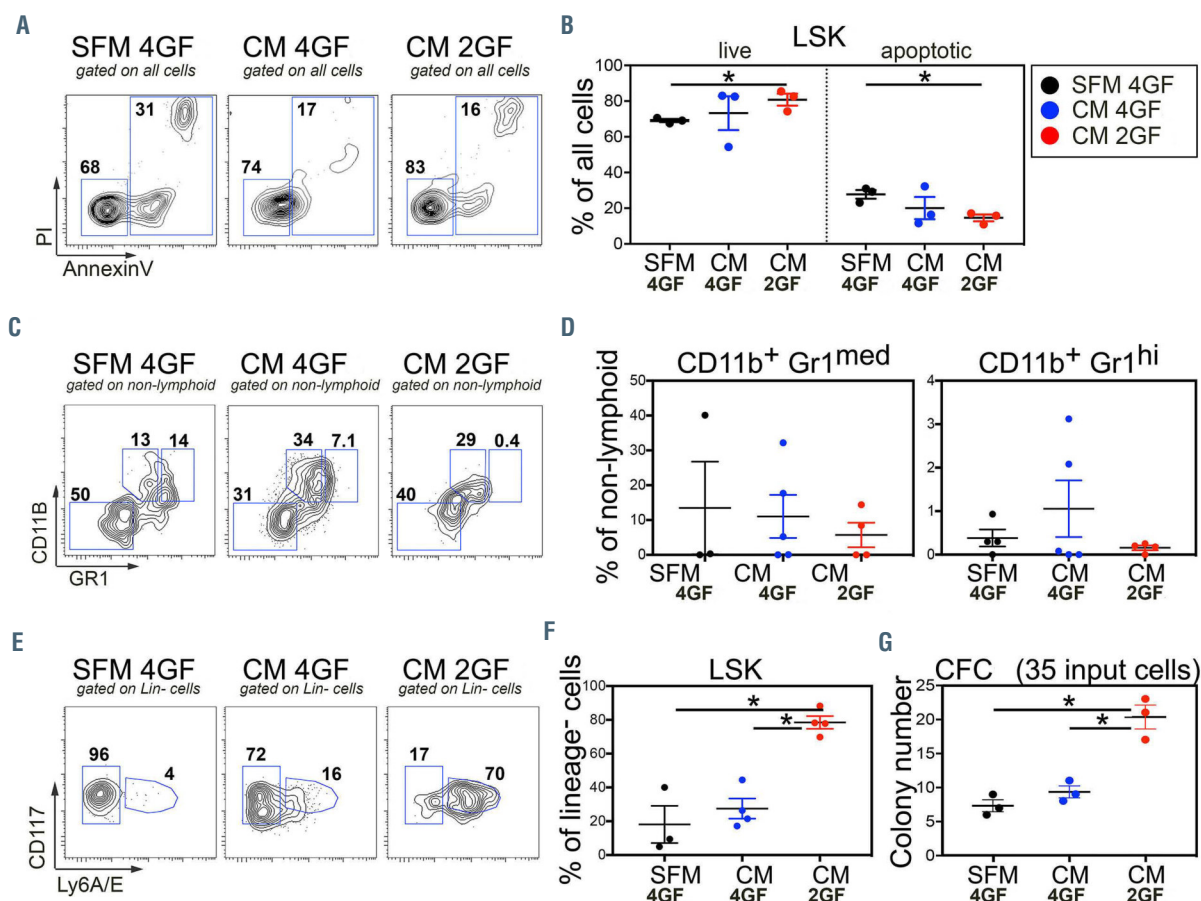


Figure 10. Flow cytometry analysis of bulk cultured LSK cells and single cell cultured CD34-SLAM cells. (A) Representative flow cytometry plots of Annexin V positive LSK cells after 48 hours culture in SFM, MEF-CM with 4 and 2GF. (B) Analysis of Annexin V FACS in percentage of life cells and Annexin V positive cells. (C) Representative flow cytometry plots of Gr1^{med}CD11b⁺ and Gr1⁺CD11b⁺ cells. (D) Dot plots in percentage of pooled single cell cultured CD34⁻ SLAM cells differentiated into Gr1^{med}CD11b⁺ and Gr1⁺CD11b⁺ after five days of culture in different media (SFM, MEF-CM with 4 or 2 GF). (E) Representative flow cytometry plots of LSK cells maintained from pooled single cell cultured CD34⁻ SLAM cells after five days of culture in different media (SFM, MEF-CM with 4

or 2 GF). (F) Dot plots in percentage of LSK cells after five days of culture in different media (SFM, MEF-CM with 4 or 2 GF). (G) Dot plots of CFU from five days of cultured (SFM, MEF-CM with 4 or 2 GF) 35 input cells. B, D, E, F and G show SFM in black dots, MEF-CM with 4GF in blue dots and MEF-CM with 2GF in red dots. All figures show three independently performed experiments within A and B n=3 and n=4 for each condition and C-F n = 3-5 plates per condition. * p-value ≤ 0.05 show significance in the comparison of SFM and MEF-CM using the Mann-Whitney U-test (Romero Marquez and Hettler et al., 2020).

The most important question was if the different culture conditions would support the self-renewal potential of the repopulating HSCs. Therefore, we transplanted 20 clones with only divided cells (≥ 2 cells/well, at day 5) into lethally irradiated recipient mice and analyzed the engraftment of the cells after five, ten and 16 weeks in the peripheral blood (Figure 11B). In accordance with the number of LSK cells and the potential to form colonies (Figure 10F and G) the engraftment in the PB of the HSCs cultured in MEF-CM with 2GF was the highest among all three conditions. Especially five weeks after transplantation MEF-CM 2GF cells show prominent engraftment. At later timepoints, stable high engraftment of cells cultured in MEF-CM 2GF was detectable in the peripheral blood (Figure 11B). Lymphoid engraftment was similar in transplanted cells from cultures with both MEF-CM 2GF and 4GF (Figure 11C). The higher levels of engraftment are mostly due to an enhanced myeloid engraftment, which was not so prominent in transplantations with cells from MEF-CM 4GF cultures (Figure 11D). Additionally, we found the highest BM engraftment in the group of MEF-CM with 2GF (Figure 11E) and significant more CD34⁻CD48⁻ LSK cells compared to the SFM 4GF group (Figure 11G). Interestingly, both MEF-CM 2GF and 4GF groups showed a higher engraftment and self-renewal capacity of CD34⁻SLAM cells in culture than the SFM with 4GF (Figure 11G) with a higher total number of HSCs recovered from animals transplanted with cells from MEF-CM 2GF cultures (Figure 11G).

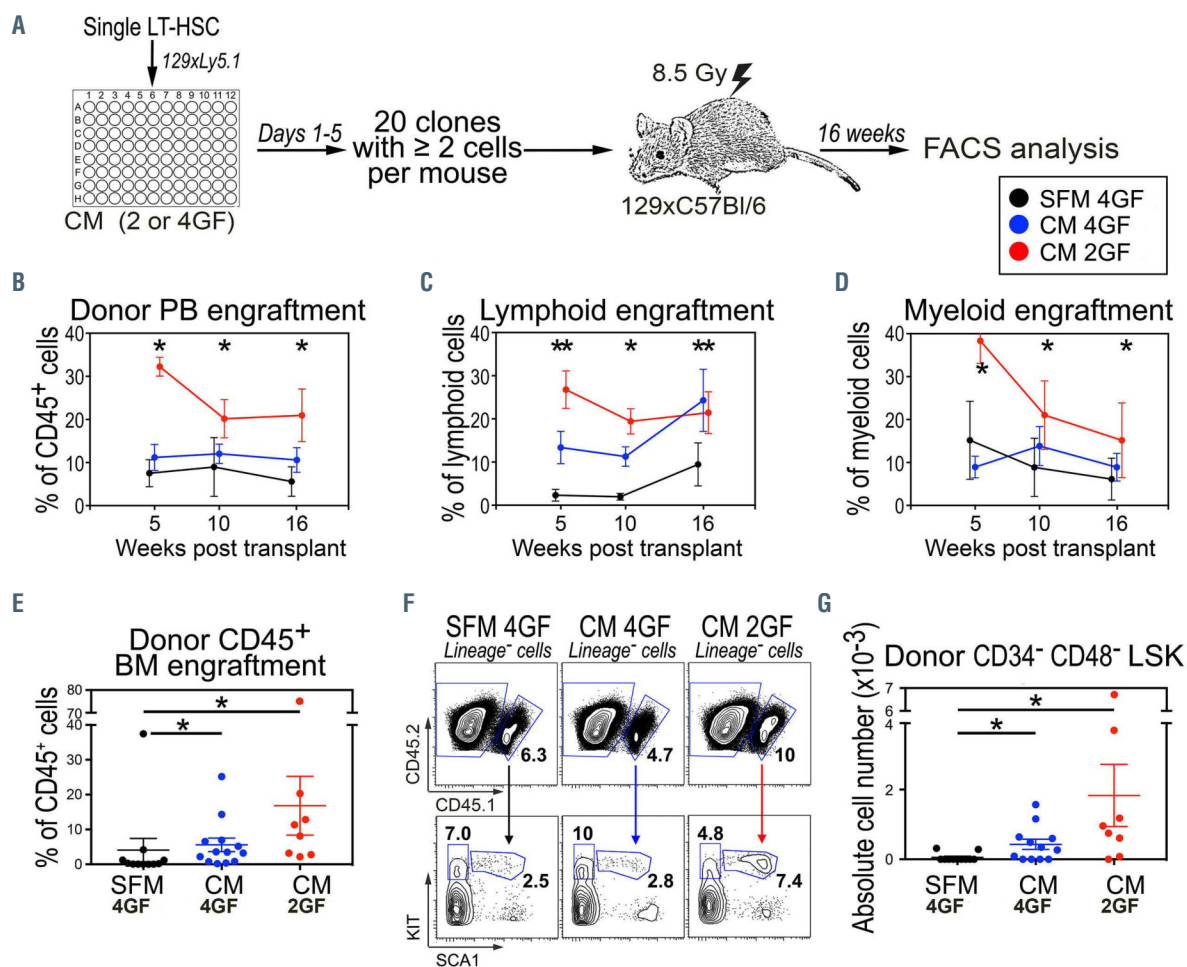


Figure 11. Transplantation experiment for self-renewal maintenance capacity of the different conditions. (A) Experimental design: Single-cell cultured 129xLy5.1 (CD45.1/CD45.2 double positive) CD34⁻ SLAM cells (cultured in SFM with 2GF and MEF-CM with 4 and 2GF) were harvested after five days, pooled and 20 clones from cells ≥ 2 clones were transplanted into lethally irradiated 129xB16 (CD45.2 positive) mice. 16 weeks after transplantation the mice were sacrificed, and the hematopoietic cell composition was analyzed using flow cytometry. (B) PB donor cell engraftment after five, ten and 16 weeks of Tx. (C) Percentage of lymphoid and (D) myeloid engraftment in the PB after five, ten and 16 weeks of Tx. (E) Percentage of donor CD45⁺ cell engraftment in the BM 16 weeks after Tx. (F) Representative gating strategy of LSK cells in the BM from transplanted cells of the different conditions (SFM 4GF, MEF-CM 4GF and MEF-CM 2GF). (G) Absolute numbers of donor CD34⁻ CD48⁻ LSK cells in the BM 16 weeks after Tx. B, C, D, E and G show SFM with 4GF in black dots, MEF-CM with 4GF in blue dots and MEF-CM with 2GF in red dots. Data shows a total of n=11 mice for SFM with 4GF n=13 for MEF-CM with 4GF and n=8 for MEF-CM with 2GF. * p-value ≤ 0.05 show significance in the comparison of SFM and MEF-CM using the Mann-Whitney U-test (Romero Marquez and Hettler et al., 2020).

3.2 Ccn2 during steady state and stress condition

3.2.1 Verification of an efficient Ccn2 knockout

To assess the importance of *Ccn2* expression for *in vitro* and *in vivo* hematopoiesis, we studied this issue in knockout models. However, the *Ccn2* knockout mice die immediately after birth due to a malformation of the skeleton (Ivkovic et al., 2003). Therefore, we used the tamoxifen-inducible Rosa26-CreER^{T2}; *Ccn2*^{fl^{ox}} mice to determine the function of *Ccn2* expression in hematopoiesis. In order to study *Ccn2* in young adult mice, we induced the *Ccn2* deletion at eight week old mice with 4x intraperitoneal tamoxifen (TAM) treatment (*Ccn2*^{Δ/Δ} mice) and confirmed successful deletion of exon 4 of the loxp-flanked *Ccn2* gene in different tissues two weeks after treatment (Figure 12). In all experiments we used the tamoxifen treated Rosa26-CreER^{T2} positive *Ccn2*^{wt/wt} mice as controls.

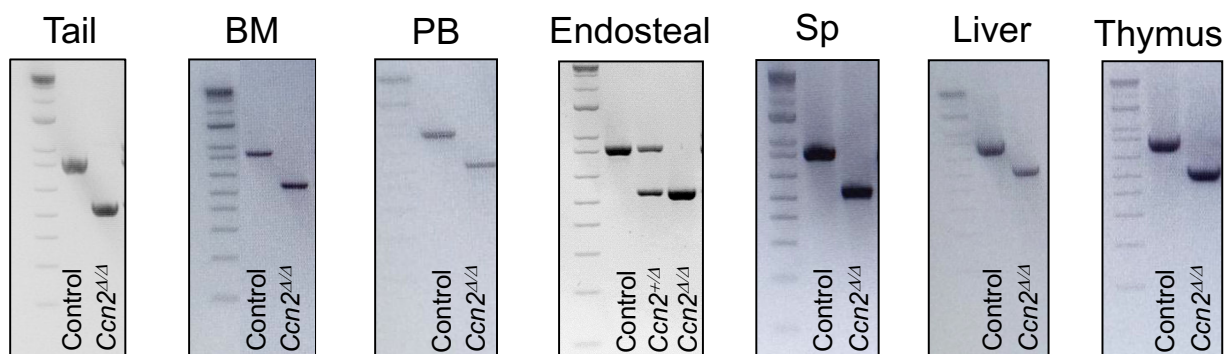


Figure 12. Verification of efficient knockout using PCR in different tissues. Tissues were isolated two weeks after intraperitoneal (i.p.) TAM treatment. PCR products from amplified *Ccn2* DNA fragments from the tail, bone marrow (BM), peripheral blood (PB) and endosteal cells, spleen (Sp), liver and thymus PCR products from amplified *Ccn2* DNA fragments.

The verification of an efficient knockout was additionally performed in a cell population known to be the putative source for *Ccn2* expression in the bone marrow niche, the mesenchymal stem and progenitor cells (MSCs) on *mRNA* level. The MSCs were grown out of the bone fragments from control and *Ccn2*^{Δ/Δ} mice and used for analysis at passage 4 (Figure 13A). In Figure 13B the efficient confirmation of the *Ccn2* knockout in cultured mesenchymal stem cells is shown.

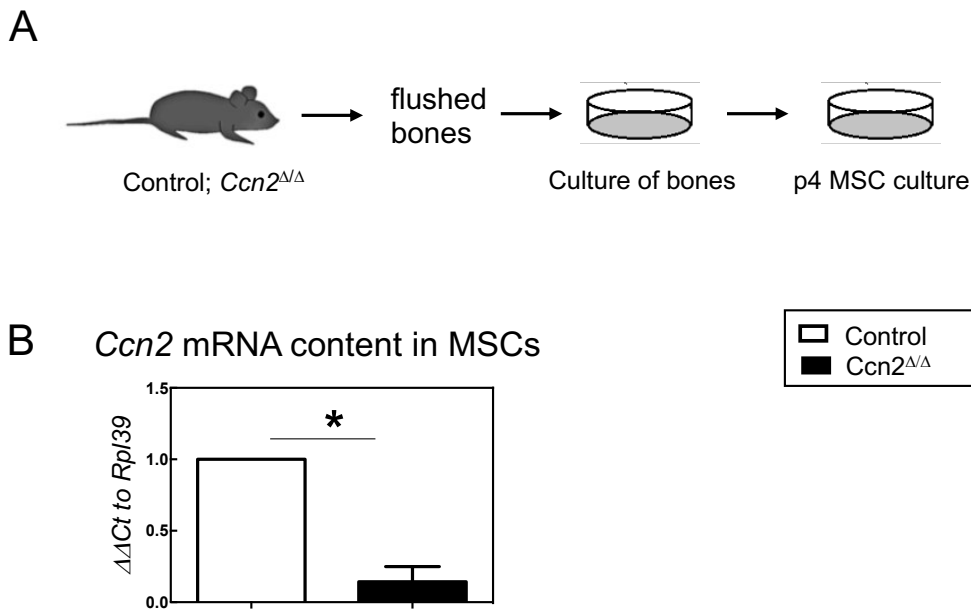


Figure 13. *Ccn2* RNA content in cultured MSCs (p4). (A) Experimental design: Bones were isolated from TAM intraperitoneal (i.p.) treated control and *Ccn2* floxed mice. BM was flushed out of the bones and bone fragments were cultured on culture dishes. Stromal cells were cultured till p4 MSCs. (B) *Ccn2* RNA content in control and *Ccn2*^{Δ/Δ} MSCs relative to housekeeping gene *Gorasp1*. Figure B shows a bar diagram of *Ccn2* mRNA content from MSCs of control: n=3 in white, and *Ccn2*^{Δ/Δ} n=3 mice in black. * p-value ≤ 0.05 show significance measurement using the Mann-Whitney U-test.

3.2.2 Function of *Ccn2* during single-cell culture stress

In a previous study the culture of HSCs in CM from UG26-1B6-sh*Ccn2* stromal cells revealed an impaired proliferation with delayed entrance in the cell cycle which was the result of increased SMAD2/3 signaling (Istvanffy et al., 2015). Using the culture system developed in section 3.1, we here wondered if CM of *Ccn2* deficient MEF cells would show similar alterations in HSC behavior.

For this purpose, we used the tamoxifen-inducible *Rosa26-CreER*^{T2}; *Ccn2*^{fl^{ox}} mice to isolate MEF cells in order to generate *Ccn2*^{Δ/Δ} MEFs. As a control we used *Rosa26-CreER*^{T2}; *Ccn2*^{wt} mice.

MEF cells were generated at gestation day E13.5. MEFs and were cultured as described in 2.2.3.1.2 Culture of Primary Cells and treated at passage one for 24 hrs with 4-OH the metabolite of tamoxifen. Afterwards the cells were cultured till passage three, the serum-free CM from control and *Ccn2*^{Δ/Δ} was prepared and a single cell assay was performed as described in 2.2.3.2 Single-Cell Culture and Figure 14A. In contrast to the previous study using CM of UG26-1B6-sh*Ccn2* CM, the single cell culture of control CD34⁻ SLAM cells in CM with or

without *Ccn2* did not show differences in clone size, suggesting no effects of *Ccn2* deletion in MEFs or the existence of redundant factors (Figure 14B).

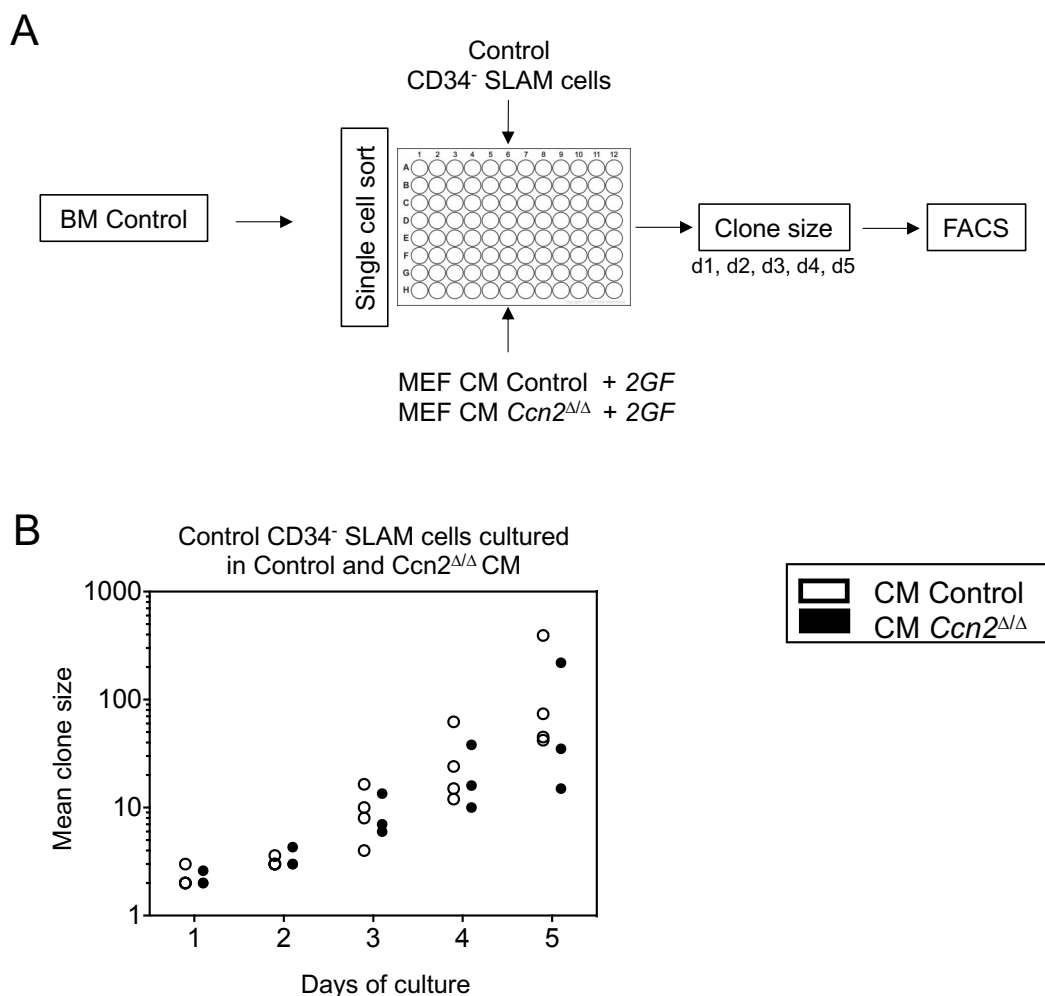


Figure 14. Single-cell cultures in control and *Ccn2*^{ΔΔ} MEF conditioned medium with 2GF. (A) Experimental design: BM isolation of ten till twelve-week-old control animals. CD34-SLAM single cell sort in 96-round-bottomed plates pre-filled with MEF-CM of control and *Ccn2*^{ΔΔ}, containing mSCF and IL-11 (2GFs). Microscopically investigation of the clone size at d1-d5 every 24 hrs. After five days the clones (<2cells/well) were harvested and analyzed per flow cytometry. The mean clone size of one SCC plate from cells cultured in control CM is shown in white and *Ccn2*^{ΔΔ} CM in black dot plots. Experiments show four different individuum's of control MEF CM and three individuum of *Ccn2*^{ΔΔ} MEF CM. * p-value ≤0.05 show significance in the comparison of control and the *Ccn2*^{ΔΔ} using the Mann-Whitney U-test.

In addition, we investigated the possible differences of the behavior of CD34⁺ SLAM cells from either control or *Ccn2*^{ΔΔ} mice in single-cell cultures using control MEF-CM.

In this experiment, the mice were treated with TAM i.p. and two weeks after the treatment the BM was isolated and verified for an efficient knockout using polymerase chain reaction (PCR). Then the BM was prepared for sorting of CD34⁺SLAM cells in the prepared single-cell plates (Figure 15A). Interestingly, the *Ccn2* knockout CD34⁺ SLAM cells revealed a significant decreased clone size after day three of culture compared to the control cells. This decrease was maintained at culture day four and five (Figure 15B).

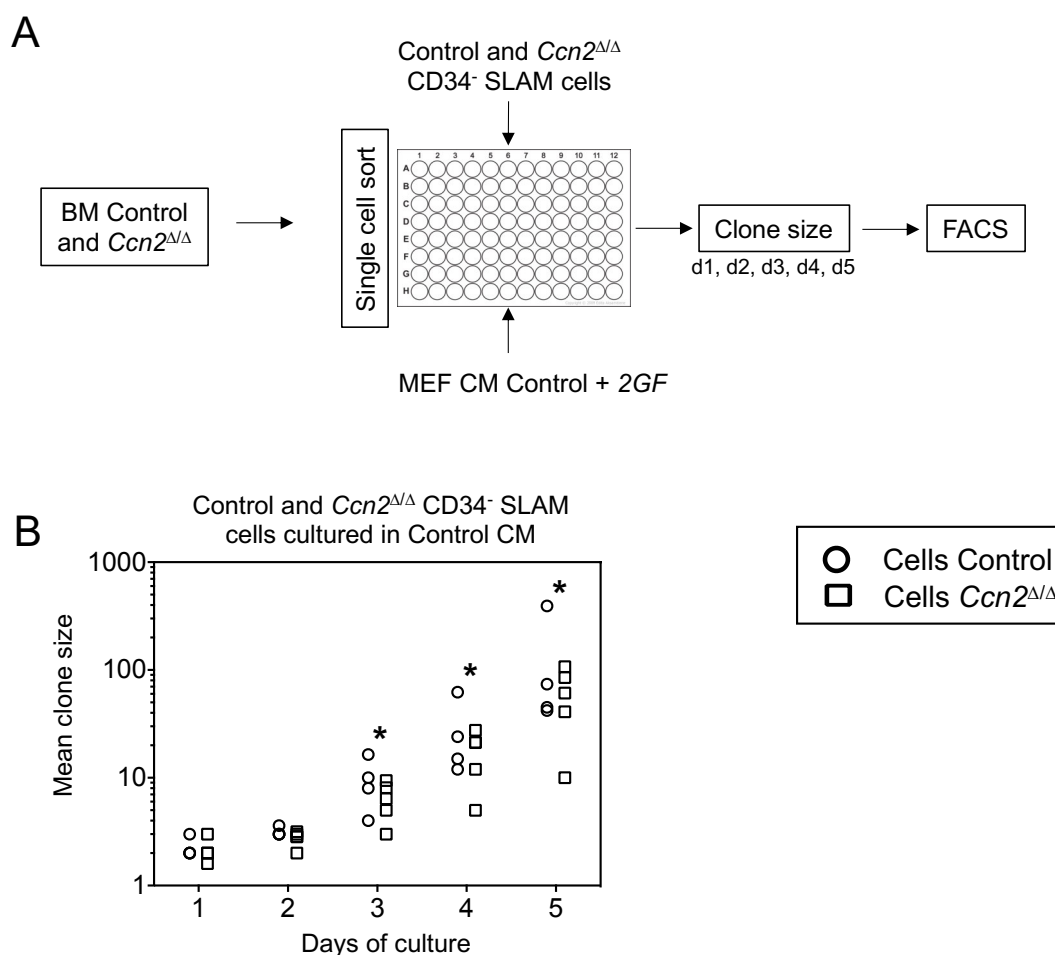


Figure 15. Single-cell cultures of control and *Ccn2*^{ΔΔ} CD34⁺ SLAM cells in control MEF conditioned medium with 2GF. (A) Experimental design: BM isolation of ten till twelve-week-old control and *Ccn2*^{ΔΔ} animals. CD34⁺SLAM single cell sort in 96-round-bottomed plates prefilled with control MEF-CM containing mSCF and IL-11 (2GFs). Microscopically investigation of the clone size at d1-d5 every 24 hrs. After five days the clones (<2cells/well) were harvested and analyzed per flow cytometry. The mean clone size of one SCC plate from control cells in white round dots and *Ccn2*^{ΔΔ} in white square dots cultured in control CM. Experiments show four different individuum's of control- and

five individuals of *Ccn2^{Δ/Δ}* CD34⁺SLAM cells. *p-value ≤ 0.05 show significance in the comparison of control and the *Ccn2^{Δ/Δ}* using the Mann-Whitney U-test.

3.2.3 *Ccn2* during steady state conditions

3.2.3.1 RNA content of *Ccn2* during steady state conditions

We then went on to find out the role of *Ccn2* expression in adult hematopoiesis *in vivo*. In a first experiment we analyzed which cells express *Ccn2* *in vivo* in adult mice at steady-state conditions. Therefore, we used B16 WT mice. In general, we found only a low expression in the hematopoietic early- (LSKs), progenitor- (CLPs and MPS) and mature cell compartments (B220⁺ B cells, CD3e⁺ T cells, Gr1⁺CD11b⁺ granulocytes and Gr1^{med}CD11b⁺ monocytes, Figure 16A). In addition, low levels of *Ccn2* expression were also noted in the stromal cell populations (MSCs, OBCs, ECs) with the highest *Ccn2* amount in the OBCs (Figure 16B) as was noted in *Ccn2*-GFP reporter mice (Wang et al., 2015).

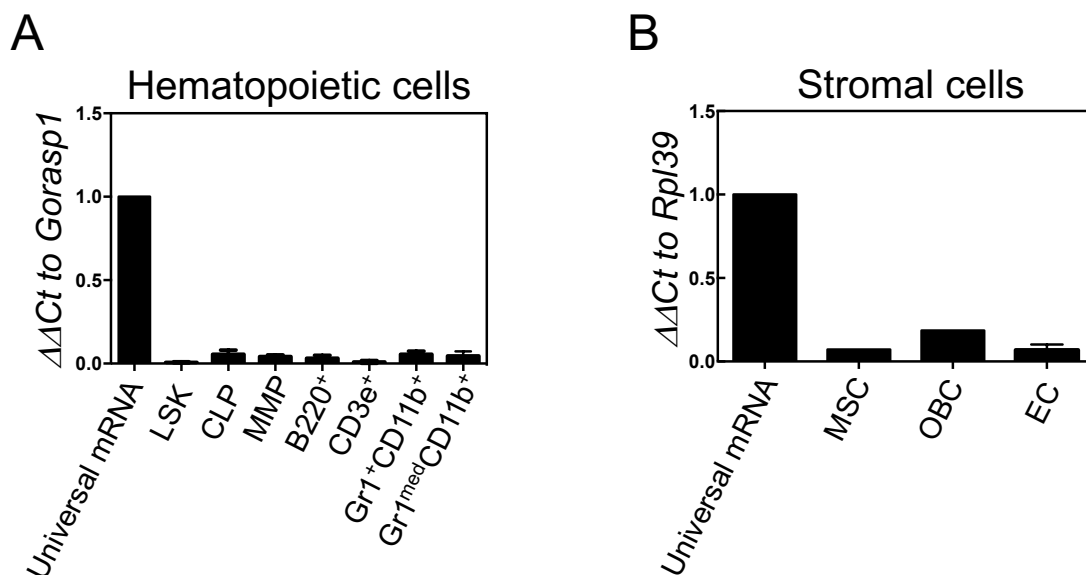


Figure 16. Relative delta delta Ct expression of *Ccn2* during steady state condition in hematopoietic- and stromal cells. (A) *Ccn2* mRNA content of LSKs, CLPs and MMPs as well as mature hematopoietic cell types like B220⁺, CD3e⁺, Gr1⁺CD11b⁺ and Gr1^{med}CD11b⁺ cells relative to housekeeping gene *Gorasp1* and *universal* mRNA. (B) *Ccn2* mRNA content of MSCs, OBCs and ECs relative to *universal* mRNA and to housekeeping gene *Rpl39* and *universal* mRNA. The mean and SEM of n = 3 is shown.

3.2.3.2 Analysis of *Ccn2* knockout during steady state in adult mice

3.2.3.2.1 Analysis of the hematopoietic cells after *Ccn2* knockout during steady state

To further explore a possible role of *Ccn2* during adult, steady state hematopoiesis we used the Rosa26-CreER^{T2} positive *Ccn2*^{wt/wt} and *Ccn2*^{fl/fl} mice and treated them for a duration of four weeks with tamoxifen. Then we determined the hematopoietic cellularity in the peripheral blood (PB), bone marrow (BM) and spleen (SP) in steady state healthy mice as shown in the experimental design Figure 17A.

In the peripheral blood (PB) the percentage of mean corpuscular hemoglobin (MCH) was significantly increased ($p=0.02$) the numbers of white blood cells (WBC), lymphocytes (Lymph), monocytes (Mono), granulocytes (Gran), red blood cells (RBC), hematocrit (HCT) and platelets (PLT) were within a normal range in the *Ccn2*^{Δ/Δ} mice compared to the littermate controls (Figure 17B).

A Experimental design



B

PB	Control (n=5)	<i>Ccn2</i> ^{Δ/Δ} (n=7)	p-Value	Significance
WBC (10 ³ /μl)	4.06	3.34	0.60	ns
Lymph (10 ³ /μl)	2.56	2.3	0.91	ns
Mono (10 ³ /μl)	0.16	0.11	0.71	ns
Gran (10 ³ /μl)	1.36	0.9	0.66	ns
RBC (10 ³ /μl)	8.21	8.32	0.90	ns
HCT %	47.86	49.43	0.78	ns
MCH %	16.86	17.33	0.02	p=0.02
PLT (10 ³ /μl)	791.8	1022	0.21	ns

Figure 17. Blood counter analysis after *Ccn2* loss in adult mice during steady state conditions.

(A) Experimental design: Eighth week old control and *Ccn2*^{fl/fl} mice were treated for four weeks with TAM food. Then the PB, BM and Sp were isolated for the analysis of the hematopoietic cell compartments. (B) Blood counter data from WBC, lymph, mono, gran, RBC, HCT, MCH and PLT of control n = 5 and *Ccn2*^{Δ/Δ} n = 7 mice. *p-value ≤0.05 show significance measurement using the Mann-Whitney U-test.

Mice lacking *Ccn2* gene showed unchanged peripheral blood, bone marrow and spleen cellularity. In contrast to the *Ccn2* knockout mice (Ivkovic et al., 2003), adult conditional tamoxifen-treated *Ccn2*^{Δ/Δ} mice reveal only a slight decrease in B220⁺ cells absolute numbers in the BM (Figure 18B) and unchanged numbers in the PB and SP (Figure 18A and C) compared to similarly treated controls. Although the CD3e⁺ T-cells population was elevated in the spleen (Figure 18C), T-cell levels were unchanged in PB and BM (Figure 18A and B). Furthermore, myeloid populations (Gr1⁺CD11b⁺ and Gr1^{med}CD11b⁺) were within normal range in the PB, BM and Sp (Figure 18A, B and C). Taken together, no gross differences were detectable during steady state conditions in adult mice when *Ccn2* deletion was induced at eighth week old mice for a duration of four weeks.

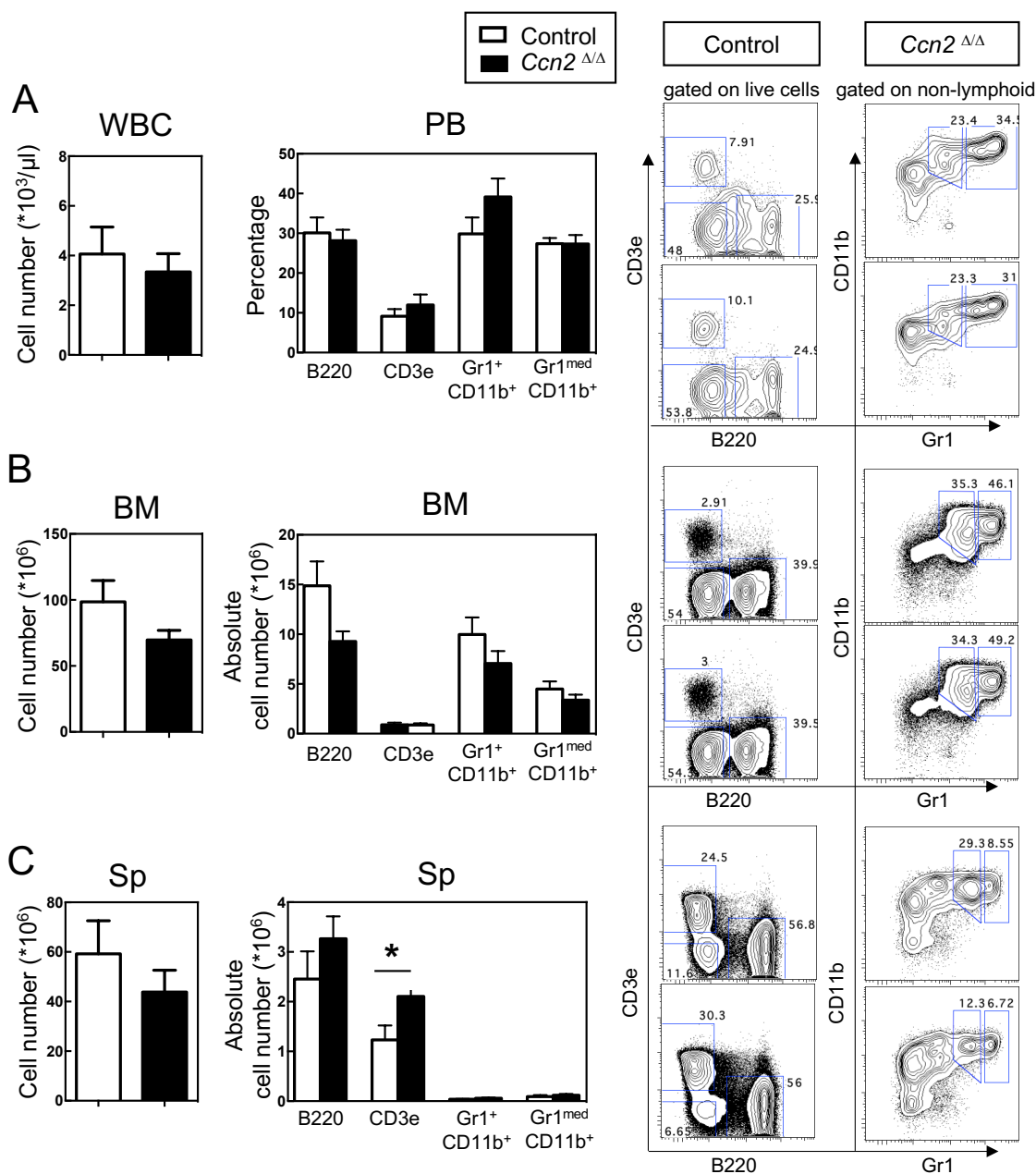


Figure 18. Hematopoietic mature cell composition after *Ccn2* deletion in the PB, BM and Sp at steady state condition. (A) Cell number of WBC in $10^3/\mu\text{l}$, and cell composition (B220⁺, CD3e⁺, Gr1⁺CD11b⁺ and Gr1^{med}CD11b⁺) in percentage of the PB and the corresponding representative gating strategy. (B) BM and (C) SP total counted cell numbers, absolute cell numbers of mature cells (B220⁺, CD3e⁺, Gr1⁺CD11b⁺ and Gr1^{med}CD11b⁺) and gating strategies. All data show the control in white and the *Ccn2*^{Δ/Δ} results in black bar graphs. Figures A, B and C show the results from two independently performed experiments with $n = 5$ for control mice and $n = 7$ for *Ccn2*^{Δ/Δ} mice. * p -value ≤ 0.05 show significance in the comparison of control and the *Ccn2*^{Δ/Δ} using the Mann-Whitney U-test.

In order to analyze possible differences in early hematopoiesis, we studied hematopoietic cell subsets in multiparameter flow cytometry (Figure 19A). Similarly, the multipotent progenitors LIN⁻, Sca1⁻, and Kit⁺ (MPs) as well as their downstream progenitors common myeloid progenitors (CMPs), megakaryocytic/ erythroid progenitors (MEPs) and granulocytic progenitors (GMPs) were within normal range (Figure 19B).

The numbers of LIN⁻, Sca1⁺, and Kit⁺ (LSK) cells as well as the more earlier CD34⁺ and CD34⁻CD150⁺ LSK subpopulations were unchanged in adult steady state *Ccn2*^{ΔΔ} mice (Figure 19C).

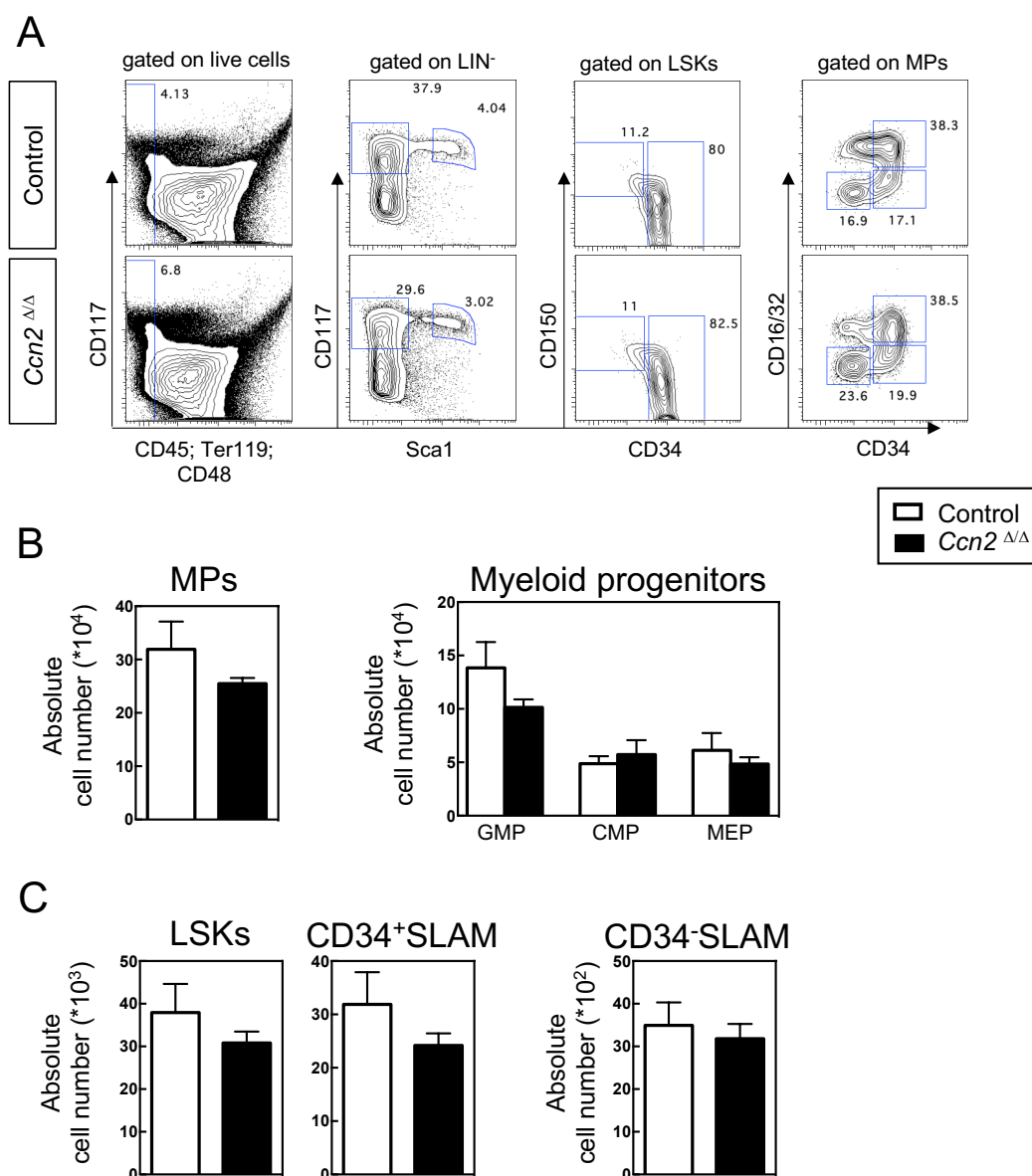


Figure 19. Early hematopoietic cell composition after *Ccn2* deletion in the BM at steady state conditions. (A) Gating strategy for hematopoietic early cells. First the lineage negative population was

separated by excluding CD45⁺, Ter119⁺ and CD48⁺ cells. Then, LSK cells were gated as CD117⁺ and Sca1⁺, while the MPs are Sca1⁻. The LSK compartment can be separated as CD34⁺LSK (ST-HSCs) and CD34⁻CD150⁺LSK (CD34-SLAM; LT-HSCs) cells. Myeloid progenitor cells were separated as CD34⁻CD16/32⁻ MEP, CD34⁺CD16/32⁻ CMPs and the CD34⁺CD16/32⁺ GMPs. (B) Absolute cell numbers of MPs and myeloid progenitor cells (GMP, CMP, MEP) and (C) absolute cell numbers of LSKs, CD34⁺LSKs and CD34-SLAM cells in the BM. All data show the control in white and the *Ccn2*^{Δ/Δ} results in black bar graphs. Figure B and C show the results from two independently performed experiments with n = 5 for control mice and n = 7 for *Ccn2*^{Δ/Δ} mice. *p-value ≤ 0.05 show significance in the comparison of control and the *Ccn2*^{Δ/Δ} using the Mann-Whitney U-test.

3.2.3.2.2 Analysis of the BM stromal cell compartment after *Ccn2* deletion during steady state

The previous experiments show that *Ccn2* deletion does not affect hematopoiesis under steady state conditions. We subsequently determined the cell number and different cell composition of the endosteal cells when *Ccn2* is deleted in adulthood using multiparameter flow cytometry (Figure 20A).

Similar to the hematopoietic compartment (Figure 18 and 19), the endosteal cell numbers (Figure 20B) as well as (CD45/Ter119)⁻ CD31⁻ stromal cellularity and different subsets such as CD31⁺ endothelial cells (ECs), CD166⁺ Sca1⁻ osteoblastic cells (OBCs) and CD166[~]/_{low} Sca1⁺ mesenchymal stem cells (MSCs) were not affected when *Ccn2* was lost (Figure 20C and 20D).

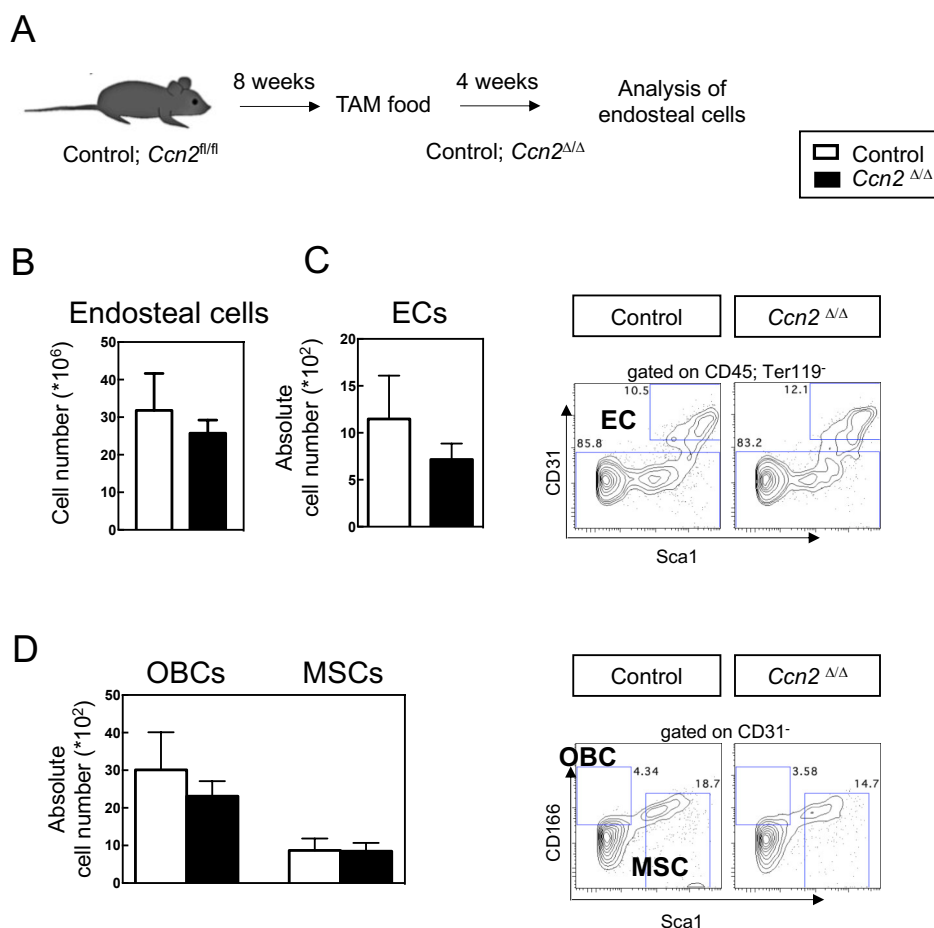


Figure 20. Endosteal cell composition after *Ccn2* deletion at steady state condition. (A) Experimental design: Eighth week old control and *Ccn2*^{fl/fl} mice were treated for four weeks with TAM food. Then the endosteal cells were isolated for the analysis of the stromal cell compartment by flow cytometry. (B) Endosteal counted cell numbers (C) absolute number of ECs and the representative gating strategy. (D) Absolute cell numbers of OBCs and MSCs and the representative gating strategy. All data show the results from two independently performed experiments with $n = 5$ for control mice and $n = 7$ for *Ccn2*^{Δ/Δ} mice. * p -value ≤ 0.05 show significance in the comparison of control and the *Ccn2*^{Δ/Δ} using the Mann-Whitney U-test

3.2.4 Ccn2 during in vivo stress conditions

As the analysis of *Ccn2* function during steady state condition in adult mice did not show any effect (chapter Results 3.3.2), but however the stress induction using single-culture showed an impaired proliferative behavior of the *Ccn2*^{Δ/Δ} HSCs we suggested a role for *Ccn2* exclusively during stress conditions in the adult hematopoiesis. This is in accordance with the role of *Ccn2* in our earlier published in vitro data (Istvánffy et al., 2015) as well as the data from others (Igarashi et al., 1993; Leask et al., 2009; Takigawa, 2018; Zang et al., 2015) which also indicated an essential role for *Ccn2* during stress conditions. Therefore, we decided to further study the impact of *Ccn2* during different short-term stress conditions such as myeloablative stress models using 5-Fluorouracil (5-FU), bacterial infection stress using lipopolysaccharide (LPS) as well as during a prolonged model using BM transplantation.

3.2.4.1 Function of Ccn2 during 5-FU induced myeloablative stress

To induce severe stress, we treated the mice with the chemotherapeutic compound 5-FU. 5-FU leads to myeloablation which activates dormant LT-HSCs to proliferate and differentiate in order to restore the hematopoietic homeostasis (Longley et al., 2003).

To study the impact of *Ccn2* expression during 5-FU-induced stress, we injected 5-FU i.p. into ten- to twelve week old control and *Ccn2*^{Δ/Δ} mice and analyzed the hematopoietic cells in the peripheral blood, spleen and bone marrow 14 days after injection (Figure 21A).

3.2.4.1.1 Function of Ccn2 during 5-FU induced myeloablative stress in hematopoiesis

The analysis showed similar recovery of the cellularity of the PB, BM and SP *Ccn2*^{Δ/Δ} compared to control littermates (Figure 21B, C, D). Overall, the percentage of B220⁺ B-cells, CD3e⁺ T-cells, Gr1⁺CD11b⁺ granulocytes or Gr1^{med}CD11b⁺ monocytes of the PB was in a normal range (Figure 21B). But, a significant 8.5-fold reduction of absolute cell numbers from CD3e⁺ T-cells was noted in the BM (Figure 21C) and a 1,66 fold reduced percentage of Gr1⁺CD11b⁺ granulocytes was observed in the SP (Figure 21D), while the other mature cell populations in the BM and SP were unaffected (Figure 21C and D).

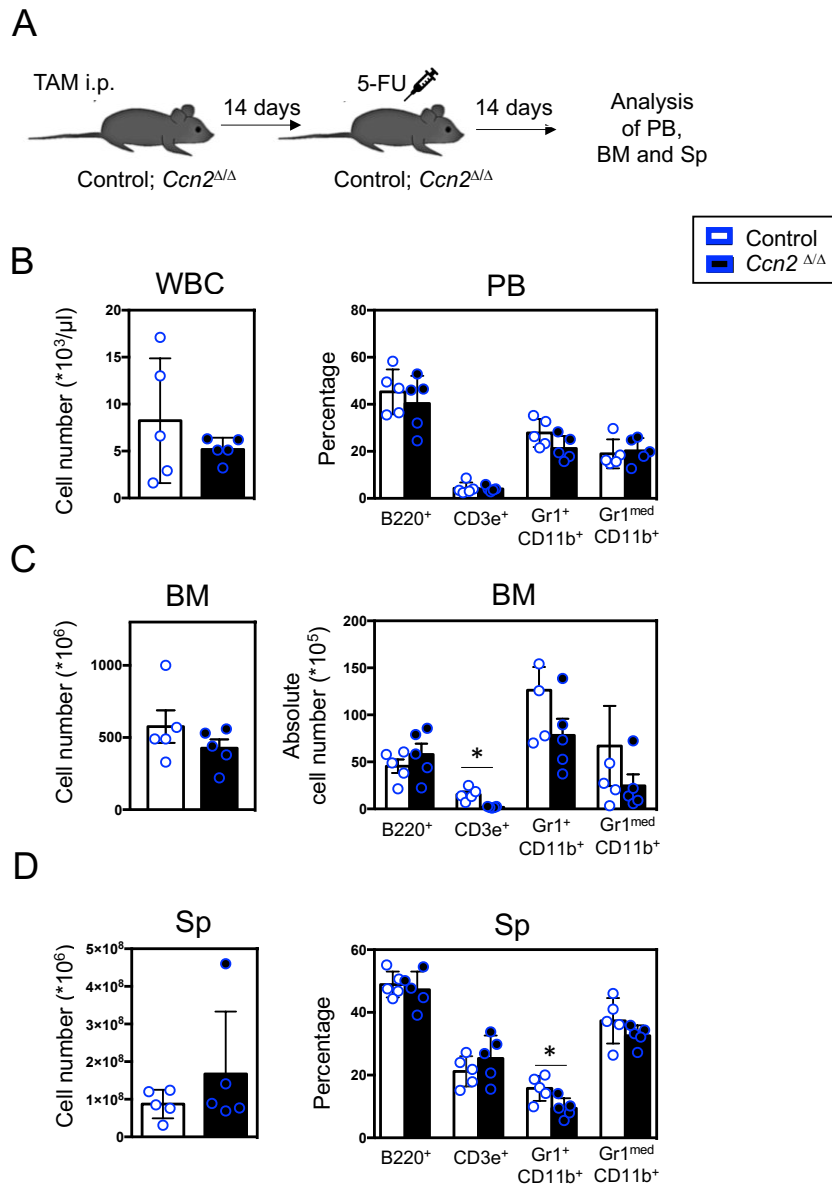


Figure 21. Mature cell populations in the PB, Sp and BM after 5-FU treatment of control and *Ccn2*^{ΔΔ} mice. (A) Experimental design: Two weeks after tamoxifen treatment (i.p.) the ten-week old control and *Ccn2*^{ΔΔ} mice were i.p injected with 5-FU (150 mg/kg). 14 days after treatment the PB, SP and BM hematopoietic cell compositions were analyzed using flow cytometry. (B) On the left the counted cell number of WBCs in the PB as 10³/μL and on the right side the percentage of B220⁺, CD3e⁺, Gr1⁺CD11b⁺, Gr1^{med}CD11b⁺ mature cell populations in the PB are shown. (C) On the left side the counted cell number of the Sp and on the right side the percentage of B220⁺, CD3e⁺, Gr1⁺CD11b⁺, Gr1^{med}CD11b⁺ mature cell populations are shown. (D) Counted cell number in the BM on the left and the percentage of B220⁺, CD3e⁺, Gr1⁺CD11b⁺, Gr1^{med}CD11b⁺ mature cell populations on the right side are shown. In all figures the control mice are shown in white bars with white dotplots that are surrounded in blue and the *Ccn2*^{ΔΔ} mice are shown in black bars with black dotplots surrounded in blue. Figure 13

show one performed experiment with n = 5 mice control mice and n = 5 *Ccn2^{ΔΔ}* mice; * p-value <0.05 show significance in the comparison of control and *Ccn2^{ΔΔ}* using the Mann-Whitney U-test.

As the 5-FU treatment also activates HSC proliferation and *Ccn2*-deleted HSCs show reduced proliferation in single cell cultures (Figure 15), we studied whether the proliferation after myeloablation would alter progenitor or stem cell compartments (Figure 22A, B and C). Contrary to the single cell results, the recruitment of dormant LT-HSCs into the cell cycle in order to repopulate the BM hematopoietic cellularity did not reveal any changes in the absolute cell numbers of the multipotent progenitor (MP) cells or their downstream common myeloid progenitor (CMP), granulocyte - monocyte progenitor (GMP)- or megakaryocyte -erythrocyte progenitor (MEP) cell composition (Figure 22B). In addition, no differences were found in the absolute cell numbers of the LSK cells, CD34⁺LSKs or in the number of CD34⁻CD150⁺LSK cells (Figure 22C).

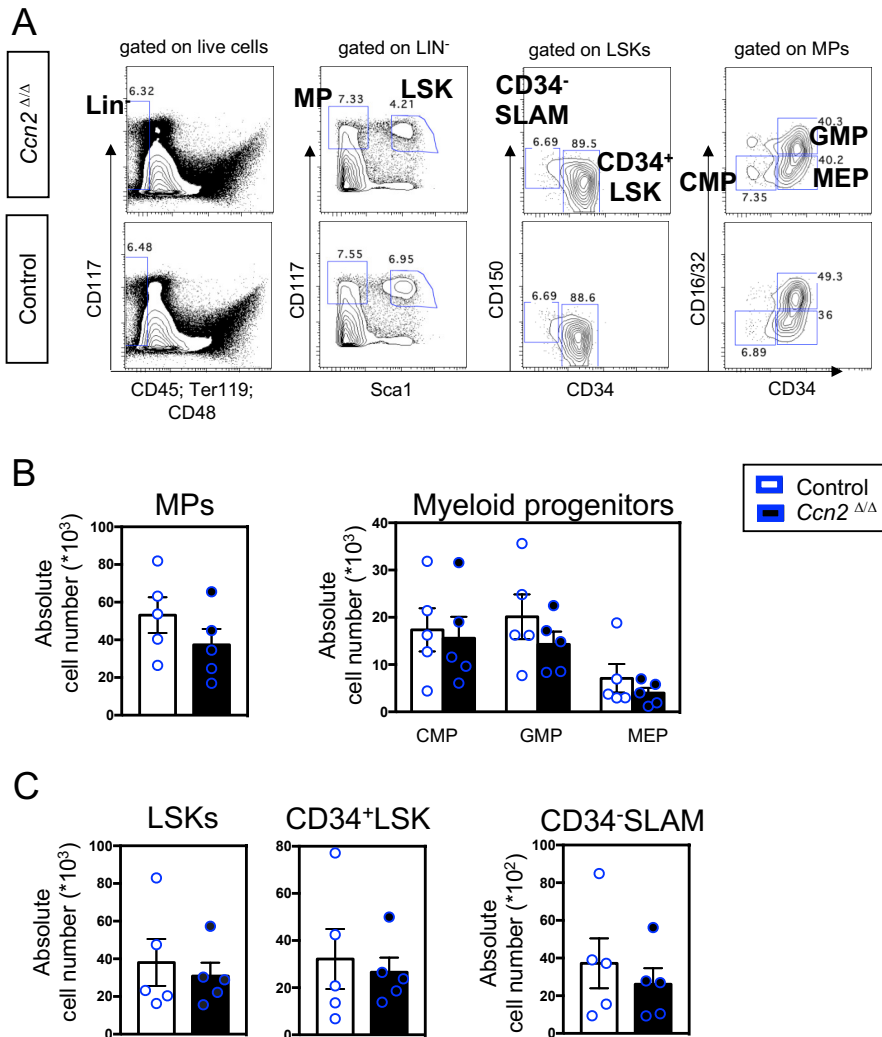


Figure 22. Myeloid progenitor and stem cells in the BM after 5-FU treatment of control and *Ccn2*^{Δ/Δ} mice. (A) Gating strategy for hematopoietic early cells. (B) Absolute number of MPs and the myeloid progenitor cell numbers of CMPs, GMPs and MEPs. (C) Absolute cell numbers of LSKs, CD34⁺LSKs and CD34-SLAM cells after 5-FU treatment in the control and *Ccn2*^{Δ/Δ} mice. In all figures the control mice are shown in white bars with white dotplots that are surrounded in blue and the *Ccn2*^{Δ/Δ} mice are shown in black bars with black dotplots surrounded in blue. Figures show one performed experiment with n = 5 mice control mice and n = 5 for *Ccn2*^{Δ/Δ} mice; *p-value ≤0.05 show significance in the comparison of control and *Ccn2*^{Δ/Δ} using the Mann-Whitney U-test.

3.2.4.1.2 Function of *Ccn2* during 5-FU induced myeloablative stress in stromal cells

Additionally, to the hematopoietic compartments we analyzed the stromal cell compartments (Figure 23A) and found unchanged total cell numbers from endosteal cells, and unaltered absolute cell numbers of endothelial cells (ECs), mesenchymal stem cells (MSCs) and osteoblastic cells (OBCs) between the 5-FU treated controls and *Ccn2*^{Δ/Δ} mice.

All in all, our results indicate that *Ccn2* expression is only marginally involved in hematopoietic recovery after 5-FU-induced hematopoietic stress (Figure 23B and C).

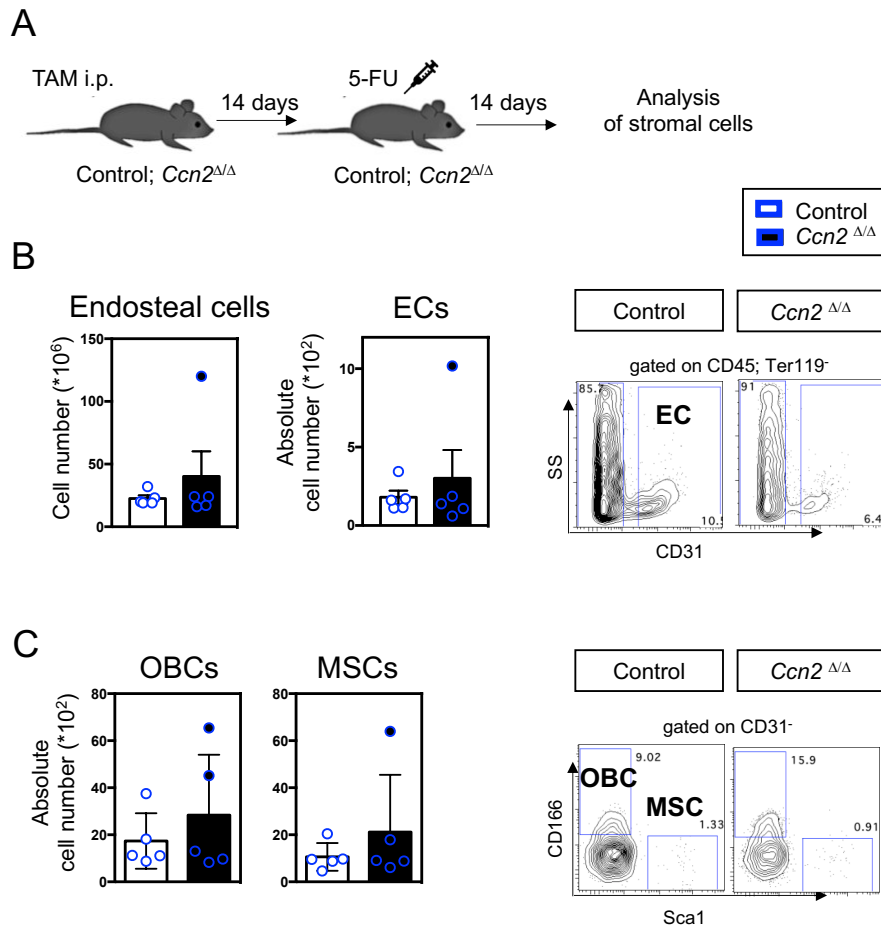


Figure 23. Stromal cell composition after 5-FU treatment of control and *Ccn2*^{Δ/Δ} mice. Experimental design: Two weeks after tamoxifen treatment (i.p.) the eight- till ten-week old control and *Ccn2*^{Δ/Δ} mice were i.p injected with 5-FU (150 mg/kg). 14 days after treatment with 5-FU the BM stromal cell compositions were analyzed using flow cytometry. (B) Endosteal total cell numbers, absolute cell number of ECs on the left side and the gating strategy on the right side are shown. (C) On the left the absolute cell numbers of OBCs and MSCs are shown and on the right side their gating strategy. In all figures the control mice are shown in white bars with white dotplots that are surrounded in blue and the *Ccn2*^{Δ/Δ} mice are shown in black bars with black dotplots surrounded in blue. Figure show one performed experiment with n = 5 mice control mice and n = 5 *Ccn2*^{Δ/Δ} mice; *p-value ≤0.05 show significance in the comparison of control and *Ccn2*^{Δ/Δ} using the Mann-Whitney U-test.

3.2.4.2 Function of *Ccn2* during inflammatory stress using lipopolysaccharide

Enhanced *Ccn2* levels are found in inflammatory diseases as well as in areas of severe tissue damage (Leask et al., 2009; Liu et al., 2012). Indeed, *Ccn2* was proposed to be an

inflammatory mediator (Abraham et al., 2008; Kular et al., 2011; Liu et al., 2012) which increases IL-6 expression in OA synovial fibroblasts (Liu et al., 2012) and plays a major role in the development of systemic sclerosis (Abraham et al., 2008). Therefore, we studied the role of *Ccn2* during the early phase of inflammatory stress. For this purpose, we treated mice with 1 µg lipopolysaccharide (LPS) to induce systemic inflammation. Mice were analyzed 24 hrs after treatment (Figure 24A).

3.2.4.2.1 Function of *Ccn2* during hematopoietic inflammatory stress

In these experiments, we observed an unchanged cellularity of WBC per $10^3/\mu\text{L}$ in the PB (Figure 24B), as well as in the in the SP (Figure 24C) or BM (Figure 24D). Additionally, the mature cell composition (B220^+ , CD3e^+ $\text{Gr1}^+\text{CD11b}^+$ and $\text{Gr1}^{\text{med}}\text{CD11b}^+$, in PB, Sp and BM, Figure 24B, C, D) was within a normal range. These data indicate no changes on the inflammatory response on mature cell numbers in *Ccn2*^{Δ/Δ} mice after 24 hrs.

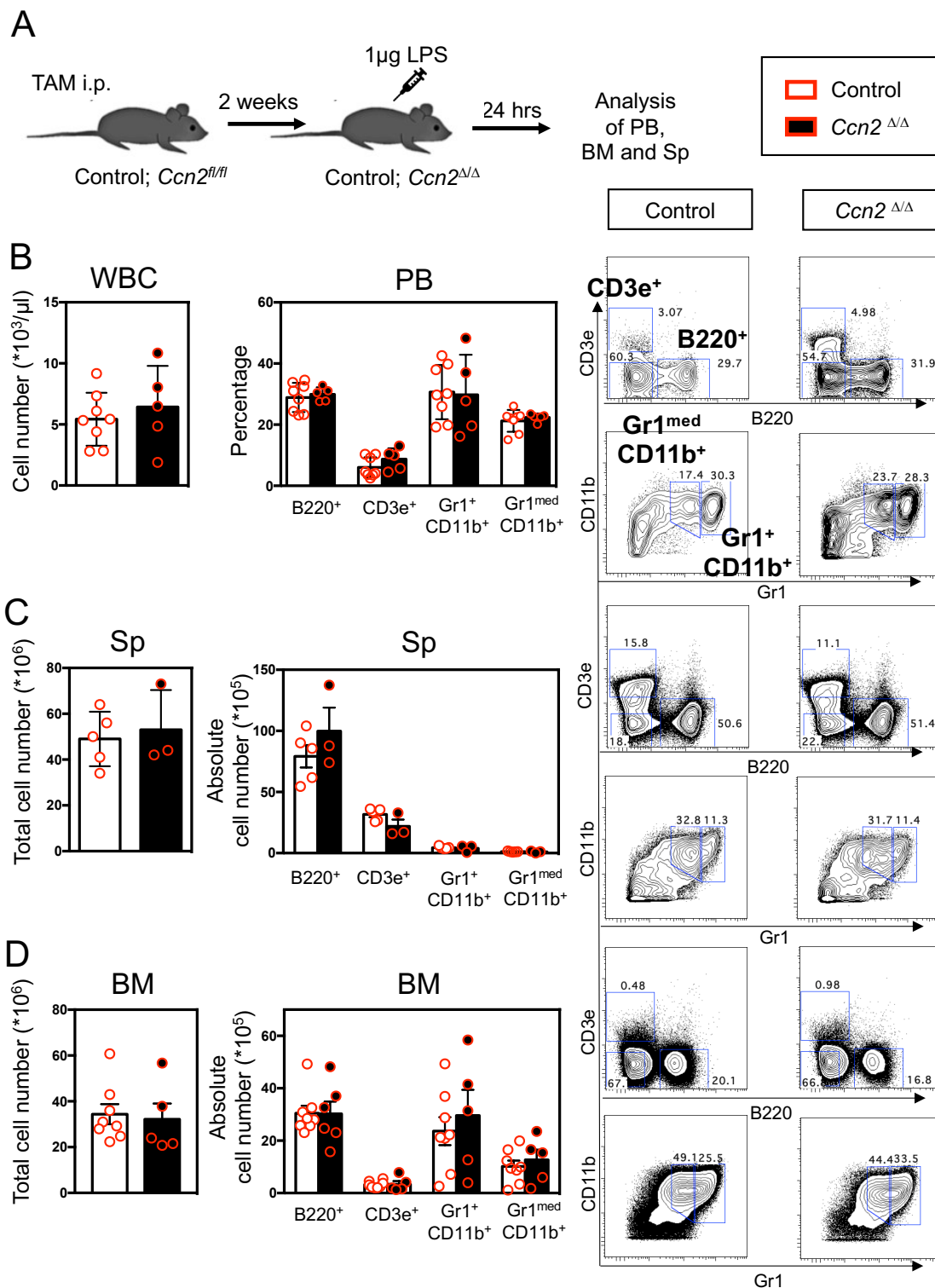


Figure 24. Mature cell populations in the PB, Sp and BM after LPS treatment of control and *Ccn2^{ΔΔ}* mice. (A) Experimental design: Two weeks after tamoxifen treatment (i.p.) the eight- till ten-week old control and *Ccn2^{ΔΔ}* mice were i.p injected with 1µg LPS. 24 hrs later the PB, SP and BM hematopoietic cell compositions were analyzed using flow cytometry. (B) Cell number of WBCs in the PB as $10^3/\mu\text{L}$ on the left, the percentage of B220⁺, CD3e⁺, Gr1⁺CD11b⁺, Gr1^{med}CD11b⁺ mature cell

populations in the middle and on the right side their gating strategy in the PB is shown. (C) Total cell number in the Sp on the left, the percentage of B220⁺, CD3e⁺, Gr1⁺CD11b⁺, Gr1^{med}CD11b⁺ mature cell populations in the middle and on the right side the gating strategy in the Sp is shown. (D) Total cell number in the BM on the left, the percentage of B220⁺, CD3e⁺, Gr1⁺CD11b⁺, Gr1^{med}CD11b⁺ mature cell populations in the middle and on the right side the gating strategy in the BM is shown. In all figures the control mice are shown in white bars with white dotplots that are surrounded in red and the *Ccn2^{ΔΔ}* mice are shown in black bars with black dotplots surrounded in red. Figures show one performed experiment in the SP with n = 5 control mice and n = 3 *Ccn2^{ΔΔ}* mice and two independently performed experiments in the BM with n = 8 control mice and n = 5 *Ccn2^{ΔΔ}* mice; *p-value ≤0.05 show significance in the comparison of control and *Ccn2^{ΔΔ}* mice using the Mann-Whitney U-test.

In addition, when analyzing the BM using flow cytometry (Figure 25A), we found that absolute numbers of MPs and the different progenitor cells CMPs, GMPs and MEPs (Figure 25B) were within a normal range. However, contrary to these progenitor populations, earlier hematopoietic compartments declined in *Ccn2^{ΔΔ}* mice after LPS treatment compared to controls.

These results indicate that in *Ccn2^{ΔΔ}* mice, mature hematopoietic and progenitor populations are not affected by LPS treatment. However, earlier LSK cells and its CD34⁺ LSK and CD34⁻ SLAM subpopulations were significantly reduced compared to control mice (Figure 25C), suggesting a relative depletion of HSCs in *Ccn2^{ΔΔ}* mice.

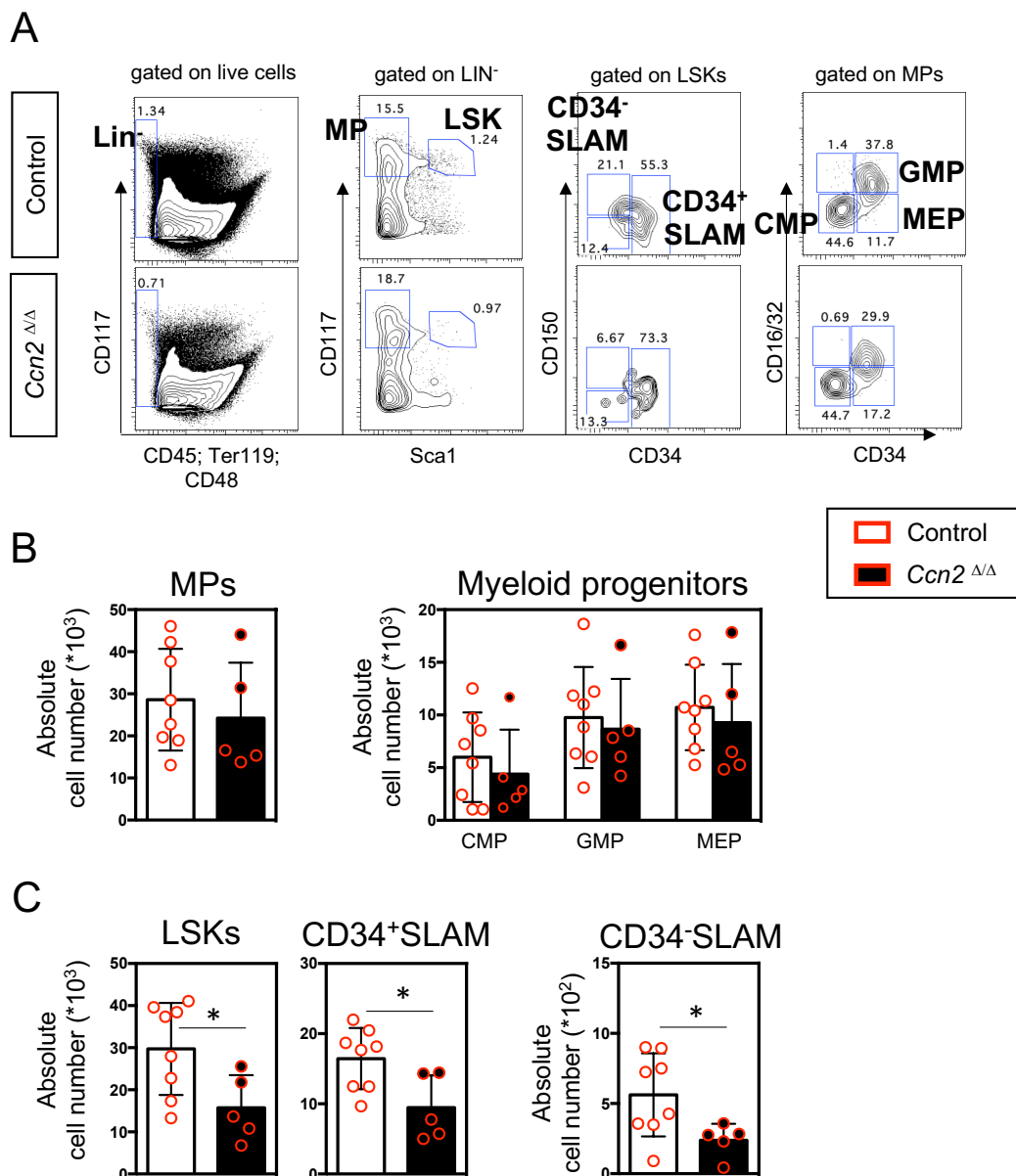


Figure 25. Myeloid progenitor and stem cells in the BM after LPS treatment of control and *Ccn2*^{Δ/Δ} mice. (A) Gating strategy for hematopoietic early cells. (B) Absolute number of MPs and the myeloid progenitor cell numbers of CMPs, GMPs and MEPs. (C) Absolute cell numbers of LSKs, ST-HSCs and LT-HSCs cells after LPS treatment in the control and *Ccn2*^{Δ/Δ} mice. In all figures the control mice are shown in white bars with white dotplots that are surrounded in red and the *Ccn2*^{Δ/Δ} mice are shown in black bars with black dotplots surrounded in red. Figures show two independently performed experiments with n = 8 control mice and n = 5 *Ccn2*^{Δ/Δ} mice; *p-value ≤0.05 show significance in the comparison of control and *Ccn2*^{Δ/Δ} mice using the Mann-Whitney U-test (generated with masterstudent Katharina Kaiser).

3.2.4.2.2 Function of *Ccn2* in inflammatory cytokine secretion during inflammatory stress

To test whether the reduced HSCs numbers in *Ccn2* deleted mice correlate to changes in systemic cytokine levels, we analyzed the inflammatory molecules inflammatory cytokines in the PB (serum) using cytokine bead assay (CBA, Figure 26A, B and C). The serum protein content of IL-10, IFN γ , and IL-12p70 in this experiment was unchanged between LPS treated *Ccn2*-deleted and control mice (data not shown). Although a relation between CCN2 and IL-6 expression was shown in human synovial fibroblasts (Liu et al., 2012), we did not detect differences in IL-6 serum levels of LPS-treated *Ccn2* ^{Δ/Δ} or control mice (Figure 26D). The protein content of TNF- α on the other hand, appears to be reduced in *Ccn2* ^{Δ/Δ} mice, but due to variation between mice this difference was not statistically significant (Figure 26D). However, *Ccn2* is necessary for the expression of the pro-inflammatory chemokine MCP-1 (CCL2) in the LPS treated mice as the concentration was significantly reduced in *Ccn2* ^{Δ/Δ} compared to control mice (Figure 26D).

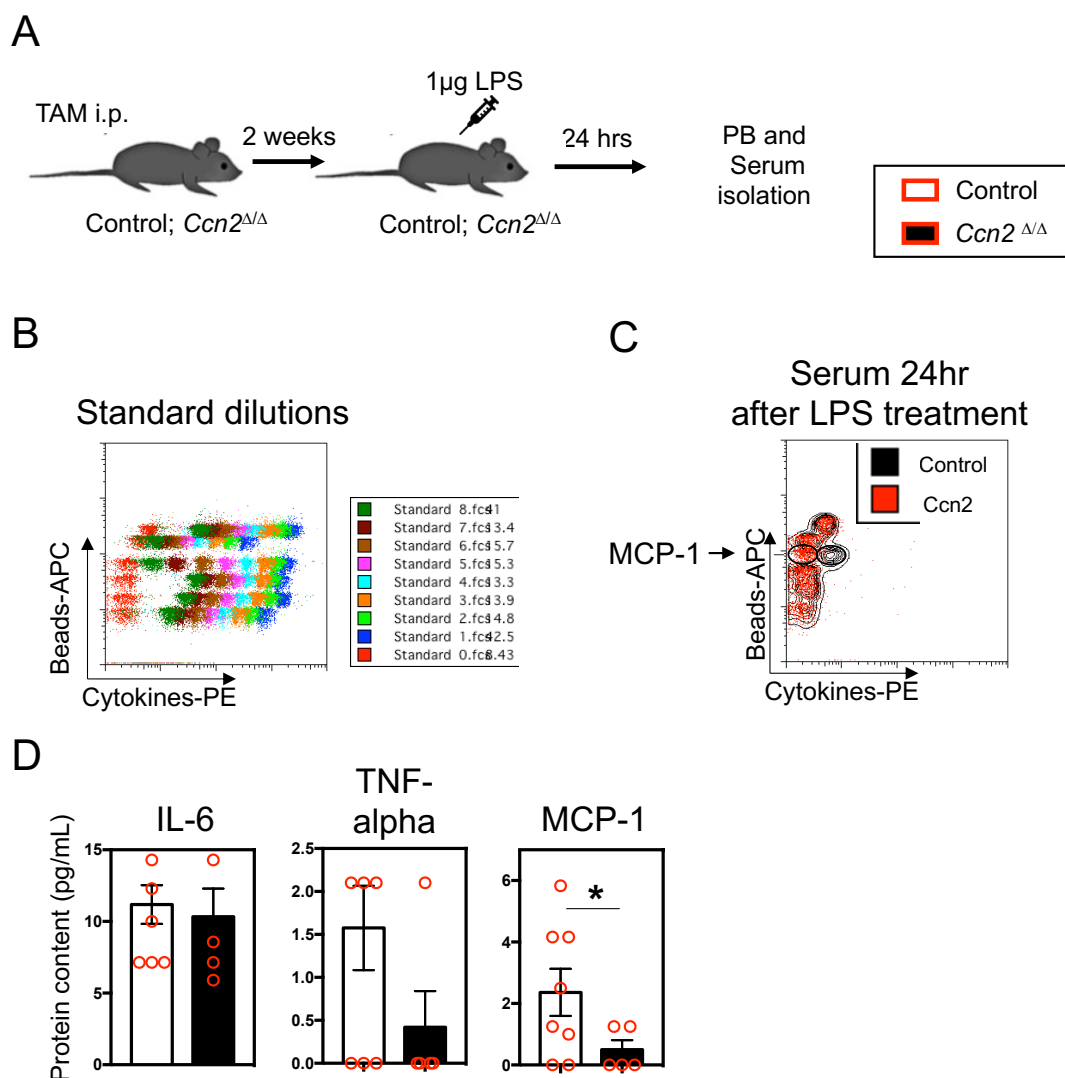


Figure 26. CBA from serum isolated of the PB after LPS treatment of control and *Ccn2*^{ΔΔ} mice. (A) Experimental design: Two weeks after tamoxifen treatment the eight- till ten-week old control and *Ccn2*^{ΔΔ} mice were i.p. injected with 1µg LPS. 24 hrs later the serum from the PB was isolated and the CBA as performed. (B) Standard dilutions for the analyzed cytokines (IL-6, IL-10, MCP-1, IFN γ , TNF- α , and IL-12p70). (C) Representative flow cytometry plot for the analysis of the cytokines in the serum of 24 hr LPS treated control (black) and *Ccn2*^{ΔΔ} (black) mice. (D) Analysis of the protein content in pg/mL from IL-6, TNF alpha and MCP-1. In all figures the control mice are shown in white bars with white dotplots that are surrounded in red and the *Ccn2*^{ΔΔ} mice are shown in black bars with black dotplots surrounded in red. Figures show two independently performed experiments with n = 8 control mice and n = 5 *Ccn2*^{ΔΔ} mice; *p-value ≤ 0.05 show significance in the comparison of control and *Ccn2*^{ΔΔ} mice using the Mann-Whitney U-test (generated in collaboration with masterstudent Katharina Kaiser).

3.2.4.2.3 Function of *Ccn2* during niche cell inflammatory stress

The previous experiments explored the hematopoietic department. Since we are mainly interested in the relevance of *Ccn2* expression in the niche, we subsequently analyzed stromal cell numbers in LPS-treated *Ccn2*^{Δ/Δ} and control mice (Figure 27A).

Here, we found no gross differences between the treated and *Ccn2*^{Δ/Δ} mice in the total cell number of non-hematopoietic endosteal cells (Figure 27B), the absolute EC numbers (Figure 27C) or the absolute number of OBCs (Figure 27D). However, a slight but, due to variation in the control mice, not significant (p=0.085) decrease of absolute cell numbers from MSCs could be observed in the *Ccn2*-deficient mice compared to the control mice (Figure 27D).

The possibly reduced MSC amount in *Ccn2*-deficient mice is inline with the view that *Ccn2* is pro-inflammatory and increasing MSC proliferation (Leask et al., 2009; Liu et al., 2012; Battula et al., 2013). Moreover, MSCs part of the BM niche were found to be a source of MCP1 (Ren et al., 2012).

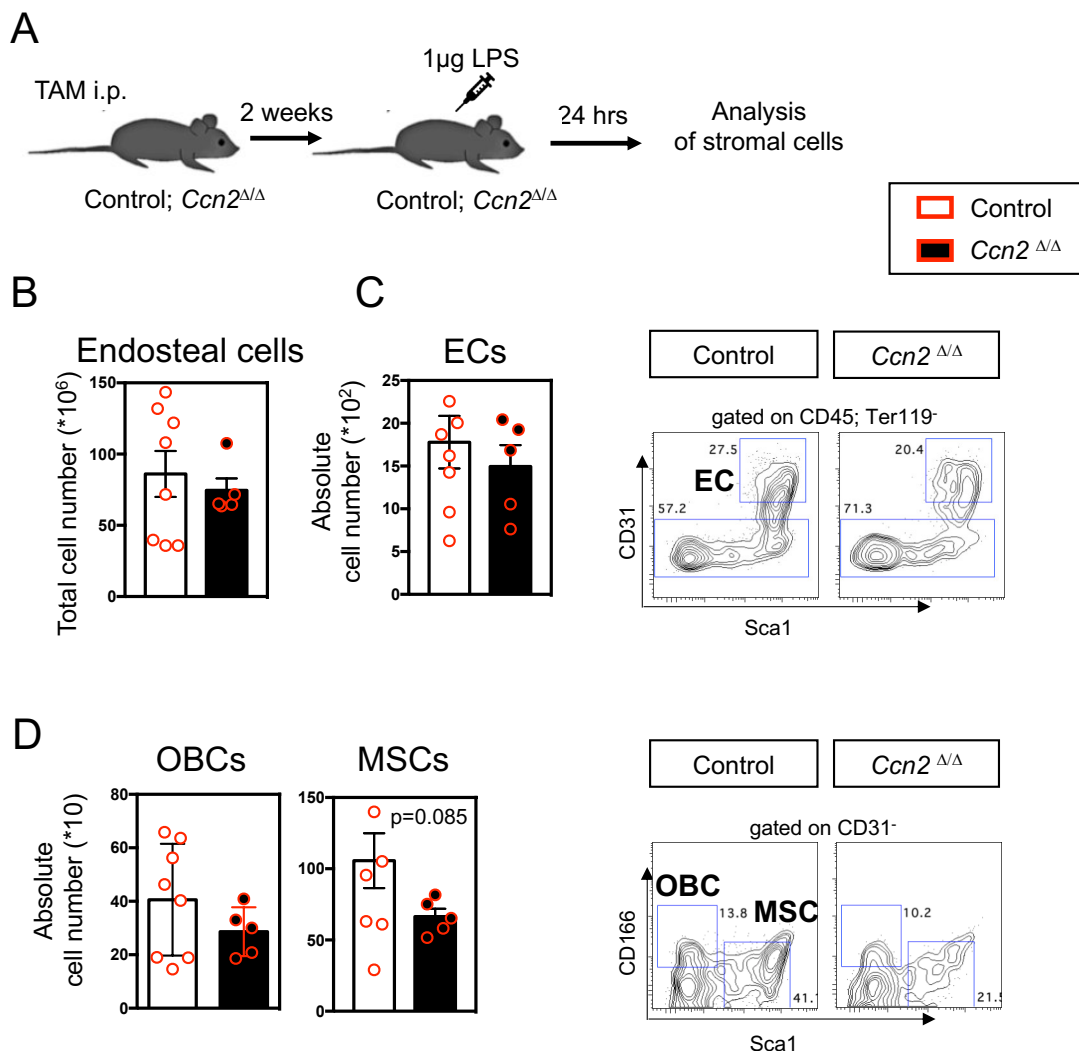


Figure 27. Stromal cell composition after LPS treatment of control and *Ccn2*^{Δ/Δ} mice. (A) Experimental design: Two weeks after tamoxifen treatment the eight- till ten-week old control and *Ccn2*^{Δ/Δ} mice were i.p. injected with 1 µg LPS. 24 hrs later the BM stromal cell compositions was analyzed using flow cytometry. (B) Endosteal total cell numbers. (C) Absolute cell number of ECs and the gating strategy. (D) Absolute cell numbers of OBCs and MSCs on the left side and their gating strategy on the right side. In all figures the control mice are shown in white bars with white dotplots that are surrounded in red and the *Ccn2*^{Δ/Δ} mice are shown in black bars with black dotplots surrounded in red. Figures show two independently performed experiments with *n* = 8 control mice and *n* = 5 *Ccn2*^{Δ/Δ} mice; **p*-value ≤0.05 show significance in the comparison of control and *Ccn2*^{Δ/Δ} mice using the Mann-Whitney U-test (generated in collaboration with masterstudent Katharina Kaiser).

3.2.4.3 Transplantation as a chronic stress model for the function of *Ccn2*

Ccn2 is known to be upregulated during stress responses triggering different signaling pathways and behavior of cells (Leask et al., 2009; Istvánffy et al., 2015). The BM transplantation model includes different stress situations (irradiation, myeloablation, regeneration) in which *Ccn2* might be involved over a longer period of time. For successful regeneration (also called repopulation), transplanted donor long-term repopulating HSCs need to home to the BM, self-renewal, proliferate, and differentiate in order to restore hematopoietic homeostasis. Irradiation will not only affect recipient hematopoietic cells, but also stromal cells with the result of an increased recipient stromal cell proliferation (Dominici et al., 2016). Aside from reduced hematopoietic and stromal cell numbers in the BM, irradiation will induce an inflammatory response with increased cytokine and chemokine secretion, including increased MCP-1 secretion, which additionally trigger hematopoietic as well as stromal cell responses. Thus, BM transplantation is a good model to study the function of *Ccn2* expression in the restoration of hematopoietic and stromal homeostasis after a complex series of stress responses.

Although the expression of *Ccn2* was not detectable in steady state HSCs and very low in niche cells (Figure 16), it might get upregulated during transplantation induced stress, so we decided to study the contribution separately in intrinsic (*Ccn2* knock out in hematopoietic) as well as extrinsic (*Ccn2* knock out in stromal cell) transplantation models.

3.2.4.3.1 Intrinsic function of *Ccn2* during chronic stress

To find out, whether *Ccn2* intrinsically regulates HSCs and donor hematopoietic regeneration in transplantation models, we treated floxed *Ccn2* and control mice with tamoxifen, isolated the bone marrow and transplanted 1500 *Ccn2*^{Δ/Δ} or control LSK cells into lethally irradiated WT mice (Figure 28A). When monitoring the transplanted mice at different timepoints after transplantation, we found that the donor engraftment in the PB was similar between transplanted donor *Ccn2*^{Δ/Δ} and control HSCs at five, ten and 16 weeks after Tx (Figure 28B). In addition, the mature hematopoietic subpopulations (B220⁺ B-cells, CD3e⁺ T-cells, Gr1⁺CD11b⁺ granulocytes, Gr1^{med}CD11b⁺ monocytes) were found at similar proportions in the PB (Figure 28C).

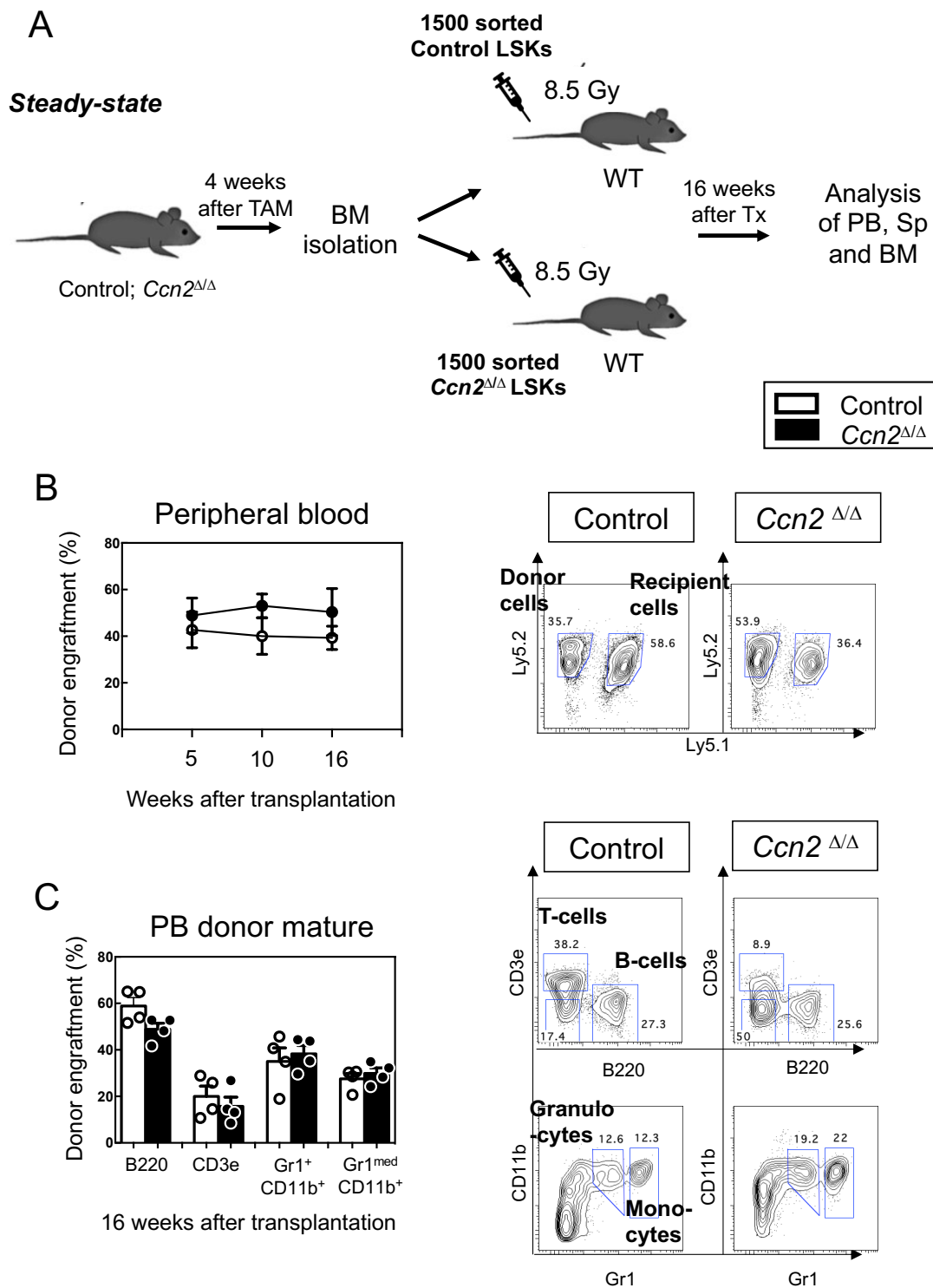


Figure 28. Engraftment in the PB of transplanted LSK cells from control and *Ccn2*^{ΔΔ} cells after four weeks of TAM treatment (i.p.) as a prolonged hematopoietic stress model. (A) Experimental design: four weeks after TAM treatment (i.p.) the BM from control and *Ccn2*^{ΔΔ} mice were isolated, pooled and sorted for LSK cells. Then 1500 LSK cells (Ly5.2) were transplanted into lethally (8.5 Gy) irradiated 129xLy5.1 (Ly5.1 and Ly5.2) WT mice. Every five, ten and 16 weeks the engraftment and cell

composition in the PB was analyzed. 16 weeks after transplantation, the mice were sacrificed and the Sp and BM cell engraftment and cell composition was determined using flow cytometry. (B) On the left: Donor cell engraftment in percentage in the PB five, ten and 16 weeks after transplantation. On the right: Representative gating strategy for the gating of Ly5.2⁺ donor cells and Ly5.1⁺Ly5.2⁺ recipient cells. (C) On the left: Percentage of donor B220⁺, CD3e⁺, Gr1⁺CD11b⁺ and Gr1^{med}CD11b⁺ cells in the PB. On the right: Gating strategy of donor mature cell populations in the PB as an example for mature cell gating. All figures show the donor cell engraftment from control hematopoietic cells in white and the *Ccn2*^{ΔΔ} hematopoietic cells in black bar and dot plots. Figures represent one performed experiment with n = 4 control mice and n = 4 *Ccn2*^{ΔΔ} mice; *p-value ≤0.05 show significance in the comparison of control and *Ccn2*^{ΔΔ} mice using the Mann-Whitney U-test.

The total cell number in the Sp (Figure 29A) and BM (Figure 29D) as well as donor cell engraftment in the SP (Figure 29B) was unchanged. However, the transplanted *Ccn2*-deleted HSCs increased myeloid engraftment in the Sp with increased Gr1⁺CD11b⁺ granulocytes and Gr1^{med}CD11b⁺ monocytes, while the lymphoid compartment (B220⁺ B cells and CD3e⁺ T-cells) was unaffected (Figure 29C).

Of further interest, donor cell engraftment in the BM was significantly enhanced from the transplanted *Ccn2*^{ΔΔ} LSK cells compared to the transplanted control LSK cells (Figure 29E). Here, the increase was attributed not only by an enhanced absolute number Gr1⁺CD11b⁺ granulocytes and Gr1^{med}CD11b⁺ monocytes, but also by an increase on of B220⁺ B-cells in the BM (Figure 29F).

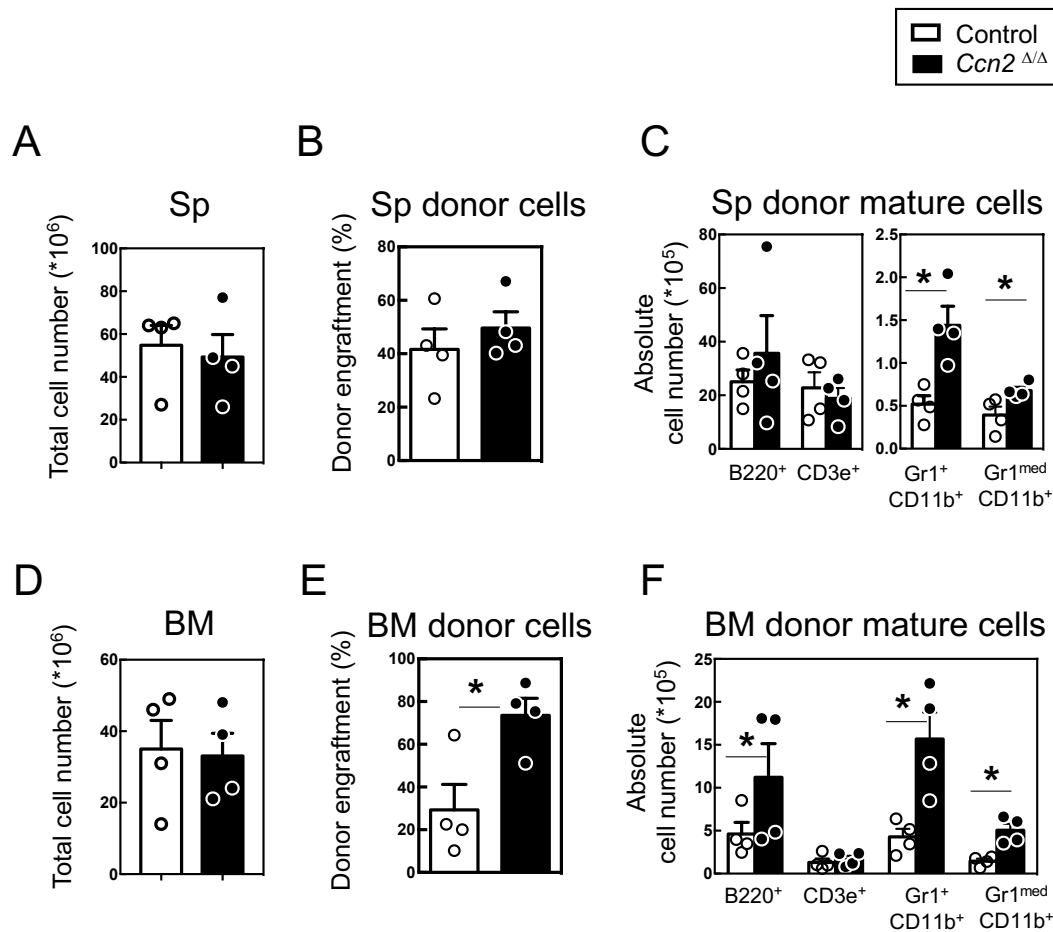


Figure 29. Mature cell engraftment in the Sp and BM of transplanted LSK cells from control and *Ccn2*^{Δ/Δ} mice as a long-term hematopoietic stress model. (A) Total cell number in the Sp. (B) Percentage of donor cell engraftment in the Sp. (C) Absolute cell number of donor B220⁺, CD3e⁺, Gr1⁺CD11b⁺, Gr1^{med}CD11b⁺ mature cell populations in the Sp. (D) Total cell number in the BM. (E) Percentage of donor cell engraftment in the BM. (F) Absolute cell number of donor B220⁺, CD3e⁺, Gr1⁺CD11b⁺, Gr1^{med}CD11b⁺ mature cell populations in the BM. All figures show the donor cell engraftment from control hematopoietic cells in white and the *Ccn2*^{Δ/Δ} hematopoietic cells in black bar and dot plots. Figures represent one performed experiment with n = 4 control mice and n = 4 *Ccn2*^{Δ/Δ} mice; *p-value ≤ 0.05 show significance in the comparison of control and *Ccn2*^{Δ/Δ} mice using the Mann-Whitney U-test.

To assess whether the increased mature cell engraftment was associated by an enhanced engraftment of more early hematopoietic stem and progenitor cell engraftment, we analyzed myeloid progenitors and HSC engraftment using flow cytometry analysis (Figure 30A). The analysis determined that the lineage-negative cell population was already elevated after transplantation of *Ccn2*^{Δ/Δ} LSK cells compared to the control LSKs (Figure 30B). Within this

population, the $KIT^+ SCA1^-$ myeloid progenitor (MP) cell population was also elevated in the mice transplanted with $Ccn2^{\Delta/\Delta}$ LSK cells (Figure 30C). Similarly, the absolute numbers of the $CD34^+$ LSK cells (ST-HSCs) were significantly elevated. But, no significant changes were detected in the the most early $CD34^-$ LSK cells (LT-HSCs, Figure 30D).

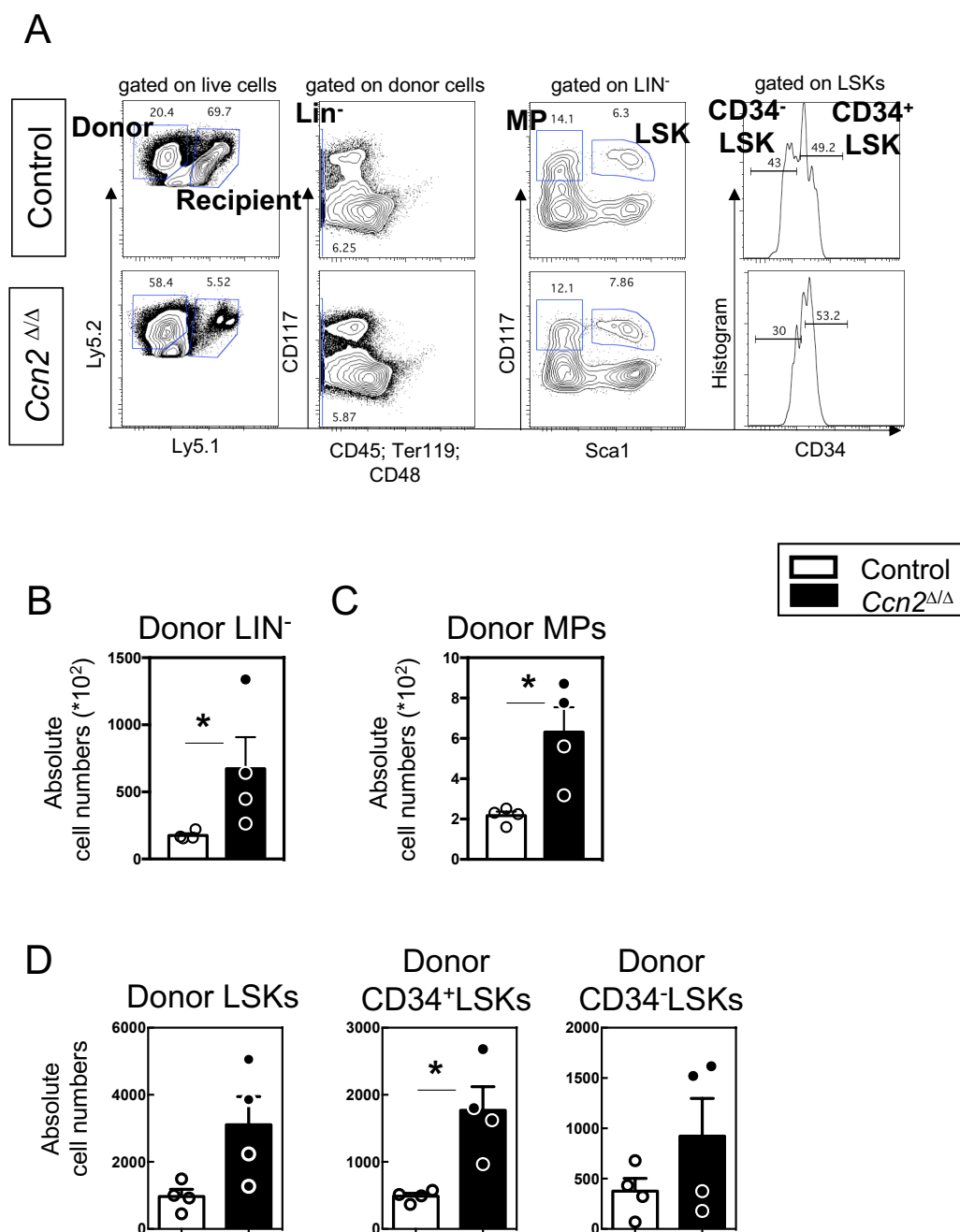


Figure 30. Hematopoietic progenitor and stem cell engraftment in the BM of transplanted LSK cells from control and $Ccn2^{\Delta/\Delta}$ mice as a long-term hematopoietic stress model. (A) Gating strategy of early hematopoietic cell population of donor cell engraftment. $Ly5.2^+$ cells were gated as donor cells. (B) Absolute cell numbers of the donor cell engrafted LIN^- cells. (C) Absolute cell numbers

of the donor cell engrafted MP cells. (C) Absolute cell number donor cell engrafted LSKs, CD34⁺LSKs- and CD34⁻LSKs cells. All figures show the donor cell engraftment from control hematopoietic cells in white and the *Ccn2^{Δ/Δ}* hematopoietic cells in black bar and dot plots. Figures represent one performed experiment with n = 4 control mice and n = 4 *Ccn2^{Δ/Δ}* mice; *p-value ≤0.05 show significance in the comparison of control and *Ccn2^{Δ/Δ}* using the Mann-Whitney U-test.

3.2.4.3.2 Isolated LSK cells from control and *Ccn2^{fl/fl}* cells transplanted as a long-term hematopoietic stress model.

In the previous experiments, *Ccn2* was deleted in all cell types four weeks prior to the isolation of HSCs and their transplantation into the 129xLy5.1 WT recipient mice (chapter 3.3.5.3.1). Since *Ccn2* was already deleted, the results of these experiments include possible effects of *Ccn2* expression on the earliest phases of engraftment: homing and perhaps the direct effects of HSC priming in the *Ccn2^{Δ/Δ}* donor environment. To exclude the effects of *Ccn2* in these these early events, we transplanted whole BM from untreated controls and RosaCre; *Ccn2^{fl/fl}* mice into lethally (8.5 Gy) irradiated 129xLy5.1 WT mice. To detect the effects of *Ccn2* expression in later engraftment, the mice were treated with Tamoxifen i.p four weeks after initial engraftment in order to knock out the *Ccn2* gene in the transplanted BM cells (Figure 31A).

This experiment analysis of PB engraftment after five (only one week after TAM treatment), ten, and 16 weeks did not reveal any significant changes in donor cell engraftment between the mice achieving controls (*Ccn2^{+/+}*) or *Ccn2^{fl/fl}* cells. Similarly, engraftment of mature cell compartments was not different in the PB at 5, 10 or 16 weeks (Figure 31B, C).

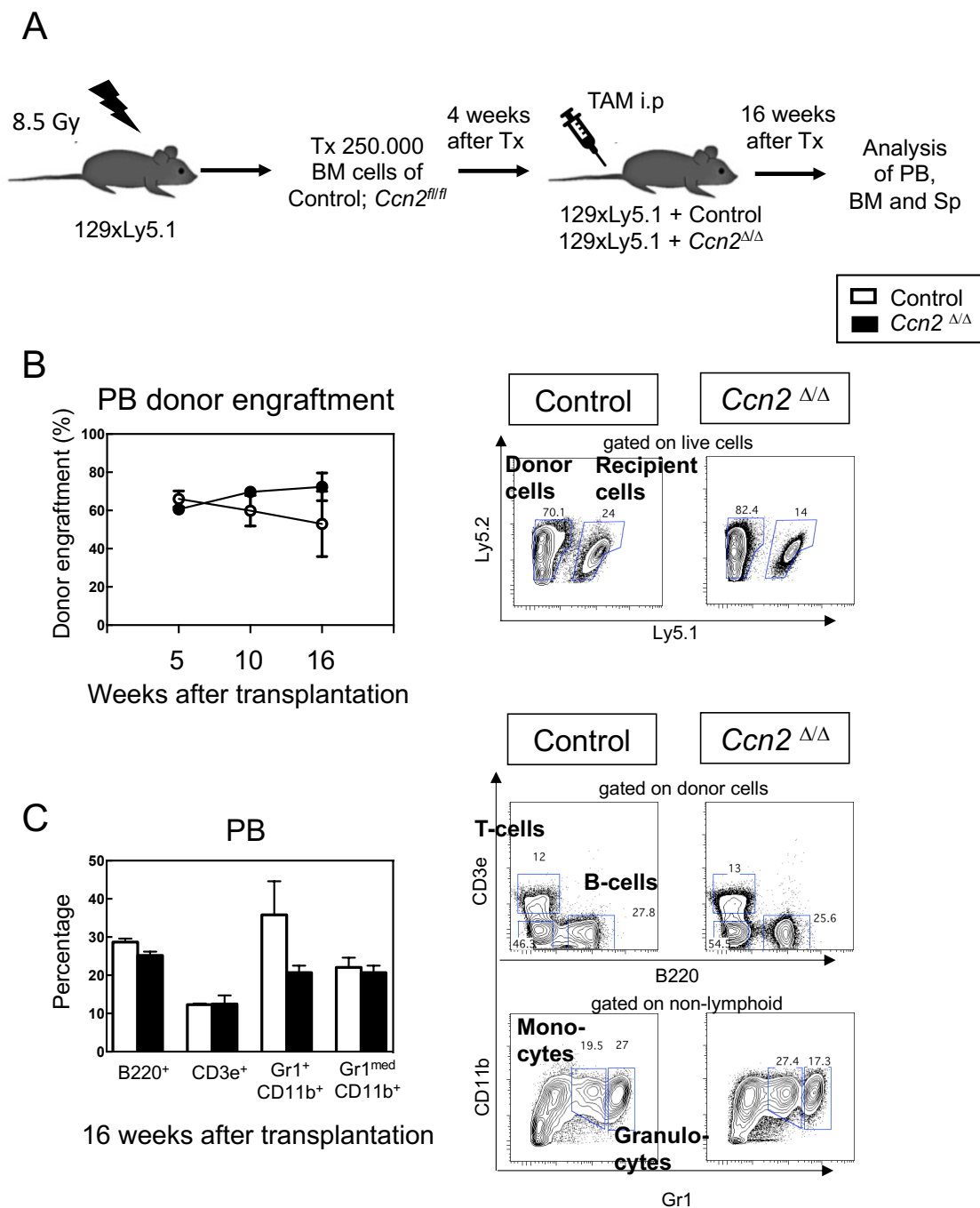


Figure 31. Engraftment in the PB of transplanted control and *Ccn2^{fl/fl}* whole BM into an WT microenvironment as a long-term hematopoietic stress model. (A) Experimental design for the long-term stress model in which WT 129xLy5.1 mice were lethally irradiated before 250.000 control and *Ccn2^{fl/fl}* whole bone marrow cells were transplanted. Four weeks after transplantation, the mice were treated with tamoxifen in order to knock out *Ccn2* in the hematopoietic cell compartments to get 129xLy5.1 + control and 129xLy5.1 + *Ccn2^{Δ/Δ}* chimera mice. Every five, ten and 16 weeks the engraftment and cell composition in the PB was analyzed. 16 weeks after transplantation the mice were sacrificed and the PB was analyzed using flow cytometry. (B) Donor cell engraftment in percentage in the PB five, ten and 16 weeks after transplantation and the representative gating strategy for the gating

of Ly5.2⁺ donor cells or Ly5.1⁺Ly5.2⁺ recipient cells. (C) Example for the gating of donor B220⁺, CD3e⁺, Gr1⁺CD11b⁺, Gr1^{med}CD11b⁺ mature cell populations in percentage. Here shown in the PB. In all figures the engraftment of the control hematopoietic cells is shown in white- and *Ccn2*^{Δ/Δ} hematopoietic cells are shown in black bar graphs. Figures show one performed experiment with n = 2 mice recipient control mice and n = 4 for recipient *Ccn2*^{Δ/Δ} mice; *p-value ≤0.05 show significance in the comparison of control and *Ccn2*^{Δ/Δ} using the Mann-Whitney U-test.

In addition, the Sp and BM did not reveal any significant differences in total cell number or engraftment (Figure 32A, B, D and E). Beside a reduced granulocyte (Gr1⁺CD11b⁺) engraftment in the Sp or no changes in the mature cellularity between the control and the *Ccn2*^{Δ/Δ} hematopoietic cells regenerated in the WT microenvironment 16 weeks after transplantation were found (Figure 32C and F).

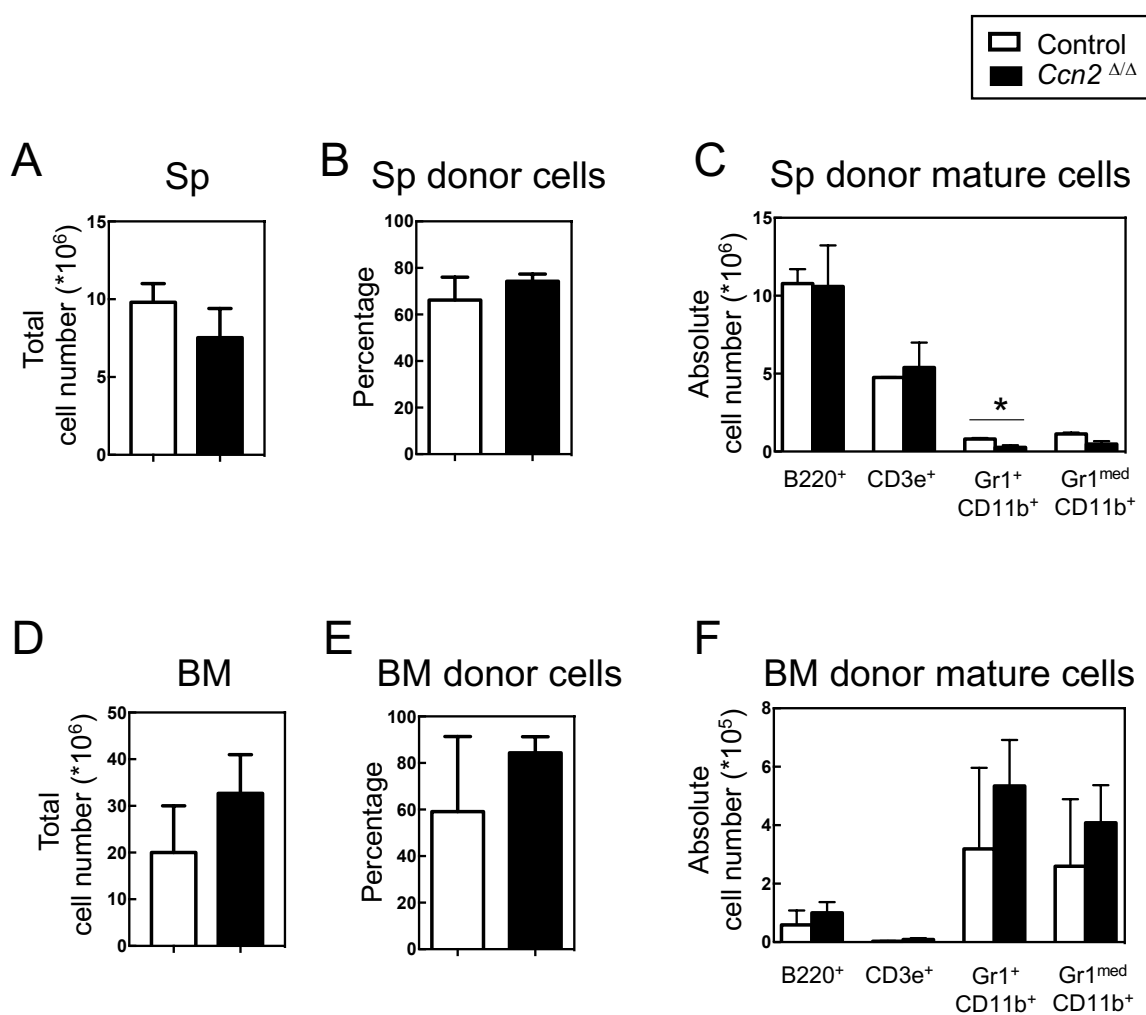


Figure 32. Mature cell engraftment in the Sp and BM of transplanted control and *Ccn2*^{fl/fl} whole BM into an WT microenvironment as a long-term hematopoietic stress model. (A) Total cell

number in the Sp. (B) Percentage of donor cell engraftment in the Sp. (C) Absolute cell number of donor B220⁺, CD3e⁺, Gr1⁺CD11b⁺, Gr1^{med}CD11b⁺ mature cell populations in the Sp. (D) Total cell number in the BM. (E) Percentage of donor cell engraftment in the BM. (F) Absolute cell number of donor B220⁺, CD3e⁺, Gr1⁺CD11b⁺, Gr1^{med}CD11b⁺ mature cell populations in the BM. In all figures the engraftment of the control hematopoietic cells is shown in white and *Ccn2*^{Δ/Δ} hematopoietic cells are shown in black bar graphs. Figures show one performed experiment with n = 2 mice recipient control mice and n = 4 for recipient *Ccn2*^{Δ/Δ} mice; *p-value ≤0.05 show significance in the comparison of control and *Ccn2*^{Δ/Δ} using the Mann-Whitney U-test.

In further flow cytometry analyses (Figure 33A) the earlier hematopoietic cells in the BM, Lineage- stem and progenitor populations in the BM (Figure 33B and C) were similar between the two groups. These analyses strengthen the view that *Ccn2* expression is mostly required in HSC priming and homing after stress, but not in steady state hematopoiesis.

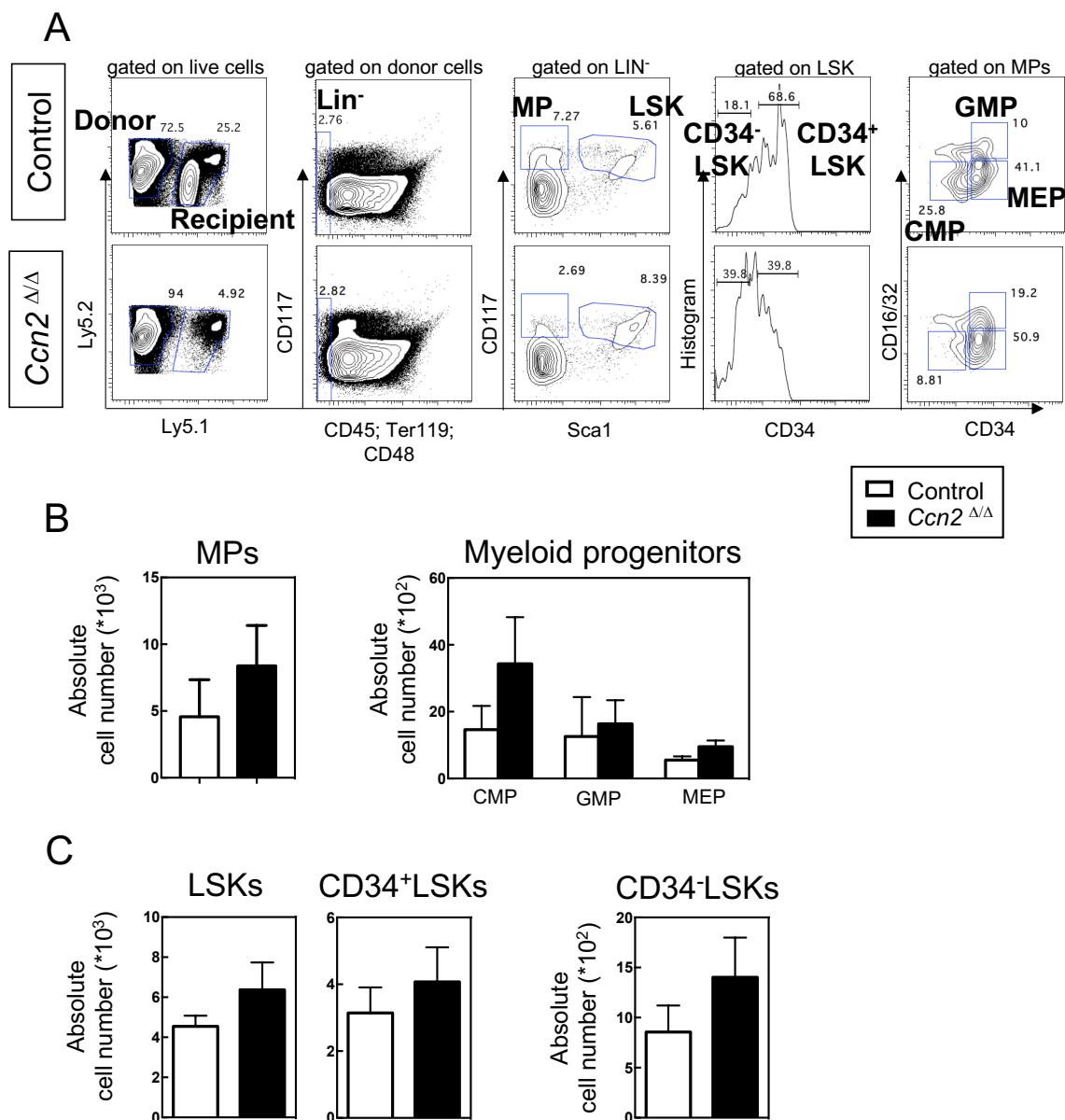


Figure 33. Hematopoietic progenitor and stem cell engraftment in the BM of transplanted control and *Ccn2*^{fl/fl} whole BM into an WT microenvironment as a long-term hematopoietic stress model. (A) Gating strategy of early cell population from donor cell engraftment. Ly5.2⁺ cells were gated as donor cells. Out of the donor cell population the lineage negative population was separated by excluding CD45⁺, Ter119⁺ and CD48⁺ cells. The LSK cells were gated as CD117⁺ and Sca1⁺ while the MPs are Sca1⁻. Out of the LSK compartment the HSCs were separated as CD34⁺LSK and CD34⁻LSK cells. The myeloid progenitor cells were gated out of the MP gate as CD34⁻CD16/32⁻ (MEPs), as CD34⁺CD16/32⁻ (CMPs) and as CD34⁺CD16/32⁺ (GMPs). (B) Absolute cell numbers of the donor cell engrafted MPs and absolute cell numbers of the CMP, MEP and GMP myeloid progenitor cells. (C) Absolute cell number of LSKs, CD34⁺LSKs and CD34⁻LSKs donor cells. In all figures the engraftment of the control hematopoietic cells is shown in white- and *Ccn2*^{Δ/Δ} hematopoietic cells are shown in black bar graphs. Figures show one performed experiment with n = 2 mice recipient control mice and n = 4 for recipient

Ccn2^{Δ/Δ} mice; *p-value ≤0.05 show significance in the comparison of control and *Ccn2^{Δ/Δ}* using the Mann-Whitney U-test.

Taken together, this single experiment suggests that the enhanced regeneration potential of *Ccn2^{Δ/Δ}* HSCs and progenitor cells, is most likely due to engraftment advantages of the HSCs because of priming in the *Ccn2^{Δ/Δ}* environment or differential homing in the WT recipients.

3.2.4.3.3 Extrinsic function of Ccn2 during prolonged stress

As *Ccn2* is mainly expressed by BM stromal cells, rather than hematopoietic cells (Cheung et al., 2014) we decided to determine the impact of *Ccn2* loss in the microenvironment during a long-term regeneration stress model. Therefore we, transplanted 300 CD34⁺CD150⁺LSK cells (LT-HSCs, 129xLy5.1) into lethally irradiated control and *Ccn2^{Δ/Δ}* mice (Figure 34A).

These experiments demonstrated that after an unchanged early recovery (five and ten weeks after transplantation), the donor cells showed reduced engraftment in the *Ccn2* deficient microenvironment in the PB 16 weeks after transplantation (Figure 34B). In accordance with this, analysis of the Sp and BM showed decreased numbers of WT donor cells in the *Ccn2^{Δ/Δ}* recipients compared to controls 16 weeks after transplantation (Figure 34D, F). Interestingly, while engraftment of CD3e⁺ T-cells or Gr1^{med}CD11b⁺ monocytes were unchanged, we found significant reductions of Gr1⁺CD11b⁺ granulocytes in the PB, Sp and BM as well as reduced B220⁺ B-cells in the SP (Figure 34C, E and G). In the BM, however, WT HSCs showed elevated BM engraftment of B220⁺ B-cells in the *Ccn2^{Δ/Δ}* recipients compared to control recipients (Figure 34G). This suggests that *Ccn2* expression in the environment may affect homing of B220⁺ B cells.

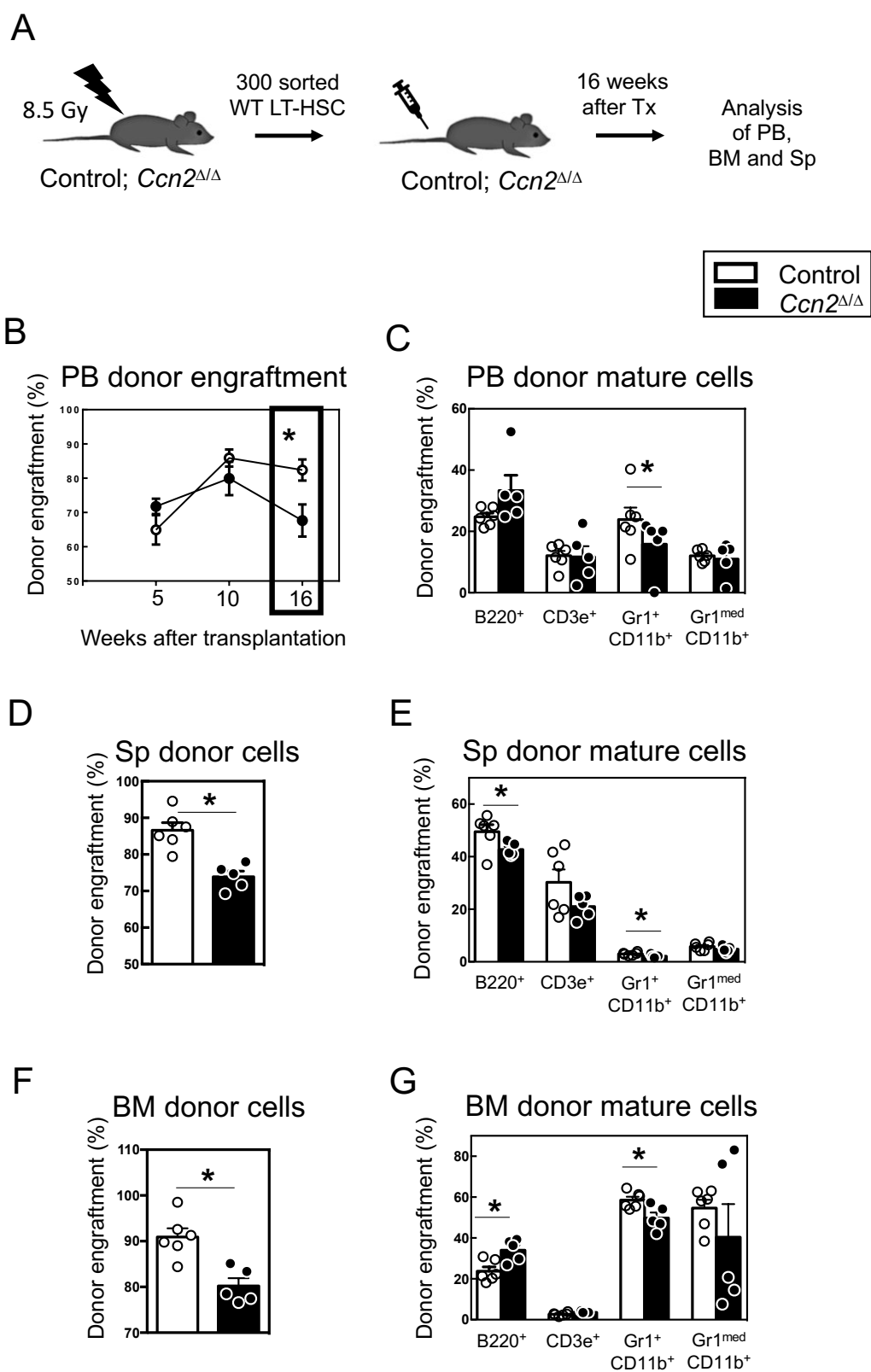


Figure 34. Engraftment of mature cell populations of transplanted WT HSCs into a *Ccn2* deficient microenvironment as a long-term hematopoietic stress model. (A) Experimental design for the

long-term stress model in which control and *Ccn2^{Δ/Δ}* mice were lethally irradiated before 300 WT CD34⁺SLAM cells from 129xLy5.1 mice were transplanted. Every five, ten and 16 weeks the engraftment and cell composition in the PB was analyzed. 16 weeks after transplantation the mice were sacrificed and the PB, Sp and BM was analyzed using flow cytometry. (B) Donor cell engraftment in percentage in the PB five, ten and 16 weeks after transplantation. (C) Donor cell engraftment in percentage of B220⁺, CD3e⁺, Gr1⁺CD11b⁺, Gr1^{med}CD11b⁺ mature cell populations in the PB. (D) Donor cell engraftment in percentage in the Sp and (F) in the BM. (E) Percentage of B220⁺, CD3e⁺, Gr1⁺CD11b⁺, Gr1^{med}CD11b⁺ donor cell populations in the Sp and (G) in the BM. In all figures the WT HSCs regenerated in the control microenvironment is shown in white- and the cells regenerated in the *Ccn2* deficient microenvironment is shown in black bar and dotplot graphs. Figures show two independently performed experiments with n = 6 control mice and n = 5 *Ccn2^{Δ/Δ}* mice; *p-value ≤0.05 show significance in the comparison of control and *Ccn2^{Δ/Δ}* mice using the Mann-Whitney U-test.

The changes in numbers of mature subtypes in the PB, Sp and BM could be caused by underlying changes in earlier stem and progenitors. Analysis of these donor cells in recipient BM showed unchanged numbers of MPs (Figure 35B). But, a significant impaired WT engraftment of CD34⁺SLAM (ST-HSC, Figure 35D) was found in the *Ccn2^{Δ/Δ}* recipients, whereas donor CD34⁺SLAM (LT-HSCs, Figure 35E) were unchanged in the *Ccn2^{Δ/Δ}* recipients.

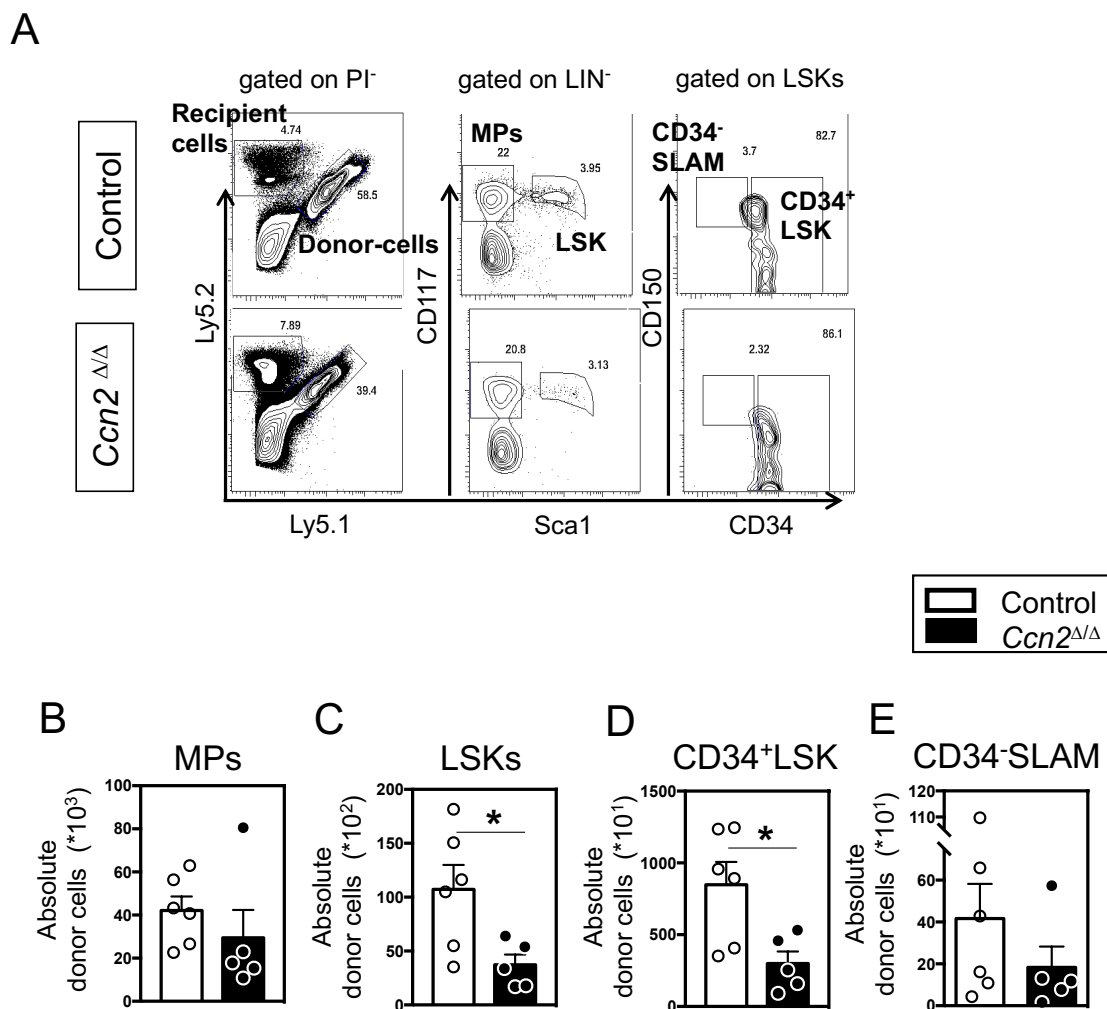


Figure 35. Engraftment of MPs and HSCs of transplanted WT HSCs into a *Ccn2* deficient microenvironment as a long-term hematopoietic stress model. (A) Gating strategy of donor LT-HSC engraftment in the BM. (B) Donor cell engraftment in absolute cell numbers of the MPs, (C) LSKs, (D) ST-HSCs and (E) LT-HSCs in the BM. In all figures the WT HSC regenerated in the control microenvironment is shown in white- and the cells regenerated in the *Ccn2* deficient microenvironment is shown in black bar and dotplot graphs. Figures show two independently performed experiments with $n = 6$ control mice and $n = 5$ *Ccn2*^{Δ/Δ} mice; * p -value ≤ 0.05 show significance in the comparison of control and *Ccn2*^{Δ/Δ} mice using the Mann-Whitney U-test.

In summary, these results suggest that loss of environmental *Ccn2* in recipient mice results in decreased regeneration of WT cells with impaired HSC self-renewal and possible reduced myeloid cell differentiation.

3.2.4.4 Ccn2 during irradiation stress

Bone marrow transplantation includes another form of stress – the total body irradiation. Irradiation was shown to induce *Ccn2* expression in the spleen, kidney and liver (Zhang et al., 2015). We wondered if and which cells might induce *Ccn2* after irradiation in the bone marrow. Additionally, we studied the impact of *Ccn2* loss after irradiation on the niche cells and hematopoietic cells.

3.2.4.4.1 Irradiation stress induced CCN2 content in the bones

As a first experiment we decided to treat, 129xB16 mice with cytotoxic lethal dose of irradiation (8.5 Gy). After 24 hours, the mice were sacrificed and the bone slices from the tibia of non-irradiated (steady-state) and irradiated mice were stained for the CCN2 protein.

During steady-state conditions the CCN2 expression was detectable in the bone slices, including hematopoietic cells and megakaryocytes (Figure, 36 (untreated, CCN2 in green)). One day after irradiation, CCN2 protein expression strongly increases compared to the steady-state condition but not as abundantly in megakaryocytes (Figure, 36 (irradiation, CCN2 in bone slices)).

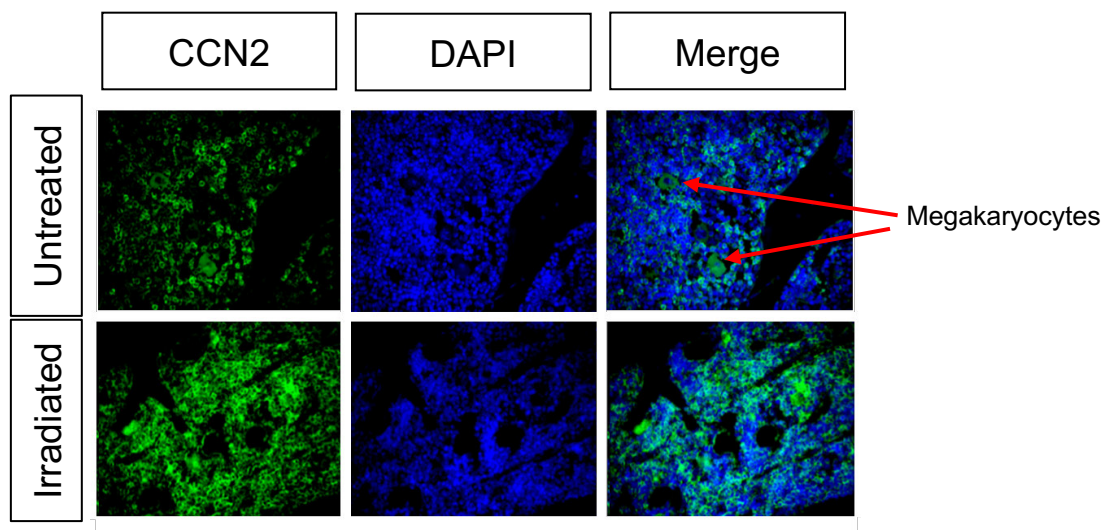


Figure 36. CCN2 protein expression during steady-state and after irradiation. CCN2 expression in green (left side) in bone slices of untreated and 24 hrs after 8.5 Gy irradiation of 129xB16 mice. Staining of the nucleus with DAPI in blue (middle) and the merged pictures CCN2 in green and nucleus in blue (right side, data generated in cooperation with Rouzanna Istvánffy).

3.2.4.4.2 Irradiation stress induced *Ccn2* RNA content in hematopoietic- and stromal cells

In order to determine changes in *Ccn2* expression in different cell types during irradiation (IR) stress conditions we performed RT-PCR on sorted BM cell populations (Figure 37A).

By sublethal irradiation method (4.5Gy) only a part of dividing cells die, allowing the isolation of enough cells for analysis. As *Ccn2* is an immediate early response to stress gene we decided to isolate the BM and BM stromal cells of Rosa26CreEr^{T2} positive and *Ccn2*^{wt/wt} control mice five hours after irradiation. Interestingly, already five hours after irradiation the percentage of B220⁺ B-cells and Gr1^{med}CD11b⁺ monocytes was significantly reduced and the Gr1⁺CD11b⁺ granulocytes significantly increased, while the numbers of CD3e⁺ T-cells was not changed compared to the unirradiated mice (Figure 37B).

Additionally, the numbers of Lin⁻Sca1⁻Kit⁺ multipotent progenitors (MPs) cells, CD48⁻ LSKs and CD34⁺ CD48⁻ LSK cells (ST-HSCs) were significantly reduced whereas the most early cells CD34⁻ CD48⁻ CD150⁺ LSK cells (LT-HSCs) were increased after irradiation compared to the untreated mice (Figure 37C).

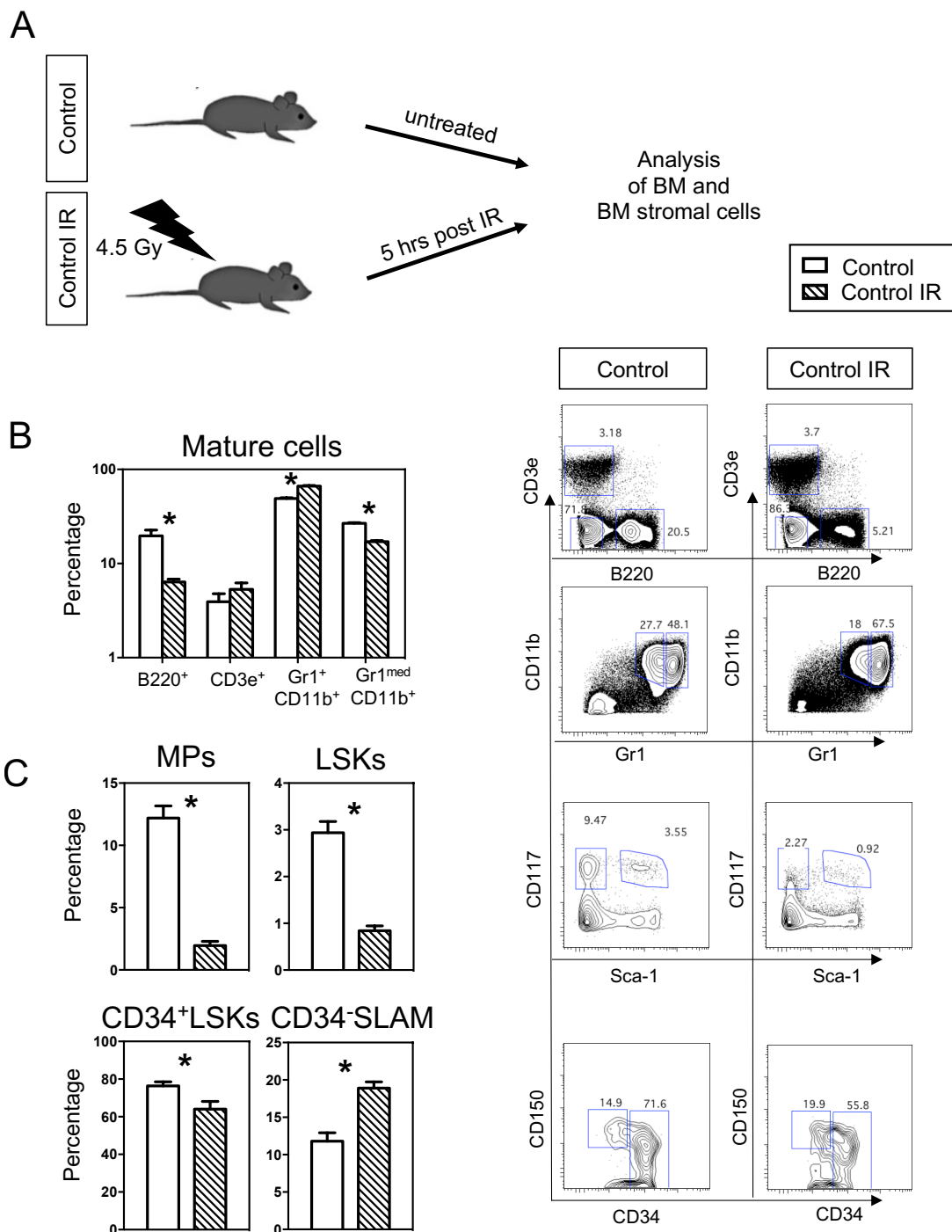


Figure 37. Hematopoietic cell composition after five hours of irradiation (IR). (A) Experimental design: Rosa26CreEr^{T2} positive Ccn2^{Wt/Wt} mice were irradiated with 4.5 Gy and analyzed five hours after irradiation. As controls the Rosa26CreEr^{T2} positive Ccn2^{Wt/Wt} untreated mice were used. The cell composition was analyzed using flow cytometry. (B) Mature cell numbers in percentage of B220⁺, CD3e⁺, Gr1⁺CD11b⁺, Gr1^{med}CD11b⁺ cells and the gating strategy. (C) MPs, LSKs, CD34⁺- and CD34-SLAM cell numbers in percentage and the gating strategy. Figures B, and C show bar diagrams of untreated control mice: n = 4 in white, and control irradiated n = 4 mice in black and white stripes; *p-

value ≤ 0.05 show significance in the comparison of untreated mice and controls using the Mann-Whitney U-test (generated in collaboration with masterstudent Katharina Kaiser).

Also the sorted LSK cells and ECs (Figure 38A) showed a tendency of reduced numbers after irradiation. Compared to these cells, the OBC and MSC numbers were unchanged (Figure 38A).

In hematopoietic cells, irradiation induces a 3-fold and 1.5-fold increase in granulocytes and LSK cells, respectively (Figure 38B). When evaluating *Ccn2* gene expression, we found that OBCs showed 20-fold increase after irradiation, whereas expression of *Ccn2* in ECs and MSCs remained unchanged (Figure 38C).

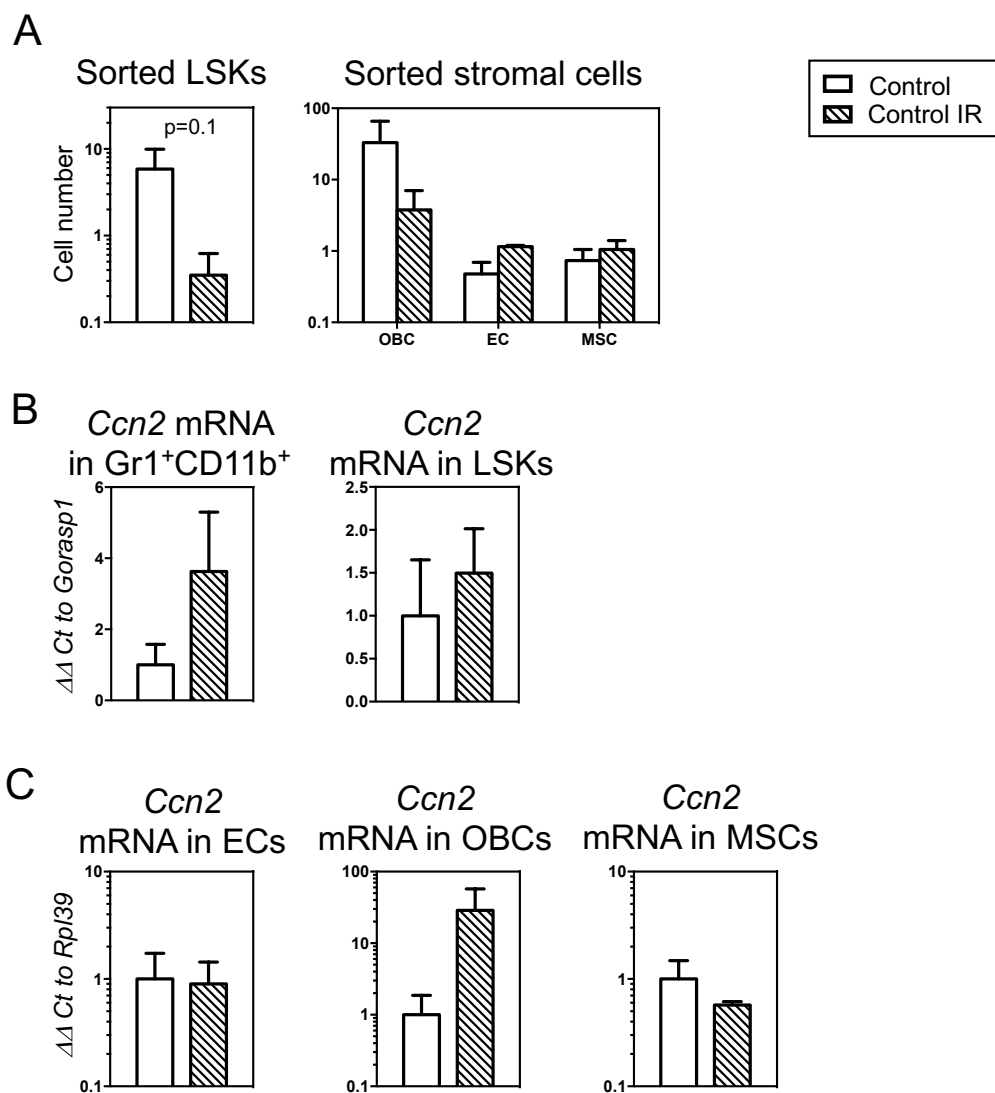


Figure 38. *Ccn2* expression in 4.5 Gy irradiated hematopoietic- and stromal cells compared to untreated cells. (A) Cell numbers of sorted LSK cells and EC, OBC and MSC stromal cells. (B) *Ccn2*

mRNA content in untreated and 4.5 Gy irradiated Gr1⁺CD11b⁺ and LSK cells relative to housekeeping gene *Gorasp1*. (C) *Ccn2* mRNA content in untreated and 4.5 Gy irradiated ECs, OBCs and MSCs relative to housekeeping gene *Rpl39*. Figure A shows a bar diagrams of control untreated mice: n = 4 in white, and control irradiated mice: n = 4 in black and white stripes; Figure B and C show the mRNA content as a bar diagrams of three pooled control untreated mice in white, and control irradiated mice in black and white stripes. Three independently performed experiments are shown in B and two independently performed experiments are shown in C; *p-value ≤ 0.05 show significance in the comparison of *Ccn2* content of untreated and irradiated controls using the Mann-Whitney U-test (generated in collaboration with masterstudent Katharina Kaiser).

3.2.4.4.3 Irradiation stress induced CCN2 protein upregulation in hematopoietic- and stromal cells

The results at Figure 38C, show that *Ccn2* mRNA content is rapidly increased after total-body irradiation, especially in the OBC compartment. To validate the results of the *Ccn2* mRNA analyses on the protein level, we isolated cells and pooled three adult (eight- to twelve-week-old) untreated and sublethal irradiated (after 24 hours) 129xB16 (WT) mice and stained the hematopoietic and stromal cells for CCN2 protein using immunofluorescence (Figure 39A).

The results show, that the irradiation does not change the CCN2 protein levels in CD3 ϵ ⁺ lymphoid cells or in the myeloid compartments of Gr1⁺CD11b⁺ and Gr1^{med}CD11b⁺ cells (Figure 39B). However, in the B220⁺ cells the CCN2 expression is significantly reduced 24 hours after irradiation (Figure 39B). Interestingly, in the earlier hematopoietic cell populations like the MPs and LSK cells the CCN2 protein content is similar in untreated and irradiated WT mice (Figure 39C).

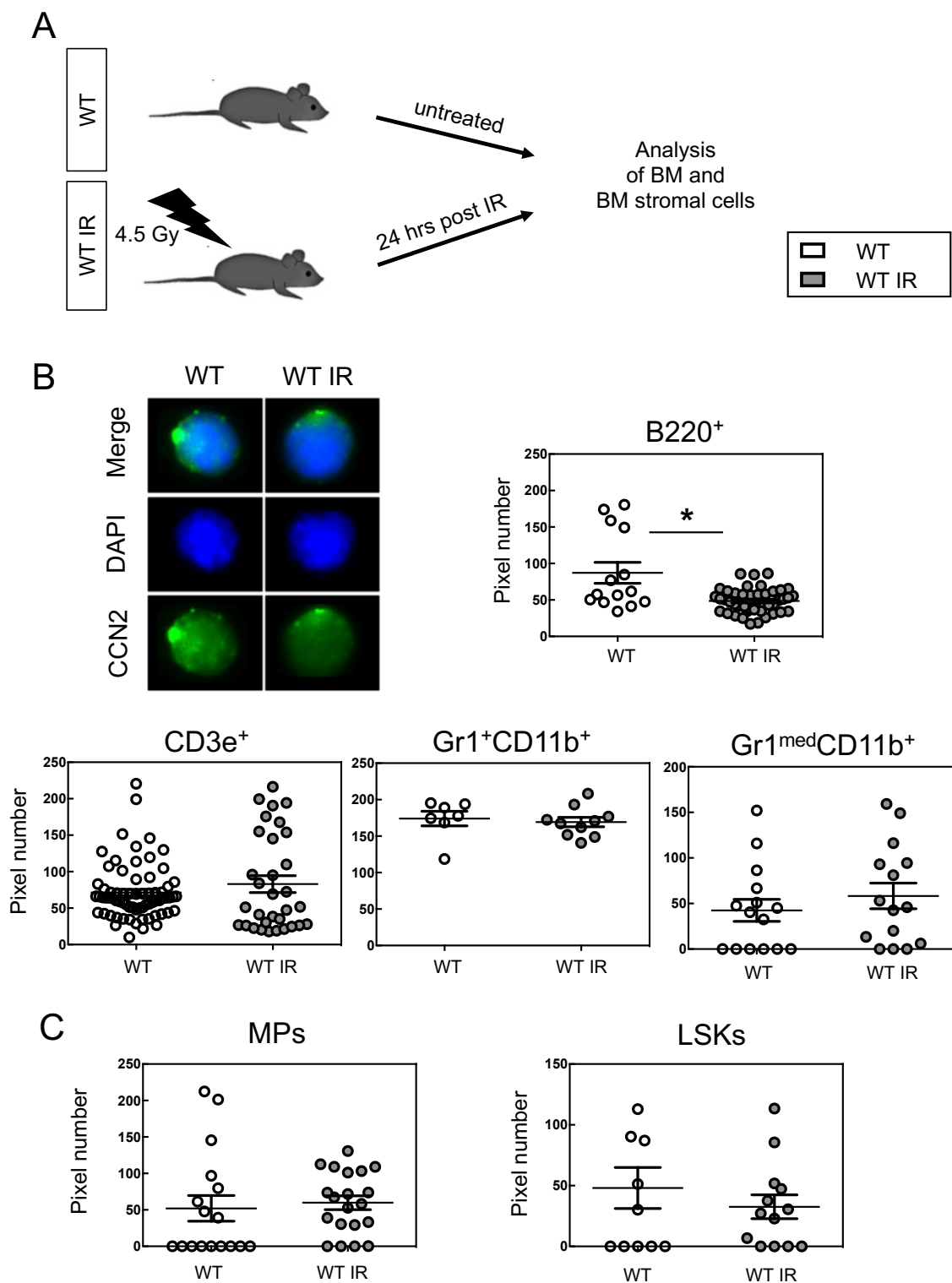


Figure 39. CCN2 protein content 24hrs after irradiation (IR) in different hematopoietic cell populations. (A) Experimental design of untreated and 4.5 Gy irradiated 129xB16 mice sacrificed 24hrs after irradiation to analyze the protein content of CCN2 in hematopoietic- and stromal cells. (B) Representative immunofluorescence staining for the CCN2 protein in green, the nuclei staining with

DAPI in blue and the merged picture of B220⁺ cells from untreated and irradiated WT mice. CCN2 protein content as pixel number of untreated and treated B220⁺, CD3e⁺, Gr1⁺CD11b⁺, Gr1^{med}CD11b⁺ cells. (C) CCN2 protein content as pixel number of untreated and treated MPs and LSKs. Figures B, and C show dot plots of a group of three WT untreated pooled mice in white, and three WT sublethal irradiated pooled mice in grey; *p-value ≤ 0.05 show significance in the comparison of untreated and sublethal irradiated WT using the Mann-Whitney U-test (generated in collaboration with masterstudent Anna Hasenkopf).

Importantly, irradiation significantly increases the CCN2 level in OBCs compared to the untreated controls (Figure 40A and 40B). Similar to the *Ccn2* mRNA analyses, the CCN2 protein expression in the stromal cell EC- and MSC compartments was unchanged by irradiation (Figure 40C).

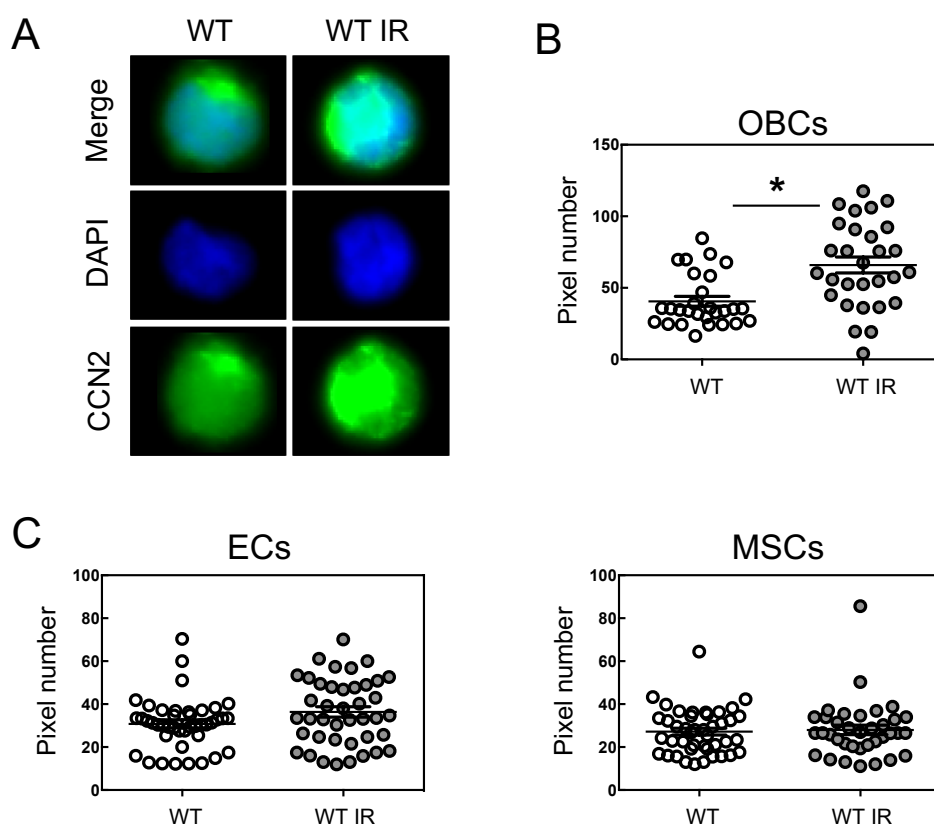


Figure 40. CCN2 protein content 24hrs after irradiation (IR) in different stromal cell populations.

(A) Representative immunofluorescence staining for the CCN2 protein in green, the nuclei staining with DAPI in blue and the merged picture of Sca1⁺CD166⁺ OBCs from untreated and irradiated WT mice. CCN2 protein content as pixel number of untreated and treated Sca1⁺CD166⁺ OBCs, Sca1⁺CD31⁺ ECs and Sca1⁺CD166⁻ MSCs. Figures show dot plots of a group of three pooled untreated WT mice in white, and three pooled sublethal irradiated WT mice in grey; *p-value ≤ 0.05 show significance in the

comparison of untreated and sublethal irradiated WT using the Mann-Whitney U-test (generated in collaboration with masterstudent Anna Hasenkopf).

3.2.4.4.4 *Ccn2* function in stromal cell recovery after 4.5 Gy irradiation

Prior to transplantation, recipients are usually myeloablated using irradiation or cytostatic treatment. Since in our transplantation model, we irradiate mice to condition recipients, we investigated the effects of irradiation on BM stromal cell populations at different time points after irradiation in order to analyse the role of *Ccn2* during stromal cell recovery we used *Ccn2^{ΔΔ}* and control mice. Due to practical reasons of studying mice over longer periods after irradiation, we did not use a lethal dose of irradiation (as in the transplantation model), but chose to irradiate with a sublethal dose of 4,5 Gy, that will already induce *Ccn2* as shown in chapter 3.2.3.4.2/3. Then five and 14 days after irradiation (5d IR, 14d IR) we sacrificed the mice and analysed the stromal cell compartment by flow cytometry (Figure 41A and 41B).

In the first analysis, the number of ECs, OBCs and MSCs were assessed in the endosteal region of the BM (crushed bones remaining in BM after central BM was flushed) during steady state and after irradiation stress. During steady state conditions, similar numbers of the endosteal cells or ECs, OBCs or MSCs were detectable in control and *Ccn2^{ΔΔ}* mice (Figure 41C, D, E, F).

After irradiation, the number of endosteal cells was reduced after five and 14 days (5d and 14d, Figure 41C). However, irradiation did not affect the total number of endosteal cells when comparing control and *Ccn2^{ΔΔ}* mice. Interestingly, five days after irradiation, ECs were significantly increased in *Ccn2^{ΔΔ}* mice (Figure 41D). Fourteen days after irradiation, cell numbers in all groups were recovered and unchanged.

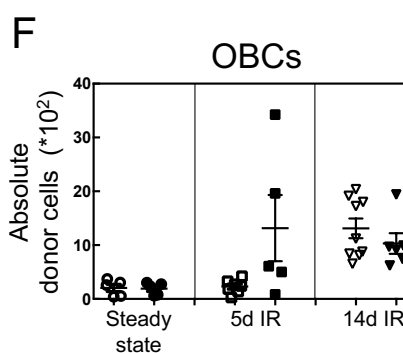
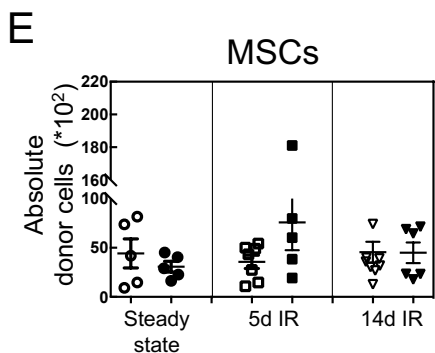
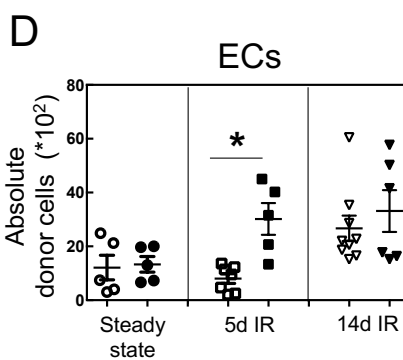
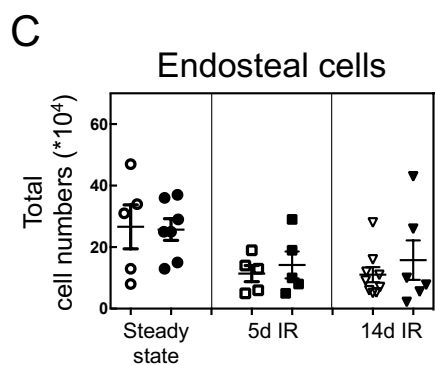
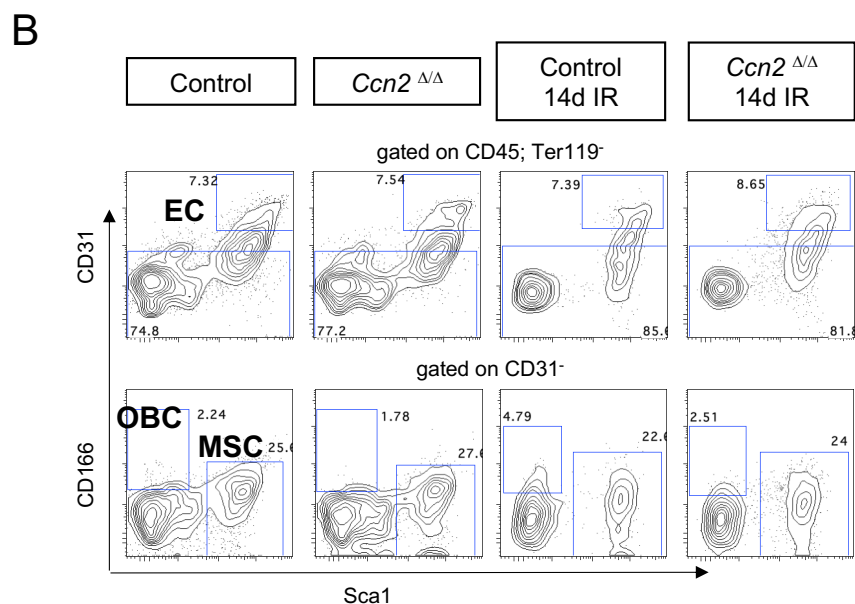
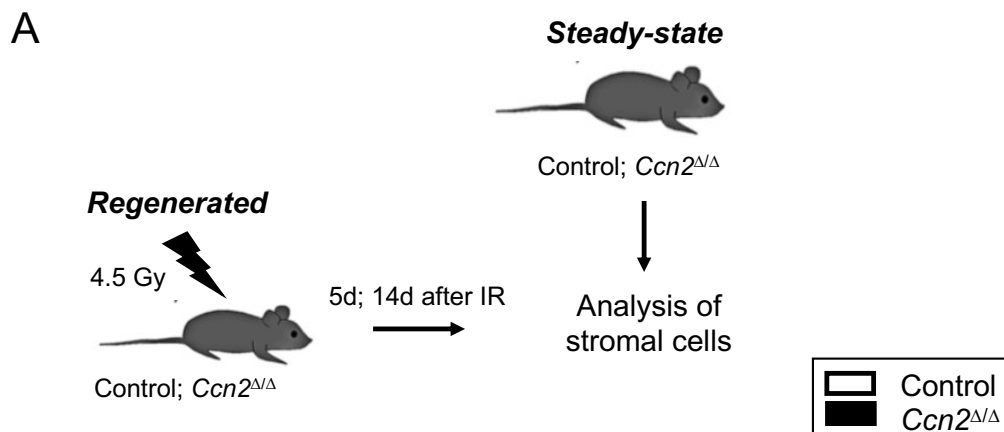


Figure 41. Stromal cells after sublethal irradiation (IR) of control and *Ccn2^{Δ/Δ}* mice as short-term stress model. (A) Experimental design: two weeks after TAM treatment the mice were sublethal (4.5 Gy) irradiated and sacrificed five, and 14 days after irradiation. Additionally untreated mice (steady-state) were used as controls in the different experiments. The bone marrow stromal cells were isolated as endosteal cells from the different groups for analysis. (B) Representative gating strategy for the gating of ECs as CD45⁺Ter119⁻Sca1⁺CD31⁺ cells, the OBCs as CD45⁺Ter119⁻CD31⁻Sca1⁺CD166⁺ cells and the MSCs as CD45⁻Ter119⁻CD31⁻Sca1⁺CD166⁻ in steady-state and 14 days after IR of control and *Ccn2^{Δ/Δ}* mice. (C) Counted total cell numbers of endosteal cells at steady-state, five and 14 days after IR. (D) Absolute cell numbers of ECs at steady-state, five and 14 days after IR. (E) Absolute cell numbers of MSCs at steady-state, five and 14 days after IR. (F) Absolute cell numbers of OBCs at steady-state, five and 14 days after IR. All figures show the steady state results in round shaped dot plots, the five days irradiated in squared dot plots and the 14 days irradiated in triangled dot plots. Control cells are shown in white and the *Ccn2^{Δ/Δ}* cells in black dot plots. Figures represent two performed experiments with steady-state control n = 5 and *Ccn2^{Δ/Δ}* n = 7, five days irradiated control n = 5 and *Ccn2^{Δ/Δ}* n = 5, 14 days irradiated control n = 4 and *Ccn2^{Δ/Δ}* n = 3 mice. *p-value ≤0.05 show significance in the comparison of control and *Ccn2^{Δ/Δ}* mice using the Mann-Whitney U-test.

To determine whether, MSCs might show altered cellular functions, despite that no differences were found in their cell numbers after irradiation, we cultured the collagenase digested bone chips until passage four (Landspersky et al., 2022, Figure 42A).

In a first experiment, we investigated the ability of MSCs to adhere to plastic isolated from 14d IR and steady state mice (Figure 42B). This experiment revealed reduced adherence of *Ccn2^{Δ/Δ}* MSCs from steady state mice. Fourteen days after irradiation, plastic adherence was unchanged between the two groups. But, MSCs from irradiated mice also showed reduced plastic adherence in contrast to steady state MSCs. Interestingly, the MSCs from *Ccn2^{Δ/Δ}* mice, adhered similarly as the MSCs isolated from both irradiated groups.

To determine the potential of the plastic-adhered MSCs to form fibroblast-like colonies (grown from CFU-Fs), we cultured the adhered cells and found that MSCs from irradiated mice (five and 14 days) show reduced colony formation. However, the frequency of CFU-F is not affected in *Ccn2^{Δ/Δ}* MSCs (Figure 42C).

Since the number of cells adhering to plastic is reduced in *Ccn2^{Δ/Δ}* MSCs, this finding could suggest that the reduced adherence of these cells is not due to reduced CFU-F adherence.

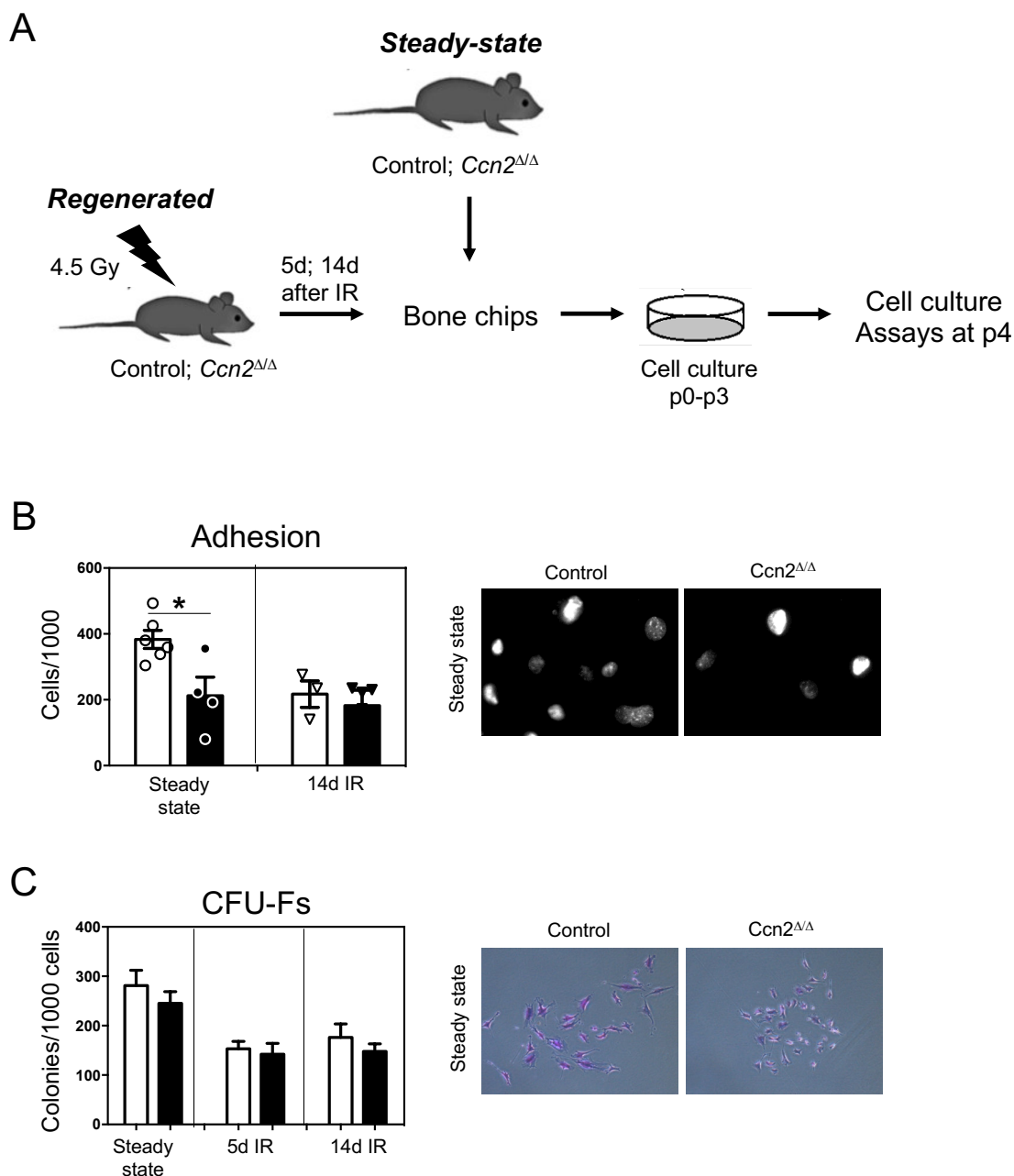


Figure 42. Adhesion and CFU-F potential at steady-state and after sublethal irradiation of control and *Ccn2*^{Δ/Δ} as short-term stress model. (A) Experimental design: control and *Ccn2*^{Δ/Δ} mice were sublethal (4.5 Gy) irradiated and sacrificed five and 14 days after irradiation. Additionally untreated mice (steady-state) were used as controls in the different experiments. After the BM and endosteal cells were isolated, the bone chips were cultured in MSC media till passage three until the experiments were performed at p4. (B) Adherent cells counted from 1000 cultured cells per control and *Ccn2*^{Δ/Δ} MSCs at steady state and after 14 days of irradiation. (C) Number of CFU-Fs per 1000 cultured cells from control and *Ccn2*^{Δ/Δ} MSCs at steady state and after five and 14 days of irradiation. All figures show the results of the control in white and the results from *Ccn2*^{Δ/Δ} MSCs black bar graphs. Figures represent two

performed experiments for steady-state and 14 days after irradiation and one performed experiment after five days of irradiation. *p-value ≤ 0.05 show significance in the comparison of control and *Ccn2^{ΔΔ}* using the Mann-Whitney U-test (generated in collaboration with masterstudent Katharina Kaiser).

The fibroblast-like colonies can be expanded to MSCs, which have the potential to differentiate *in vitro* into adipocytes, osteoblasts and chondrocytes (Friedenstein et al., 1976; Mendez-Ferrer et al., 2010; Oswald et al., 2004; Wang et al., 2006). As CCN2 was reported to be important for a balanced MSCs differentiation (Battula et al., 2013; Schutze et al., 2005; Wang et al., 2009), we were interested in the differentiation potential of control and *Ccn2^{ΔΔ}* MSCs isolated from mice during steady state conditions and after sublethal irradiation. Two different assays were performed in order to answer this question.

In the first type of assay, differentiation of p4 MSCs was induced using media containing growth factors, known to induce an adipogenic or osteogenic differentiation of the MSCs (see Materials and Methods 2.1.6.1 Ordered buffer, medium and solution). Here, we found a similar adipogenic differentiation as measured by the formation of lipid droplets of control and *Ccn2^{ΔΔ}* MSCs when MSCs were isolated from the bone chips of steady state as well as sublethal irradiated mice (5d and 14d after IR, Figure 43A).

Interestingly, despite that *Ccn2* appears to be expressed and regulated most in OBCs, the osteogenic potential as measured by calcium deposits was unchanged in MSCs isolated from steady state mice but reduced in *Ccn2* deleted MSCs when compared to control cells five days after irradiation (Figure 43B). 14 days after IR no differences between the two groups were detectable. Generally, irradiation reduced the deposited calcium five and 14 days after irradiation and reached a significantly reduction five days after irradiation in the *Ccn2^{ΔΔ}* MSCs when compared to the untreated *Ccn2^{ΔΔ}* MSCs (Figure 43B).

In the second type of assay, MSCs were cultured without passaging until a spontaneous differentiation of the MSCs into adipocytes or osteoblasts became visible. As for the induced differentiation, there was no alteration detectable in adipo- or osteogenic potential between control and *Ccn2^{ΔΔ}* MSCs isolated during steady state or 14 days after irradiation. Interestingly, *Ccn2^{ΔΔ}* MSCs showed an increased adipogenic potential when isolated from sublethal irradiated mice compared to MSCs from steady state *Ccn2^{ΔΔ}* mice (Figure 43C). In accordance with an increased adipogenic potential of MSCs from irradiated mice, their osteogenic potential was slightly reduced (not significant, Figure 43D).

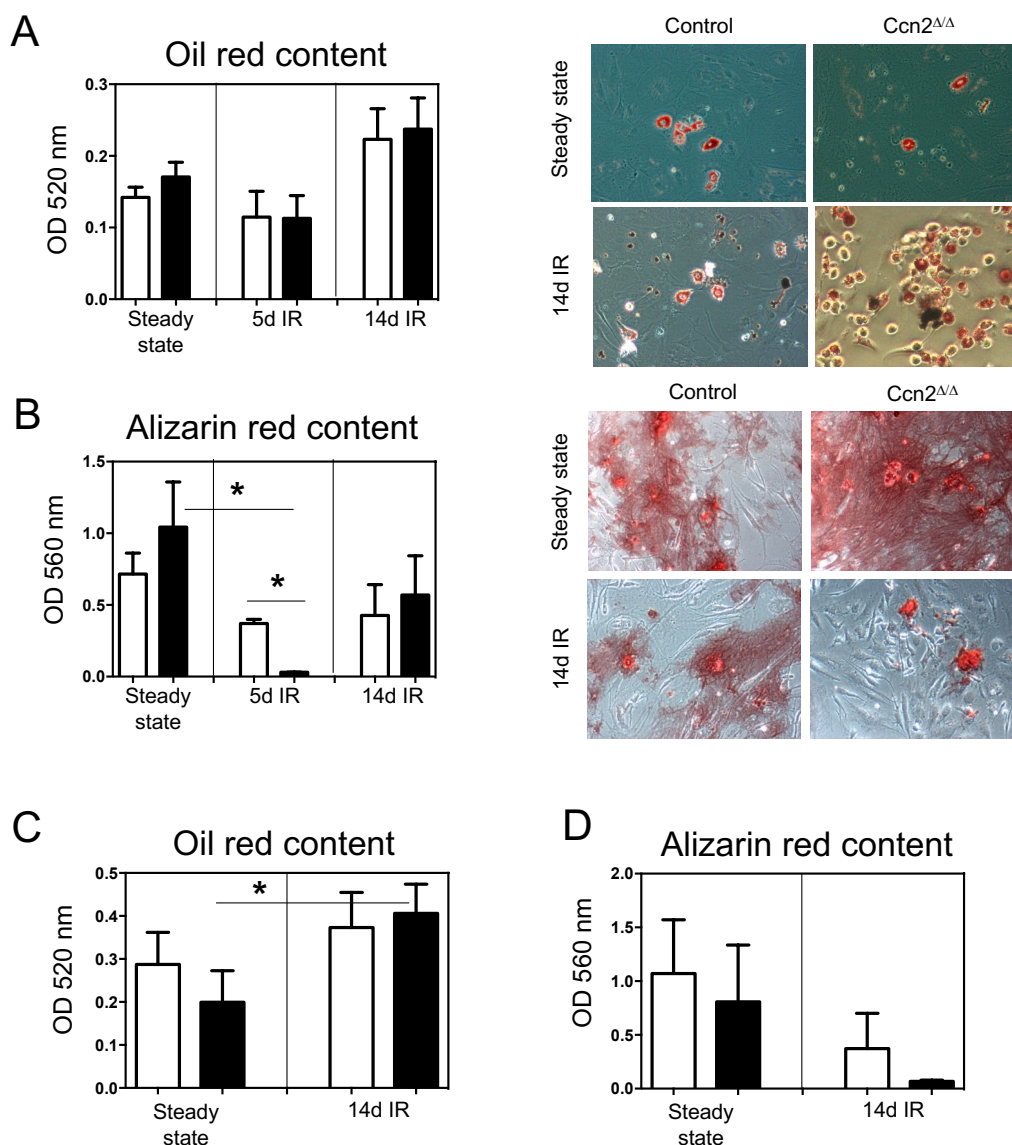


Figure 43. Induced and spontaneous adipogenic and osteogenic differentiation at steady state and after sublethal irradiation of control and *Ccn2^{ΔΔ}* as short-term stress model. (A) Induced adipogenic differentiation as detected by oil red content at OD 520 nm for control and *Ccn2^{ΔΔ}* MSCs at steady state and after five and 14 days of irradiation. (B) Induced osteogenic differentiation as detected by alizarin red content at OD 560 nm for control and *Ccn2^{ΔΔ}* MSCs at steady state and after five and 14 days of irradiation. (C) Spontaneous adipogenic differentiation as detected by oil red content at OD 520 nm for control and *Ccn2^{ΔΔ}* MSCs at steady state and after 14 days of irradiation. (D) Spontaneous osteogenic differentiation as detected by alizarin red content at OD 560 nm for control and *Ccn2^{ΔΔ}* MSCs at steady state and after 14 days of irradiation. All figures show the results of the control in white and the results from *Ccn2^{ΔΔ}* MSCs black bar graphs. Figures represent two performed experiments for steady state and 14 days after irradiation and one performed experiment after five days of irradiation. *p-value ≤ 0.05 show significance in the comparison of control and *Ccn2^{ΔΔ}* using the Mann-Whitney U-test (data generated in collaboration with masterstudent Katharina Kaiser).

Ccn2 was additionally reported to be important during wound healing (Kapoor et al., 2008; Shi-Wen et al., 2008). To imitate tissue wounding, we used a so-called scratch assay. Six, twelve and 24 hours after scratching, the confluence of the cells growing into the initial scratch was measured. Using this method, no differences were found between the MSCs isolated from control or *Ccn2*^{Δ/Δ} mice during steady state or after sublethal irradiation (Figure 44A, B, C). Additionally, no significant changes were measurable between the MSCs from untreated and irradiated groups in general (Figure 44A, B, C).

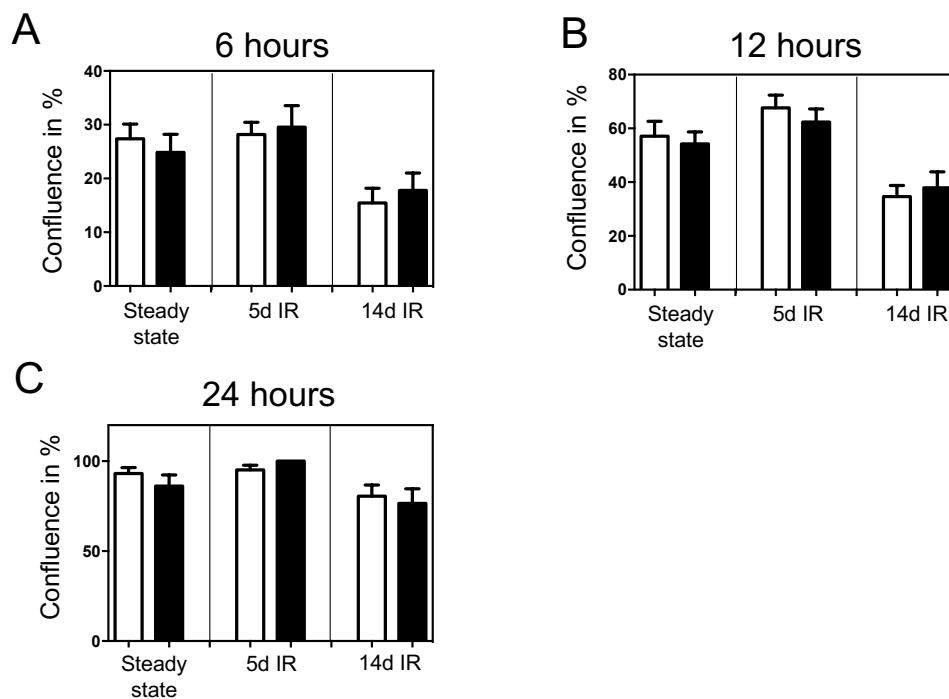


Figure 44. Wound healing potential of MSC at steady state and after sublethal irradiation of control and *Ccn2*^{Δ/Δ} as short-term stress model. (A) Confluence in percentage after six hours of the initial scratch in control and *Ccn2*^{Δ/Δ} MSCs at steady state and after five and 14 days of irradiation. (B) Confluence in percentage after twelve hours of the initial scratch in control and *Ccn2*^{Δ/Δ} MSCs at steady state and after five and 14 days of irradiation. (C) Confluence in percentage after 24 hours of the initial scratch in control and *Ccn2*^{Δ/Δ} MSCs at steady state and after five and 14 days of irradiation. All figures show the results of the control in white and the results from *Ccn2*^{Δ/Δ} MSCs black bar graphs. Figures represent two performed experiments for steady state and 14 days after irradiation and one performed experiment after five days of irradiation. *p-value ≤0.05 show significance in the comparison of control and *Ccn2*^{Δ/Δ} using the Mann-Whitney U-test (data generated in collaboration with masterstudent Katharina Kaiser).

It was reported, that shCCN2 in human MSCs lead to reduced proliferation in cell culture (Battula et al., 2013). To investigate the proliferation potential of MSCs isolated from mice 14 days after irradiation over a long series of passages, we cultured the control and *Ccn2^{ΔΔ}* MSCs until growth stopped.. Unexpectedly, the *Ccn2*-deficient MSCs proliferated to more cumulative population doublings (control 13, *Ccn2^{ΔΔ}* 30 PD), with a higher number of MSCs surviving beyond passage 31 (control 0/5, and *Ccn2^{ΔΔ}* 4/6; Figure 45A).

The enhanced cumulative PD and the increased survival suggest possible changes in MSC senescence. Indeed, a previous publication showed that CCN2 increased cellular senescence in fibroblasts (Jun and Lau et al., 2017), implicating that reduced *Ccn2* expression might reduce senescence and lead to increased PD. To study this hypothesis, we induced cellular senescence in p4 MSCs by culture of the cells for one week without medium change. After this, the number of β -galactosidase positive cells was determined. Although no changes were found between the control and *Ccn2^{ΔΔ}* MSCs in the steady state groups as well as in the irradiated groups (five and 14 days) (Figure 45B), the irradiation in the control group (five days after irradiation) increased significantly the numbers of blue stained cells when compared to the steady state and 14 days after irradiation (Figure 45B). In comparison to that 14 days after irradiation of *Ccn2^{ΔΔ}* MSCs, a reduced number of blue stained cells was measurable compared to the untreated ones (Figure 45B).

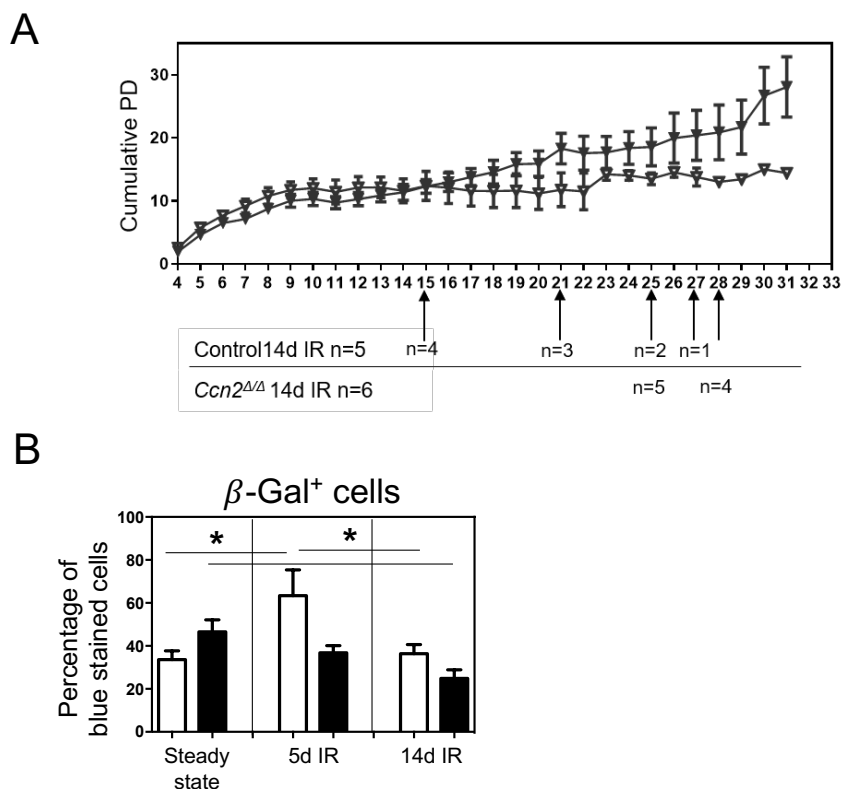


Figure 45. Growth potential and senescence of MSC at steady state and after sublethal irradiation of control and *Ccn2*^{Δ/Δ} as short-term stress model. (A) Cumulative population doubling of MSCs 14 days after irradiation. (B) Percentage of β -galactosidase positive cells (blue stained cells) in control and *Ccn2*^{Δ/Δ} MSCs at steady state and after five and 14 days of irradiation. All figures show the results of the control in white and the results from *Ccn2*^{Δ/Δ} MSCs black bar graphs. Figures represent two performed experiments for steady state and 14 days after irradiation and one performed experiment after five days of irradiation. *p-value ≤ 0.05 show significance in the comparison of control and *Ccn2*^{Δ/Δ} using the Mann-Whitney U-test (data generated in collaboration with masterstudent Katharina Kaiser).

To test whether cytokine expression was altered in *Ccn2*-deleted 14d IR MSCs, we analyzed the cell supernatant upon inflammatory molecules using cytokine bead assay (CBA). While IL-10, IFN γ , and IL-12p70 was undetectable (data not shown), Rantes and TGF- β 1, were expressed but slightly decreased in the supernatant of *Ccn2*-deleted 14d IR MSCs (Figure 46). The protein content of TNF- α was unchanged (Figure 46). However, as in serum of LPS-treated mice, the supernatant from *Ccn2* deleted 14d IR MSCs showed significantly reduced pro-inflammatory chemokine MCP-1 (CCL2) as compared to the supernatant of control 14d IR MSCs (Figure 46).

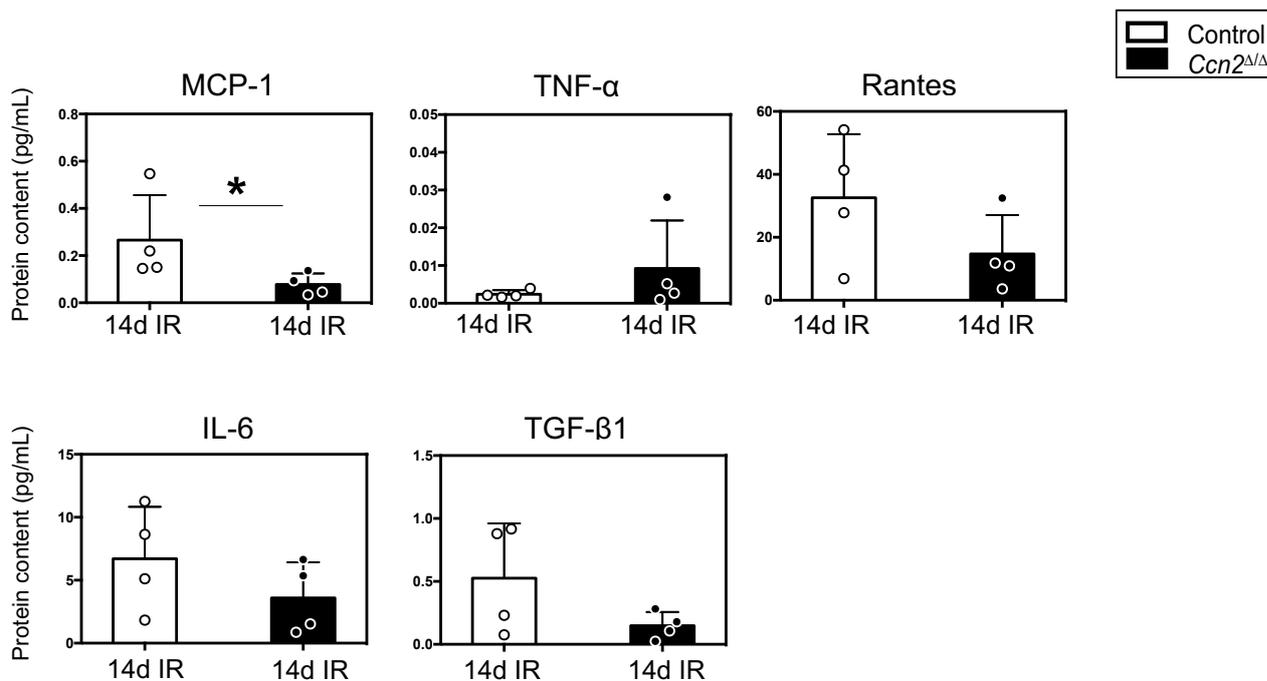


Figure 46. CBA from stromal cells 14 days after irradiation of control and *Ccn2*^{Δ/Δ} mice. (A) Analysis of the protein content in pg/mL from MCP-1, TNF- α , Rantes, IL-6 and TGF- β 1. In all figures the control mice are shown in white bars with white dotplots that are surrounded in red and the *Ccn2*^{Δ/Δ} mice are shown in black bars with black dotplots. Figures show one performed experiment with n = 4 control mice and n = 4 *Ccn2*^{Δ/Δ} mice; *p-value ≤ 0.05 show significance in the comparison of control and *Ccn2*^{Δ/Δ} mice using the Mann-Whitney U-test.

3.2.4.4.5 *Ccn2* function in hematopoietic cell recovery after 4.5 Gy irradiation

Although there were minor differences in the stromal cell numbers and functions between *Ccn2*^{Δ/Δ} and control stromal cells, there might be a direct effect of *Ccn2* loss on hematopoiesis. Previous results had demonstrated, that cocultures of irradiated *Ccn2*-knockdown stromal cells with HSCs results in decreased stem cell numbers, proliferation, and impaired differentiation, with increased cellular senescence and a loss of HSC function (Istvánffy et al. 2015). In addition, total-body irradiation of WT mice rapidly upregulates the expression of *Ccn2* and CCN2 in OBCs (Figure 38C and 40B), suggesting a role of *Ccn2* in the stress response of these cells to irradiation. Thus, we hypothesized that 4,5Gy sublethal irradiation (IR) of *Ccn2*^{Δ/Δ} mice would alter hematopoietic composition and the behavior of HSCs.

To study this, we first analyzed possible changes in the mature subpopulations of the PB during steady state, as well as five- and 14-days post irradiation (14d IR) We found no alterations between control and *Ccn2*^{Δ/Δ} mice in the percentage of B220⁺, CD3e⁺ or Gr1⁺CD11b⁺ cells at all time points (Figure 47A, B; C). Gr1^{med}CD11b⁺ cells were unchanged during steady state

and 5d post irradiation (5d IR). However, a significantly increased percentage of Gr1^{med}CD11b⁺ cells (monocytes) was found in the PB of *Ccn2*^{ΔΔ} compared to controls 14d IR (Figure 47D).

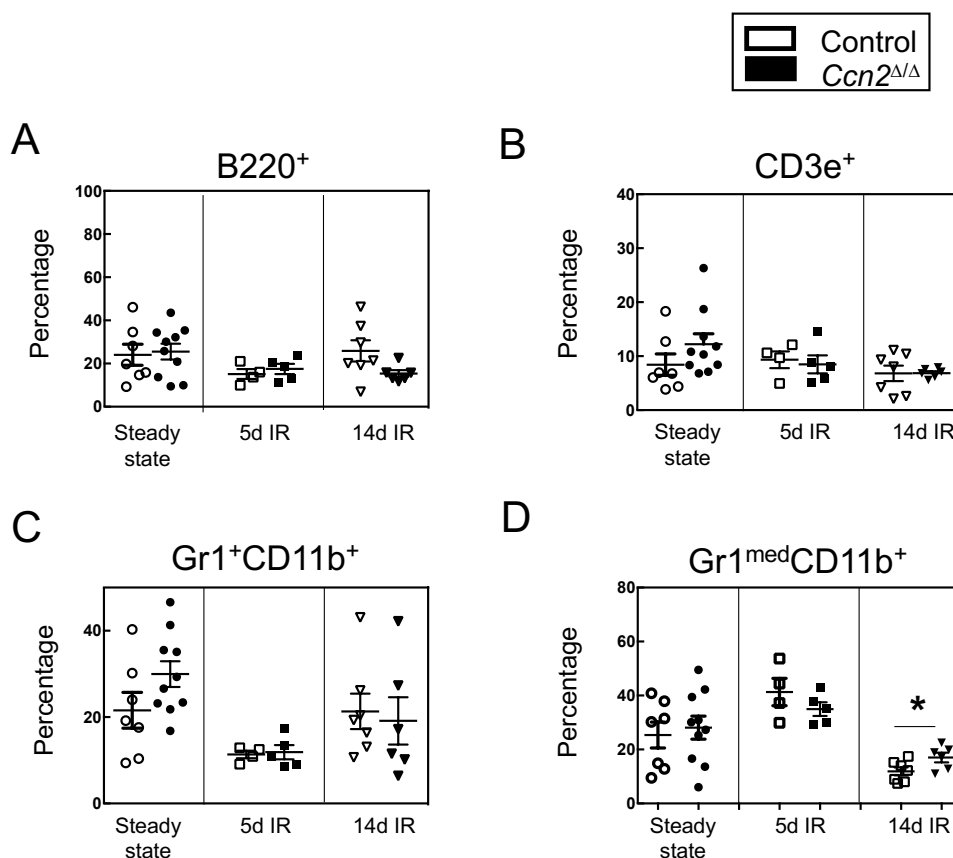


Figure 47. PB cells after sublethal irradiation (IR) of control and *Ccn2*^{ΔΔ} as short-term stress model. (A) Percentage cell numbers of B220⁺ B-cells in the BM during steady state, five and 14 days after IR. (B) Percentage cell numbers of CD3e⁺ T-cells in the BM during steady state, five and 14 days after (C) Percentage cell numbers of Gr1⁺CD11b⁺ granulocytes in the BM during steady state, five and 14 days after IR. (D) Percentage cell numbers of Gr1^{med}CD11b⁺ monocytes in the BM during steady state, five and 14 days after IR. All figures show the steady state results in round shaped dot plots, the five days irradiated in squared dot plots and the 14 days irradiated in triangled dot plots. Control cells are shown in white and the *Ccn2*^{ΔΔ} cells in black dot plots. Figures represent three (steady state) or two (5d IR, 14d IR) performed experiments with steady state control n = 7 and *Ccn2*^{ΔΔ} n = 10, five days irradiated control n = 4 and *Ccn2*^{ΔΔ} n = 5, 14 days irradiated control n = 7 and *Ccn2*^{ΔΔ} n = 6 mice. *p-value ≤0.05 show significance in the comparison of ontrol and *Ccn2*^{ΔΔ} mice using the Mann- Whitney U-test.

When analyzing the calculated total cell numbers and the flow cytometry analyzed mature subpopulations in the four long bones of the BM, we did not find significant changes between controls and the *Ccn2^{Δ/Δ}* during steady state, or 5d and 14d IR conditions. However, as expected after IR, the total BM cell numbers and, consequently, mature subpopulations, were reduced compared to the untreated (steady-state) situation five days after irradiation. Fourteen days IR the cell numbers already regenerated to the cell numbers prior to irradiation. Although no significant changes in the total BM cell numbers were detectable 5d and 14d IR, the absolute increase in Gr1^{med}CD11b⁺ cells 14d IR resulted in a nearly significant reduction of the total BM cell numbers of these cells in *Ccn2^{Δ/Δ}* mice ((Figure 48A, B, C, D, E), p=0.07).

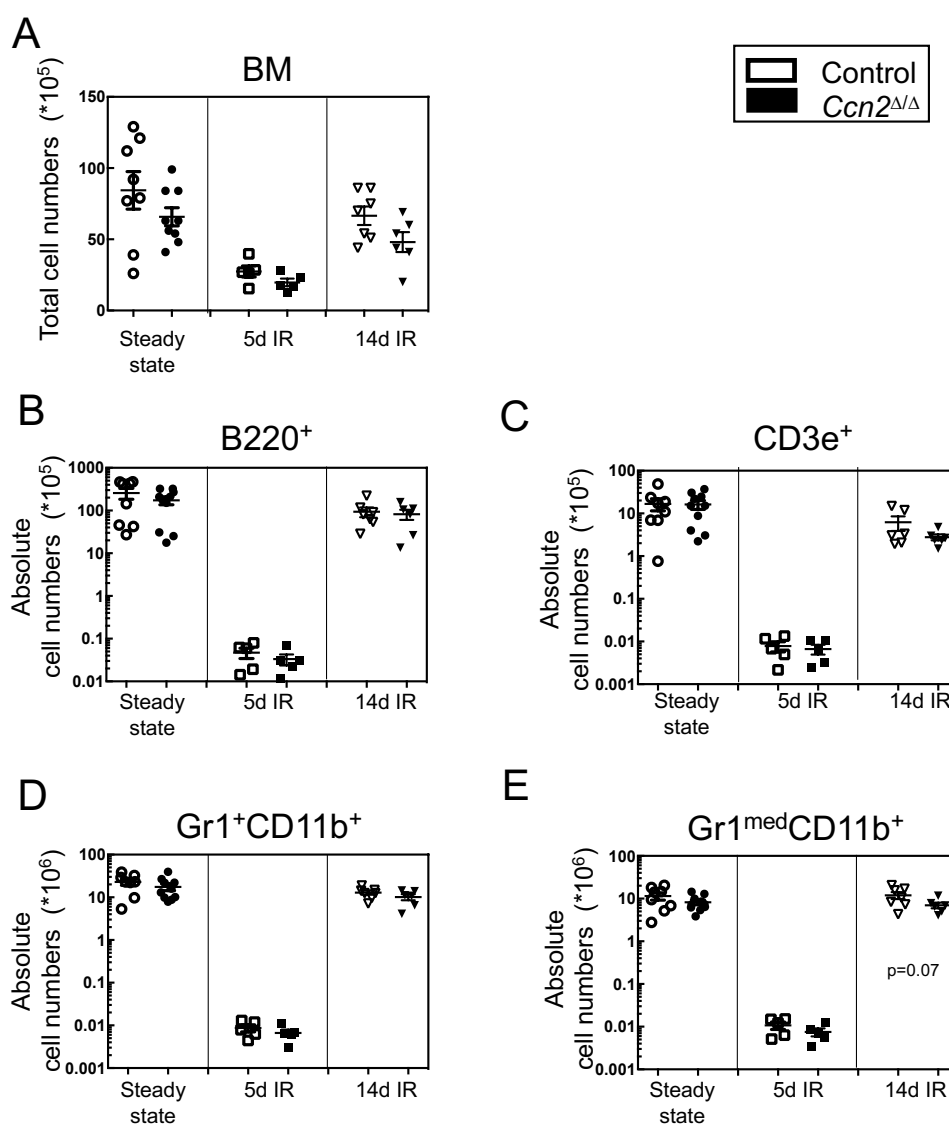


Figure 48. Hematopoietic mature cells after sublethal irradiation (IR) of control and *Ccn2^{Δ/Δ}* as short-term stress model. (A) Counted total cell numbers in the BM during steady state, five and 14

days after IR. Absolute cell numbers during steady state, five and 14 days after IR of (B) B220⁺ B-cells, (C) CD3e⁺ T-cells, (D) Gr1⁺CD11b⁺ granulocytes and (E) Gr1^{med}CD11b⁺ monocytes. All figures show the steady state results in round shaped dot plots, the five days irradiated in squared dot plots and the 14 days irradiated in triangled dot plots. Control cells are shown in white and the *Ccn2*^{Δ/Δ} cells in black dot plots. Figures represent three (steady state) or two (5d IR, 14d IR) performed experiments with steady state control n = 7 and *Ccn2*^{Δ/Δ} n = 10, five days irradiated control n = 4 and *Ccn2*^{Δ/Δ} n = 5, 14 days irradiated control n = 7 and *Ccn2*^{Δ/Δ} n = 6 mice. *p-value ≤ 0.05 show significance in the comparison of control and *Ccn2*^{Δ/Δ} mice using the Mann-Whitney U-test.

When focusing on the progenitor cell compartment, we found that the loss of *Ccn2* expression does not affect MPs, CMPs, MEPs and GMP numbers during steady state conditions or 14d after IR (Figures 49A, C, D, E). Interestingly, where mature cells regenerate to almost pre-IR numbers, the progenitors seem to be progressively declining from 5d to 14d IR. Furthermore, during early IR recovery (5d IR), the absolute numbers of CMPs (Figure 49C), MEPs (Figure 49D) and GMPs (Figure 49E) are significantly reduced in *Ccn2*^{Δ/Δ} mice compared to controls, even though MP numbers were similar 5d after IR (Figure 49A).

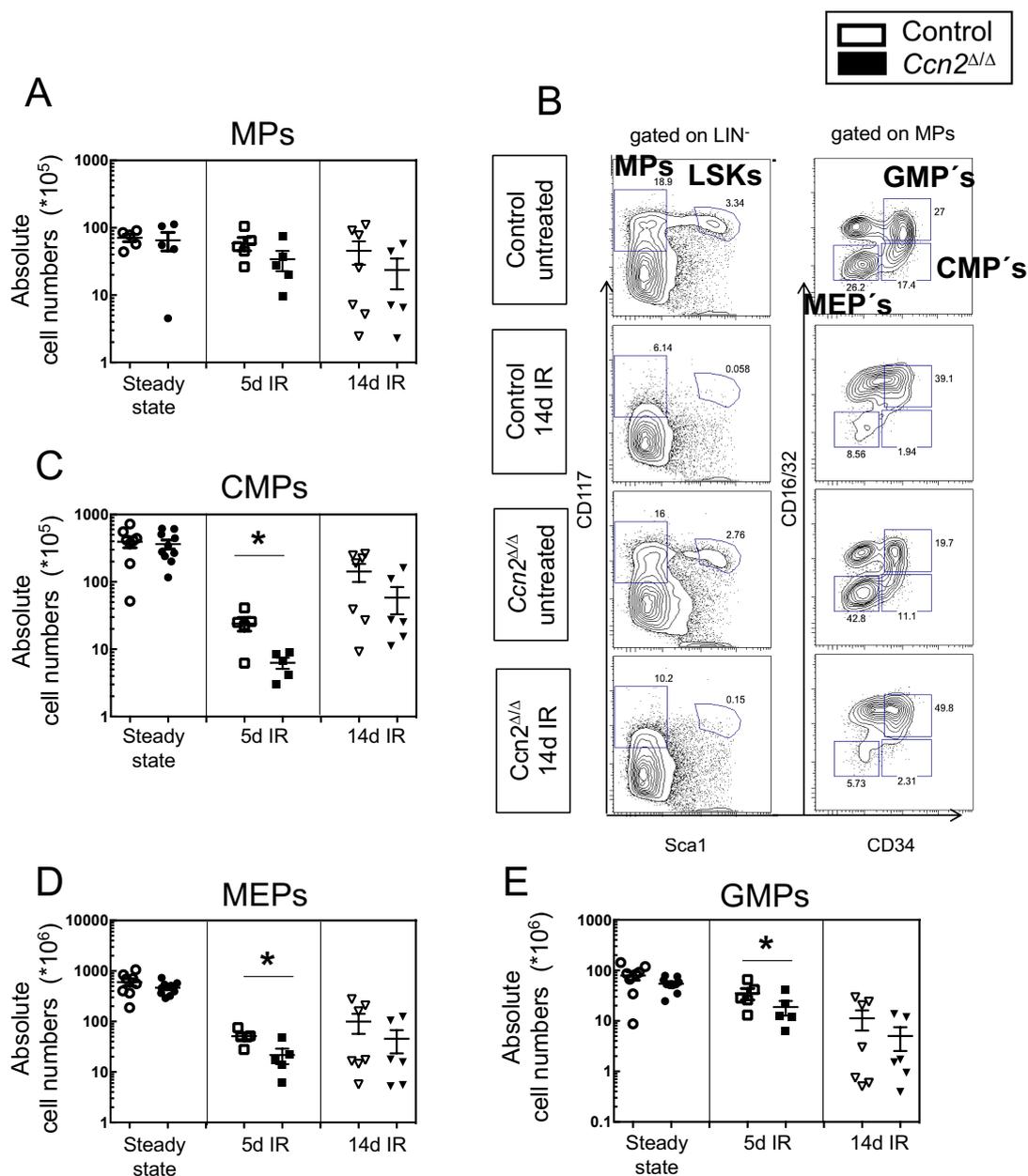


Figure 49. Hematopoietic myeloid progenitor cells after sublethal irradiation (IR) of control and *Ccn2*^{Δ/Δ} as short-term stress model. Representative gating strategy for the gating of MPs as CD45⁺Ter119⁺Sca1⁺CD117⁺ cells, the MEPs as CD45⁺Ter119⁺Sca1⁺CD117⁺CD34⁺CD16/32⁺ cells, the CMPs as CD45⁺Ter119⁺Sca1⁺CD117⁺CD34⁺CD16/32⁺ cells, and the GMPs as CD45⁺Ter119⁺Sca1⁺CD117⁺CD34⁺CD16/32⁺ cells in steady-state and 14 days after IR of control and *Ccn2*^{Δ/Δ} mice. Absolute cell numbers five and 14 days after IR of (A) MPs (B) CMPs (C) MEPs and (D) GMPs. All figures show the steady state results in round shaped dot plots, the five days irradiated in squared dot plots and the 14 days irradiated in triangled dot plots. Control cells are shown in white and the *Ccn2*^{Δ/Δ} cells in black dot plots. Figures represent three (steady state) or two (5d IR, 14d IR) performed experiments with steady state control n = 7 and *Ccn2*^{Δ/Δ} n = 10, five days irradiated control n = 4 and *Ccn2*^{Δ/Δ} n = 5, 14

days irradiated control $n = 7$ and $Ccn2^{\Delta/\Delta}$ $n = 6$ mice. * p -value ≤ 0.05 show significance in the comparison of control and $Ccn2^{\Delta/\Delta}$ mice using the Mann-Whitney U-test.

The analysis of the earliest hematopoietic cells in the stem cell hierarchy showed no significant changes in the cell numbers of the LSK, $CD34^+ LSK$ cell populations prior to IR (Figure 50A, B,C). After IR, no significant alterations were found during early recovery (5d IR) or 14 days of irradiation. Interestingly, however, the earliest HSC-enriched $CD34^- LSK$ cells were nearly significantly reduced in $Ccn2^{\Delta/\Delta}$ mice 14d after IR ($p=0.065$, Figure 50C).

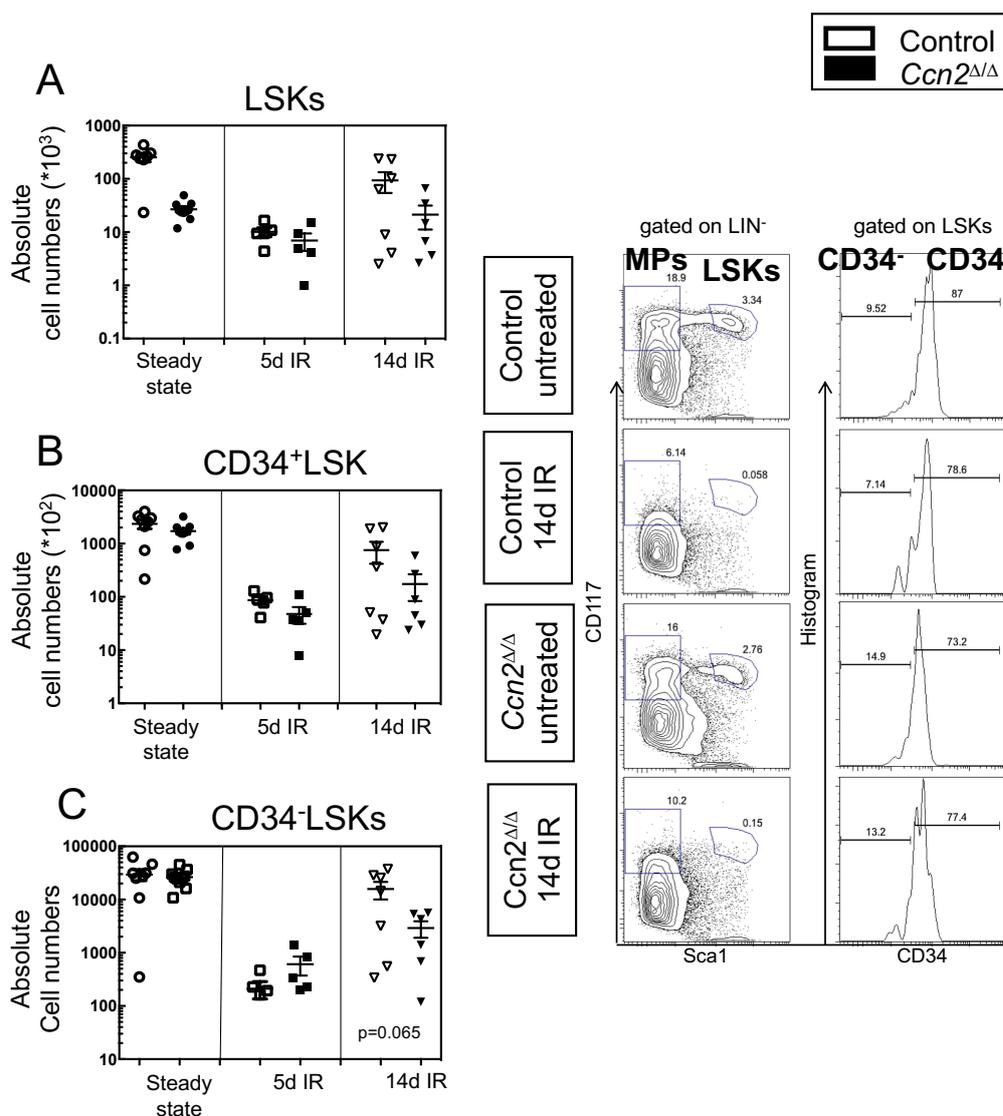


Figure 50. Hematopoietic stem cells after sublethal irradiation (IR) of control and $Ccn2^{\Delta/\Delta}$ as short-term stress model. Representative gating strategy for the gating of LSKs as $CD45-Ter119^- Sca1^+ CD117^+$ cells, the $CD34^+ LSKs$ and the $CD34^- LSKs$ in steady-state and 14 days after IR of control

and *Ccn2^{ΔΔ}* mice. Absolute cell numbers during steady state, five and 14 days after IR in (A) LSKs (B) CD34⁺LSKs (C) CD34⁻LSKs. All figures show the steady state results in round shaped dot plots, the five days irradiated in squared dot plots and the 14 days irradiated in triangled dot plots. Control cells are shown in white and the *Ccn2^{ΔΔ}* cells in black dot plots. Figures represent three (steady state) or two (5d IR, 14d IR) performed experiments with steady state control n = 7 and *Ccn2^{ΔΔ}* n = 10, five days irradiated control n = 4 and *Ccn2^{ΔΔ}* n = 5, 14 days irradiated control n = 7 and *Ccn2^{ΔΔ}* n = 6 mice. *p-value ≤0.05 show significance in the comparison of control and *Ccn2^{ΔΔ}* mice using the Mann-Whitney U-test

3.2.4.4.6 Functional analysis of irradiated *Ccn2^{ΔΔ}* HSCs using transplantation

The lower numbers of CMPs, MEPs, and GMPs, without significant reductions in LSKs, and LT-HSCs is in line with the view that irradiation reduces the ability of LT-HSCs to regenerate the progenitor cell compartment in the BM (Wang et al., 2006, Shao et al., 2014). Therefore, we tested the *in vivo* hematopoiesis-repopulating ability of control and *Ccn2^{ΔΔ}* LSKs isolated 14d IR by transplanting 1500 control or *Ccn2^{ΔΔ}* LSKs into lethally irradiated congenic 129xLy5.1 recipient mice (Figure 51A).

Here we found that five weeks after transplantation, engraftment of *Ccn2^{ΔΔ}* LSKs was slightly but not significantly lower than the engraftment of their control counterparts. Importantly, however, we found almost no engraftment in the PB at ten and 16 weeks after transplantation (Figure 51B). When analyzing the PB cellularity, we found no differences in the percentage of the lymphoid engraftment (B220⁺ and CD3ε⁺ cells), however myeloid engraftment (Gr1⁺CD11b⁺ and Gr1^{med}CD11b⁺) in the PB was dramatically decreased (Figure 51C).

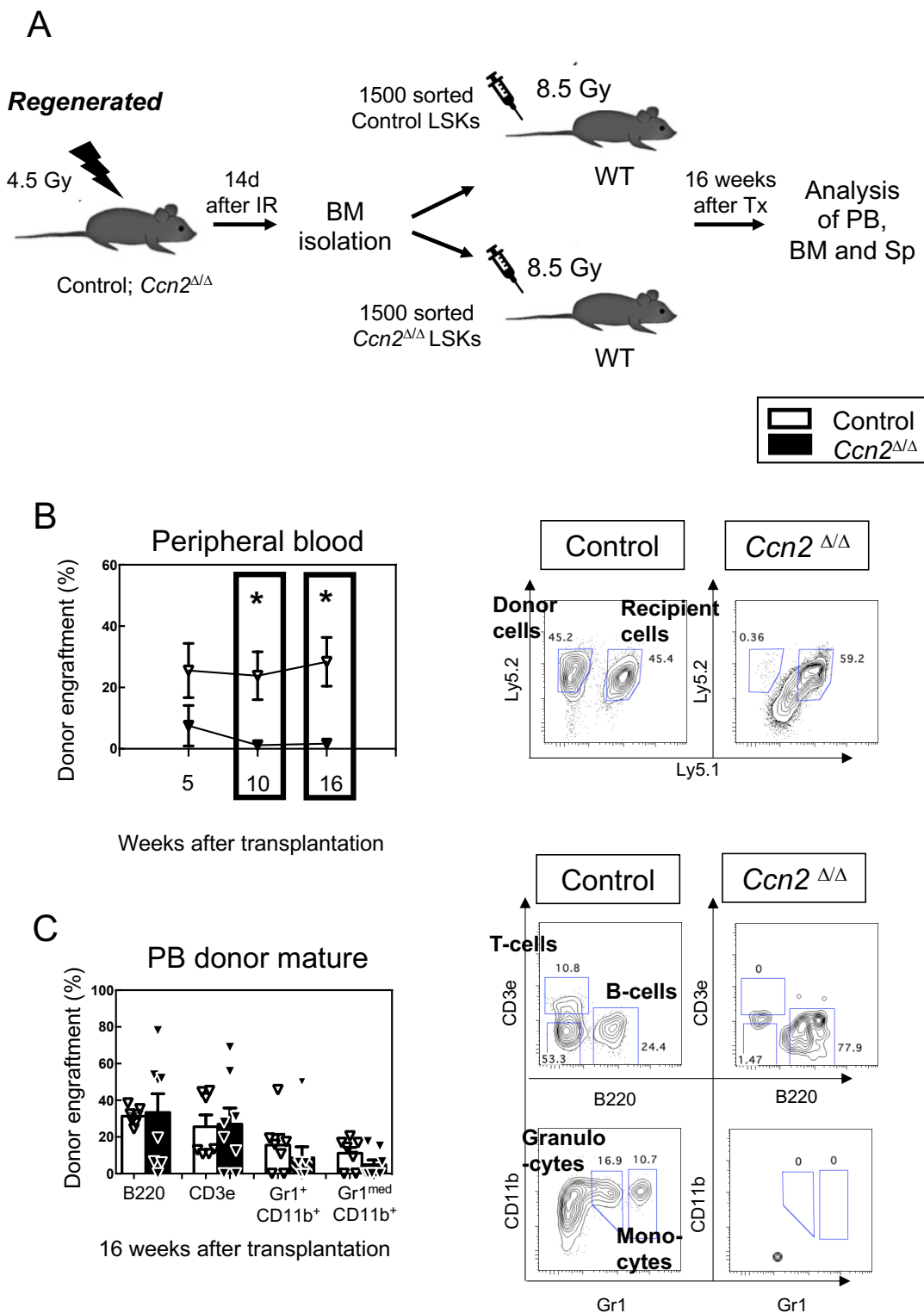


Figure 51. Engraftment in the PB of transplanted LSK cells from sublethal irradiated (IR) and 14 days regenerated control and *Ccn2*^{ΔΔ} cells as a long-term hematopoietic stress model. (A) Experimental design: 14 days after sublethal (4.5 Gy) irradiation the BM from control and *Ccn2*^{ΔΔ} mice were isolated, pooled per group and sorted for LSK cells. Then, 1500 from the regenerated LSK cells were transplanted into lethally (8.5 Gy) irradiated WT mice. Five, ten and 16 weeks after transplantation

the PB engraftment and mature cell composition was determined. 16 weeks after transplantation the Sp and BM cell engraftment and cell composition was analyzed using flow cytometry. (B) Donor cell engraftment in percentage of the PB five, ten and 16 weeks after Tx. Representative gating strategy for the gating of Ly5.2⁺ donor cells or Ly5.1⁺Ly5.2⁺ recipient cells. (C) Percentage of donor cell engrafted B220⁺, CD3e⁺, Gr1⁺CD11b⁺ and Gr1^{med}CD11b⁺ cells in the PB. Gating strategy of donor mature cell populations in the PB as an example for mature cell gating. All figures show the donor cell engraftment from 14 days regenerated control hematopoietic cells in white- and the *Ccn2^{ΔΔ}* hematopoietic cells in black bar and dot plots. Figures represent two performed experiments with n = 7 control mice and n = 8 *Ccn2^{ΔΔ}* mice; *p-value ≤0.05 show significance in the comparison of control and *Ccn2^{ΔΔ}* mice using the Mann-Whitney U-test.

The engraftment failure of the irradiated *Ccn2^{ΔΔ}* LSK cells at late time points after transplantation was also detectable in the Sp and BM when comparing donor engraftment of *Ccn2^{ΔΔ}* cells (in percentage) to their controls (Figure 52B, E). This was accompanied by a severely reduced engraftment of the myeloid cells in the Sp (Figure 52C), and both mature lymphoid and myeloid populations in the BM (Figure 52F).

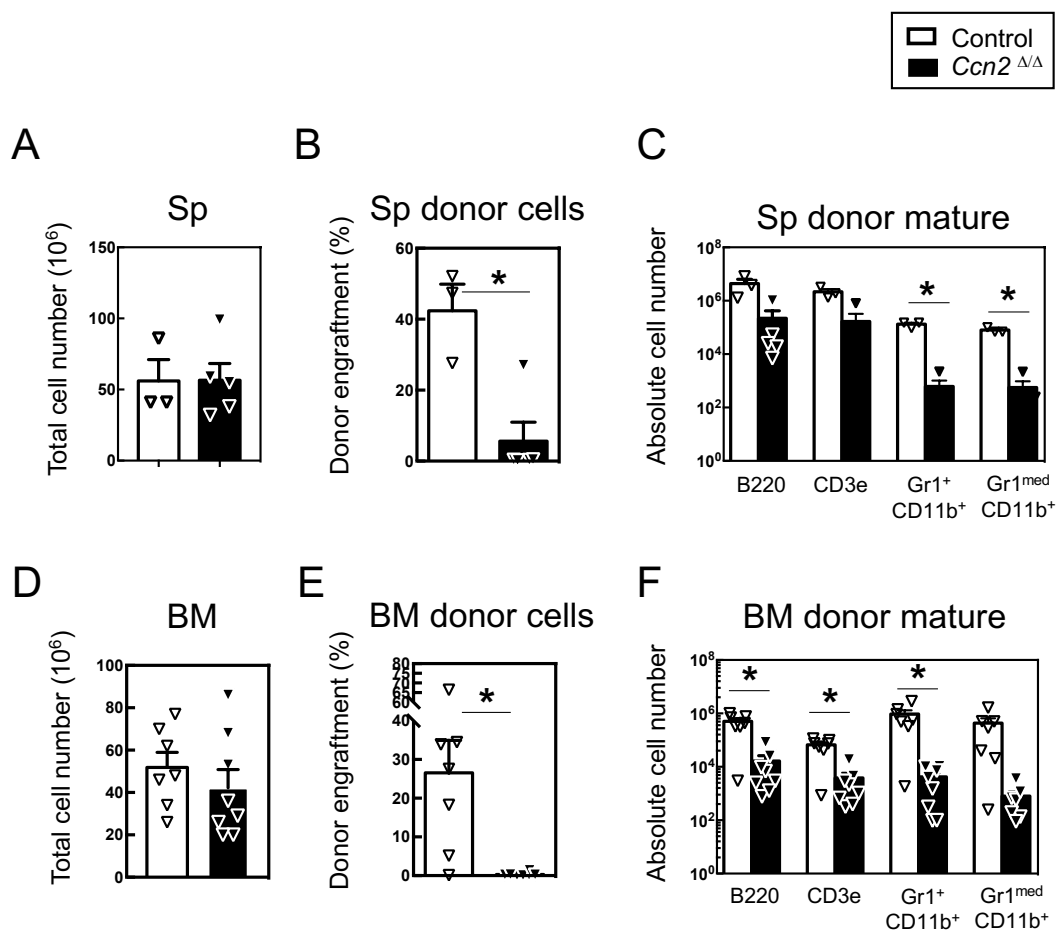


Figure 52. Mature cell engraftment in the Sp and BM of transplanted LSK cells from sublethal irradiated and 14 days regenerated control and *Ccn2*^{Δ/Δ} cells as a long-term hematopoietic stress model. (A) Total cell number in the Sp. (B) Percentage of donor cell engraftment in the Sp. (C) Absolute cell number of donor B220⁺, CD3e⁺, Gr1⁺CD11b⁺, Gr1^{med}CD11b⁺ mature cell populations in the Sp. (D) Total cell number in the BM. (E) Percentage of donor cell engraftment in the BM. (F) Absolute cell number of donor B220⁺, CD3e⁺, Gr1⁺CD11b⁺, Gr1^{med}CD11b⁺ mature cell populations in the BM. All figures show the donor cell engraftment from 14 days regenerated control hematopoietic cells in white- and the *Ccn2*^{Δ/Δ} hematopoietic cells in black bar and dot plots. Figures represent one performed experiment with n = 3 control mice and n = 5 *Ccn2*^{Δ/Δ} mice for the Sp and two performed experiments with n = 7 control mice and n = 8 *Ccn2*^{Δ/Δ} mice; *p-value ≤0.05 show significance in the comparison of control and *Ccn2*^{Δ/Δ} mice using the Mann-Whitney U-test.

When analyzing the engraftment of the earliest hematopoietic cells, we found that none of the early hematopoietic cell types were detectable in the mice receiving LSK cells from *Ccn2*^{Δ/Δ} 14d IR (Figure 53A). Indeed, even lineage-negative *Ccn2*^{Δ/Δ} donor cells (Figure 53B)

were not detectable, and, consequently, their MP, LSK, CD34⁺ and CD34⁻ LSK subpopulations (Figure 53C,D).

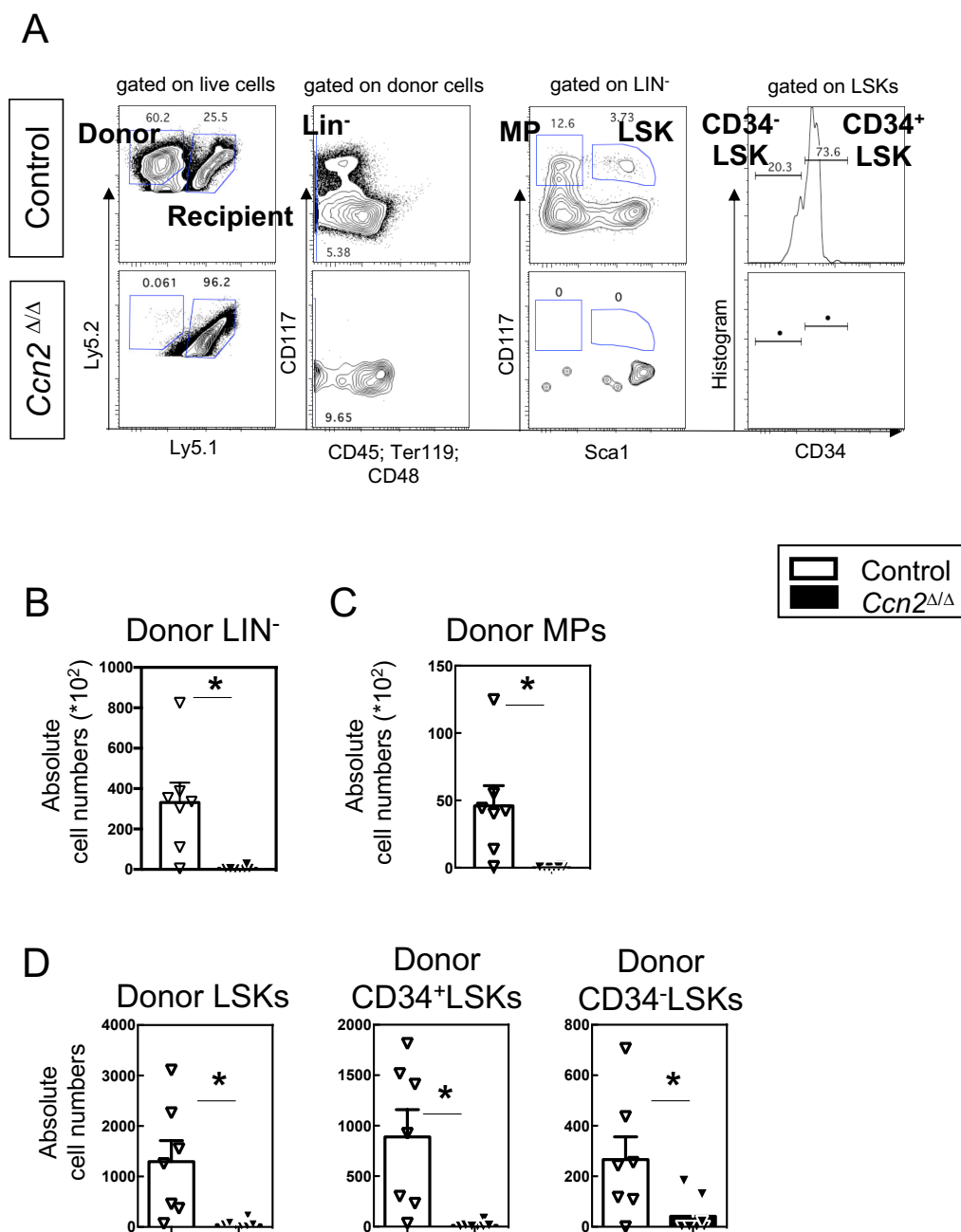


Figure 53. Hematopoietic progenitor and stem cell engraftment in the BM of transplanted LSK cells from sublethal irradiated and 14 days regenerated control and *Ccn2*^{Δ/Δ} cells as a long-term hematopoietic stress model. (A) Gating strategy of early cell population of donor cell engraftment. (B) Absolute cell numbers of the donor cell engrafted LIN⁻ cell numbers. (C) Absolute cell numbers of the donor cell engrafted MP cell numbers. (D) Absolute cell number of donor cell engrafted LSKs, CD34⁺LSKs and CD34⁻LSKs cells. All figures show the donor cell engraftment from 14 days regenerated

control hematopoietic cells in white- and the *Ccn2^{ΔΔ}* hematopoietic cells in black bar and dot plots. Figures represent two performed experiments with n = 7 control mice and n = 8 *Ccn2^{ΔΔ}* mice; *p-value ≤0.05 show significance in the comparison of control and *Ccn2^{ΔΔ}* mice using the Mann-Whitney U-test.

3.2.4.4.7 Functional analysis of irradiated *Ccn2^{ΔΔ}* HSCs using AnnexinV and BrdU-FACS

To exclude that the decreased engraftment of the HSCs from irradiated *Ccn2^{ΔΔ}* mice is caused by increased apoptotic cell death or impaired proliferation, we studied these possibilities using Annexin V and BrdU-FACS analysis (Figure 54A). Since most cell death events occur early after irradiation, we studied Annexin V two days after irradiation in LSK cells. The anionic phospholipid phosphatidylserine (PS) changes from the inner to the outer membrane in apoptotic cells. Annexin V binds PS on the outer membrane and marks apoptotic cells (Koopmann et al., 1994). However, two days after irradiation we found no increase in Annexin V⁺ *Ccn2^{ΔΔ}* LSK cells (Figure 54B).

To analyze possible changes in the proliferation behavior of LSK cells, we labeled all cells in S-phase five days after irradiation using i.p. BrdU injection. Our previous results (Figure 49) suggested that hematopoietic regeneration of the progenitor compartment is most divergent between controls and *Ccn2^{ΔΔ}* mice at this time point after irradiation. Indeed, we found a significant elevation of the *Ccn2^{ΔΔ}* LSK cells in active cell cycle 5d IR compared to control LSKs 5d IR, which show a larger population of LSKs retaining in the G0/G1-phase of the cell cycle (Figure 54C).

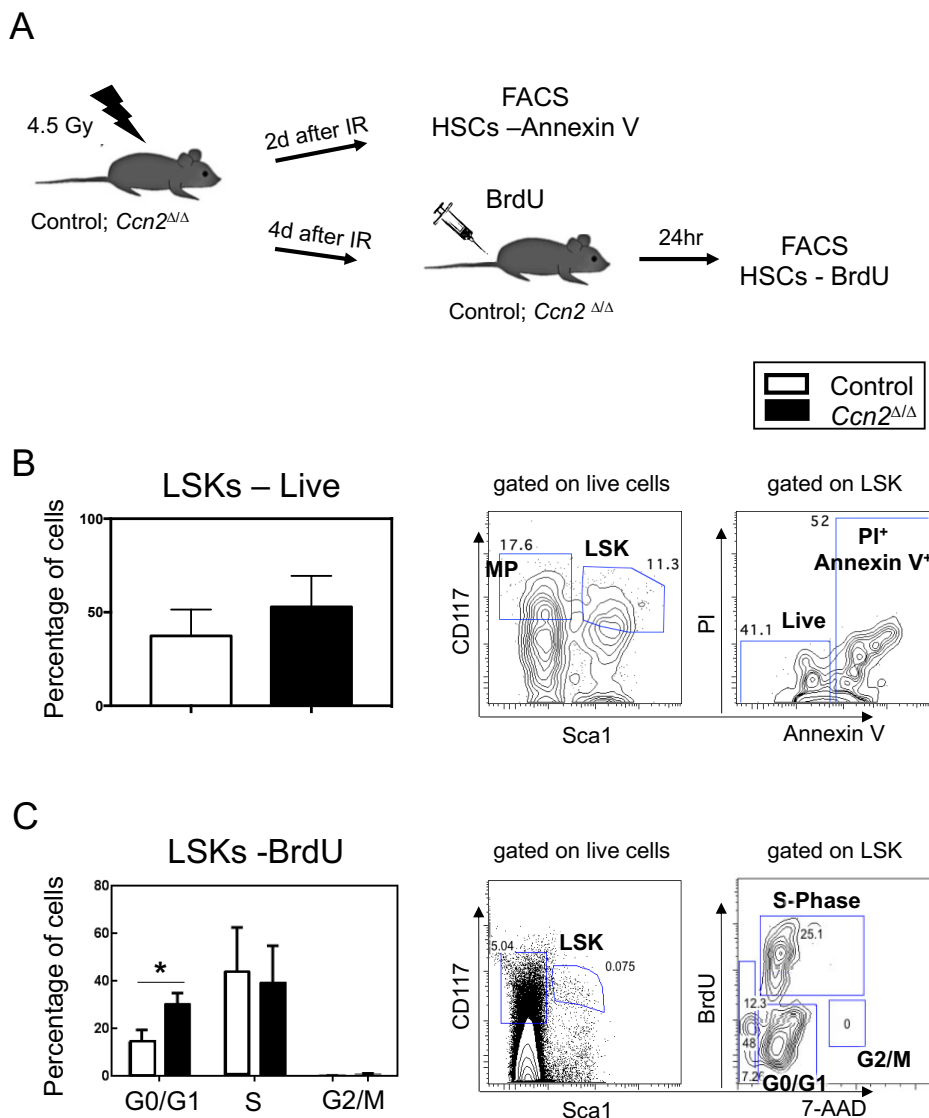


Figure 54. Annexin V and BrdU treatment of IR LSK cells. (A) Experimental design: 2 days after sublethal (4.5 Gy) irradiation the BM from control and *Ccn2*^{Δ/Δ} mice was isolated for Annexin V flow cytometry. 4 days IR mice were treated with BrdU, sacrificed (5d after IR) and BM was isolated and prepared for flow cytometry. (B) Percentage of alive LSK cells and corresponding flow cytometry plots. (C) Percentage of G0/G1-, S-, and G2/M-phase of LSK cells in percentage with the corresponding flow cytometry plots. Figures represent one performed experiment for Annexin V and two performed experiments for BrdU assay with control n = 4 and *Ccn2*^{Δ/Δ} n = 5; *p-value ≤0.05 show significance in the comparison of control and *Ccn2*^{Δ/Δ} mice using the Mann-Whitney U-test.

3.2.4.4.8 Functional analysis of irradiated *Ccn2^{ΔΔ}* HSCs using Immunofluorescence staining

To assess possible underlying mechanisms of the dichotomy between elevated cell numbers in G0/G1 phase of the *Ccn2^{ΔΔ}* LSK cells and reduced regeneration of the progenitor compartment, we first studied possible differences between the presence of cell cycle inhibitors 14d IR. In the first experiments, we studied similarities of the *Ccn2^{ΔΔ}* and control 14d IR and the LSK cells co-cultured on *Ccn2*-knockdown stromal cells we published previously (Istvanffy et al., 2015). For all of the following experiments, mice were sublethal irradiated, and 14d IR, cells were sorted and prepared for immunofluorescence staining. For these experiments, we could not study the HSC-enriched fraction of CD34- CD48- LSK cells due to too low cell numbers after sorting. Instead, we studied LSK cells (Figure 55A).

In first experiments, we evaluated possible changes in the expression of the acetylated p53 between irradiated control and *Ccn2*-deleted LSK cells. Here, in line with possible senescence, we found an increased content of the active form of p53, acetylated p53 in the LSK cells from irradiated *Ccn2^{ΔΔ}* mice (Figure 55B). Furthermore, the protein expression of the G1 to S-Phase gate keeper p27^{KIP} (CDKN1B) was also elevated in the *Ccn2^{ΔΔ}* group 14d post IR (Figure 55C). In accordance with that we found downregulation of Cyclin D1 (Figure 55D), which is necessary for S-Phase entrance, in *Ccn2^{ΔΔ}* 14d IR.

As the cell cycle inhibition might be the result of an enhanced DNA damage, we stained for a marker for DNA double stranded brakes (DSB), the phosphorylated histone, H2AX. Indeed, 14 days after irradiation the number of the gamma H2AX in accumulated foci was significantly increased in the irradiated *Ccn2*-deleted LSK cells (Figure 55E). In accordance with the increase in DSB, Comet-Assay was performed. *Ccn2*-deleted LSK cells displayed an increased tail, or length of the Comet, meaning more DNA damage.. Additionally, we compared the length of the tail from untreated control and *Ccn2^{ΔΔ}* and the 14 days irradiated once. As for the gamma H2AX staining the Comet-Assay (Figure 55F) confirmed the theory that the LSK cells from irradiated *Ccn2^{ΔΔ}* mice after 14 days still harbor the DSB while the controls were able to repair their DSB and showed the same Comet length as the untreated controls. Additionally, the untreated *Ccn2^{ΔΔ}* LSK cells showed a normal length of the comet.

Taken together, LSKs from sublethal irradiated *Ccn2^{ΔΔ}*, show increased BrdU incorporation and inhibited cell cycle progression into S-phase through elevated Ac-p53 and p27Kip1 and reduced Cyclin D1 probably caused by enhanced DSB as indicated by elevated gamma H2AX and enhanced Comets.

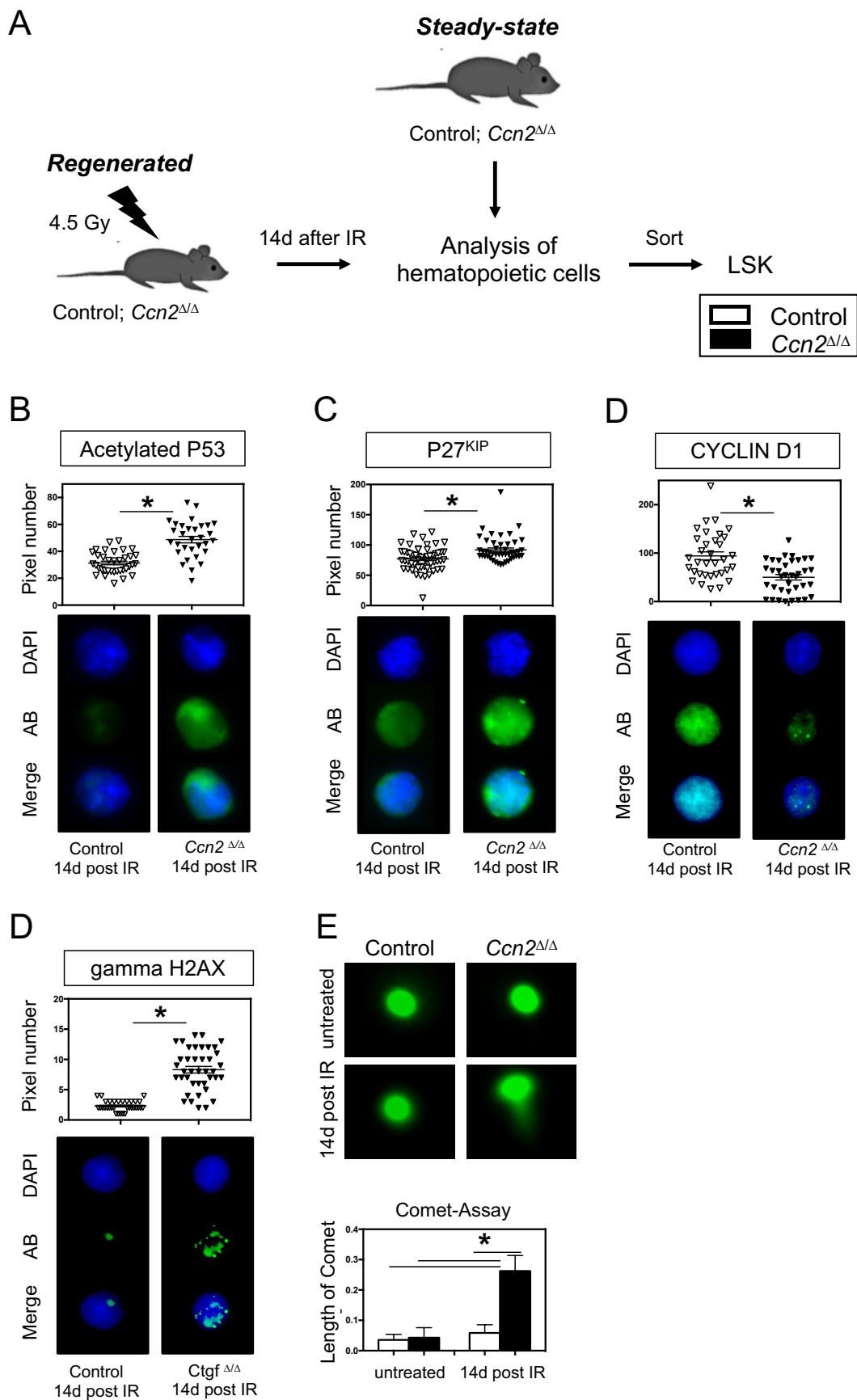


Figure 55. Immunofluorescence staining of sublethal irradiated and Comet assay from irradiated and steady state control and *Ccn2^{ΔΔ}* mice. (A) Experimental design: control and *Ccn2^{ΔΔ}* mice were sublethal irradiated (4.5 Gy) and 14 days after irradiation the BM was isolated from irradiated and additionally from steady state mice. LSK cells were sorted and prepared for immunofluorescence staining. (B) The immunofluorescence staining of acetylated P53 is shown, as well as for (C) P27^{KIP}, (D) CYCLIN D1 (E) gamma H2AX and (F) Comet Assay 14 days IR control and *Ccn2^{ΔΔ}*. The measurement of the fluorescence intensity in pixel number and the representative immunofluorescence staining of the nuclei staining in dapi (blue), the measured protein (AB, green), the merged once (blue and green) from the control on the left side *Ccn2^{ΔΔ}* mice on the right side is shown. In all figures the control in white- and the *Ccn2^{ΔΔ}* is shown in black dotplot graphs. *p-value ≤ 0.05 show significance in the comparison of control and *Ccn2^{ΔΔ}* using the Mann-Whitney U-test.

In our previous co-culture stress model LSK cells co-cultured on *Ccn2* knockdown stromal cells revealed enhanced DNA damage as shown by increased gamma H2AX with reduced Cyclin D1 (Istvanffy et al., 2015). This cells additionally showed an increased p-SMAD2/3 signaling indicating an impaired TGF- β 1 signaling (Istvanffy et al., 2015). Furthermore, an increased β -catenin signaling was detected suggesting an enhanced Wnt signaling (Istvanffy et al., 2015).

As we saw similar results with the impaired cell cycle progression and enhanced DNA damage response in *Ccn2^{ΔΔ}* 14d IR mice, we suggested an altered TGF- β 1 and Wnt signaling.

Unexpectedly, the protein level of p-SMAD2/3 was similar (Figure 56A), indicating an unaffected SMAD signaling in the LSK cells isolated from control or *Ccn2^{ΔΔ}* mice 14d IR.

On the other hand, similar to our previous study, reduction of both cyclin D1 (Figure 55D) and β -catenin (Figure 56B) were detected in the LSK cells of *Ccn2^{ΔΔ}* mice when compared to controls 14d IR, suggesting reduced canonical Wnt signaling.

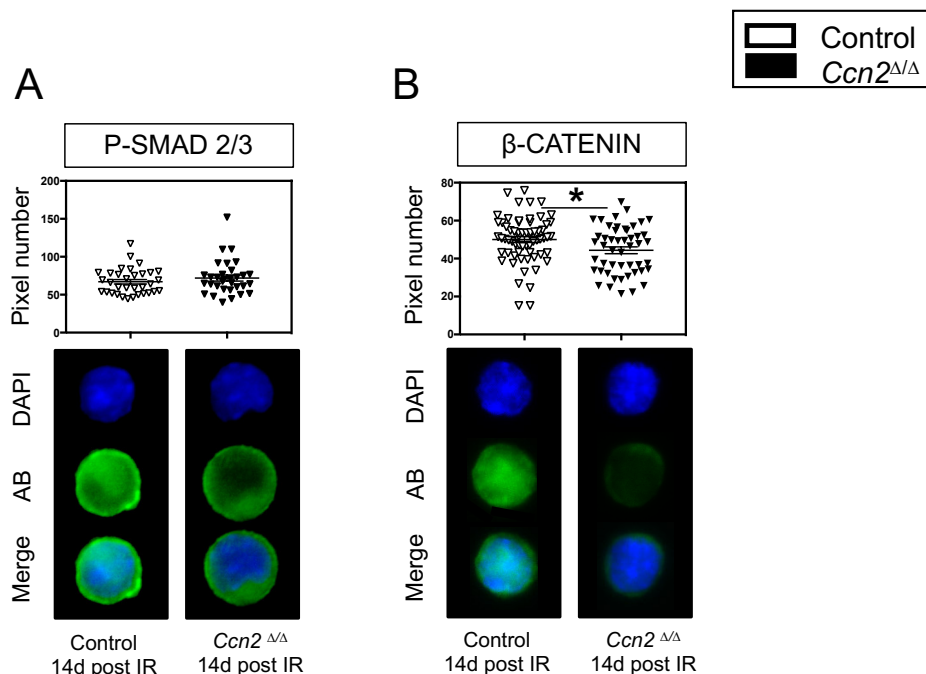


Figure 56. Immunofluorescence staining of sublethally irradiated control and *Ccn2*^{Δ/Δ} mice. (A) The immunofluorescence staining of P-SMAD 2/3 and (B) The immunofluorescence staining of β-Catenin 14d IR control and *Ccn2*^{Δ/Δ}. The measurement of the fluorescence intensity in pixel number and the representative immunofluorescence staining of the nuclei staining in dapi (blue), the measured protein (AB, green), the merged once (blue and green) from the control on the left side *Ccn2*^{Δ/Δ} mice on the right side is shown. In all figures the control in white- and the *Ccn2*^{Δ/Δ} is shown in black dotplot graphs. *p-value ≤0.05 show significance in the comparison of control and *Ccn2*^{Δ/Δ} using the Mann-Whitney U-test.

The inhibition of cell cycle progression in LSKs from sublethally irradiated *Ccn2*^{Δ/Δ}, together with the increase in BrdU incorporation may be caused by impaired S-phase activation of the cells in cell cycle. An important pathway regulating cell cycle progression from G1 to S-phase and myelopoiesis is the STAT3 pathway (Hirano et al., 2000; Zhang et al., 2010). Thus, we stained LSK cells from sublethally irradiated control and *Ccn2*^{Δ/Δ} mice for the expression of the upstream co-receptor gp130 of the IL-6 family of cytokines and the downstream phosphorylated and activated form of STAT3. Interestingly, we found a decreased expression of both the gp130 co-receptor (Figure 57B) and phosphorylated STAT3 in LSK cells isolated from *Ccn2*^{Δ/Δ} mice 14d IR (Figure 57C).

Phosphorylated STAT3 enters the nucleus and acts as a transcription factor to regulate gene expression (Zhang et al., 2014; 2018). Here, pSTAT3 may stimulate both cell cycle progression (Kanna et al., 2018) and inhibit inflammation (Zhang et al., 2018) in HSCs. An important

intermediate in the anti-inflammatory activity of pSTAT3 is its down-regulation of the pro-inflammatory ubiquitin conjugating enzyme E2N (UBC13; *Ube2n*) (Zhang et al., 2014; 2018). Considering the involvement of *Ccn2* in inflammatory pathways (Istvanffy et al., 2015), and the involvement of UBC13 in DNA repair mechanisms during double strand breaks (Pinder et al., 2013), we stained for this conjugate UBC13 protein. Interestingly, the LSK cells from irradiated *Ccn2*-deleted mice express significantly more UBC13 compared to the controls (Figure 57D), suggesting increased inflammatory activity.

Interestingly, as we found both enhanced UBC13 and γ H2AX expression, we wondered if downstream of these to molecules the DNA repair mechanism fails in *Ccn2* ^{$\Delta\Delta$} mice 14d IR. In the repair of DNA double strand breaks, γ H2AX recruits 53BP1 to DNA repair foci (Lassmann et al., 2010; Nakamura et al., 2010). When we analysed 53BP1 localization, we found that γ H2AX with 53BP1 did not colocalize (Figure 57E). This observation supports that γ H2AX does not properly recruit the DNA repair machinery in *Ccn2* ^{$\Delta\Delta$} HSCs, despite the finding that the number of γ H2AX foci was increased (Figure 55D).

Taken together, our results are consistent with a mechanism of reduced HSC activity due to reduced anti-inflammatory gp130/STAT3 signaling and increased UBC13 signaling in LSK cells of irradiated *Ccn2* ^{$\Delta\Delta$} mice. Furthermore, the results provide evidence for an impaired DNA repair machinery in *Ccn2* ^{$\Delta\Delta$} HSCs, similar as in aged HSCs (Flach et al., 2014).

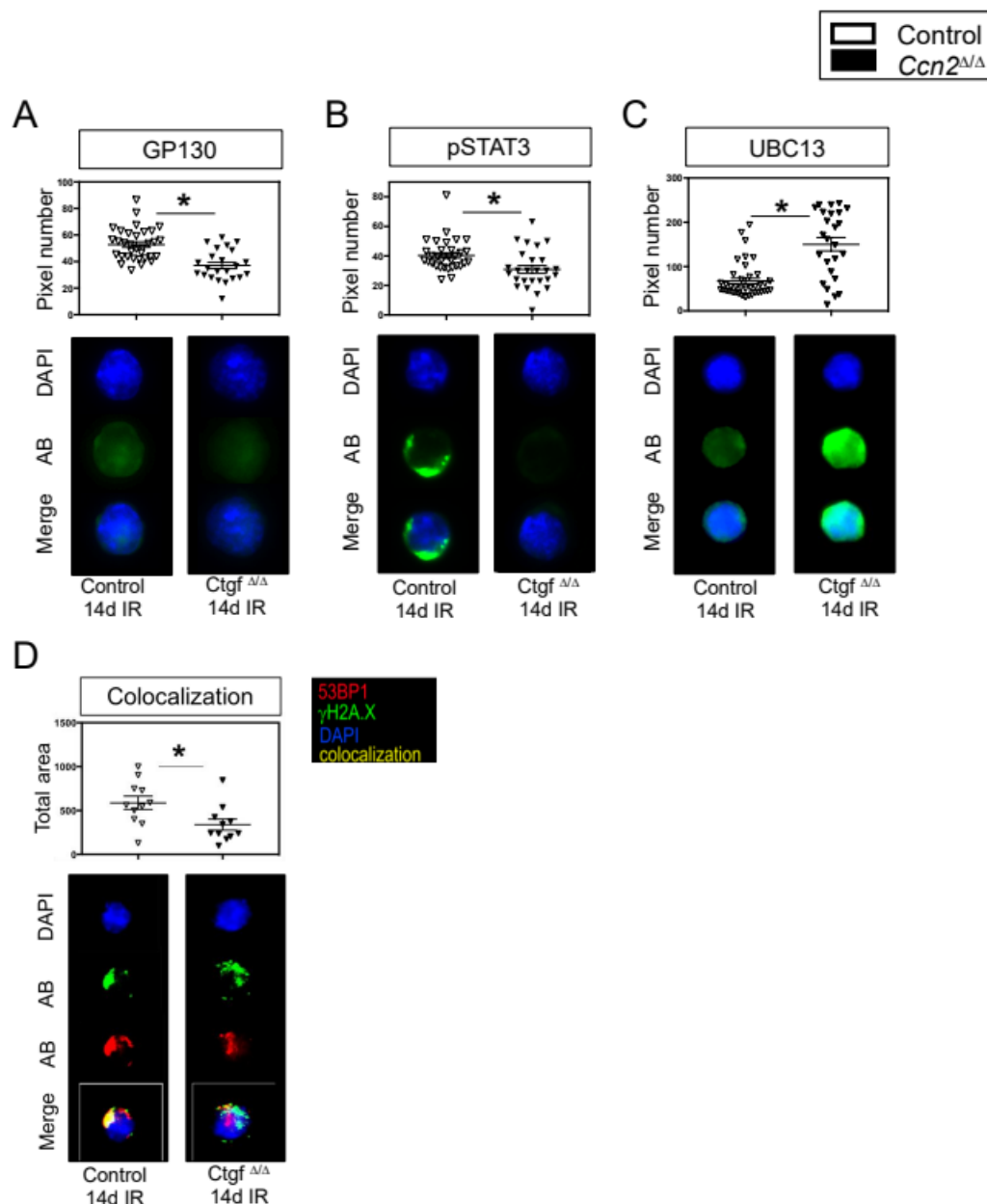


Figure 57. Immunofluorescence staining of 4.5Gy irradiated control and *Ccn2*^{Δ/Δ} mice. The immunofluorescence stainings of (A) GP-130 (B pSTAT3), (C), UBC13, (D) colocalization of gamma H2AX with 53BP1 in 14d IR of control and *Ccn2*^{Δ/Δ} LSK cells are shown. The measurement of the fluorescence intensity in pixel number and the representative immunofluorescence staining of the nuclei staining in DAPI (blue), the measured protein (antibody (AB) green or green and red), the merged once (blue and green, or blue, green and red) from the control mice on the left side, and from the *Ccn2*^{Δ/Δ} mice on the right side is shown. In all figures the control in white- and the *Ccn2*^{Δ/Δ} is shown in black dotplot graphs. *p-value ≤ 0.05 show significance in the comparison of control and *Ccn2*^{Δ/Δ} mice using the Mann-Whitney U-test.

4 Discussion

4.1 Function of *Ccn2* during steady state and stress conditions

Ccn2 was found to be an immediate-early response gene to stress (Ponticos, 2013) that in a coculture experiment of hematopoietic cells with stromal cells together with genes associated with wounding and infection is rapidly, up-regulated by the niche (Lutzny et al., 2013; Istvánffy et al., 2015, Desterke et al., 2020). This up-regulation was shown to be essential to maintain the functionality of HSCs in cell culture (Istvanffy et al., 2015).

Through the investigation of ROSA26-CreER^{T2}/*Ccn2*^{fl/fl} mice we found that *Ccn2* is dispensable during steady state conditions. But, in terms of an inflammatory response such as LPS necessary for the correct resolve of inflammatory cytokines affecting HSC numbers. Furthermore, *in vivo* irradiation and/or transplantation experiments revealed *Ccn2* to be essential to protect the functionality of LT-HSCs. Irradiated *Ccn2*^{Δ/Δ} HSCs showed a reduced γ H2AX-directed DNA repair, inflammatory cytokine secretion of stromal cells with impaired GP130/pSTAT3 signaling in HSCs and subsequent enhanced UBC13. In accordance to enhanced UBC13, γ H2A.X+ accumulates in these cells, without recruiting the DNA repair machinery. These results indicate that *Ccn2* expression is required to protect HSCs from increased DNA damage or to ensure a working DNA repair mechanism, after inflammatory/irradiation stress.

4.1.1 Single HSCs in culture with stromal MEF-CM and *Ccn2*^{Δ/Δ}-MEF-CM

I would like to refer to my publication in Haematologica (Romero Marquez and Hettler et al., 2021).

4.1.2 The function of *Ccn2* expression during different stress conditions

4.1.2.1 *Ccn2* has no impact on 5-FU-induced hematopoietic or BM niche stress

In previous experiments, our group showed that an adequate response to 5-FU-induced stress requires the expression of soluble factors by the microenvironment (Ruf et al., 2016; Landspersky et al. 2022). Thus, it was surprising to find, that 14 days after *in vivo* 5-FU treatment, no major changes in hematopoietic cell numbers in the PB, BM, or Sp, nor in the BM niche cell numbers were found in the *Ccn2*^{Δ/Δ} mice. One reason for this finding could be, that in contrast to the previous studies of *Sfrp2* and *Wnt5a*, which are mostly expressed by *Cxcl12*⁺ *Lepr*⁺ osteoprogenitors of the BM, *Ccn2* is not only expressed by *Fbn1*⁺ *Igf1*⁺ O2 osteoblasts, followed by *Col16a1*⁺ *Tnn*⁺ O1 osteoblasts, but also in *Stab2*⁺ sinusoidal

endothelial cells (Tikhonova et al., 2019). 5-FU treatment upregulates *Ccn2* expression in O1 osteoblasts and endothelial cells 1.5- and 2.3-fold, respectively. However, the highest expressors, the O2 osteoblasts, are unaffected by 5-FU treatment, resulting in only a minor increase of *Ccn2* in the total BM after 5-FU (Figure 58, Tikhonova et al., 2019).

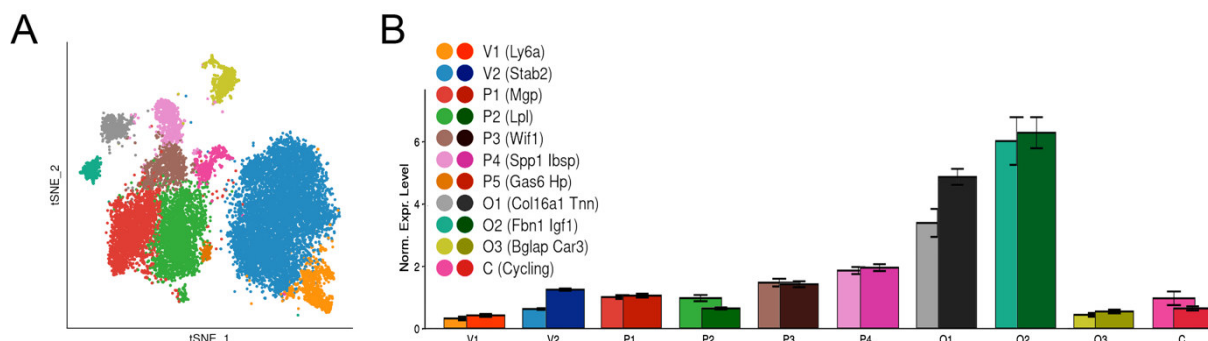


Figure 58. *Ccn2* expression in stromal cells during steady state conditions and after 5-FU treatment. (Tikhonova et al., 2019; <https://compbio.nyumc.org/niche/>). (A) Different clusters of niche cells: V1, V2: endothelial cells; P1-4: perivascular cells/MSC; O1-3: mature osteoblasts; C: cycling cells. (B) change in *Ccn2* /*Ctgf* expression after 5-FU treatment (darker colors, right columns).

Thus, although the composition of the BM changes after 5-FU treatment (especially the P2 *Cxcl12*⁺ *Lepr*⁺ *AdipoCAR* are increased), the overall *Ccn2* expression is only minimally affected. Further studies evaluating the *Ccn2* content in subpopulations of the PB or BM flush out of 5-FU treated and untreated mice would distinguish changes in subpopulation composition compared to *Ccn2* expression to each subpopulation. Moreover, as we found previously that unchanged cell numbers do not predict HSC function after 5-FU treatment (Landspersky et al., 2022), HSC function should still be evaluated by transplanting HSCs from 5-FU treated *Ccn2*^{Δ/Δ} or *Ccn2*^{wt/wt} mice.

4.1.2.1 *Ccn2* expression increases the number of HSCs in the BM during LPS stress

In our hands, consistent with the putative pro-inflammatory role of *Ccn2*, a single and low dose application of LPS, which mimics a bacterial infection, reduced immature hematopoietic populations such as LSKs, CD34⁺ and CD34⁻ SLAM cells in the *Ccn2*^{Δ/Δ} when compared to controls, without affecting more mature populations. This indicates a minor role for *Ccn2* during emergency hematopoiesis. Previously, it has been described that infections act directly on HSCs (King and Goodell, 2011). Our results in *Ccn2*^{Δ/Δ} contrast to a previous study where LPS (3mg/kg) increases WT LSKs as well as LT-HSCs cell numbers after 24 hours later (Zhang et

al., 2016). Thus, it seems likely that deletion of *Ccn2* reduces the inflammatory response leading to a decrease in HSCs already at a lower dose of injection (1 μ g/mouse).

A reduced inflammatory response of *Ccn2* ^{Δ/Δ} mice includes a reduced release of pro-inflammatory cytokines from the microenvironment (King and Goodell, 2011). Indeed, we found that *Ccn2* ^{Δ/Δ} mice show lower serum concentrations of CCL2 (MCP-1) and a tendency of reduced TNF- α after LPS treatment compared to the controls. Interestingly, besides myeloid cells, MSCs and osteoarthritis synovial fibroblasts were found to secrete MCP-1 after application with the inflammatory factors TNF- α or CCN2 (Liu et al., 2012; Ren et al., 2012). As MCP-1 was shown to attract progenitor and hematopoietic stem cells to the site of injury via CCR2 binding (Si et al., 2010) the reduced MCP-1 concentration in LPS-challenged *Ccn2* ^{Δ/Δ} mice could lead to reduced attraction of HSCs to injury sites or might reduce the attraction of HSCs into the BM causing reduced HSC numbers as shown in the *Ccn2* ^{Δ/Δ} .

It is yet unclear, which cells from the niche are affected most by LPS challenge in *Ccn2* ^{Δ/Δ} mice. MCP-1 is secreted by monocytes, macrophages, neutrophils (Evers et al., 2022; Yoshimura et al., 2014;) and in MSCs (Ren et al., 2012; Helbling et al., 2019). In both MSCs and ECs, MCP-1 is upregulated 48 hours after LPS challenge (Helbling et al., 2019). In contrast, we found reduced MCP-1 concentration in serum, without any changes in the numbers of these myeloid cells in the PB, SP and BM, as well as MSC numbers 24 hours after LPS treatment. The unchanged mature cell and stromal cellularity suggest that *MCP-1* expression is affected by *Ccn2* deletion, 24 hours after LPS challenge, rather than cell numbers.

In conclusion, our results support the view that *Ccn2* is a pro-inflammatory factor, which promotes the increase in the number of HSCs and the secretion of other pro-inflammatory cytokines such as MCP-1 and possibly TNF α .

4.1.2.2 In- and extrinsic significance of *Ccn2* expression in BM transplantation

4.1.2.2.1 Intrinsic significance of *Ccn2* expression

4.1.2.2.1.1 *Ccn2*^{ΔΔ} HSCs transplanted

We have found that adult *Ccn2*^{ΔΔ} HSC show an increased potential to engraft in WT primary recipient mice compared to controls. Here, *Ccn2*^{ΔΔ} HSC transplantation resulted in enhanced myeloid cells in the SP and increased mature myeloid cells, B-cells as well as MPs and ST-HSCs in the BM. Although this single experiment has to be repeated to make a clear statement, the increased engraftment of *Ccn2*^{ΔΔ} HSCs would suggest an enhanced number of potent HSCs. However, increased myeloid and stem cell numbers are also found in aged mice (Adolfsson et al., 2005; Florian et al., 2012), that upon serial transplantation reveal an impaired functionality with lowered self-renewal capacity (Janzen et al., 2006; Rossi et al., 2005).

Interestingly, against the general view that *Ccn2* mainly regulates HSCs extrinsically and not intrinsically (Cheung et al., 2014; Istvánffy et al., 2014), this result implies an intrinsic role for *Ccn2* in regulating HSCs during stress situations. However, *Ccn2* was knocked out two weeks before BM transplantation, with the possible result of already primed cells due to the loss of extrinsic *Ccn2* from the niche in *Ccn2*^{ΔΔ}.

Indeed, our results with HSCs in which *Ccn2* was deleted 4 weeks after engraftment, we did not find major differences in the cell numbers or differentiation of the engrafted HSCs (16 weeks after Tx). As such, this experiment supports the view of primed HSCs from *Ccn2*^{ΔΔ} leading to the altered engraftment, rather than an intrinsic role of *Ccn2*. In accordance to that, Cheung postulated that the *Ccn2*^{-/-} hematopoietic cells are primed by their niche as *Ccn2* was not expressed in the unfractionated BM, but transplanted fetal liver cells from *Ccn2*^{-/-} compared to WT mice revealed an impaired B-cell development when transplanted into a WT background (Cheung et al., 2014).

In summary, the experiments indicate that *Ccn2* loss of the niche in *Ccn2*^{ΔΔ} mice prime the HSCs leading to an altered engraftment that shares similarities with HSCs of aged mice.

4.1.2.2.2 Extrinsic *Ccn2* maintains long term repopulating functionality of HSCs

In line with the hypothesis that environmental *Ccn2* is essential for the preservation of long-term repopulating HSCs with associated myeloid engraftment, we found delayed impaired engraftment at 16 weeks after transplantation of WT cells regenerated in a *Ccn2*^{ΔΔ} microenvironment. In addition, we also found reduced numbers of WT HSCs in the PB and SP of *Ccn2*^{ΔΔ} recipients with reduced LSKs, ST-HSCs and myeloid cells (Gr1⁺CD11b⁺ cells) cells.

In the BM niche, *Ccn2* is necessary for regenerative processes and balanced MSC differentiation (Battula et al., 2013; 2017; Igarashi et al., 1993; Takigawa, 2018). In addition, although *Ccn2* is only expressed at a low level under steady state conditions, we found that irradiation, which we use as conditioning in the transplantation procedure, induces *Ccn2* (Figure 40A and B; Zhang et al., 2015). The precise role of *Ccn2* expression in BM stress responses remains to be studied. Besides the observed and described effects on HSC maintenance upon stress, it is likely that CCN2 may affect proliferation and differentiation of different BM subpopulations, thus altering the composition of the niche (Battula et al., 2013). In the latter study, human CCN2 knockdown MSCs were transplanted into NOD/SCID/IL-2rg(null) mice and differentiated mainly into adipocytes. This adipogenic microenvironment then further promoted the engraftment of leukemia cells by upregulating Leptin and SDF1 α (Battula et al., 2013). These findings are controversial, since they would imply an increased engraftment of the WT HSCs into the *Ccn2*^{Δ/Δ} microenvironment rather than reduced numbers. Against this theory, other studies showed that adipocytes impaired the hematopoietic recovery rather than promoted it (Ambrosi et al., 2017).

Taken together, niche secreted *Ccn2* seems to be necessary for a prolonged maintenance of self-renewing LT-HSCs maintaining their proliferative and differentiation potential via a possible direct or indirect mechanism.

4.1.2.1 *Ccn2* is necessary during irradiation stress

4.1.2.1.1 Osteoblastic OBCs express and upregulate CCN2 *in vivo* after irradiation

We found that total body irradiation (8.5 Gy) upregulates CCN2 in bone slices of adult mice when compared to controls (adult, steady state), 24 hours after irradiation. Analysis of BM subpopulations further showed that in OBCs, CCN2 protein was significantly enhanced, 24 hours after sublethal (4.5 Gy) irradiation. This experiment provides evidence, that in the studied BM, exclusively osteoblastic cells respond with an increased *Ccn2* expression 24 hours after irradiation. This result indicates that OBCs play a major role in CCN2-mediated responses during stress situations.

At later time points after irradiation, the inability to upregulate *Ccn2* in *Ccn2* deficient mice leads to a significant expansion of ECs and a tendency of increased OBCs (p=0.0556) five days after irradiation. Interestingly, the EC expansion is reversible, as 14 days after irradiation, the *Ccn2*^{Δ/Δ} niche looked like the niche in irradiated control mice.

Considering that *Ccn2* is upregulated by OBCs after irradiation, the increase in OBC after five days in *Ccn2^{Δ/Δ}* mice suggests that CCN2 is a negative regulator of OBC proliferation in irradiation-induced BM damage. Although high levels of CCN2 were found during different biological processes such as bone remodeling and growth in trabeculae osteoblasts (Safadi et al., 2003). Contrary to our results, a previous publication suggests that *Ccn2* expression promotes OBC proliferation rather than inhibit, as high levels of *Ccn2* were found during proliferation of early osteoblast progenitors *in vitro*, and the loss of *Ccn2* in MSCs reduces their proliferation (Battula et al., 2013). In addition, osteoblasts derived from *Ccn2* knockout mice show decreased proliferation, three days after culture (Luo et al., 2004; Mundy et al., 2014). Interestingly, seven days into the culture, cell numbers were the same with *Ccn2* knockout and control OBCs (Mundy et al., 2014). Thus, our finding that OBC numbers are normalized 14 days after irradiation, suggests *Ccn2* is relevant in the proliferative phase of the stress response, but not so much in later differentiation and regeneration stages.

4.1.2.3.2.2 Irradiation alters the behavior of *Ccn2^{Δ/Δ}* MSCs

We observed that osteogenic calcium deposition in osteogenic induced *Ccn2^{Δ/Δ}* MSCs (5d IR) was reduced, indicating impaired osteogenesis lineage, as was previously also found in human shCCN2 MSCs (Battula et al., 2013; 2017). Considering that MSCs either differentiate into osteoblasts or adipocytes (Chen et al., 2016) we would have expected an enhanced adipogenic differentiation of *Ccn2^{Δ/Δ}* MSCs (5d IR) compared to control MSCs (5d IR). However, we did not find this in our experiments.

We further found reduced MCP-1, which is strongly produced by sinusoidal ECs and CXCL12-abundant stromal cells (Helbling et al., 2019; Dolgalev and Tikhonova, 2021; Website [single cell portal](#)), in the serum of LPS treated *Ccn2^{Δ/Δ}* mice. Thus, we hypothesize that the reduced numbers of hematopoietic cells from WT HSCs in the *Ccn2^{Δ/Δ}* microenvironment could be the result of reduced support or activation due to an impaired pro-inflammatory cytokine secretion. Indeed, besides MCP-1, IL-6, Rantes (CCL5) and TGFβ-1 were on average 50% less secreted in the supernatant of *Ccn2^{Δ/Δ}* MSCs (14d IR).

Alternatively, considering that reduced MCP-1/CCL2 concentration impairs the recruitment of mature myeloid cells to the BM niche, thus possibly reducing the impact of HSC quiescence-promoting ACKR1⁺ or VCAM1⁺ macrophages in the BM (Kaur et al., Blood. 2018; Kwon et al., Cell Stem Cell. 2022).

These findings support the view that *Ccn2* loss alters the HSCs niche composition with altered release of pro-inflammatory cytokines, particularly MCP-1/CCL2, leading to a possible impaired support of the HSCs through a yet undefined mechanism.

4.1.2.3.2.2 Irradiation alters the behavior of *Ccn2*^{Δ/Δ} MSCs

In experiments to reveal a possible impaired differentiation potential of irradiated *Ccn2*^{Δ/Δ} MSCs, we found reduced calcium deposition in osteogenic induced differentiation of *Ccn2*^{Δ/Δ} MSCs (5d IR) indicating an impaired differentiation potential into the osteogenic lineage. This is in accordance to the previous published data (Battula et al., 2013; 2017) where human shCCN2-MSCs increased the ability to differentiate into adipocytes. Because MSCs either differentiate into osteoblasts or adipocytes (Chen et al., 2016) we would have expected an enhanced adipogenic differentiation of *Ccn2*^{Δ/Δ} MSCs (5d IR) compared to control MSCs (5d IR). However, the impaired osteogenic differentiation of *Ccn2*^{Δ/Δ} MSCs five days after irradiation but unchanged 14 days after irradiation supports our previous theory that *Ccn2* is relevant in the proliferative phase of the stress response, but not so much in later regeneration stages.

However, we found reduced MCP-1, which is mainly source produced by stromal cells (Huang et al., 2016), in the serum of LPS treated *Ccn2*^{Δ/Δ} mice. Thus, we hypothesize that the reduced numbers of hematopoietic cells from WT HSCs in the *Ccn2*^{Δ/Δ} microenvironment could be the result of reduced support or activation due to an impaired pro-inflammatory cytokine secretion. Indeed, besides MCP-1, IL-6, Rantes (CCL5) and TGFβ-1 were on average 50% less secreted in the supernatant of *Ccn2*^{Δ/Δ} MSCs (14d IR).

These findings support the view that *Ccn2* loss alters the HSCs niche composition with altered release of pro-inflammatory cytokines leading to a possible impaired support of the HSCs.

4.1.2.3.2.3 *Ccn2* loss during irradiation stress impairs HSC function

Besides the BM niche, we also studied hematopoietic regeneration at different time points after sublethal irradiation. Whereas 5d IR the hematopoietic system is at the nadir of cell degeneration, 14d IR the hematopoietic microenvironment in the BM is restored while the white blood cell number in the PB is 50% of pre-irradiation numbers (Dominici 2009; Jin et al., 2014).

Our findings of reduced myeloid progenitor compartment 5d after IR that after 14d IR was restored with the result of slowly decreasing LT- stem cell numbers (0.065) which harbor a

reduced repopulating ability, supports the earlier view that *Ccn2* is essential for the maintenance of self-renewing LT-HSCs (Istvánffy et al., 2015).

As we showed increased myelopoiesis in the transplantation of non-irradiated *Ccn2*^{ΔΔ} LT-HSCs, and decreased myeloid progenitor cells 5d IR, this finding could signify that in line with its pro-inflammatory activity, extrinsic *Ccn2* stimulates myelopoiesis. The mechanisms underlying this pro-myeloid effect are as yet unclear, but our cytokine analyses of the supernatant from MSCs 14d IR and the serum after LPS treatment suggest that CCN2 might regulate the release of MCP-1, TNF- α , and other pro-inflammatory cytokines.

MCP-1/CCL2 for example was documented to stimulate the myeloid proliferation but also myeloid cell survival by reducing apoptosis through upregulation of antiapoptotic proteins Bcl-2, Bcl-XL and cFLIPL (Amano et al., 2014; Li et al., 2015; Roca et al., 2009). Similarly, IL-6 is also known as an activator of myelopoiesis during inflammation (Ishihara and Hirano, 2002). Our results, thus, suggest, that the rapid upregulation of microenvironmental CCN2 in the inflammatory response is an essential mechanism to induce cytokines required to regulate the myeloid cell pool during stress responses.

In addition, in line with our previous *in vitro* study (Istvánffy et al., 2015), the loss repopulating activity of HSCs in irradiated *Ccn2*^{ΔΔ} mice, and the reduced cell cycle of LSK cells (increased G0/G1 state), suggests a similar function of CCN2 in the maintenance of LT-HSC during stress responses.

4.1.2.3.2.4.1 HSC functionality in vivo does not involve CCN2-dependent TGF β /SMAD2/3 signaling

In line with the observed impaired proliferative response of *Ccn2*^{ΔΔ} stressed HSCs, we observed that LSK cells from *Ccn2*^{ΔΔ} 14d IR increase acetylated p53 and p27^{KIP} (CDKN1B) while reducing Cyclin D1. As aged HSCs show inefficient DNA damage repair, and are impaired in repopulating activity (Flach et al., 2014), we wondered if DNA damage accumulates in *Ccn2*^{ΔΔ} HSCs like aged HSCs. Indeed, we found highly increased DNA damage indicator γ H2A.X+ nuclear foci in *Ccn2*^{ΔΔ} 14d IR, which did not form active 53BP1+ DNA repair foci when compared to controls 14d IR. In addition, increased length of DNA comets in *Ccn2*^{ΔΔ} 14d IR confirms inefficient DNA repair in these cells, while controls 14d IR were unchanged and comparable to steady state *Ccn2*^{ΔΔ} and controls.

In our previous *in vitro* study, using cocultures of HSCs with sh*Ccn2* stromal cells we found that inefficient DNA repair in HSCs cultured on sh*Ccn2* stroma was strongly associated with increased signaling through SMAD2/3 in the LT-HSCs (Istvánffy et al., 2015). Surprisingly, in

our in vivo 14d IR model, we did not find activation of SMAD2/3 signaling in the *Ccn2^{ΔΔ}* LSK cells compared to controls.

4.1.2.3.2.4.1 HSC functionality is dependent from CCN2/gp130/STAT3/UBC13 signaling

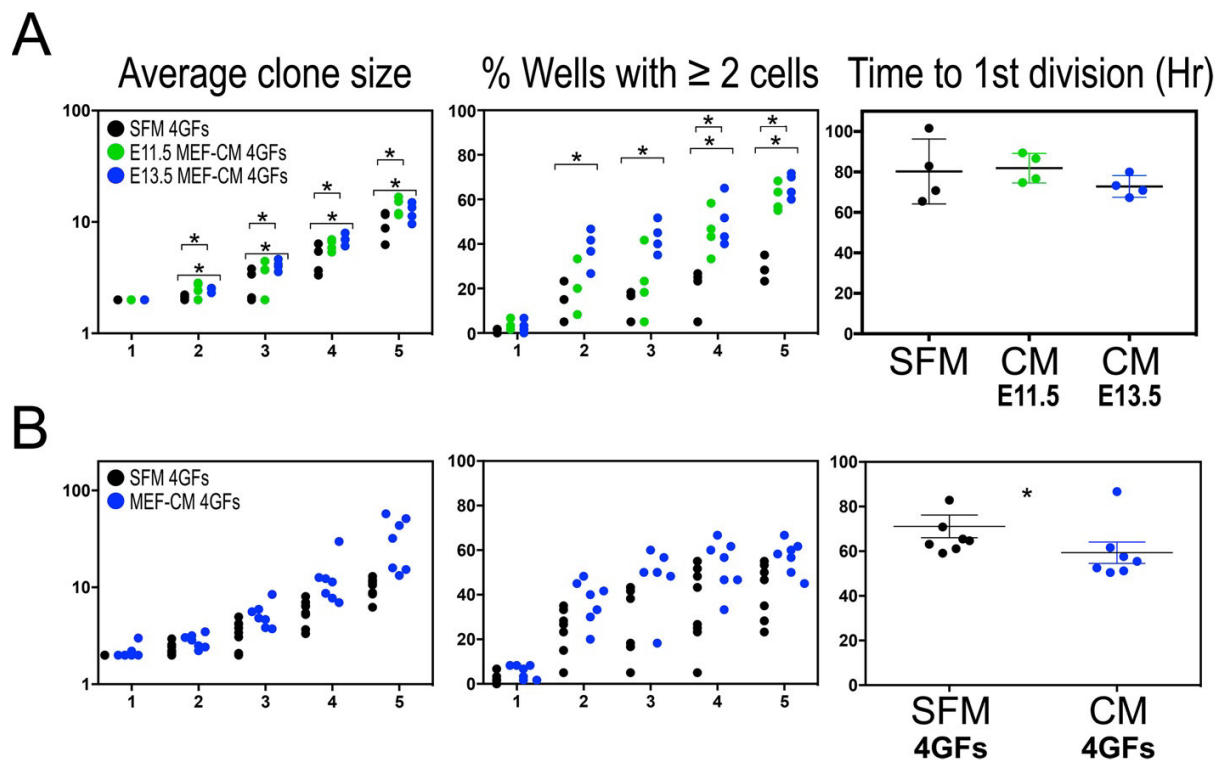
In accordance with reduced inflammatory cytokines, we found reduced gp130 and phosphorylated STAT3 signaling in *Ccn2^{ΔΔ}* 14d IR, compared to control 14d IR. Since activation of STAT3 down-regulates the pro-inflammatory ubiquitin E2 ligase UBC13/UBE2N (Zhang et al., 2018), we also analyzed UBC13 in control and *Ccn2^{ΔΔ}* 14d IR LSK cells. UBC13 is necessary at G1 phase reparation of irradiation induced “dirty” DSBs and NHEJ-dependent DNA repair in 50% and 70% of irradiation induced DSBs (Akagawa et al., 2020) and its deletion impairs hematopoiesis (Wu et al., 2009). Downstream UBC13 ubiquitinates γ H2A.X+ which initiates further repair mechanisms (Akagawa et al., 2020). Considering that irradiated *Ccn2^{ΔΔ}* 14d IR show elevation of DNA damage foci although both γ H2A.X+ and UBC13 are also increased, suggests that *Ccn2^{ΔΔ}* 14d IR LSK cells either, excessively proliferate and accumulate DNA damage (replicative stress), or are unable to repair their irradiation-induced DNA damage due to an impaired DNA repair mechanism downstream of ubiquitinated γ H2A.X+. The first hypothesis is supported by the finding that UBC13 promotes the pro-inflammatory NF- κ B signaling pathway by ubiquitination of inhibitory regulators such as I κ B, leading to increased proliferation of myeloid cells through accumulation of DNA damage (Zhang et al., 2018) and upregulation of Jagged 1 on niche cells (Rupec et al., 2005). Surprisingly, we found reduced expression of the I κ B inhibitor IKK- β in *Ccn2^{ΔΔ}* 14d IR compared to controls (data not shown), thus suggesting decreased NF- κ B signaling (Hodge et al., 2016; Xiao et al., 2005). Also, we did not find increased proliferation with elevated numbers of HSCs in stressed *Ccn2^{ΔΔ}*. The second theory of an impaired DNA repair mechanism downstream of γ H2A.X+ and UBC13 is more likely. While *Ccn2^{ΔΔ}* 14d IR HSCs would possibly still gain their DSB through the cause of irradiation, WT HSCs proliferating in *Ccn2^{ΔΔ}* stroma would gain the DSB through proliferation, leading to slowly reduced numbers of HSCs, as we already detected in *Ccn2^{ΔΔ}*-MEF single cell assay or extrinsic transplantation experiments. A possible mechanism important for the following DDR mechanism is the colocalization of γ H2A.X+ with 53BP1 (Lassmann et al., 2010; Nakamura et al., 2010;). Indeed, in *Ccn2^{ΔΔ}* 14d IR HSCs compared to controls, we found a significant decreased co-localization of γ H2A.X+ with 53BP1, supporting the idea that γ H2AX fails to recruit the DNA repair machinery to form DNA repair foci in stressed *Ccn2^{ΔΔ}* HSCs.

The thesis period did, unfortunately, not leave time to pin down the two different hypotheses. In the future, investigations should study I κ B, Rel/NF κ B, and other molecules of the DNA repair

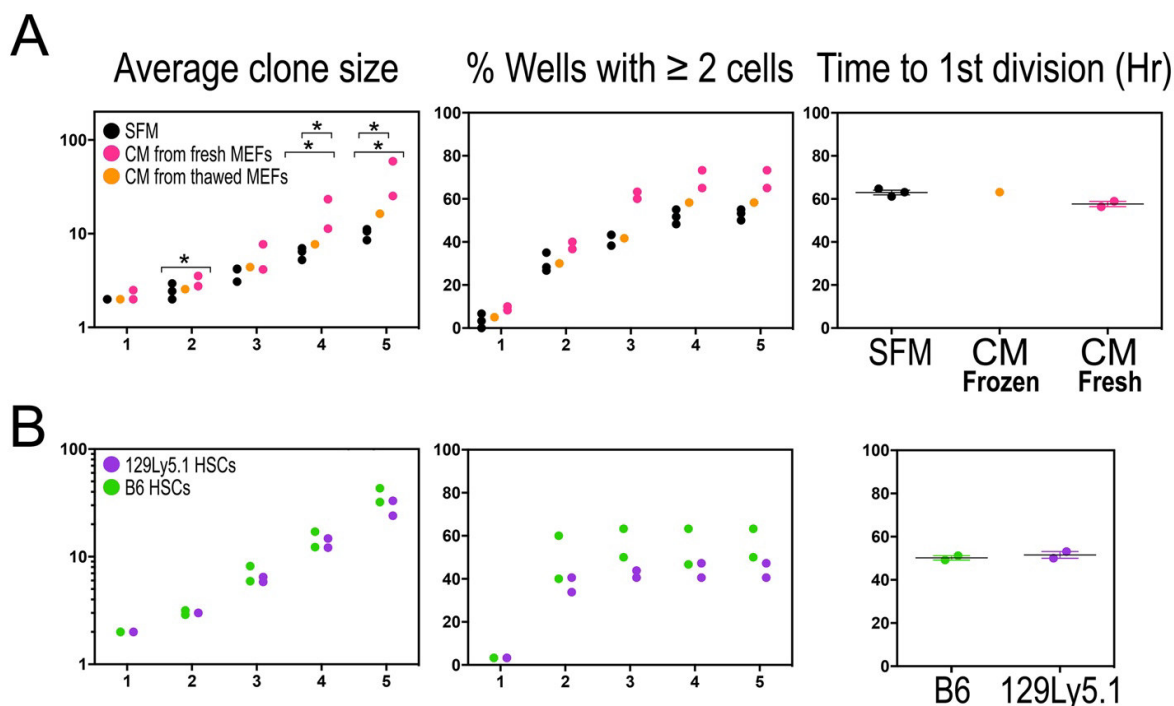
foci such as Ku79/80, RAD51, and DNA-PK in more detail. Furthermore, since UBC13 regulates NF κ B activation and DNA repair through two different E3 ubiquitin ligases acting as a switch between the two pathways: UVE1A and MMS2, respectively (Wu et al., 2020) analyses of these two molecules may give insights on how the switch between DNA repair or NF κ B signaling operates in *Ccn2* ^{Δ/Δ} 14d IR HSCs.

In summary, deletion of *Ccn2* expression *in vivo* is required for maintaining stem cells after stress-induced inflammation. The results in this thesis support a mechanism whereby CCN2 upregulates the expression of pro-inflammatory factors (cytokines, gp130), and anti-inflammatory up-regulation of pSTAT3 signaling through down-regulation of UBC13. Furthermore, *Ccn2* deletion leads to an inefficient co-localization γ H2A.X+ with 53BP1 which impairs DDR and the progressing loss of functional HSCs. Considering CCN2 is upregulated both in several solid cancers (Cheng et al., 2014; Chien et al., 2004; Hou et al., 2018; Jiang et al., 2019) and hematopoietic acute lymphoblastic leukemia (Ross et al., 2003; Sala-Torra et al., 2007; Vorwerk et al., 2000), this thesis strongly suggests the CCN2/gp130/STAT3/UBC13 pathway as a novel therapeutic target for these cancers.

Supplementary Data



Supplementary Figure 1. MEF-CM enhances CD34-SLAM cell number with decreased time to first division. MEF-CM was generated from E.11.5 and E.13.5 (Materials and Methods) and 129xLy5.1 CD34-SLAM cells were cultured in SFM or MEF-CM media with the addition of 4GFs. Mean result of clones cultured in one 96-well plate are shown as dot plots in a total of four independent experiments. Left plot: average clone size/plate. Middle plot: percentage of wells with > 2 cells/plate. Right plot: time to 1st division in (hrs). (B) Differences of MEF-CM from individual E13.5 embryos in three independently performed single cell experiments. CD34-SLAM cells were cultivated in SFM or MEF-CM with 4GF. Left plot: average clone size/plate. Middle plot: percentage of wells with > 2 cells/plate. Right plot: time to 1st division in (hrs). SFM in black dots, E11.5 MEF-CM with 4GF in green dots and E13.5 MEF-CM with 4GF in blue dots. * p-value < 0.05 show significance in the comparison of SFM and MEF-CM (2GF and 4GF) using the Mann-Whitney U-test (Romero Marquez and Hettler et al., 2020).



Supplementary Figure 2. Single cell culture optimization in MEF-CM. MEF-CM was generated from E.13.5 (Materials and Methods). Freshly generated CM was compared to CM generated from cells thawed before the experiment. Mean result of clones cultured in one 96-well plate are shown as dot plots. Left plot: average clone size/plate. Middle plot: percentage of wells with $>- 2$ cells/plate. Right plot: time to 1st division in (hrs). (B) Differences of CD34-SLAM cells isolated from 129Ly5.1 or B16 mice cultured in MEF-CM 4GF. Left plot: average clone size/plate. Middle plot: percentage of wells with $>- 2$ cells/plate. Right plot: time to 1st division in (hrs). SFM in black dots, CM from fresh MEFs in pink dots, CM from thawed MEFs in orange dots, B16 HSCs in green dots and 129Ly5.1 HSC in purple dots. E13.5 MEF-CM with 4GF in blue dots. * p-value <0.05 show significance in the comparison of SFM and MEF-CM (2GF and 4GF) using the Mann-Whitney U-test (Romero Marquez and Hettler et al., 2020).

5 Summary

Preservation of functional hematopoietic stem cells (HSCs) is the main function of the bone marrow microenvironment, regulating the dormancy, activation, self-renewal and differentiation. Previously our group demonstrated in coculture assays with HSCs on shCcn2-stromal cells, that the pro-inflammatory factor Cellular Communication Network factor 2 (*Ccn2*) is necessary for the maintenance of CD34⁺CD150⁺ LSK (LT-HSCs) and the entrance of dormant (G0) HSCs into the cell cycle.

Here, we investigated the *in vivo* role of *Ccn2* in adult steady state and stress induced hematopoiesis.

At steady state, in line with a low expression of *Ccn2*, its loss did not affect hematopoietic or stromal cell composition.

Interestingly, inflammatory stress such as LPS treatment in *Ccn2^{Δ/Δ}* mice resulted in reduced pro-inflammatory cytokine MCP-1 and lower numbers of LSK as well as CD34⁺ LSK, short-term (ST-) and long-term (LT-) repopulating HSCs already 24hrs after treatment. Moreover, in transplantation experiments where we transplanted WT LT-HSCs into *Ccn2^{Δ/Δ}* and control mice the lacking support of stromal cell *Ccn2* resulted in reduced donor cell engraftment with impaired numbers of myeloid cells, LSKs and ST-HSCs. Irradiation studies revealed that *Ccn2* exclusively gets upregulated in osteoblastic cells and is necessary for osteogenic differentiation of MSCs five days after irradiation. Moreover, 14 days after irradiation (14d IR) cultured MSCs secreted less MCP-1 and 50% reduced IL-6, Rantes and TGF-β1 indicating an impaired inflammatory response when *Ccn2* is lost. Five days after irradiation, we found reduced numbers of myeloid progenitor cells that after 14 days were restored. Although further numbers of hematopoietic cells were unchanged in irradiated *Ccn2^{Δ/Δ}* mice compared to controls, the functionality of *Ccn2^{Δ/Δ}* HSC 14d IR was strongly impaired as their ability to engraft in WT recipient was apparent. Irradiated *Ccn2^{Δ/Δ}* HSCs, displayed a cell cycle arrest at G0/G1 state of cell cycle as demonstrated with BrDU incorporation as well as increased p53, p27^{KIP} and reduced Cyclin-D1. Consistent with that we found increased γH2AX and an enhanced DNA comet length of *Ccn2^{Δ/Δ}* HSCs 14d IR, explaining their impaired ability to engraft in WT recipient mice. Further investigation on molecular level revealed, an unchanged TGF-β1/SMAD2/3 signaling. However, in line with reduced pro-inflammatory cytokines of *Ccn2^{Δ/Δ}* MSCs 14d IR we found reduced GP130, p-STAT3 and a subsequent increase of UBC13. Although first DNA repair mechanisms are active in *Ccn2^{Δ/Δ}* HSCs 14d IR as shown by enhanced UBC13 and γH2AX, colocalization of γH2AX with 53BP1 was reduced, indicating an impaired DNA repair mechanism when *Ccn2* is lost. The latter may explain the DNA damage discovered in *Ccn2^{Δ/Δ}* HSCs 14d IR.

Summarized this thesis shows that *Ccn2* is dispensable at steady state conditions. However, during irradiation stress mainly osteoblastic *Ccn2* seems to be necessary for the secretion of pro-inflammatory cytokines of the niche that ensures a correct HSC behavior in terms of hematopoietic stress. Furthermore, *Ccn2* is essential for a correct DNA repair mechanism that

especially during inflammatory stress induced HSC proliferation, is required for the maintenance of LT-HSCs.

6 Zusammenfassung

Die Erhaltung funktioneller hämatopoetischer Stammzellen (HSZ) ist die Hauptaufgabe der Knochenmarks-Nische, die neben der Ruhephase, Aktivierung, und Selbsterneuerung auch die Differenzierung der HSZ reguliert.

In einer vorangegangenen Studie, in welcher *in vitro* HSZs auf shCcn2-Stammzellen kultiviert wurden, konnte gezeigt werden, dass der stressinduzierte pro-inflammatorische Faktor „Cellular Communication Network factor 2“ (Ccn2) für den Erhalt von Langzeit (LZ)-HSZs notwendig ist da es von (G0-phase) CD34⁺CD150⁺ LSK-HSZs benötigt wird, um in den Zellzyklus einzutreten.

Hier untersuchten wir die *in vivo* Rolle von *Ccn2* im unbehandelten und stress-induzierten Zustand.

Im unbehandelten Zustand, in welchem die Expression von *Ccn2* gering ist, hat dessen Verlust keine Auswirkungen auf die Zusammensetzung von Blut- oder Stromazellen. Interessanterweise führte inflammatorischer Stress wie etwa eine LPS-Behandlung bei *Ccn2^{Δ/Δ}* Mäusen bereits 24 Stunden nach der Behandlung zu einer Verringerung des pro-inflammatorischen Zytokins MCP-1 sowie einer geringeren Anzahl von LSKs, Kurzzeit und Langzeit repopulierende HSZs. In Transplantationsexperimenten, in welchen WT CD34⁺CD150⁺LSKs in *Ccn2^{Δ/Δ}* und Kontrollmäuse wurden, führte der Verlust von Stromazellen sekretiertes CCN2 zu einem verminderten Engraftment der Spenderzellen mit einer geringeren Anzahl von myeloider Zellen, LSKs sowie Kurzzeit proliferierender -HSZs. Bestrahlungsstudien zeigten, dass *Ccn2* ausschließlich in osteoblastischen Zellen hochreguliert wird und für die osteogene Differenzierung von MSCs fünf Tage nach Bestrahlung notwendig ist. Darüber hinaus sezernierten kultivierte MSCs 14 Tage nach Bestrahlung (14d IR) weniger MCP-1 und 50 % weniger IL-6, Rantes und TGF-1, was auf eine beeinträchtigte Entzündungsreaktion bei Verlust von *Ccn2* hinweist. Fünf Tage nach Bestrahlung fanden wir eine verringerte Anzahl myeloider Vorläuferzellen, die nach 14 Tagen wiederhergestellt war. Obwohl die Anzahl hämatopoetischer Zellen in bestrahlten *Ccn2^{Δ/Δ}* im Vergleich zu den Kontrollen unverändert blieb, war die HSZ-Funktionalität 14 Tage nach Bestrahlung stark beeinträchtigt, was durch ihre verminderte Repopulationsfähigkeit in WT-Empfänger verdeutlicht wurde. Bestrahlte *Ccn2^{Δ/Δ}* HSZ wiesen einen Zellzyklus-Stillstand im G0/G1-Stadium des Zellzyklus auf, wie mit BrDU-Inkorporation nachgewiesen wurde, sowie

erhöhtes p53, p27Kip und reduziertes Cyclin-D1. In Übereinstimmung damit fanden wir eine erhöhte H2AX und eine erhöhte DNA-Komet-Länge von *Ccn2^{Δ/Δ}* HSZs 14d IR, was ihre eingeschränkte Fähigkeit zur Transplantation in WT-Empfängermäuse erklärt. Weitere Untersuchungen auf molekularer Ebene zeigten eine unveränderte TGF-1/SMAD2/3-Signalübertragung. In Übereinstimmung mit den verringerten pro-inflammatorischen Zytokinen der *Ccn2^{Δ/Δ}* MSCs 14d IR fanden wir jedoch eine Verringerung von Gp130, p-Stat3 und einen anschließenden Anstieg von UBC13. Obwohl die ersten DNA-Reparaturmechanismen in *Ccn2^{Δ/Δ}* HSZ 14d IR aktiv sind, wie durch erhöhte UBC13 und H2AX gezeigt wird, war die Kollokalisierung von H2AX mit 53BP1 reduziert, was auf einen beeinträchtigten DNA-Reparaturmechanismus hinweist, wenn *Ccn2* verloren geht.

Zusammengefasst zeigt diese Arbeit, dass *Ccn2* unter normalen Bedingungen entbehrlich ist. Bei Bestrahlungsstress wird *Ccn2* jedoch hauptsächlich von osteoblastische Zellen exprimiert. Es konnte gezeigt werden, dass *Ccn2* für die Sekretion von pro-inflammatorischen Zytokinen in der Nische notwendig ist, die ein korrektes Verhalten der HSZ bei hämatopoetischer Stress gewährleistet. Darüber hinaus ist *Ccn2* essenziell für einen korrekten DNA-Reparaturmechanismus, der insbesondere während der durch Entzündungsstress induzierten HSZ-Proliferation für die Aufrechterhaltung von LZ-HSZs erforderlich ist.

7 Appendices

7.1 List of Figures

Figure 1. Mouse hematopoietic hierarchy model.....	3
Figure 2. The central niche and the endosteal niche.....	9
Figure 3. Gp130/JAK/STAT signaling.....	15
Figure 4. Canonical and noncanonical NF- κ B. IL-1 β or TNF- α bind specific receptors and activate the canonical pathway through phosphorylation of I κ B components (β , ϵ , or γ (NEMO)) by I κ B kinase (IKK)..	17
Figure 5. DNA damage induced apoptosis.....	21
Figure 6. CCN family members.....	26
Figure 7. CCN2 and its binding partners.....	27
Figure 8. Representative picture for the genotyping of <i>Ccn2</i> conditional mice.....	54
Figure 9. Single-cell cultures in SFM and MEF conditioned medium with 2GF and 4GF.....	70
Figure 10. Flow cytometry analysis of bulk cultured LSK cells and single cell cultured CD34-SLAM cells.....	72
Figure 11. Transplantation experiment for self-renewal maintenance capacity of the different conditions.....	74
Figure 12. Verification of efficient knockout using PCR in different tissues.....	75
Figure 13. <i>Ccn2</i> RNA content in cultured MSCs (p4).....	76
Figure 14. Single-cell cultures in control and <i>Ccn2</i> ^{Δ/Δ} MEF conditioned medium with 2GF...	77
Figure 15. Single-cell cultures of control and <i>Ccn2</i> ^{Δ/Δ} CD34 ⁻ SLAM cells in control MEF conditioned medium with 2GF.	78
Figure 16. Relative delta delta Ct expression of <i>Ccn2</i> during steady state condition in hematopoietic- and stromal cells..	79
Figure 17. Blood counter analysis after <i>Ccn2</i> loss in adult mice during steady state conditions.	80
Figure 18. Hematopoietic mature cell composition after <i>Ccn2</i> deletion in the PB, BM and Sp at steady state condition.	82

Figure 19. Early hematopoietic cell composition after <i>Ccn2</i> deletion in the BM at steady state conditions.....	83
Figure 20. Endosteal cell composition after <i>Ccn2</i> deletion at steady state condition.	85
Figure 21. Mature cell populations in the PB, Sp and BM after 5-FU treatment of control and <i>Ccn2^{Δ/Δ}</i> mice.. ..	87
Figure 22. Myeloid progenitor and stem cells in the BM after 5-FU treatment of control and <i>Ccn2^{Δ/Δ}</i> mice.....	89
Figure 23. Stromal cell composition after 5-FU treatment of control and <i>Ccn2^{Δ/Δ}</i> mice.. ..	90
Figure 24. Mature cell populations in the PB, Sp and BM after LPS treatment of control and <i>Ccn2^{Δ/Δ}</i> mice.	92
Figure 25. Myeloid progenitor and stem cells in the BM after LPS treatment of control and <i>Ccn2^{Δ/Δ}</i> mice.	94
Figure 26. CBA from serum isolated of the PB after LPS treatment of control and <i>Ccn2^{Δ/Δ}</i> mice.	96
Figure 27. Stromal cell composition after LPS treatment of control and <i>Ccn2^{Δ/Δ}</i> mice.....	98
Figure 28. Engraftment in the PB of transplanted LSK cells from control and <i>Ccn2^{Δ/Δ}</i> cells after four weeks of TAM treatment (i.p.) as a prolonged hematopoietic stress model.....	100
Figure 29. Mature cell engraftment in the Sp and BM of transplanted LSK cells from control and <i>Ccn2^{Δ/Δ}</i> mice as a long-term hematopoietic stress model.	102
Figure 30. Hematopoietic progenitor and stem cell engraftment in the BM of transplanted LSK cells from control and <i>Ccn2^{Δ/Δ}</i> mice as a long-term hematopoietic stress model.....	103
Figure 31. Engraftment in the PB of transplanted control and <i>Ccn2^{fl/fl}</i> whole BM into an WT microenvironment as a long-term hematopoietic stress model.....	105
Figure 32. Mature cell engraftment in the Sp and BM of transplanted control and <i>Ccn2^{fl/fl}</i> whole BM into an WT microenvironment as a long-term hematopoietic stress model.....	106
Figure 33. Hematopoietic progenitor and stem cell engraftment in the BM of transplanted control and <i>Ccn2^{fl/fl}</i> whole BM into an WT microenvironment as a long-term hematopoietic stress model.....	108
Figure 34. Engraftment of mature cell populations of transplanted WT HSCs into a <i>Ccn2</i> deficient microenvironment as a long-term hematopoietic stress model.. ..	110

Figure 35. Engraftment of MPs and HSCs of transplanted WT HSCs into a <i>Ccn2</i> deficient microenvironment as a long-term hematopoietic stress model.....	112
Figure 36. CCN2 protein expression during steady-state and after irradiation.....	113
Figure 37. Hematopoietic cell composition after five hours of irradiation (IR).	115
Figure 38. <i>Ccn2</i> expression in 4.5 Gy irradiated hematopoietic- and stromal cells compared to untreated cells.....	116
Figure 39. CCN2 protein content 24hrs after irradiation (IR) in different hematopoietic cell populations.....	118
Figure 40. CCN2 protein content 24hrs after irradiation (IR) in different stromal cell populations.	119
Figure 41. Stromal cells after sublethal irradiation (IR) of control and <i>Ccn2</i> ^{ΔΔ} mice as short-term stress model.	122
Figure 42. Adhesion and CFU-F potential at steady-state and after sublethal irradiation of control and <i>Ccn2</i> ^{ΔΔ} as short-term stress model.....	123
Figure 43. Induced and spontaneous adipogenic and osteogenic differentiation at steady state and after sublethal irradiation of control and <i>Ccn2</i> ^{ΔΔ} as short-term stress model.....	125
Figure 44. Wound healing potential of MSC at steady state and after sublethal irradiation of control and <i>Ccn2</i> ^{ΔΔ} as short-term stress model.....	126
Figure 45. Growth potential and senescence of MSC at steady state and after sublethal irradiation of control and <i>Ccn2</i> ^{ΔΔ} as short-term stress model..	128
Figure 46. CBA from stromal cells 14 days after irradiation of control and <i>Ccn2</i> ^{ΔΔ} mice....	129
Figure 47. PB cells after sublethal irradiation (IR) of control and <i>Ccn2</i> ^{ΔΔ} as short-term stress model.	130
Figure 48. Hematopoietic mature cells after sublethal irradiation (IR) of control and <i>Ccn2</i> ^{ΔΔ} as short-term stress model.	131
Figure 49. Hematopoietic myeloid progenitor cells after sublethal irradiation (IR) of control and <i>Ccn2</i> ^{ΔΔ} as short-term stress model.....	133
Figure 50. Hematopoietic stem cells after sublethal irradiation (IR) of control and <i>Ccn2</i> ^{ΔΔ} as short-term stress model.	134

Figure 51. Engraftment in the PB of transplanted LSK cells from sublethal irradiated (IR) and 14 days regenerated control and <i>Ccn2^{ΔΔ}</i> cells as a long-term hematopoietic stress model..	136
Figure 52. Mature cell engraftment in the Sp and BM of transplanted LSK cells from sublethal irradiated and 14 days regenerated control and <i>Ccn2^{ΔΔ}</i> cells as a long-term hematopoietic stress model.....	138
Figure 53. Hematopoietic progenitor and stem cell engraftment in the BM of transplanted LSK cells from sublethal irradiated and 14 days regenerated control and <i>Ccn2^{ΔΔ}</i> cells as a long-term hematopoietic stress model.	139
Figure 54. Annexin V and BrdU treatment of IR LSK cells.	141
Figure 55. Immunofluorescence staining of sublethal irradiated and Comet assay from irradiated and steady state control and <i>Ccn2^{ΔΔ}</i> mice.....	144
Figure 56. Immunofluorescence staining of sublethal irradiated control and <i>Ccn2^{ΔΔ}</i> mice.	145
Figure 57. Immunofluorescence staining of 4.5Gy irradiated control and <i>Ccn2^{ΔΔ}</i> mice.	147
Figure 58. <i>Ccn2</i> expression in stromal cells during steady state conditions and after 5-FU treatment.....	149

7.2 List of Tables

Table 1. List of used consumption-utensils.....	36
Table 2. List of used machines and equipment's	38
Table 3. List of used Software's.....	38
Table 4. List of used chemicals.....	39
Table 5. List of used biological reagents	40
Table 6. List of ordered buffers, medium and solution.....	41
Table 7. List of self-made buffers, medium and solution	43
Table 8. List of used kits	43
Table 9. List of used primary antibodies for flow cytometry	45
Table 10. List of used primary antibodies for immunofluorescence.....	48
Table 11. List of used secondary antibodies for FACS.....	48

Table 12. List of used secondary antibodies for immunofluorescence	48
Table 13. List of PCR primers.....	49
Table 14. List of RT-PCR primers.....	49
Table 15. List of used vectors.....	50
Table 16. List of used cell lines.....	50
Table 17. List of used mice strains	51
Table 18. Content PCR scheme	52
Table 19. PCR programs	53
Table 20. Genomic DNA elimination and reverse-transcription master mix preparation	55
Table 21. RT-PCR pipette scheme	55

8 Publications

9 Acknowledgments

10 References

- Abd El Kader, T., Kubota, S., Nishida, T., Hattori, T., Aoyama, E., Janune, D., Hara, E. S., Ono, M., Tabata, Y., Kuboki, T., & Takigawa, M. (2014, Feb). The regenerative effects of CCN2 independent modules on chondrocytes in vitro and osteoarthritis models in vivo. *Bone*, 59, 180-188. <https://doi.org/10.1016/j.bone.2013.11.010>
- Abdel-Wahab, N., Weston, B. S., Roberts, T., & Mason, R. M. (2002, Oct). Connective tissue growth factor and regulation of the mesangial cell cycle: role in cellular hypertrophy. *J Am Soc Nephrol*, 13(10), 2437-2445. <https://doi.org/10.1097/01.asn.0000031828.58276.02>
- Abraham, D. (2008, Oct). Connective tissue growth factor: growth factor, matricellular organizer, fibrotic biomarker or molecular target for anti-fibrotic therapy in SSC? *Rheumatology (Oxford)*, 47 Suppl 5, v8-9. <https://doi.org/10.1093/rheumatology/ken278>
- Abreu, J. G., Ketpura, N. I., Reversade, B., & De Robertis, E. M. (2002, Aug). Connective-tissue growth factor (CTGF) modulates cell signalling by BMP and TGF-beta. *Nat Cell Biol*, 4(8), 599-604. <https://doi.org/10.1038/ncb826>
- Abreu, J. G., Ketpura, N. I., Reversade, B., & De Robertis, E. M. (2002, 2002/08/01). Connective-tissue growth factor (CTGF) modulates cell signalling by BMP and TGF- β . *Nature Cell Biology*, 4(8), 599-604. <https://doi.org/10.1038/ncb826>
- Adolfsson, J., Borge, O. J., Bryder, D., Theilgaard-Mönch, K., Astrand-Grundström, I., Sitnicka, E., Sasaki, Y., & Jacobsen, S. E. (2001, Oct). Upregulation of Flt3 expression within the bone marrow Lin(-)Sca1(+)c-kit(+) stem cell compartment is accompanied by loss of

- self-renewal capacity. *Immunity*, 15(4), 659-669. [https://doi.org/10.1016/s1074-7613\(01\)00220-5](https://doi.org/10.1016/s1074-7613(01)00220-5)
- Adolfsson, J., Månsson, R., Buza-Vidas, N., Hultquist, A., Liuba, K., Jensen, C. T., Bryder, D., Yang, L., Borge, O.-J., Thoren, L. A. M., Anderson, K., Sitnicka, E., Sasaki, Y., Sigvardsson, M., & Jacobsen, S. E. W. (2005, 2005/04/22/). Identification of Flt3+ Lympho-Myeloid Stem Cells Lacking Erythro-Megakaryocytic Potential: A Revised Road Map for Adult Blood Lineage Commitment. *Cell*, 121(2), 295-306. <https://doi.org/https://doi.org/10.1016/j.cell.2005.02.013>
- Adolfsson, J., Månsson, R., Buza-Vidas, N., Hultquist, A., Liuba, K., Jensen, C. T., Bryder, D., Yang, L., Borge, O. J., Thoren, L. A., Anderson, K., Sitnicka, E., Sasaki, Y., Sigvardsson, M., & Jacobsen, S. E. (2005, Apr 22). Identification of Flt3+ lympho-myeloid stem cells lacking erythro-megakaryocytic potential a revised road map for adult blood lineage commitment. *Cell*, 121(2), 295-306. <https://doi.org/10.1016/j.cell.2005.02.013>
- Aggarwal, B. B. (2003, Sep). Signalling pathways of the TNF superfamily: a double-edged sword. *Nat Rev Immunol*, 3(9), 745-756. <https://doi.org/10.1038/nri1184>
- Ahmed, M. S., Øie, E., Vinge, L. E., Yndestad, A., Øystein Andersen, G., Andersson, Y., Attramadal, T., & Attramadal, H. (2004, Mar). Connective tissue growth factor--a novel mediator of angiotensin II-stimulated cardiac fibroblast activation in heart failure in rats. *J Mol Cell Cardiol*, 36(3), 393-404. <https://doi.org/10.1016/j.yjmcc.2003.12.004>
- Akagawa, R., Trinh, H. T., Saha, L. K., Tsuda, M., Hirota, K., Yamada, S., Shibata, A., Kanemaki, M. T., Nakada, S., Takeda, S., & Sasanuma, H. (2020, Apr 24). UBC13-Mediated Ubiquitin Signaling Promotes Removal of Blocking Adducts from DNA Double-Strand Breaks. *iScience*, 23(4), 101027. <https://doi.org/10.1016/j.isci.2020.101027>
- Akashi, K., Traver, D., Miyamoto, T., & Weissman, I. L. (2000, Mar 9). A clonogenic common myeloid progenitor that gives rise to all myeloid lineages. *Nature*, 404(6774), 193-197. <https://doi.org/10.1038/35004599>
- Akira, S. (2003, Oct 3). Toll-like receptor signaling. *J Biol Chem*, 278(40), 38105-38108. <https://doi.org/10.1074/jbc.R300028200>
- Akira, S., & Kishimoto, T. (1992, Jun). IL-6 and NF-IL6 in acute-phase response and viral infection. *Immunol Rev*, 127, 25-50. <https://doi.org/10.1111/j.1600-065x.1992.tb01407.x>
- Akira, S., Takeda, K., & Kaisho, T. (2001, Aug). Toll-like receptors: critical proteins linking innate and acquired immunity. *Nat Immunol*, 2(8), 675-680. <https://doi.org/10.1038/90609>

- Alfaro, M. P., Deskins, D. L., Wallus, M., DasGupta, J., Davidson, J. M., Nanney, L. B., M, A. G., Gannon, M., & Young, P. P. (2013, Jan). A physiological role for connective tissue growth factor in early wound healing. *Lab Invest*, *93*(1), 81-95. <https://doi.org/10.1038/labinvest.2012.162>
- Almendral, J. M., Sommer, D., Macdonald-Bravo, H., Burckhardt, J., Perera, J., & Bravo, R. (1988, May). Complexity of the early genetic response to growth factors in mouse fibroblasts. *Mol Cell Biol*, *8*(5), 2140-2148. <https://doi.org/10.1128/mcb.8.5.2140-2148.1988>
- Amano, S. U., Cohen, J. L., Vangala, P., Tencerova, M., Nicoloso, S. M., Yawe, J. C., Shen, Y., Czech, M. P., & Aouadi, M. (2014, Jan 7). Local proliferation of macrophages contributes to obesity-associated adipose tissue inflammation. *Cell Metab*, *19*(1), 162-171. <https://doi.org/10.1016/j.cmet.2013.11.017>
- Ambrosi, T. H., Scialdone, A., Graja, A., Gohlke, S., Jank, A. M., Bocian, C., Woelk, L., Fan, H., Logan, D. W., Schürmann, A., Saraiva, L. R., & Schulz, T. J. (2017, Jun 1). Adipocyte Accumulation in the Bone Marrow during Obesity and Aging Impairs Stem Cell-Based Hematopoietic and Bone Regeneration. *Cell Stem Cell*, *20*(6), 771-784.e776. <https://doi.org/10.1016/j.stem.2017.02.009>
- Aoyama, E., Hattori, T., Hoshijima, M., Araki, D., Nishida, T., Kubota, S., & Takigawa, M. (2009, May 27). N-terminal domains of CCN family 2/connective tissue growth factor bind to aggrecan. *Biochem J*, *420*(3), 413-420. <https://doi.org/10.1042/bj20081991>
- Arai, F., Hirao, A., Ohmura, M., Sato, H., Matsuoka, S., Takubo, K., Ito, K., Koh, G. Y., & Suda, T. (2004, Jul 23). Tie2/angiopoietin-1 signaling regulates hematopoietic stem cell quiescence in the bone marrow niche. *Cell*, *118*(2), 149-161. <https://doi.org/10.1016/j.cell.2004.07.004>
- Arnott, J. A., Lambi, A. G., Mundy, C., Hendsi, H., Pixley, R. A., Owen, T. A., Safadi, F. F., & Popoff, S. N. (2011). The role of connective tissue growth factor (CTGF/CCN2) in skeletogenesis. *Crit Rev Eukaryot Gene Expr*, *21*(1), 43-69. <https://doi.org/10.1615/critreveukargeneexpr.v21.i1.40>
- Arnott, J. A., Zhang, X., Sanjay, A., Owen, T. A., Smock, S. L., Rehman, S., DeLong, W. G., Safadi, F. F., & Popoff, S. N. (2008, May). Molecular requirements for induction of CTGF expression by TGF-beta1 in primary osteoblasts. *Bone*, *42*(5), 871-885. <https://doi.org/10.1016/j.bone.2008.01.006>
- Askmyr, M., Sims, N. A., Martin, T. J., & Purton, L. E. (2009, Aug). What is the true nature of the osteoblastic hematopoietic stem cell niche? *Trends Endocrinol Metab*, *20*(6), 303-309. <https://doi.org/10.1016/j.tem.2009.03.004>

- Asri, A., Sabour, J., Atashi, A., & Soleimani, M. (2016). Homing in hematopoietic stem cells: focus on regulatory role of CXCR7 on SDF1a/CXCR4 axis. *Excli j*, *15*, 134-143. <https://doi.org/10.17179/excli2014-585>
- Audet, J., Miller, C. L., Eaves, C. J., & Piret, J. M. (2002, Nov 20). Common and distinct features of cytokine effects on hematopoietic stem and progenitor cells revealed by dose-response surface analysis. *Biotechnol Bioeng*, *80*(4), 393-404. <https://doi.org/10.1002/bit.10399>
- Audet, J., Miller, C. L., Rose-John, S., Piret, J. M., & Eaves, C. J. (2001, Feb 13). Distinct role of gp130 activation in promoting self-renewal divisions by mitogenically stimulated murine hematopoietic stem cells. *Proc Natl Acad Sci U S A*, *98*(4), 1757-1762. <https://doi.org/10.1073/pnas.98.4.1757>
- Austin, T. W., Solar, G. P., Ziegler, F. C., Liem, L., & Matthews, W. (1997, May 15). A role for the Wnt gene family in hematopoiesis: expansion of multilineage progenitor cells. *Blood*, *89*(10), 3624-3635.
- Babic, A. M., Chen, C. C., & Lau, L. F. (1999, Apr). Fisp12/mouse connective tissue growth factor mediates endothelial cell adhesion and migration through integrin alphavbeta3, promotes endothelial cell survival, and induces angiogenesis in vivo. *Mol Cell Biol*, *19*(4), 2958-2966. <https://doi.org/10.1128/mcb.19.4.2958>
- Baccin, C., Al-Sabah, J., Velten, L., Helbling, P. M., Grünschläger, F., Hernández-Malmierca, P., Nombela-Arrieta, C., Steinmetz, L. M., Trumpp, A., & Haas, S. (2020, 2020/01/01). Combined single-cell and spatial transcriptomics reveal the molecular, cellular and spatial bone marrow niche organization. *Nature Cell Biology*, *22*(1), 38-48. <https://doi.org/10.1038/s41556-019-0439-6>
- Bai, K. J., Chen, B. C., Pai, H. C., Weng, C. M., Yu, C. C., Hsu, M. J., Yu, M. C., Ma, H. P., Wu, C. H., Hong, C. Y., Kuo, M. L., & Lin, C. H. (2013, Jan). Thrombin-induced CCN2 expression in human lung fibroblasts requires the c-Src/JAK2/STAT3 pathway. *J Leukoc Biol*, *93*(1), 101-112. <https://doi.org/10.1189/jlb.0911449>
- Baksh, D., Boland, G. M., & Tuan, R. S. (2007, Aug 1). Cross-talk between Wnt signaling pathways in human mesenchymal stem cells leads to functional antagonism during osteogenic differentiation. *J Cell Biochem*, *101*(5), 1109-1124. <https://doi.org/10.1002/jcb.21097>
- Barriga, F., Ramírez, P., Wietstruck, A., & Rojas, N. (2012). Hematopoietic stem cell transplantation: clinical use and perspectives. *Biol Res*, *45*(3), 307-316. <https://doi.org/10.4067/s0716-97602012000300012>
- Baryawno, N., Przybylski, D., Kowalczyk, M. S., Kfoury, Y., Severe, N., Gustafsson, K., Kokkaliaris, K. D., Mercier, F., Tabaka, M., Hofree, M., Dionne, D., Papazian, A., Lee, D., Ashenberg, O., Subramanian, A., Vaishnav, E. D., Rozenblatt-Rosen, O., Regev, A.,

- & Scadden, D. T. (2019, Jun 13). A Cellular Taxonomy of the Bone Marrow Stroma in Homeostasis and Leukemia. *Cell*, 177(7), 1915-1932.e1916. <https://doi.org/10.1016/j.cell.2019.04.040>
- Batey, K., Kim, J., Brinster, L., Gonzalez-Matias, G., Wu, Z., Solorzano, S., Chen, J., Feng, X., & Young, N. S. (2022, Jan). Residual effects of busulfan and irradiation on murine hematopoietic stem and progenitor cells. *Exp Hematol*, 105, 22-31. <https://doi.org/10.1016/j.exphem.2021.11.001>
- Battula, V. L., Chen, Y., Cabreira Mda, G., Ruvolo, V., Wang, Z., Ma, W., Konoplev, S., Shpall, E., Lyons, K., Strunk, D., Bueso-Ramos, C., Davis, R. E., Konopleva, M., & Andreeff, M. (2013, Jul 18). Connective tissue growth factor regulates adipocyte differentiation of mesenchymal stromal cells and facilitates leukemia bone marrow engraftment. *Blood*, 122(3), 357-366. <https://doi.org/10.1182/blood-2012-06-437988>
- Battula, V. L., Le, P. M., Sun, J. C., Nguyen, K., Yuan, B., Zhou, X., Sonnylal, S., McQueen, T., Ruvolo, V., Michel, K. A., Ling, X., Jacamo, R., Shpall, E., Wang, Z., Rao, A., Al-Atrash, G., Konopleva, M., Davis, R. E., Harrington, M. A., Cahill, C. W., Bueso-Ramos, C., & Andreeff, M. (2017, Jul 6). AML-induced osteogenic differentiation in mesenchymal stromal cells supports leukemia growth. *JCI Insight*, 2(13). <https://doi.org/10.1172/jci.insight.90036>
- Beg, A. A., Sha, W. C., Bronson, R. T., Ghosh, S., & Baltimore, D. (1995, Jul 13). Embryonic lethality and liver degeneration in mice lacking the RelA component of NF-kappa B. *Nature*, 376(6536), 167-170. <https://doi.org/10.1038/376167a0>
- Benveniste, P., Frelin, C., Janmohamed, S., Barbara, M., Herrington, R., Hyam, D., & Iscove, N. N. (2010, Jan 8). Intermediate-term hematopoietic stem cells with extended but time-limited reconstitution potential. *Cell Stem Cell*, 6(1), 48-58. <https://doi.org/10.1016/j.stem.2009.11.014>
- Bernad, A., Kopf, M., Kulbacki, R., Weich, N., Koehler, G., & Gutierrez-Ramos, J. C. (1994, Dec). Interleukin-6 is required in vivo for the regulation of stem cells and committed progenitors of the hematopoietic system. *Immunity*, 1(9), 725-731. [https://doi.org/10.1016/s1074-7613\(94\)80014-6](https://doi.org/10.1016/s1074-7613(94)80014-6)
- Birbrair, A., & Frenette, P. S. (2016, Apr). Niche heterogeneity in the bone marrow. *Ann N Y Acad Sci*, 1370(1), 82-96. <https://doi.org/10.1111/nyas.13016>
- Blank, U., & Karlsson, S. (2015, Jun 4). TGF- β signaling in the control of hematopoietic stem cells. *Blood*, 125(23), 3542-3550. <https://doi.org/10.1182/blood-2014-12-618090>
- Blom, I. E., Goldschmeding, R., & Leask, A. (2002, Oct). Gene regulation of connective tissue growth factor: new targets for antifibrotic therapy? *Matrix Biol*, 21(6), 473-482. [https://doi.org/10.1016/s0945-053x\(02\)00055-0](https://doi.org/10.1016/s0945-053x(02)00055-0)

- Boag, J. M., Beesley, A. H., Firth, M. J., Freitas, J. R., Ford, J., Brigstock, D. R., de Klerk, N. H., & Kees, U. R. (2007, Sep). High expression of connective tissue growth factor in pre-B acute lymphoblastic leukaemia. *Br J Haematol*, *138*(6), 740-748. <https://doi.org/10.1111/j.1365-2141.2007.06739.x>
- Bonavida, B. (1991). Immunomodulatory effect of tumor necrosis factor. *Biotherapy*, *3*(2), 127-133. <https://doi.org/10.1007/bf02172085>
- Bork, P. (1993, Jul 26). The modular architecture of a new family of growth regulators related to connective tissue growth factor. *FEBS Lett*, *327*(2), 125-130. [https://doi.org/10.1016/0014-5793\(93\)80155-n](https://doi.org/10.1016/0014-5793(93)80155-n)
- Boulais, P. E., & Frenette, P. S. (2015, Apr 23). Making sense of hematopoietic stem cell niches. *Blood*, *125*(17), 2621-2629. <https://doi.org/10.1182/blood-2014-09-570192>
- Bradford, G. B., Williams, B., Rossi, R., & Bertoncello, I. (1997, May). Quiescence, cycling, and turnover in the primitive hematopoietic stem cell compartment. *Exp Hematol*, *25*(5), 445-453.
- Bradham, D. M., Igarashi, A., Potter, R. L., & Grotendorst, G. R. (1991, Sep). Connective tissue growth factor: a cysteine-rich mitogen secreted by human vascular endothelial cells is related to the SRC-induced immediate early gene product CEF-10. *J Cell Biol*, *114*(6), 1285-1294. <https://doi.org/10.1083/jcb.114.6.1285>
- Brigstock, D. R., Steffen, C. L., Kim, G. Y., Vegunta, R. K., Diehl, J. R., & Harding, P. A. (1997, Aug 8). Purification and characterization of novel heparin-binding growth factors in uterine secretory fluids. Identification as heparin-regulated Mr 10,000 forms of connective tissue growth factor. *J Biol Chem*, *272*(32), 20275-20282. <https://doi.org/10.1074/jbc.272.32.20275>
- Brouckaert, P., Libert, C., Everaerd, B., Takahashi, N., Cauwels, A., & Fiers, W. (1993, Apr). Tumor necrosis factor, its receptors and the connection with interleukin 1 and interleukin 6. *Immunobiology*, *187*(3-5), 317-329. [https://doi.org/10.1016/s0171-2985\(11\)80347-5](https://doi.org/10.1016/s0171-2985(11)80347-5)
- Brown, Z., Strieter, R. M., Neild, G. H., Thompson, R. C., Kunkel, S. L., & Westwick, J. (1992, Jul). IL-1 receptor antagonist inhibits monocyte chemotactic peptide 1 generation by human mesangial cells. *Kidney Int*, *42*(1), 95-101. <https://doi.org/10.1038/ki.1992.266>
- Bruns, I., Lucas, D., Pinho, S., Ahmed, J., Lambert, M. P., Kunisaki, Y., Scheiermann, C., Schiff, L., Poncz, M., Bergman, A., & Frenette, P. S. (2014, Nov). Megakaryocytes regulate hematopoietic stem cell quiescence through CXCL4 secretion. *Nat Med*, *20*(11), 1315-1320. <https://doi.org/10.1038/nm.3707>

- Buckley, S. M., Ulloa-Montoya, F., Abts, D., Oostendorp, R. A., Dzierzak, E., Ekker, S. C., & Verfaillie, C. M. (2011, Jan). Maintenance of HSC by Wnt5a secreting AGM-derived stromal cell line. *Exp Hematol*, *39*(1), 114-123.e111-115.
<https://doi.org/10.1016/j.exphem.2010.09.010>
- Burda, P., Laslo, P., & Stopka, T. (2010, Jul). The role of PU.1 and GATA-1 transcription factors during normal and leukemogenic hematopoiesis. *Leukemia*, *24*(7), 1249-1257.
<https://doi.org/10.1038/leu.2010.104>
- Burkly, L., Hession, C., Ogata, L., Reilly, C., Marconi, L. A., Olson, D., Tizard, R., Cate, R., & Lo, D. (1995, Feb 9). Expression of relB is required for the development of thymic medulla and dendritic cells. *Nature*, *373*(6514), 531-536.
<https://doi.org/10.1038/373531a0>
- Butler, J. M., Nolan, D. J., Vertes, E. L., Varnum-Finney, B., Kobayashi, H., Hooper, A. T., Seandel, M., Shido, K., White, I. A., Kobayashi, M., Witte, L., May, C., Shawber, C., Kimura, Y., Kitajewski, J., Rosenwaks, Z., Bernstein, I. D., & Rafii, S. (2010, Mar 5). Endothelial cells are essential for the self-renewal and repopulation of Notch-dependent hematopoietic stem cells. *Cell Stem Cell*, *6*(3), 251-264.
<https://doi.org/10.1016/j.stem.2010.02.001>
- Cabezas-Wallscheid, N., Buettner, F., Sommerkamp, P., Klimmeck, D., Ladell, L., Thalheimer, F. B., Pastor-Flores, D., Roma, L. P., Renders, S., Zeisberger, P., Przybylla, A., Schönberger, K., Scognamiglio, R., Altamura, S., Florian, C. M., Fawaz, M., Vonficht, D., Tesio, M., Collier, P., Pavlinic, D., Geiger, H., Schroeder, T., Benes, V., Dick, T. P., Rieger, M. A., Stegle, O., & Trumpp, A. (2017, May 18). Vitamin A-Retinoic Acid Signaling Regulates Hematopoietic Stem Cell Dormancy. *Cell*, *169*(5), 807-823.e819.
<https://doi.org/10.1016/j.cell.2017.04.018>
- Calvi, L. M., Adams, G. B., Weibrecht, K. W., Weber, J. M., Olson, D. P., Knight, M. C., Martin, R. P., Schipani, E., Divieti, P., Bringham, F. R., Milner, L. A., Kronenberg, H. M., & Scadden, D. T. (2003, Oct 23). Osteoblastic cells regulate the haematopoietic stem cell niche. *Nature*, *425*(6960), 841-846. <https://doi.org/10.1038/nature02040>
- Cao, X., Wu, X., Frassica, D., Yu, B., Pang, L., Xian, L., Wan, M., Lei, W., Armour, M., Tryggestad, E., Wong, J., Wen, C. Y., Lu, W. W., & Frassica, F. J. (2011). Irradiation induces bone injury by damaging bone marrow microenvironment for stem cells. *Proceedings of the National Academy of Sciences*, *108*(4), 1609-1614.
<https://doi.org/10.1073/pnas.1015350108>
- Caplan, A. I. (1991, Sep). Mesenchymal stem cells. *J Orthop Res*, *9*(5), 641-650.
<https://doi.org/10.1002/jor.1100090504>
- Capron, C., Lacout, C., Lécluse, Y., Jalbert, V., Chagraoui, H., Charrier, S., Galy, A., Bennaceur-Griscelli, A., Cramer-Bordé, E., & Vainchenker, W. (2010, Aug 26). A major role of

- TGF-beta1 in the homing capacities of murine hematopoietic stem cell/progenitors. *Blood*, 116(8), 1244-1253. <https://doi.org/10.1182/blood-2009-05-221093>
- Carbonneau, C. L., Despars, G., Rojas-Sutterlin, S., Fortin, A., Le, O., Hoang, T., & Beauséjour, C. M. (2012, Jan 19). Ionizing radiation-induced expression of INK4a/ARF in murine bone marrow-derived stromal cell populations interferes with bone marrow homeostasis. *Blood*, 119(3), 717-726. <https://doi.org/10.1182/blood-2011-06-361626>
- Caux, C., Saeland, S., Favre, C., Duvert, V., Mannoni, P., & Banchereau, J. (1990, Jun 15). Tumor necrosis factor-alpha strongly potentiates interleukin-3 and granulocyte-macrophage colony-stimulating factor-induced proliferation of human CD34+ hematopoietic progenitor cells. *Blood*, 75(12), 2292-2298.
- Chamberlain, G., Fox, J., Ashton, B., & Middleton, J. (2007, Nov). Concise review: mesenchymal stem cells: their phenotype, differentiation capacity, immunological features, and potential for homing. *Stem Cells*, 25(11), 2739-2749. <https://doi.org/10.1634/stemcells.2007-0197>
- Chambers, R. C., Leoni, P., Blanc-Brude, O. P., Wembridge, D. E., & Laurent, G. J. (2000, Nov 10). Thrombin is a potent inducer of connective tissue growth factor production via proteolytic activation of protease-activated receptor-1. *J Biol Chem*, 275(45), 35584-35591. <https://doi.org/10.1074/jbc.M003188200>
- Chan, C. K., Chen, C. C., Luppen, C. A., Kim, J. B., DeBoer, A. T., Wei, K., Helms, J. A., Kuo, C. J., Kraft, D. L., & Weissman, I. L. (2009, Jan 22). Endochondral ossification is required for haematopoietic stem-cell niche formation. *Nature*, 457(7228), 490-494. <https://doi.org/10.1038/nature07547>
- Chan, J. Y., & Watt, S. M. (2001, Mar). Adhesion receptors on haematopoietic progenitor cells. *Br J Haematol*, 112(3), 541-557. <https://doi.org/10.1046/j.1365-2141.2001.02439.x>
- Charrier, A., Chen, R., Chen, L., Kemper, S., Hattori, T., Takigawa, M., & Brigstock, D. R. (2014, Jun). Connective tissue growth factor (CCN2) and microRNA-21 are components of a positive feedback loop in pancreatic stellate cells (PSC) during chronic pancreatitis and are exported in PSC-derived exosomes. *Journal of cell communication and signaling*, 8(2), 147-156. <https://doi.org/10.1007/s12079-014-0220-3>
- Charrier, A. L., & Brigstock, D. R. (2010, Aug). Connective tissue growth factor production by activated pancreatic stellate cells in mouse alcoholic chronic pancreatitis. *Lab Invest*, 90(8), 1179-1188. <https://doi.org/10.1038/labinvest.2010.82>
- Che, H., Wang, Y., Li, Y., Lv, J., Li, H., Liu, Y., Dong, R., Sun, Y., Xu, X., Zhao, J., & Wang, L. (2020, Nov). Inhibition of microRNA-150-5p alleviates cardiac inflammation and fibrosis via targeting Smad7 in high glucose-treated cardiac fibroblasts. *J Cell Physiol*, 235(11), 7769-7779. <https://doi.org/10.1002/jcp.29386>

- Chen, C. C., & Lau, L. F. (2009, Apr). Functions and mechanisms of action of CCN matricellular proteins. *Int J Biochem Cell Biol*, 41(4), 771-783. <https://doi.org/10.1016/j.biocel.2008.07.025>
- Chen, J.-q., Ou, Y.-l., Huang, Z.-p., Hong, Y.-g., Tao, Y.-p., Wang, Z.-g., Ni, J.-s., Hao, L.-q., & Lin, H. (2019, 2019/07/08). MicroRNA-212-3p inhibits the Proliferation and Invasion of Human Hepatocellular Carcinoma Cells by Suppressing CTGF expression. *Scientific Reports*, 9(1), 9820. <https://doi.org/10.1038/s41598-019-46088-w>
- Chen, M. F., Lin, C. T., Chen, W. C., Yang, C. T., Chen, C. C., Liao, S. K., Liu, J. M., Lu, C. H., & Lee, K. D. (2006, Sep 1). The sensitivity of human mesenchymal stem cells to ionizing radiation. *Int J Radiat Oncol Biol Phys*, 66(1), 244-253. <https://doi.org/10.1016/j.ijrobp.2006.03.062>
- Chen, Q., Shou, P., Zheng, C., Jiang, M., Cao, G., Yang, Q., Cao, J., Xie, N., Velletri, T., Zhang, X., Xu, C., Zhang, L., Yang, H., Hou, J., Wang, Y., & Shi, Y. (2016, Jul). Fate decision of mesenchymal stem cells: adipocytes or osteoblasts? *Cell Death Differ*, 23(7), 1128-1139. <https://doi.org/10.1038/cdd.2015.168>
- Cheng, T., Rodrigues, N., Shen, H., Yang, Y., Dombkowski, D., Sykes, M., & Scadden, D. T. (2000, Mar 10). Hematopoietic stem cell quiescence maintained by p21cip1/waf1. *Science*, 287(5459), 1804-1808. <https://doi.org/10.1126/science.287.5459.1804>
- Cheng, T. Y., Wu, M. S., Hua, K. T., Kuo, M. L., & Lin, M. T. (2014, Feb 21). Cyr61/CTGF/Nov family proteins in gastric carcinogenesis. *World J Gastroenterol*, 20(7), 1694-1700. <https://doi.org/10.3748/wjg.v20.i7.1694>
- Cheshier, S. H., Morrison, S. J., Liao, X., & Weissman, I. L. (1999, Mar 16). In vivo proliferation and cell cycle kinetics of long-term self-renewing hematopoietic stem cells. *Proc Natl Acad Sci U S A*, 96(6), 3120-3125. <https://doi.org/10.1073/pnas.96.6.3120>
- Cheung, L. C., Strickland, D. H., Howlett, M., Ford, J., Charles, A. K., Lyons, K. M., Brigstock, D. R., Goldschmeding, R., Cole, C. H., Alexander, W. S., & Kees, U. R. (2014, Jul). Connective tissue growth factor is expressed in bone marrow stromal cells and promotes interleukin-7-dependent B lymphopoiesis. *Haematologica*, 99(7), 1149-1156. <https://doi.org/10.3324/haematol.2013.102327>
- Cheung, T. H., & Rando, T. A. (2013, Jun). Molecular regulation of stem cell quiescence. *Nat Rev Mol Cell Biol*, 14(6), 329-340. <https://doi.org/10.1038/nrm3591>
- Chien, W., Kumagai, T., Miller, C. W., Desmond, J. C., Frank, J. M., Said, J. W., & Koeffler, H. P. (2004, Dec 17). Cyr61 suppresses growth of human endometrial cancer cells. *J Biol Chem*, 279(51), 53087-53096. <https://doi.org/10.1074/jbc.M410254200>

- Chotinantakul, K., & Leeansaksiri, W. (2012). Hematopoietic stem cell development, niches, and signaling pathways. *Bone Marrow Res*, 2012, 270425. <https://doi.org/10.1155/2012/270425>
- Chowdhury, I., & Chaqour, B. (2004, Nov). Regulation of connective tissue growth factor (CTGF/CCN2) gene transcription and mRNA stability in smooth muscle cells. Involvement of RhoA GTPase and p38 MAP kinase and sensitivity to actin dynamics. *Eur J Biochem*, 271(22), 4436-4450. <https://doi.org/10.1111/j.1432-1033.2004.04382.x>
- Christensen, J. L., & Weissman, I. L. (2001, Dec 4). Flk-2 is a marker in hematopoietic stem cell differentiation: a simple method to isolate long-term stem cells. *Proc Natl Acad Sci U S A*, 98(25), 14541-14546. <https://doi.org/10.1073/pnas.261562798>
- Cicha, I., & Goppelt-Struebe, M. (2009, Mar-Apr). Connective tissue growth factor: context-dependent functions and mechanisms of regulation. *Biofactors*, 35(2), 200-208. <https://doi.org/10.1002/biof.30>
- Cobas, M., Wilson, A., Ernst, B., Mancini, S. J., MacDonald, H. R., Kemler, R., & Radtke, F. (2004, Jan 19). Beta-catenin is dispensable for hematopoiesis and lymphopoiesis. *J Exp Med*, 199(2), 221-229. <https://doi.org/10.1084/jem.20031615>
- Cooker, L. A., Peterson, D., Rambow, J., Riser, M. L., Riser, R. E., Najmabadi, F., Brigstock, D., & Riser, B. L. (2007, Jul). TNF-alpha, but not IFN-gamma, regulates CCN2 (CTGF), collagen type I, and proliferation in mesangial cells: possible roles in the progression of renal fibrosis. *Am J Physiol Renal Physiol*, 293(1), F157-165. <https://doi.org/10.1152/ajprenal.00508.2006>
- Coppé, J. P., Desprez, P. Y., Krtolica, A., & Campisi, J. (2010). The senescence-associated secretory phenotype: the dark side of tumor suppression. *Annu Rev Pathol*, 5, 99-118. <https://doi.org/10.1146/annurev-pathol-121808-102144>
- Costa, S., & Reagan, M. R. (2019). Therapeutic Irradiation: Consequences for Bone and Bone Marrow Adipose Tissue. *Front Endocrinol (Lausanne)*, 10, 587. <https://doi.org/10.3389/fendo.2019.00587>
- Crippa, S., & Bernardo, M. E. (2018, Dec). Mesenchymal Stromal Cells: Role in the BM Niche and in the Support of Hematopoietic Stem Cell Transplantation. *Hemasphere*, 2(6), e151. <https://doi.org/10.1097/hs9.000000000000151>
- Cushing, S. D., Berliner, J. A., Valente, A. J., Territo, M. C., Navab, M., Parhami, F., Gerrity, R., Schwartz, C. J., & Fogelman, A. M. (1990, Jul). Minimally modified low density lipoprotein induces monocyte chemotactic protein 1 in human endothelial cells and smooth muscle cells. *Proc Natl Acad Sci U S A*, 87(13), 5134-5138. <https://doi.org/10.1073/pnas.87.13.5134>

- Czabotar, P. E., Lessene, G., Strasser, A., & Adams, J. M. (2014, Jan). Control of apoptosis by the BCL-2 protein family: implications for physiology and therapy. *Nat Rev Mol Cell Biol*, 15(1), 49-63. <https://doi.org/10.1038/nrm3722>
- Dendooven, A., Gerritsen, K. G., Nguyen, T. Q., Kok, R. J., & Goldschmeding, R. (2011, Jun). Connective tissue growth factor (CTGF/CCN2) ELISA: a novel tool for monitoring fibrosis. *Biomarkers*, 16(4), 289-301. <https://doi.org/10.3109/1354750x.2011.561366>
- Deng, L., Wang, C., Spencer, E., Yang, L., Braun, A., You, J., Slaughter, C., Pickart, C., & Chen, Z. J. (2000, Oct 13). Activation of the I κ B kinase complex by TRAF6 requires a dimeric ubiquitin-conjugating enzyme complex and a unique polyubiquitin chain. *Cell*, 103(2), 351-361. [https://doi.org/10.1016/s0092-8674\(00\)00126-4](https://doi.org/10.1016/s0092-8674(00)00126-4)
- Desterke, C., Petit, L., Sella, N., Chevallier, N., Cabeli, V., Coquelin, L., Durand, C., Oostendorp, R. A. J., Isambert, H., Jaffredo, T., & Charbord, P. (2020, Jun 26). Inferring Gene Networks in Bone Marrow Hematopoietic Stem Cell-Supporting Stromal Niche Populations. *iScience*, 23(6), 101222. <https://doi.org/10.1016/j.isci.2020.101222>
- Ding, L., & Morrison, S. J. (2013, Mar 14). Haematopoietic stem cells and early lymphoid progenitors occupy distinct bone marrow niches. *Nature*, 495(7440), 231-235. <https://doi.org/10.1038/nature11885>
- Ding, L., Saunders, T. L., Enikolopov, G., & Morrison, S. J. (2012, Jan 25). Endothelial and perivascular cells maintain haematopoietic stem cells. *Nature*, 481(7382), 457-462. <https://doi.org/10.1038/nature10783>
- Doan, P. L., Himgburg, H. A., Helms, K., Russell, J. L., Fixsen, E., Quarmyne, M., Harris, J. R., Deoliviera, D., Sullivan, J. M., Chao, N. J., Kirsch, D. G., & Chute, J. P. (2013, Mar). Epidermal growth factor regulates hematopoietic regeneration after radiation injury. *Nat Med*, 19(3), 295-304. <https://doi.org/10.1038/nm.3070>
- Dolgalev, I., & Tikhonova, A. N. (2021). Connecting the Dots: Resolving the Bone Marrow Niche Heterogeneity. *Front Cell Dev Biol*, 9, 622519. <https://doi.org/10.3389/fcell.2021.622519>
- Domen, J., Gandy, K. L., & Weissman, I. L. (1998, Apr 1). Systemic overexpression of BCL-2 in the hematopoietic system protects transgenic mice from the consequences of lethal irradiation. *Blood*, 91(7), 2272-2282.
- Dominici, M., Rasini, V., Bussolari, R., Chen, X., Hofmann, T. J., Spano, C., Bernabei, D., Veronesi, E., Bertoni, F., Paolucci, P., Conte, P., & Horwitz, E. M. (2009). Restoration and reversible expansion of the osteoblastic hematopoietic stem cell niche after marrow radioablation. *Blood*, 114(11), 2333-2343. <https://doi.org/10.1182/blood-2008-10-183459>

- Doulatov, S., Notta, F., Laurenti, E., & Dick, J. E. (2012, Feb 3). Hematopoiesis: a human perspective. *Cell Stem Cell*, *10*(2), 120-136.
<https://doi.org/10.1016/j.stem.2012.01.006>
- Dzierzak, E., & Speck, N. A. (2008, Feb). Of lineage and legacy: the development of mammalian hematopoietic stem cells. *Nat Immunol*, *9*(2), 129-136.
<https://doi.org/10.1038/ni1560>
- Ebbe, S., Phalen, E., & Yee, T. (1986). Postirradiation thrombocytopoiesis: suppression, recovery, compensatory states, and macromegakaryocytosis. *Prog Clin Biol Res*, *215*, 71-89.
- Escobar, G., Lopez-Vilchez, I., Diaz-Ricart, M., White, J. G., & Galan, A. M. (2008). Internalization of tissue factor by platelets. *Thromb Res*, *122 Suppl 1*, S37-41.
[https://doi.org/10.1016/s0049-3848\(08\)70017-3](https://doi.org/10.1016/s0049-3848(08)70017-3)
- Esplin, B. L., Shimazu, T., Welner, R. S., Garrett, K. P., Nie, L., Zhang, Q., Humphrey, M. B., Yang, Q., Borghesi, L. A., & Kincade, P. W. (2011, May 1). Chronic exposure to a TLR ligand injures hematopoietic stem cells. *J Immunol*, *186*(9), 5367-5375.
<https://doi.org/10.4049/jimmunol.1003438>
- Esplin, B. L., Shimazu, T., Welner, R. S., Garrett, K. P., Nie, L., Zhang, Q., Humphrey, M. B., Yang, Q., Borghesi, L. A., & Kincade, P. W. (2011). Chronic exposure to a TLR ligand injures hematopoietic stem cells. *Journal of immunology (Baltimore, Md. : 1950)*, *186*(9), 5367-5375. <https://doi.org/10.4049/jimmunol.1003438>
- Essers, M. A., Offner, S., Blanco-Bose, W. E., Waibler, Z., Kalinke, U., Duchosal, M. A., & Trumpp, A. (2009, Apr 16). IFN α activates dormant haematopoietic stem cells in vivo. *Nature*, *458*(7240), 904-908. <https://doi.org/10.1038/nature07815>
- Essers, M. A., & Trumpp, A. (2010, Oct). Targeting leukemic stem cells by breaking their dormancy. *Mol Oncol*, *4*(5), 443-450. <https://doi.org/10.1016/j.molonc.2010.06.001>
- Evers, T. M. J., Sheikhhassani, V., Haks, M. C., Storm, C., Ottenhoff, T. H. M., & Mashaghi, A. (2022, Jan 21). Single-cell analysis reveals chemokine-mediated differential regulation of monocyte mechanics. *iScience*, *25*(1), 103555.
<https://doi.org/10.1016/j.isci.2021.103555>
- Ewen, M. E., Sluss, H. K., Whitehouse, L. L., & Livingston, D. M. (1993, Sep 24). TGF β inhibition of Cdk4 synthesis is linked to cell cycle arrest. *Cell*, *74*(6), 1009-1020.
[https://doi.org/10.1016/0092-8674\(93\)90723-4](https://doi.org/10.1016/0092-8674(93)90723-4)
- Fabregat, I., & Caballero-Díaz, D. (2018). Transforming Growth Factor- β -Induced Cell Plasticity in Liver Fibrosis and Hepatocarcinogenesis. *Front Oncol*, *8*, 357.
<https://doi.org/10.3389/fonc.2018.00357>

- Fahmy-Garcia, S., van Driel, M., Witte-Buoma, J., Walles, H., van Leeuwen, J., van Osch, G., & Farrell, E. (2018, Feb). NELL-1, HMGB1, and CCN2 Enhance Migration and Vasculogenesis, But Not Osteogenic Differentiation Compared to BMP2. *Tissue Eng Part A*, 24(3-4), 207-218. <https://doi.org/10.1089/ten.TEA.2016.0537>
- Fiedler, T., Salamon, A., Adam, S., Herzmann, N., Taubenheim, J., & Peters, K. (2013, 2013/11/01/). Impact of bacteria and bacterial components on osteogenic and adipogenic differentiation of adipose-derived mesenchymal stem cells. *Experimental Cell Research*, 319(18), 2883-2892. <https://doi.org/https://doi.org/10.1016/j.yexcr.2013.08.020>
- Fiedler, T., Salamon, A., Adam, S., Herzmann, N., Taubenheim, J., & Peters, K. (2013, Nov 1). Impact of bacteria and bacterial components on osteogenic and adipogenic differentiation of adipose-derived mesenchymal stem cells. *Exp Cell Res*, 319(18), 2883-2892. <https://doi.org/10.1016/j.yexcr.2013.08.020>
- Flach, J., Bakker, S. T., Mohrin, M., Conroy, P. C., Pietras, E. M., Reynaud, D., Alvarez, S., Diolaiti, M. E., Ugarte, F., Forsberg, E. C., Le Beau, M. M., Stohr, B. A., Méndez, J., Morrison, C. G., & Passegué, E. (2014, Aug 14). Replication stress is a potent driver of functional decline in ageing haematopoietic stem cells. *Nature*, 512(7513), 198-202. <https://doi.org/10.1038/nature13619>
- Fleming, H. E., Janzen, V., Lo Celso, C., Guo, J., Leahy, K. M., Kronenberg, H. M., & Scadden, D. T. (2008, Mar 6). Wnt signaling in the niche enforces hematopoietic stem cell quiescence and is necessary to preserve self-renewal in vivo. *Cell Stem Cell*, 2(3), 274-283. <https://doi.org/10.1016/j.stem.2008.01.003>
- Florian, Maria C., Dörr, K., Niebel, A., Daria, D., Schrezenmeier, H., Rojewski, M., Filippi, M.-D., Hasenberg, A., Gunzer, M., Scharffetter-Kochanek, K., Zheng, Y., & Geiger, H. (2012, 2012/05/04/). Cdc42 Activity Regulates Hematopoietic Stem Cell Aging and Rejuvenation. *Cell Stem Cell*, 10(5), 520-530. <https://doi.org/https://doi.org/10.1016/j.stem.2012.04.007>
- Florian, M. C., Dörr, K., Niebel, A., Daria, D., Schrezenmeier, H., Rojewski, M., Filippi, M. D., Hasenberg, A., Gunzer, M., Scharffetter-Kochanek, K., Zheng, Y., & Geiger, H. (2012, May 4). Cdc42 activity regulates hematopoietic stem cell aging and rejuvenation. *Cell Stem Cell*, 10(5), 520-530. <https://doi.org/10.1016/j.stem.2012.04.007>
- Franzoso, G., Carlson, L., Xing, L., Poljak, L., Shores, E. W., Brown, K. D., Leonardi, A., Tran, T., Boyce, B. F., & Siebenlist, U. (1997, Dec 15). Requirement for NF-kappaB in osteoclast and B-cell development. *Genes Dev*, 11(24), 3482-3496. <https://doi.org/10.1101/gad.11.24.3482>
- Frasconi, F., Testa, N. G., & Lord, B. I. (1982, Jul). The relative spatial distribution of erythroid progenitor cells (BFUe and CFUe) in the normal mouse femur. *Cell Tissue Kinet*, 15(4), 447-455. <https://doi.org/10.1111/j.1365-2184.1982.tb01062.x>

- Frazier, K., Williams, S., Kothapalli, D., Klapper, H., & Grotendorst, G. R. (1996, Sep). Stimulation of fibroblast cell growth, matrix production, and granulation tissue formation by connective tissue growth factor. *J Invest Dermatol*, 107(3), 404-411. <https://doi.org/10.1111/1523-1747.ep12363389>
- Frenette, P. S., Pinho, S., Lucas, D., & Scheiermann, C. (2013). Mesenchymal stem cell: keystone of the hematopoietic stem cell niche and a stepping-stone for regenerative medicine. *Annu Rev Immunol*, 31, 285-316. <https://doi.org/10.1146/annurev-immunol-032712-095919>
- Friedenstein, A. J., Chailakhyan, R. K., Latsinik, N. V., Panasyuk, A. F., & Keiliss-Borok, I. V. (1974, Apr). Stromal cells responsible for transferring the microenvironment of the hemopoietic tissues. Cloning in vitro and retransplantation in vivo. *Transplantation*, 17(4), 331-340. <https://doi.org/10.1097/00007890-197404000-00001>
- Friedenstein, A. J., Gorskaja, J. F., & Kulagina, N. N. (1976, Sep). Fibroblast precursors in normal and irradiated mouse hematopoietic organs. *Exp Hematol*, 4(5), 267-274.
- Fröbel, J., Landspersky, T., Percin, G., Schreck, C., Rahmig, S., Ori, A., Nowak, D., Essers, M., Waskow, C., & Oostendorp, R. A. J. (2021). The Hematopoietic Bone Marrow Niche Ecosystem. *Front Cell Dev Biol*, 9, 705410. <https://doi.org/10.3389/fcell.2021.705410>
- Fuchs, E., Tumber, T., & Guasch, G. (2004, 2004/03/19/). Socializing with the Neighbors: Stem Cells and Their Niche. *Cell*, 116(6), 769-778. [https://doi.org/https://doi.org/10.1016/S0092-8674\(04\)00255-7](https://doi.org/https://doi.org/10.1016/S0092-8674(04)00255-7)
- Fukushima, T., Tanaka, Y., Hamey, F. K., Chang, C. H., Oki, T., Asada, S., Hayashi, Y., Fujino, T., Yonezawa, T., Takeda, R., Kawabata, K. C., Fukuyama, T., Umemoto, T., Takubo, K., Takizawa, H., Goyama, S., Ishihama, Y., Honda, H., Göttgens, B., & Kitamura, T. (2019, Dec 17). Discrimination of Dormant and Active Hematopoietic Stem Cells by G(0) Marker Reveals Dormancy Regulation by Cytoplasmic Calcium. *Cell Rep*, 29(12), 4144-4158.e4147. <https://doi.org/10.1016/j.celrep.2019.11.061>
- Gao, R., & Brigstock, D. R. (2004, Mar 5). Connective tissue growth factor (CCN2) induces adhesion of rat activated hepatic stellate cells by binding of its C-terminal domain to integrin alpha(v)beta(3) and heparan sulfate proteoglycan. *J Biol Chem*, 279(10), 8848-8855. <https://doi.org/10.1074/jbc.M313204200>
- Gao, R., & Brigstock, D. R. (2005, Sep). Connective tissue growth factor (CCN2) in rat pancreatic stellate cell function: integrin alpha5beta1 as a novel CCN2 receptor. *Gastroenterology*, 129(3), 1019-1030. <https://doi.org/10.1053/j.gastro.2005.06.067>
- Gekas, C., Dieterlen-Lièvre, F., Orkin, S. H., & Mikkola, H. K. (2005, Mar). The placenta is a niche for hematopoietic stem cells. *Dev Cell*, 8(3), 365-375. <https://doi.org/10.1016/j.devcel.2004.12.016>

- Goldman, D. C., Bailey, A. S., Pfaffle, D. L., Al Masri, A., Christian, J. L., & Fleming, W. H. (2009, Nov 12). BMP4 regulates the hematopoietic stem cell niche. *Blood*, *114*(20), 4393-4401. <https://doi.org/10.1182/blood-2009-02-206433>
- Grabher, C., Payne, E. M., Johnston, A. B., Bolli, N., Lechman, E., Dick, J. E., Kanki, J. P., & Look, A. T. (2011). Zebrafish microRNA-126 determines hematopoietic cell fate through c-Myb. *Leukemia*, *25*(3), 506-514. <https://doi.org/10.1038/leu.2010.280>
- Green, D. E., & Rubin, C. T. (2014, Jun). Consequences of irradiation on bone and marrow phenotypes, and its relation to disruption of hematopoietic precursors. *Bone*, *63*, 87-94. <https://doi.org/10.1016/j.bone.2014.02.018>
- Greenbaum, A., Hsu, Y. M., Day, R. B., Schuettpelz, L. G., Christopher, M. J., Borgerding, J. N., Nagasawa, T., & Link, D. C. (2013, Mar 14). CXCL12 in early mesenchymal progenitors is required for haematopoietic stem-cell maintenance. *Nature*, *495*(7440), 227-230. <https://doi.org/10.1038/nature11926>
- Gressner, O. A., Peredniene, I., & Gressner, A. M. (2011, Jan 14). Connective tissue growth factor reacts as an IL-6/STAT3-regulated hepatic negative acute phase protein. *World J Gastroenterol*, *17*(2), 151-163. <https://doi.org/10.3748/wjg.v17.i2.151>
- Grotendorst, G. R. (1997, Sep). Connective tissue growth factor: a mediator of TGF-beta action on fibroblasts. *Cytokine Growth Factor Rev*, *8*(3), 171-179. [https://doi.org/10.1016/s1359-6101\(97\)00010-5](https://doi.org/10.1016/s1359-6101(97)00010-5)
- Grotendorst, G. R., Okochi, H., & Hayashi, N. (1996, Apr). A novel transforming growth factor beta response element controls the expression of the connective tissue growth factor gene. *Cell Growth Differ*, *7*(4), 469-480.
- Gu, J., Liu, X., Wang, Q. X., Tan, H. W., Guo, M., Jiang, W. F., & Zhou, L. (2012, Oct 1). Angiotensin II increases CTGF expression via MAPKs/TGF-β1/TRAF6 pathway in atrial fibroblasts. *Exp Cell Res*, *318*(16), 2105-2115. <https://doi.org/10.1016/j.yexcr.2012.06.015>
- Guo, F., Carter, D. E., & Leask, A. (2011). Mechanical tension increases CCN2/CTGF expression and proliferation in gingival fibroblasts via a TGFβ-dependent mechanism. *PLoS One*, *6*(5), e19756. <https://doi.org/10.1371/journal.pone.0019756>
- Hall-Glenn, F., Aivazi, A., Akopyan, L., Ong, J. R., Baxter, R. R., Benya, P. D., Goldschmeding, R., van Nieuwenhoven, F. A., Hunziker, E. B., & Lyons, K. M. (2013, Aug). CCN2/CTGF is required for matrix organization and to protect growth plate chondrocytes from cellular stress. *Journal of cell communication and signaling*, *7*(3), 219-230. <https://doi.org/10.1007/s12079-013-0201-y>

- Hall-Glenn, F., De Young, R. A., Huang, B. L., van Handel, B., Hofmann, J. J., Chen, T. T., Choi, A., Ong, J. R., Benya, P. D., Mikkola, H., Iruela-Arispe, M. L., & Lyons, K. M. (2012). CCN2/connective tissue growth factor is essential for pericyte adhesion and endothelial basement membrane formation during angiogenesis. *PLoS One*, 7(2), e30562. <https://doi.org/10.1371/journal.pone.0030562>
- Hamada, T., Möhle, R., Hesselgesser, J., Hoxie, J., Nachman, R. L., Moore, M. A., & Rafii, S. (1998, Aug 3). Transendothelial migration of megakaryocytes in response to stromal cell-derived factor 1 (SDF-1) enhances platelet formation. *J Exp Med*, 188(3), 539-548. <https://doi.org/10.1084/jem.188.3.539>
- Haylock, D. N., & Nilsson, S. K. (2006, Sep). Osteopontin: a bridge between bone and blood. *Br J Haematol*, 134(5), 467-474. <https://doi.org/10.1111/j.1365-2141.2006.06218.x>
- He, X., Wang, H., Jin, T., Xu, Y., Mei, L., & Yang, J. (2016). TLR4 Activation Promotes Bone Marrow MSC Proliferation and Osteogenic Differentiation via Wnt3a and Wnt5a Signaling. *PLoS One*, 11(3), e0149876. <https://doi.org/10.1371/journal.pone.0149876>
- Heinrich, P. C., Behrmann, I., Müller-Newen, G., Schaper, F., & Graeve, L. (1998, Sep 1). Interleukin-6-type cytokine signalling through the gp130/Jak/STAT pathway. *Biochem J*, 334 (Pt 2)(Pt 2), 297-314. <https://doi.org/10.1042/bj3340297>
- Helbling, P. M., Piñeiro-Yáñez, E., Gerosa, R., Boettcher, S., Al-Shahrour, F., Manz, M. G., & Nombela-Arrieta, C. (2019, Dec 3). Global Transcriptomic Profiling of the Bone Marrow Stromal Microenvironment during Postnatal Development, Aging, and Inflammation. *Cell Rep*, 29(10), 3313-3330.e3314. <https://doi.org/10.1016/j.celrep.2019.11.004>
- Henry, E., & Arcangeli, M. L. (2021, Feb). How Hematopoietic Stem Cells Respond to Irradiation: Similarities and Differences between Low and High Doses of Ionizing Radiations. *Exp Hematol*, 94, 11-19. <https://doi.org/10.1016/j.exphem.2020.12.001>
- Himburg, H. A., Doan, P. L., Quarmyne, M., Yan, X., Sasine, J., Zhao, L., Hancock, G. V., Kan, J., Pohl, K. A., Tran, E., Chao, N. J., Harris, J. R., & Chute, J. P. (2017, Jan). Dickkopf-1 promotes hematopoietic regeneration via direct and niche-mediated mechanisms. *Nat Med*, 23(1), 91-99. <https://doi.org/10.1038/nm.4251>
- Hirano, T., Ishihara, K., & Hibi, M. (2000, May 15). Roles of STAT3 in mediating the cell growth, differentiation and survival signals relayed through the IL-6 family of cytokine receptors. *Oncogene*, 19(21), 2548-2556. <https://doi.org/10.1038/sj.onc.1203551>
- Ho, Y. H., & Méndez-Ferrer, S. (2020, Jan). Microenvironmental contributions to hematopoietic stem cell aging. *Haematologica*, 105(1), 38-46. <https://doi.org/10.3324/haematol.2018.211334>

- Hodge, C. D., Spyrapopoulos, L., & Glover, J. N. (2016, Sep 27). Ubc13: the Lys63 ubiquitin chain building machine. *Oncotarget*, 7(39), 64471-64504. <https://doi.org/10.18632/oncotarget.10948>
- Hodohara, K., Fujii, N., Yamamoto, N., & Kaushansky, K. (2000, Feb 1). Stromal cell-derived factor-1 (SDF-1) acts together with thrombopoietin to enhance the development of megakaryocytic progenitor cells (CFU-MK). *Blood*, 95(3), 769-775.
- <Hoesel and Schmid 2013.pdf>
- Hoesel, B., & Schmid, J. A. (2013, Aug 2). The complexity of NF- κ B signaling in inflammation and cancer. *Mol Cancer*, 12, 86. <https://doi.org/10.1186/1476-4598-12-86>
- Holbourn, K. P., Acharya, K. R., & Perbal, B. (2008). The CCN family of proteins: structure-function relationships. *Trends in biochemical sciences*, 33(10), 461-473. <https://doi.org/10.1016/j.tibs.2008.07.006>
- Holbourn, K. P., Perbal, B., & Ravi Acharya, K. (2009, Mar). Proteins on the catwalk: modelling the structural domains of the CCN family of proteins. *Journal of cell communication and signaling*, 3(1), 25-41. <https://doi.org/10.1007/s12079-009-0048-4>
- Holmes, A., Abraham, D. J., Sa, S., Shiwen, X., Black, C. M., & Leask, A. (2001, Apr 6). CTGF and SMADs, maintenance of scleroderma phenotype is independent of SMAD signaling. *J Biol Chem*, 276(14), 10594-10601. <https://doi.org/10.1074/jbc.M010149200>
- Holyoake, T. L., Freshney, M. G., McNair, L., Parker, A. N., McKay, P. J., Steward, W. P., Fitzsimons, E., Graham, G. J., & Pragnell, I. B. (1996, Jun 1). Ex vivo expansion with stem cell factor and interleukin-11 augments both short-term recovery posttransplant and the ability to serially transplant marrow. *Blood*, 87(11), 4589-4595.
- Honjo, T., Kubota, S., Kamioka, H., Sugawara, Y., Ishihara, Y., Yamashiro, T., Takigawa, M., & Takano-Yamamoto, T. (2012, Dec). Promotion of Ccn2 expression and osteoblastic differentiation by actin polymerization, which is induced by laminar fluid flow stress. *Journal of cell communication and signaling*, 6(4), 225-232. <https://doi.org/10.1007/s12079-012-0177-z>
- Hooper, A. T., Butler, J. M., Nolan, D. J., Kranz, A., Iida, K., Kobayashi, M., Kopp, H. G., Shido, K., Petit, I., Yanger, K., James, D., Witte, L., Zhu, Z., Wu, Y., Pytowski, B., Rosenwaks, Z., Mittal, V., Sato, T. N., & Rafii, S. (2009, Mar 6). Engraftment and reconstitution of hematopoiesis is dependent on VEGFR2-mediated regeneration of sinusoidal endothelial cells. *Cell Stem Cell*, 4(3), 263-274. <https://doi.org/10.1016/j.stem.2009.01.006>

- Horwitz, B. H., Scott, M. L., Cherry, S. R., Bronson, R. T., & Baltimore, D. (1997, Jun). Failure of lymphopoiesis after adoptive transfer of NF-kappaB-deficient fetal liver cells. *Immunity*, 6(6), 765-772. [https://doi.org/10.1016/s1074-7613\(00\)80451-3](https://doi.org/10.1016/s1074-7613(00)80451-3)
- Hoshijima, M., Hattori, T., Inoue, M., Araki, D., Hanagata, H., Miyauchi, A., & Takigawa, M. (2006, Feb 20). CT domain of CCN2/CTGF directly interacts with fibronectin and enhances cell adhesion of chondrocytes through integrin alpha5beta1. *FEBS Lett*, 580(5), 1376-1382. <https://doi.org/10.1016/j.febslet.2006.01.061>
- Hou, C. H., Yang, R. S., & Tsao, Y. T. (2018, Sep). Connective tissue growth factor stimulates osteosarcoma cell migration and induces osteosarcoma metastasis by upregulating VCAM-1 expression. *Biochem Pharmacol*, 155, 71-81. <https://doi.org/10.1016/j.bcp.2018.06.015>
- Hu, L., Yin, X., Zhang, Y., Pang, A., Xie, X., Yang, S., Zhu, C., Li, Y., Zhang, B., Huang, Y., Tian, Y., Wang, M., Cao, W., Chen, S., Zheng, Y., Ma, S., Dong, F., Hao, S., Feng, S., Ru, Y., Cheng, H., Jiang, E., & Cheng, T. (2021, Jun 17). Radiation-induced bystander effects impair transplanted human hematopoietic stem cells via oxidative DNA damage. *Blood*, 137(24), 3339-3350. <https://doi.org/10.1182/blood.2020007362>
- Igarashi, A., Nashiro, K., Kikuchi, K., Sato, S., Ihn, H., Fujimoto, M., Grotendorst, G. R., & Takehara, K. (1996, Apr). Connective tissue growth factor gene expression in tissue sections from localized scleroderma, keloid, and other fibrotic skin disorders. *J Invest Dermatol*, 106(4), 729-733. <https://doi.org/10.1111/1523-1747.ep12345771>
- Igarashi, A., Okochi, H., Bradham, D. M., & Grotendorst, G. R. (1993, Jun). Regulation of connective tissue growth factor gene expression in human skin fibroblasts and during wound repair. *Mol Biol Cell*, 4(6), 637-645. <https://doi.org/10.1091/mbc.4.6.637>
- Ikuta, K., & Weissman, I. L. (1992, Feb 15). Evidence that hematopoietic stem cells express mouse c-kit but do not depend on steel factor for their generation. *Proc Natl Acad Sci U S A*, 89(4), 1502-1506. <https://doi.org/10.1073/pnas.89.4.1502>
- Inaba, M., & Yamashita, Y. M. (2012, Oct 5). Asymmetric stem cell division: precision for robustness. *Cell Stem Cell*, 11(4), 461-469. <https://doi.org/10.1016/j.stem.2012.09.003>
- Inoki, I., Shiomi, T., Hashimoto, G., Enomoto, H., Nakamura, H., Makino, K., Ikeda, E., Takata, S., Kobayashi, K., & Okada, Y. (2002, Feb). Connective tissue growth factor binds vascular endothelial growth factor (VEGF) and inhibits VEGF-induced angiogenesis. *Faseb j*, 16(2), 219-221. <https://doi.org/10.1096/fj.01-0332fje>
- Iotsova, V., Caamaño, J., Loy, J., Yang, Y., Lewin, A., & Bravo, R. (1997, Nov). Osteopetrosis in mice lacking NF-kappaB1 and NF-kappaB2. *Nat Med*, 3(11), 1285-1289. <https://doi.org/10.1038/nm1197-1285>

- Ishibashi, T., Kimura, H., Shikama, Y., Uchida, T., Kariyone, S., Hirano, T., Kishimoto, T., Takatsuki, F., & Akiyama, Y. (1989, Sep). Interleukin-6 is a potent thrombopoietic factor in vivo in mice. *Blood*, *74*(4), 1241-1244.
- Ishihara, K., & Hirano, T. (2002, Aug-Oct). IL-6 in autoimmune disease and chronic inflammatory proliferative disease. *Cytokine Growth Factor Rev*, *13*(4-5), 357-368. [https://doi.org/10.1016/s1359-6101\(02\)00027-8](https://doi.org/10.1016/s1359-6101(02)00027-8)
- Istvánffy, R., Vilne, B., Schreck, C., Ruf, F., Pagel, C., Grziwok, S., Henkel, L., Prazeres da Costa, O., Berndt, J., Stümpflen, V., Götze, K. S., Schiemann, M., Peschel, C., Mewes, H.-W., & Oostendorp, R. A. J. (2015). Stroma-Derived Connective Tissue Growth Factor Maintains Cell Cycle Progression and Repopulation Activity of Hematopoietic Stem Cells In Vitro. *Stem cell reports*, *5*(5), 702-715. <https://doi.org/10.1016/j.stemcr.2015.09.018>
- Ivkovic, S., Yoon, B. S., Popoff, S. N., Safadi, F. F., Libuda, D. E., Stephenson, R. C., Daluiski, A., & Lyons, K. M. (2003, Jun). Connective tissue growth factor coordinates chondrogenesis and angiogenesis during skeletal development. *Development*, *130*(12), 2779-2791. <https://doi.org/10.1242/dev.00505>
- Iwai, K. (2012, Jul). Diverse ubiquitin signaling in NF- κ B activation. *Trends Cell Biol*, *22*(7), 355-364. <https://doi.org/10.1016/j.tcb.2012.04.001>
- Iwasa, M., Fujii, S., Fujishiro, A., Maekawa, T., Andoh, A., Takaori-Kondo, A., Ichinohe, T., & Miura, Y. (2021, May). Impact of 2 Gy γ -irradiation on the hallmark characteristics of human bone marrow-derived MSCs. *Int J Hematol*, *113*(5), 703-711. <https://doi.org/10.1007/s12185-020-03072-9>
- Janzen, V., Forkert, R., Fleming, H. E., Saito, Y., Waring, M. T., Dombkowski, D. M., Cheng, T., DePinho, R. A., Sharpless, N. E., & Scadden, D. T. (2006, Sep 28). Stem-cell ageing modified by the cyclin-dependent kinase inhibitor p16INK4a. *Nature*, *443*(7110), 421-426. <https://doi.org/10.1038/nature05159>
- Jeannot, G., Scheller, M., Scarpellino, L., Duboux, S., Gardiol, N., Back, J., Kuttler, F., Malanchi, I., Birchmeier, W., Leutz, A., Huelsken, J., & Held, W. (2008, Jan 1). Long-term, multilineage hematopoiesis occurs in the combined absence of beta-catenin and gamma-catenin. *Blood*, *111*(1), 142-149. <https://doi.org/10.1182/blood-2007-07-102558>
- Jenkins, B. J., Grail, D., Nheu, T., Najdovska, M., Wang, B., Waring, P., Inglese, M., McLoughlin, R. M., Jones, S. A., Topley, N., Baumann, H., Judd, L. M., Giraud, A. S., Boussioutas, A., Zhu, H. J., & Ernst, M. (2005, Aug). Hyperactivation of Stat3 in gp130 mutant mice promotes gastric hyperproliferation and desensitizes TGF-beta signaling. *Nat Med*, *11*(8), 845-852. <https://doi.org/10.1038/nm1282>

- Jeong, M., Piao, Z. H., Kim, M. S., Lee, S. H., Yun, S., Sun, H. N., Yoon, S. R., Chung, J. W., Kim, T. D., Jeon, J. H., Lee, J., Kim, H. N., Choi, J. Y., & Choi, I. (2009, Aug 15). Thioredoxin-interacting protein regulates hematopoietic stem cell quiescence and mobilization under stress conditions. *J Immunol*, *183*(4), 2495-2505. <https://doi.org/10.4049/jimmunol.0804221>
- Jia, Q., Dong, Q., & Qin, L. (2016, Jan 12). CCN: core regulatory proteins in the microenvironment that affect the metastasis of hepatocellular carcinoma? *Oncotarget*, *7*(2), 1203-1214. <https://doi.org/10.18632/oncotarget.6209>
- Jiang, Y., Sun, A., Zhao, Y., Ying, W., Sun, H., Yang, X., Xing, B., Sun, W., Ren, L., Hu, B., Li, C., Zhang, L., Qin, G., Zhang, M., Chen, N., Zhang, M., Huang, Y., Zhou, J., Zhao, Y., Liu, M., Zhu, X., Qiu, Y., Sun, Y., Huang, C., Yan, M., Wang, M., Liu, W., Tian, F., Xu, H., Zhou, J., Wu, Z., Shi, T., Zhu, W., Qin, J., Xie, L., Fan, J., Qian, X., & He, F. (2019, Mar). Proteomics identifies new therapeutic targets of early-stage hepatocellular carcinoma. *Nature*, *567*(7747), 257-261. <https://doi.org/10.1038/s41586-019-0987-8>
- Jin, J., Wang, Y., Wang, J., Xu, Y., Chen, S. L., Wang, J. P., & Su, Y. P. (2014, May). Impaired hematopoiesis and delayed thrombopoietic recovery following sublethal irradiation in SRC-3 knockout mice. *Mol Med Rep*, *9*(5), 1629-1633. <https://doi.org/10.3892/mmr.2014.2043>
- Johansson, B. M., & Wiles, M. V. (1995, Jan). Evidence for involvement of activin A and bone morphogenetic protein 4 in mammalian mesoderm and hematopoietic development. *Mol Cell Biol*, *15*(1), 141-151. <https://doi.org/10.1128/mcb.15.1.141>
- Joliot, V., Martinerie, C., Dambine, G., Plassiart, G., Brisac, M., Crochet, J., & Perbal, B. (1992, Jan). Proviral rearrangements and overexpression of a new cellular gene (nov) in myeloblastosis-associated virus type 1-induced nephroblastomas. *Mol Cell Biol*, *12*(1), 10-21. <https://doi.org/10.1128/mcb.12.1.10-21.1992>
- Jun, J. I., & Lau, L. F. (2010, Jul). The matricellular protein CCN1 induces fibroblast senescence and restricts fibrosis in cutaneous wound healing. *Nat Cell Biol*, *12*(7), 676-685. <https://doi.org/10.1038/ncb2070>
- Jun, J. I., & Lau, L. F. (2017, Mar). CCN2 induces cellular senescence in fibroblasts. *Journal of cell communication and signaling*, *11*(1), 15-23. <https://doi.org/10.1007/s12079-016-0359-1>
- Kaasbøll, O. J., Gadicherla, A. K., Wang, J. H., Monsen, V. T., Hagelin, E. M. V., Dong, M. Q., & Attramadal, H. (2018, Nov 16). Connective tissue growth factor (CCN2) is a matricellular preproprotein controlled by proteolytic activation. *J Biol Chem*, *293*(46), 17953-17970. <https://doi.org/10.1074/jbc.RA118.004559>
- Kang, H., Chen, I. M., Wilson, C. S., Bedrick, E. J., Harvey, R. C., Atlas, S. R., Devidas, M., Mullighan, C. G., Wang, X., Murphy, M., Ar, K., Wharton, W., Borowitz, M. J.,

- Bowman, W. P., Bhojwani, D., Carroll, W. L., Camitta, B. M., Reaman, G. H., Smith, M. A., Downing, J. R., Hunger, S. P., & Willman, C. L. (2010, Feb 18). Gene expression classifiers for relapse-free survival and minimal residual disease improve risk classification and outcome prediction in pediatric B-precursor acute lymphoblastic leukemia. *Blood*, *115*(7), 1394-1405. <https://doi.org/10.1182/blood-2009-05-218560>
- Kanna, R., Choudhary, G., Ramachandra, N., Steidl, U., Verma, A., & Shastri, A. (2018, Sep). STAT3 inhibition as a therapeutic strategy for leukemia. *Leuk Lymphoma*, *59*(9), 2068-2074. <https://doi.org/10.1080/10428194.2017.1397668>
- Kapoor, M., Liu, S., Huh, K., Parapuram, S., Kennedy, L., & Leask, A. (2008, Oct 13). Connective tissue growth factor promoter activity in normal and wounded skin. *Fibrogenesis Tissue Repair*, *1*(1), 3. <https://doi.org/10.1186/1755-1536-1-3>
- Kawabata, K., Ujikawa, M., Egawa, T., Kawamoto, H., Tachibana, K., Iizasa, H., Katsura, Y., Kishimoto, T., & Nagasawa, T. (1999, May 11). A cell-autonomous requirement for CXCR4 in long-term lymphoid and myeloid reconstitution. *Proc Natl Acad Sci U S A*, *96*(10), 5663-5667. <https://doi.org/10.1073/pnas.96.10.5663>
- Kawata, K., Eguchi, T., Kubota, S., Kawaki, H., Oka, M., Minagi, S., & Takigawa, M. (2006, Jun 30). Possible role of LRP1, a CCN2 receptor, in chondrocytes. *Biochem Biophys Res Commun*, *345*(2), 552-559. <https://doi.org/10.1016/j.bbrc.2006.04.109>
- Kawata, K., Kubota, S., Eguchi, T., Aoyama, E., Moritani, N. H., Kondo, S., Nishida, T., & Takigawa, M. (2012, Jun 15). Role of LRP1 in transport of CCN2 protein in chondrocytes. *J Cell Sci*, *125*(Pt 12), 2965-2972. <https://doi.org/10.1242/jcs.101956>
- Keller, J. R., Jacobsen, S. E., Sill, K. T., Ellingsworth, L. R., & Ruscetti, F. W. (1991, Aug 15). Stimulation of granulopoiesis by transforming growth factor beta: synergy with granulocyte/macrophage-colony-stimulating factor. *Proc Natl Acad Sci U S A*, *88*(16), 7190-7194. <https://doi.org/10.1073/pnas.88.16.7190>
- Kent, D. G., Copley, M. R., Benz, C., Wöhrer, S., Dykstra, B. J., Ma, E., Cheyne, J., Zhao, Y., Bowie, M. B., Zhao, Y., Gasparetto, M., Delaney, A., Smith, C., Marra, M., & Eaves, C. J. (2009, Jun 18). Prospective isolation and molecular characterization of hematopoietic stem cells with durable self-renewal potential. *Blood*, *113*(25), 6342-6350. <https://doi.org/10.1182/blood-2008-12-192054>
- Khatib-Massalha, E., & Méndez-Ferrer, S. (2022). Megakaryocyte Diversity in Ontogeny, Functions and Cell-Cell Interactions. *Front Oncol*, *12*, 840044. <https://doi.org/10.3389/fonc.2022.840044>
- Kiel, M. J., Acar, M., Radice, G. L., & Morrison, S. J. (2009). Hematopoietic stem cells do not depend on N-cadherin to regulate their maintenance. *Cell Stem Cell*, *4*(2), 170-179. <https://doi.org/10.1016/j.stem.2008.10.005>

- Kiel, M. J., & Morrison, S. J. (2008, Apr). Uncertainty in the niches that maintain haematopoietic stem cells. *Nat Rev Immunol*, *8*(4), 290-301. <https://doi.org/10.1038/nri2279>
- Kiel, M. J., Radice, G. L., & Morrison, S. J. (2007, 2007/08/16/). Lack of Evidence that Hematopoietic Stem Cells Depend on N-Cadherin-Mediated Adhesion to Osteoblasts for Their Maintenance. *Cell Stem Cell*, *1*(2), 204-217. <https://doi.org/https://doi.org/10.1016/j.stem.2007.06.001>
- Kiel, M. J., Yilmaz, O. H., Iwashita, T., Yilmaz, O. H., Terhorst, C., & Morrison, S. J. (2005, Jul 1). SLAM family receptors distinguish hematopoietic stem and progenitor cells and reveal endothelial niches for stem cells. *Cell*, *121*(7), 1109-1121. <https://doi.org/10.1016/j.cell.2005.05.026>
- Kieslinger, M., Hiechinger, S., Dobрева, G., Consalez, G. G., & Grosschedl, R. (2010, 2010/10/08/). Early B Cell Factor 2 Regulates Hematopoietic Stem Cell Homeostasis in a Cell-Nonautonomous Manner. *Cell Stem Cell*, *7*(4), 496-507. <https://doi.org/https://doi.org/10.1016/j.stem.2010.07.015>
- Kikuchi, T., Kubota, S., Asaumi, K., Kawaki, H., Nishida, T., Kawata, K., Mitani, S., Tabata, Y., Ozaki, T., & Takigawa, M. (2008, Jun). Promotion of bone regeneration by CCN2 incorporated into gelatin hydrogel. *Tissue Eng Part A*, *14*(6), 1089-1098. <https://doi.org/10.1089/tea.2007.0167>
- Kim, A., Shim, S., Kim, M. J., Myung, J. K., & Park, S. (2018, Jun 18). Mesenchymal stem cell-mediated Notch2 activation overcomes radiation-induced injury of the hematopoietic system. *Sci Rep*, *8*(1), 9277. <https://doi.org/10.1038/s41598-018-27666-w>
- Kim, S. J., & Letterio, J. (2003, 2003/09/01). Transforming growth factor- β signaling in normal and malignant hematopoiesis. *Leukemia*, *17*(9), 1731-1737. <https://doi.org/10.1038/sj.leu.2403069>
- Kimura, A., & Kishimoto, T. (2010, Jul). IL-6: regulator of Treg/Th17 balance. *Eur J Immunol*, *40*(7), 1830-1835. <https://doi.org/10.1002/eji.201040391>
- King, K. Y., & Goodell, M. A. (2011, Sep 9). Inflammatory modulation of HSCs: viewing the HSC as a foundation for the immune response. *Nat Rev Immunol*, *11*(10), 685-692. <https://doi.org/10.1038/nri3062>
- Kishimoto, T. (1989, Jul). The biology of interleukin-6. *Blood*, *74*(1), 1-10.
- Komori, T., Yagi, H., Nomura, S., Yamaguchi, A., Sasaki, K., Deguchi, K., Shimizu, Y., Bronson, R. T., Gao, Y. H., Inada, M., Sato, M., Okamoto, R., Kitamura, Y., Yoshiki, S., & Kishimoto, T. (1997, 1997/05/30/). Targeted Disruption of Cbfa1 Results in a

- Complete Lack of Bone Formation owing to Maturation Arrest of Osteoblasts. *Cell*, 89(5), 755-764. [https://doi.org/https://doi.org/10.1016/S0092-8674\(00\)80258-5](https://doi.org/https://doi.org/10.1016/S0092-8674(00)80258-5)
- Kondo, M., Weissman, I. L., & Akashi, K. (1997, Nov 28). Identification of clonogenic common lymphoid progenitors in mouse bone marrow. *Cell*, 91(5), 661-672. [https://doi.org/10.1016/s0092-8674\(00\)80453-5](https://doi.org/10.1016/s0092-8674(00)80453-5)
- Kondo, S., Kubota, S., Shimo, T., Nishida, T., Yosimichi, G., Eguchi, T., Sugahara, T., & Takigawa, M. (2002, May). Connective tissue growth factor increased by hypoxia may initiate angiogenesis in collaboration with matrix metalloproteinases. *Carcinogenesis*, 23(5), 769-776. <https://doi.org/10.1093/carcin/23.5.769>
- Kondo, S., Tanaka, N., Kubota, S., Mukudai, Y., Yosimichi, G., Sugahara, T., & Takigawa, M. (2006, Jan). Novel angiogenic inhibitor DN-9693 that inhibits post-transcriptional induction of connective tissue growth factor (CTGF/CCN2) by vascular endothelial growth factor in human endothelial cells. *Mol Cancer Ther*, 5(1), 129-137. <https://doi.org/10.1158/1535-7163.Mct-05-0097>
- Koopman, G., Reutelingsperger, C. P., Kuijten, G. A., Keehnen, R. M., Pals, S. T., & van Oers, M. H. (1994, Sep 1). Annexin V for flow cytometric detection of phosphatidylserine expression on B cells undergoing apoptosis. *Blood*, 84(5), 1415-1420.
- Krizhanovsky, V., Yon, M., Dickins, R. A., Hearn, S., Simon, J., Miething, C., Yee, H., Zender, L., & Lowe, S. W. (2008, Aug 22). Senescence of activated stellate cells limits liver fibrosis. *Cell*, 134(4), 657-667. <https://doi.org/10.1016/j.cell.2008.06.049>
- Kular, L., Pakradouni, J., Kitabgi, P., Laurent, M., & Martinerie, C. (2011, Mar). The CCN family: a new class of inflammation modulators? *Biochimie*, 93(3), 377-388. <https://doi.org/10.1016/j.biochi.2010.11.010>
- Landspersky, T., Saçma, M., Rivière, J., Hecker, J. S., Hettler, F., Hameister, E., Brandstetter, K., Istvánffy, R., Romero Marquez, S., Ludwig, R., Götz, M., Buck, M., Wolf, M., Schiemann, M., Ruland, J., Strunk, D., Shimamura, A., Myers, K., Yamaguchi, T. P., Kieslinger, M., Leonhardt, H., Bassermann, F., Götze, K. S., Geiger, H., Schreck, C., & Oostendorp, R. A. J. (2022, Feb 3). Autophagy in mesenchymal progenitors protects mice against bone marrow failure after severe intermittent stress. *Blood*, 139(5), 690-703. <https://doi.org/10.1182/blood.2021011775>
- Lapidot, T., & Kollet, O. (2002, Oct). The essential roles of the chemokine SDF-1 and its receptor CXCR4 in human stem cell homing and repopulation of transplanted immune-deficient NOD/SCID and NOD/SCID/B2m(null) mice. *Leukemia*, 16(10), 1992-2003. <https://doi.org/10.1038/sj.leu.2402684>
- Lasky, J. A., Ortiz, L. A., Tonthat, B., Hoyle, G. W., Corti, M., Athas, G., Lungarella, G., Brody, A., & Friedman, M. (1998, Aug). Connective tissue growth factor mRNA expression is

- upregulated in bleomycin-induced lung fibrosis. *Am J Physiol*, 275(2), L365-371.
<https://doi.org/10.1152/ajplung.1998.275.2.L365>
- Lassmann, M., Hänscheid, H., Gassen, D., Biko, J., Meineke, V., Reiners, C., & Scherthan, H. (2010, Aug). In vivo formation of gamma-H2AX and 53BP1 DNA repair foci in blood cells after radioiodine therapy of differentiated thyroid cancer. *J Nucl Med*, 51(8), 1318-1325. <https://doi.org/10.2967/jnumed.109.071357>
- Laug, R., Fehrholz, M., Schütze, N., Kramer, B. W., Krump-Konvalinkova, V., Speer, C. P., & Kunzmann, S. (2012). IFN- γ and TNF- α synergize to inhibit CTGF expression in human lung endothelial cells. *PLoS One*, 7(9), e45430.
<https://doi.org/10.1371/journal.pone.0045430>
- Leary, A. G., Ikebuchi, K., Hirai, Y., Wong, G. G., Yang, Y.-C., Clark, S. C., & Ogawa, M. (1988, 1988/06/01/). Synergism Between Interleukin-6 and Interleukin-3 in Supporting Proliferation of Human Hematopoietic Stem Cells: Comparison With Interleukin- α . *Blood*, 71(6), 1759-1763.
<https://doi.org/https://doi.org/10.1182/blood.V71.6.1759.1759>
- Leask, A. (2009, Jun 1). Signaling in fibrosis: targeting the TGF beta, endothelin-1 and CCN2 axis in scleroderma. *Front Biosci (Elite Ed)*, 1(1), 115-122.
<https://doi.org/10.2741/e12>
- Leask, A., & Abraham, D. J. (2006, Dec 1). All in the CCN family: essential matricellular signaling modulators emerge from the bunker. *J Cell Sci*, 119(Pt 23), 4803-4810.
<https://doi.org/10.1242/jcs.03270>
- Lecault, V., Vaninsberghe, M., Sekulovic, S., Knapp, D. J., Wohrer, S., Bowden, W., Viel, F., McLaughlin, T., Jarandehi, A., Miller, M., Falconnet, D., White, A. K., Kent, D. G., Copley, M. R., Taghipour, F., Eaves, C. J., Humphries, R. K., Piret, J. M., & Hansen, C. L. (2011, May 22). High-throughput analysis of single hematopoietic stem cell proliferation in microfluidic cell culture arrays. *Nat Methods*, 8(7), 581-586.
<https://doi.org/10.1038/nmeth.1614>
- Leguit, R. J., Raymakers, R. A. P., Hebeda, K. M., & Goldschmeding, R. (2021, Mar). CCN2 (Cellular Communication Network factor 2) in the bone marrow microenvironment, normal and malignant hematopoiesis. *Journal of cell communication and signaling*, 15(1), 25-56. <https://doi.org/10.1007/s12079-020-00602-2>
- Li, B., Bailey, A. S., Jiang, S., Liu, B., Goldman, D. C., & Fleming, W. H. (2010, Jan). Endothelial cells mediate the regeneration of hematopoietic stem cells. *Stem Cell Res*, 4(1), 17-24. <https://doi.org/10.1016/j.scr.2009.08.001>
- Li, F., Zhang, R., Hu, C., Ran, Q., Xiang, Y., Xiang, L., Chen, L., Yang, Y., Li, S. C., Zhang, G., & Li, Z. (2021). Irradiation Haematopoiesis Recovery Orchestrated by IL-12/IL-12R β 1/TYK2/STAT3-Initiated Osteogenic Differentiation of Mouse Bone Marrow-

- Derived Mesenchymal Stem Cells. *Front Cell Dev Biol*, 9, 729293. <https://doi.org/10.3389/fcell.2021.729293>
- Li, Y., Zheng, Y., Li, T., Wang, Q., Qian, J., Lu, Y., Zhang, M., Bi, E., Yang, M., Reu, F., Yi, Q., & Cai, Z. (2015, Sep 15). Chemokines CCL2, 3, 14 stimulate macrophage bone marrow homing, proliferation, and polarization in multiple myeloma. *Oncotarget*, 6(27), 24218-24229. <https://doi.org/10.18632/oncotarget.4523>
- Liles, W. C., Broxmeyer, H. E., Rodger, E., Wood, B., Hübel, K., Cooper, S., Hangoc, G., Bridger, G. J., Henson, G. W., Calandra, G., & Dale, D. C. (2003, Oct 15). Mobilization of hematopoietic progenitor cells in healthy volunteers by AMD3100, a CXCR4 antagonist. *Blood*, 102(8), 2728-2730. <https://doi.org/10.1182/blood-2003-02-0663>
- Liotta, F., Angeli, R., Cosmi, L., Fili, L., Manuelli, C., Frosali, F., Mazzinghi, B., Maggi, L., Pasini, A., Lisi, V., Santarasci, V., Consoloni, L., Angelotti, M. L., Romagnani, P., Parronchi, P., Krampera, M., Maggi, E., Romagnani, S., & Annunziato, F. (2008, Jan). Toll-like receptors 3 and 4 are expressed by human bone marrow-derived mesenchymal stem cells and can inhibit their T-cell modulatory activity by impairing Notch signaling. *Stem Cells*, 26(1), 279-289. <https://doi.org/10.1634/stemcells.2007-0454>
- Liu, S., & Leask, A. (2011, Aug). CCN2 is not required for skin development. *Journal of cell communication and signaling*, 5(3), 179-182. <https://doi.org/10.1007/s12079-011-0129-z>
- Liu, S. C., Hsu, C. J., Chen, H. T., Tsou, H. K., Chuang, S. M., & Tang, C. H. (2012). CTGF increases IL-6 expression in human synovial fibroblasts through integrin-dependent signaling pathway. *PLoS One*, 7(12), e51097. <https://doi.org/10.1371/journal.pone.0051097>
- Lo Celso, C., Fleming, H. E., Wu, J. W., Zhao, C. X., Miake-Lye, S., Fujisaki, J., Côté, D., Rowe, D. W., Lin, C. P., & Scadden, D. T. (2009, Jan 1). Live-animal tracking of individual haematopoietic stem/progenitor cells in their niche. *Nature*, 457(7225), 92-96. <https://doi.org/10.1038/nature07434>
- Longley, D. B., Harkin, D. P., & Johnston, P. G. (2003, May). 5-fluorouracil: mechanisms of action and clinical strategies. *Nat Rev Cancer*, 3(5), 330-338. <https://doi.org/10.1038/nrc1074>
- Lord, B. I., Testa, N. G., & Hendry, J. H. (1975, Jul). The relative spatial distributions of CFUs and CFUc in the normal mouse femur. *Blood*, 46(1), 65-72.
- Lu, H., Kojima, K., Battula, V. L., Korchin, B., Shi, Y., Chen, Y., Spong, S., Thomas, D. A., Kantarjian, H., Lock, R. B., Andreeff, M., & Konopleva, M. (2014, Mar). Targeting connective tissue growth factor (CTGF) in acute lymphoblastic leukemia preclinical models: anti-CTGF monoclonal antibody attenuates leukemia growth. *Ann Hematol*, 93(3), 485-492. <https://doi.org/10.1007/s00277-013-1939-2>

- Luft, F. C. (2008, Jan). CCN2, the connective tissue growth factor. *J Mol Med (Berl)*, *86*(1), 1-3. <https://doi.org/10.1007/s00109-007-0287-x>
- Luis, T. C., Weerkamp, F., Naber, B. A., Baert, M. R., de Haas, E. F., Nikolic, T., Heuvelmans, S., De Krijger, R. R., van Dongen, J. J., & Staal, F. J. (2009, Jan 15). Wnt3a deficiency irreversibly impairs hematopoietic stem cell self-renewal and leads to defects in progenitor cell differentiation. *Blood*, *113*(3), 546-554. <https://doi.org/10.1182/blood-2008-06-163774>
- Luo, Q., Kang, Q., Si, W., Jiang, W., Park, J. K., Peng, Y., Li, X., Luu, H. H., Luo, J., Montag, A. G., Haydon, R. C., & He, T. C. (2004, Dec 31). Connective tissue growth factor (CTGF) is regulated by Wnt and bone morphogenetic proteins signaling in osteoblast differentiation of mesenchymal stem cells. *J Biol Chem*, *279*(53), 55958-55968. <https://doi.org/10.1074/jbc.M407810200>
- Luskey, B. D., Rosenblatt, M., Zsebo, K., & Williams, D. A. (1992, Jul 15). Stem cell factor, interleukin-3, and interleukin-6 promote retroviral-mediated gene transfer into murine hematopoietic stem cells. *Blood*, *80*(2), 396-402.
- Lutzny, G., Kocher, T., Schmidt-Supprian, M., Rudelius, M., Klein-Hitpass, L., Finch, A. J., Dürig, J., Wagner, M., Haferlach, C., Kohlmann, A., Schnittger, S., Seifert, M., Wanninger, S., Zaborsky, N., Oostendorp, R., Ruland, J., Leitges, M., Kuhnt, T., Schäfer, Y., Lampl, B., Peschel, C., Egle, A., & Ringshausen, I. (2013, Jan 14). Protein kinase c- β -dependent activation of NF- κ B in stromal cells is indispensable for the survival of chronic lymphocytic leukemia B cells in vivo. *Cancer Cell*, *23*(1), 77-92. <https://doi.org/10.1016/j.ccr.2012.12.003>
- Lyman, S. D., & Jacobsen, S. E. (1998, Feb 15). c-kit ligand and Flt3 ligand: stem/progenitor cell factors with overlapping yet distinct activities. *Blood*, *91*(4), 1101-1134.
- Ma, Q., Jones, D., Borghesani, P. R., Segal, R. A., Nagasawa, T., Kishimoto, T., Bronson, R. T., & Springer, T. A. (1998, Aug 4). Impaired B-lymphopoiesis, myelopoiesis, and derailed cerebellar neuron migration in CXCR4- and SDF-1-deficient mice. *Proc Natl Acad Sci U S A*, *95*(16), 9448-9453. <https://doi.org/10.1073/pnas.95.16.9448>
- Ma, Y. D., Park, C., Zhao, H., Oduro, K. A., Jr., Tu, X., Long, F., Allen, P. M., Teitelbaum, S. L., & Choi, K. (2009, Nov 12). Defects in osteoblast function but no changes in long-term repopulating potential of hematopoietic stem cells in a mouse chronic inflammatory arthritis model. *Blood*, *114*(20), 4402-4410. <https://doi.org/10.1182/blood-2008-12-196311>
- Maes, C., Kobayashi, T., Selig, M. K., Torrekens, S., Roth, S. I., Mackem, S., Carmeliet, G., & Kronenberg, H. M. (2010, Aug 17). Osteoblast precursors, but not mature osteoblasts, move into developing and fractured bones along with invading blood vessels. *Dev Cell*, *19*(2), 329-344. <https://doi.org/10.1016/j.devcel.2010.07.010>

- Marshall, C. J., Kinnon, C., & Thrasher, A. J. (2000, Aug 15). Polarized expression of bone morphogenetic protein-4 in the human aorta-gonad-mesonephros region. *Blood*, *96*(4), 1591-1593.
- Mazo, I. B., Massberg, S., & von Andrian, U. H. (2011, Oct). Hematopoietic stem and progenitor cell trafficking. *Trends Immunol*, *32*(10), 493-503. <https://doi.org/10.1016/j.it.2011.06.011>
- McElroy, S. L., & Reijo Pera, R. A. (2008, Sep 1). Culturing human embryonic stem cells with mouse embryonic fibroblast feeder cells. *CSH Protoc*, *2008*, pdb.prot5042. <https://doi.org/10.1101/pdb.prot5042>
- Mende, N., Jolly, A., Percin, G. I., Günther, M., Rostovskaya, M., Krishnan, S. M., Oostendorp, R. A. J., Dahl, A., Anastassiadis, K., Höfer, T., & Waskow, C. (2019, Oct 10). Prospective isolation of nonhematopoietic cells of the niche and their differential molecular interactions with HSCs. *Blood*, *134*(15), 1214-1226. <https://doi.org/10.1182/blood.2019000176>
- Méndez-Ferrer, S., Michurina, T. V., Ferraro, F., Mazloom, A. R., Macarthur, B. D., Lira, S. A., Scadden, D. T., Ma'ayan, A., Enikolopov, G. N., & Frenette, P. S. (2010). Mesenchymal and haematopoietic stem cells form a unique bone marrow niche. *Nature*, *466*(7308), 829-834. <https://doi.org/10.1038/nature09262>
- Mercurio, S., Latinkic, B., Itasaki, N., Krumlauf, R., & Smith, J. C. (2004, May). Connective-tissue growth factor modulates WNT signalling and interacts with the WNT receptor complex. *Development*, *131*(9), 2137-2147. <https://doi.org/10.1242/dev.01045>
- Mikkola, H. K., & Orkin, S. H. (2006, Oct). The journey of developing hematopoietic stem cells. *Development*, *133*(19), 3733-3744. <https://doi.org/10.1242/dev.02568>
- Miller, C. L., & Eaves, C. J. (1997, Dec 9). Expansion in vitro of adult murine hematopoietic stem cells with transplantable lympho-myeloid reconstituting ability. *Proc Natl Acad Sci U S A*, *94*(25), 13648-13653. <https://doi.org/10.1073/pnas.94.25.13648>
- Mise-Omata, S., Alles, N., Fukazawa, T., Aoki, K., Ohya, K., Jimi, E., Obata, Y., & Doi, T. (2014, Nov). NF- κ B RELA-deficient bone marrow macrophages fail to support bone formation and to maintain the hematopoietic niche after lethal irradiation and stem cell transplantation. *Int Immunol*, *26*(11), 607-618. <https://doi.org/10.1093/intimm/dxu062>
- Mitroulis, I., Chen, L. S., Singh, R. P., Kourtzelis, I., Economopoulou, M., Kajikawa, T., Troullinaki, M., Ziogas, A., Ruppova, K., Hosur, K., Maekawa, T., Wang, B., Subramanian, P., Tonn, T., Verginis, P., von Bonin, M., Wobus, M., Bornhäuser, M., Grinenko, T., Di Scala, M., Hidalgo, A., Wielockx, B., Hajishengallis, G., & Chavakis, T. (2017, Oct 2). Secreted protein Del-1 regulates myelopoiesis in the hematopoietic

- stem cell niche. *The Journal of clinical investigation*, 127(10), 3624-3639.
<https://doi.org/10.1172/jci92571>
- Mohrin, M., Bourke, E., Alexander, D., Warr, M. R., Barry-Holson, K., Le Beau, M. M., Morrison, C. G., & Passegué, E. (2010, Aug 6). Hematopoietic stem cell quiescence promotes error-prone DNA repair and mutagenesis. *Cell Stem Cell*, 7(2), 174-185.
<https://doi.org/10.1016/j.stem.2010.06.014>
- Molofsky, A. V., Pardal, R., & Morrison, S. J. (2004, 2004/12/01/). Diverse mechanisms regulate stem cell self-renewal. *Current Opinion in Cell Biology*, 16(6), 700-707.
<https://doi.org/https://doi.org/10.1016/j.ceb.2004.09.004>
- Moore, M. A., & Metcalf, D. (1970, Mar). Ontogeny of the haemopoietic system: yolk sac origin of in vivo and in vitro colony forming cells in the developing mouse embryo. *Br J Haematol*, 18(3), 279-296. <https://doi.org/10.1111/j.1365-2141.1970.tb01443.x>
- Mori, T., Kawara, S., Shinozaki, M., Hayashi, N., Kakinuma, T., Igarashi, A., Takigawa, M., Nakanishi, T., & Takehara, K. (1999, Oct). Role and interaction of connective tissue growth factor with transforming growth factor-beta in persistent fibrosis: A mouse fibrosis model. *J Cell Physiol*, 181(1), 153-159. [https://doi.org/10.1002/\(sici\)1097-4652\(199910\)181:1<153::Aid-jcp16>3.0.Co;2-k](https://doi.org/10.1002/(sici)1097-4652(199910)181:1<153::Aid-jcp16>3.0.Co;2-k)
- Morita, Y., Ema, H., & Nakauchi, H. (2010, Jun 7). Heterogeneity and hierarchy within the most primitive hematopoietic stem cell compartment. *J Exp Med*, 207(6), 1173-1182.
<https://doi.org/10.1084/jem.20091318>
- Morrison, S. J., & Scadden, D. T. (2014, Jan 16). The bone marrow niche for haematopoietic stem cells. *Nature*, 505(7483), 327-334. <https://doi.org/10.1038/nature12984>
- Morrison, S. J., & Spradling, A. C. (2008, Feb 22). Stem cells and niches: mechanisms that promote stem cell maintenance throughout life. *Cell*, 132(4), 598-611.
<https://doi.org/10.1016/j.cell.2008.01.038>
- Morrison, S. J., Wandycz, A. M., Hemmati, H. D., Wright, D. E., & Weissman, I. L. (1997, May). Identification of a lineage of multipotent hematopoietic progenitors. *Development*, 124(10), 1929-1939. <https://doi.org/10.1242/dev.124.10.1929>
- Morrison, S. J., & Weissman, I. L. (1994, Nov). The long-term repopulating subset of hematopoietic stem cells is deterministic and isolatable by phenotype. *Immunity*, 1(8), 661-673. [https://doi.org/10.1016/1074-7613\(94\)90037-x](https://doi.org/10.1016/1074-7613(94)90037-x)
- Mosteo, L., Storer, J., Batta, K., Searle, E. J., Duarte, D., & Wiseman, D. H. (2021). The Dynamic Interface Between the Bone Marrow Vascular Niche and Hematopoietic Stem Cells in Myeloid Malignancy. *Front Cell Dev Biol*, 9, 635189.
<https://doi.org/10.3389/fcell.2021.635189>

- Moussad, E. E., & Brigstock, D. R. (2000, Sep-Oct). Connective tissue growth factor: what's in a name? *Mol Genet Metab*, *71*(1-2), 276-292. <https://doi.org/10.1006/mgme.2000.3059>
- Moxey-Mims, M. M., Simms, H. H., Frank, M. M., Lin, E. Y., & Gaither, T. A. (1991, Sep 15). The effects of IL-1, IL-2, and tumor necrosis factor on polymorphonuclear leukocyte Fc gamma receptor-mediated phagocytosis. IL-2 down-regulates the effect of tumor necrosis factor. *J Immunol*, *147*(6), 1823-1830.
- Muehlich, S., Schneider, N., Hinkmann, F., Garlichs, C. D., & Goppelt-Struebe, M. (2004, Aug). Induction of connective tissue growth factor (CTGF) in human endothelial cells by lysophosphatidic acid, sphingosine-1-phosphate, and platelets. *Atherosclerosis*, *175*(2), 261-268. <https://doi.org/10.1016/j.atherosclerosis.2004.04.011>
- Müller, A. M., Medvinsky, A., Strouboulis, J., Grosveld, F., & Dzierzak, E. (1994, Jul). Development of hematopoietic stem cell activity in the mouse embryo. *Immunity*, *1*(4), 291-301. [https://doi.org/10.1016/1074-7613\(94\)90081-7](https://doi.org/10.1016/1074-7613(94)90081-7)
- Mundy, C., Gannon, M., & Popoff, S. N. (2014, May). Connective tissue growth factor (CTGF/CCN2) negatively regulates BMP-2 induced osteoblast differentiation and signaling. *J Cell Physiol*, *229*(5), 672-681. <https://doi.org/10.1002/jcp.24491>
- Murphy, M., Godson, C., Cannon, S., Kato, S., Mackenzie, H. S., Martin, F., & Brady, H. R. (1999, Feb 26). Suppression subtractive hybridization identifies high glucose levels as a stimulus for expression of connective tissue growth factor and other genes in human mesangial cells. *J Biol Chem*, *274*(9), 5830-5834. <https://doi.org/10.1074/jbc.274.9.5830>
- Nagai, Y., Garrett, K. P., Ohta, S., Bahrn, U., Kouro, T., Akira, S., Takatsu, K., & Kincade, P. W. (2006). Toll-like receptors on hematopoietic progenitor cells stimulate innate immune system replenishment. *Immunity*, *24*(6), 801-812. <https://doi.org/10.1016/j.immuni.2006.04.008>
- Nagasawa, T., Hirota, S., Tachibana, K., Takakura, N., Nishikawa, S.-i., Kitamura, Y., Yoshida, N., Kikutani, H., & Kishimoto, T. (1996, 1996/08/01). Defects of B-cell lymphopoiesis and bone-marrow myelopoiesis in mice lacking the CXC chemokine PBSF/SDF-1. *Nature*, *382*(6592), 635-638. <https://doi.org/10.1038/382635a0>
- Nakagawa, M. M., & Rathinam, C. V. (2018, Nov 20). Constitutive Activation of the Canonical NF-κB Pathway Leads to Bone Marrow Failure and Induction of Erythroid Signature in Hematopoietic Stem Cells. *Cell Rep*, *25*(8), 2094-2109.e2094. <https://doi.org/10.1016/j.celrep.2018.10.071>
- Nakamura, A. J., Rao, V. A., Pommier, Y., & Bonner, W. M. (2010, 2010/01/15). The complexity of phosphorylated H2AX foci formation and DNA repair assembly at DNA double-strand breaks. *Cell Cycle*, *9*(2), 389-397. <https://doi.org/10.4161/cc.9.2.10475>

- Nakamura, A. J., Rao, V. A., Pommier, Y., & Bonner, W. M. (2010, Jan 15). The complexity of phosphorylated H2AX foci formation and DNA repair assembly at DNA double-strand breaks. *Cell Cycle*, *9*(2), 389-397. <https://doi.org/10.4161/cc.9.2.10475>
- Nakamura, Y., Arai, F., Iwasaki, H., Hosokawa, K., Kobayashi, I., Gomei, Y., Matsumoto, Y., Yoshihara, H., & Suda, T. (2010, Sep 2). Isolation and characterization of endosteal niche cell populations that regulate hematopoietic stem cells. *Blood*, *116*(9), 1422-1432. <https://doi.org/10.1182/blood-2009-08-239194>
- Nakamura-Ishizu, A., Takubo, K., Fujioka, M., & Suda, T. (2014, Nov 14). Megakaryocytes are essential for HSC quiescence through the production of thrombopoietin. *Biochem Biophys Res Commun*, *454*(2), 353-357. <https://doi.org/10.1016/j.bbrc.2014.10.095>
- Nakashima, K., Zhou, X., Kunkel, G., Zhang, Z., Deng, J. M., Behringer, R. R., & de Crombrughe, B. (2002, Jan 11). The novel zinc finger-containing transcription factor osterix is required for osteoblast differentiation and bone formation. *Cell*, *108*(1), 17-29. [https://doi.org/10.1016/s0092-8674\(01\)00622-5](https://doi.org/10.1016/s0092-8674(01)00622-5)
- Nakauchi, H., Sudo, K., & Ema, H. (2001, Jun). Quantitative assessment of the stem cell self-renewal capacity. *Ann N Y Acad Sci*, *938*, 18-24; discussion 24-15. <https://doi.org/10.1111/j.1749-6632.2001.tb03570.x>
- Negahdaripour, M., Nezafat, N., & Ghasemi, Y. (2016, Dec). A panoramic review and in silico analysis of IL-11 structure and function. *Cytokine Growth Factor Rev*, *32*, 41-61. <https://doi.org/10.1016/j.cytogfr.2016.06.002>
- Nilsson, S. K., Johnston, H. M., Whitty, G. A., Williams, B., Webb, R. J., Denhardt, D. T., Bertocello, I., Bendall, L. J., Simmons, P. J., & Haylock, D. N. (2005, Aug 15). Osteopontin, a key component of the hematopoietic stem cell niche and regulator of primitive hematopoietic progenitor cells. *Blood*, *106*(4), 1232-1239. <https://doi.org/10.1182/blood-2004-11-4422>
- Nishida, T., Kubota, S., Fukunaga, T., Kondo, S., Yosimichi, G., Nakanishi, T., Takano-Yamamoto, T., & Takigawa, M. (2003, Aug). CTGF/Hcs24, hypertrophic chondrocyte-specific gene product, interacts with perlecan in regulating the proliferation and differentiation of chondrocytes. *J Cell Physiol*, *196*(2), 265-275. <https://doi.org/10.1002/jcp.10277>
- Nishioka, M., Ogawa, E., Kinose, D., Haruna, A., Ohara, T., Ito, I., Hoshino, Y., Ito, Y., Matsumoto, H., Niimi, A., Mio, T., Chin, K., Hirai, T., Muro, S., & Mishima, M. (2010, May). Lipopolysaccharide induced connective tissue growth factor gene expression in human bronchial epithelial cells. *Respirology*, *15*(4), 669-676. <https://doi.org/10.1111/j.1440-1843.2010.01742.x>

- O'Brien, T. P., Yang, G. P., Sanders, L., & Lau, L. F. (1990, Jul). Expression of *cyr61*, a growth factor-inducible immediate-early gene. *Mol Cell Biol*, *10*(7), 3569-3577. <https://doi.org/10.1128/mcb.10.7.3569-3577.1990>
- O'Connell, R. M., Kahn, D., Gibson, W. S. J., Round, J. L., Scholz, R. L., Chaudhuri, A. A., Kahn, M. E., Rao, D. S., & Baltimore, D. (2010, 2010/10/29/). MicroRNA-155 Promotes Autoimmune Inflammation by Enhancing Inflammatory T Cell Development. *Immunity*, *33*(4), 607-619. <https://doi.org/https://doi.org/10.1016/j.immuni.2010.09.009>
- Ogawa, M., Tajima, F., Ito, T., Sato, T., Laver, J. H., & Deguchi, T. (2001, Jun). CD34 expression by murine hematopoietic stem cells. Developmental changes and kinetic alterations. *Ann N Y Acad Sci*, *938*, 139-145. <https://doi.org/10.1111/j.1749-6632.2001.tb03583.x>
- Ogilvy, S., Metcalf, D., Print, C. G., Bath, M. L., Harris, A. W., & Adams, J. M. (1999, Dec 21). Constitutive Bcl-2 expression throughout the hematopoietic compartment affects multiple lineages and enhances progenitor cell survival. *Proc Natl Acad Sci U S A*, *96*(26), 14943-14948. <https://doi.org/10.1073/pnas.96.26.14943>
- Ohta, M., Greenberger, J. S., Anklesaria, P., Bassols, A., & Massagué, J. (1987, Oct 8-14). Two forms of transforming growth factor-beta distinguished by multipotential haematopoietic progenitor cells. *Nature*, *329*(6139), 539-541. <https://doi.org/10.1038/329539a0>
- Olson, T. S., Caselli, A., Otsuru, S., Hofmann, T. J., Williams, R., Paolucci, P., Dominici, M., & Horwitz, E. M. (2013, Jun 27). Megakaryocytes promote murine osteoblastic HSC niche expansion and stem cell engraftment after radioablative conditioning. *Blood*, *121*(26), 5238-5249. <https://doi.org/10.1182/blood-2012-10-463414>
- Oostendorp, R. A., & Dörmer, P. (1997, Feb). VLA-4-mediated interactions between normal human hematopoietic progenitors and stromal cells. *Leuk Lymphoma*, *24*(5-6), 423-435. <https://doi.org/10.3109/10428199709055581>
- Oostendorp, R. A., Harvey, K. N., Kusadasi, N., de Bruijn, M. F., Saris, C., Ploemacher, R. E., Medvinsky, A. L., & Dzierzak, E. A. (2002, Feb 15). Stromal cell lines from mouse aorta-gonads-mesonephros subregions are potent supporters of hematopoietic stem cell activity. *Blood*, *99*(4), 1183-1189. <https://doi.org/10.1182/blood.v99.4.1183>
- Oostendorp, R. A., Medvinsky, A. J., Kusadasi, N., Nakayama, N., Harvey, K., Orelia, C., Ottersbach, K., Covey, T., Ploemacher, R. E., Saris, C., & Dzierzak, E. (2002, May 15). Embryonal subregion-derived stromal cell lines from novel temperature-sensitive SV40 T antigen transgenic mice support hematopoiesis. *J Cell Sci*, *115*(Pt 10), 2099-2108. <https://doi.org/10.1242/jcs.115.10.2099>
- Oostendorp, R. A., Robin, C., Steinhoff, C., Marz, S., Bräuer, R., Nuber, U. A., Dzierzak, E. A., & Peschel, C. (2005, Jun-Jul). Long-term maintenance of hematopoietic stem cells does

- not require contact with embryo-derived stromal cells in cocultures. *Stem Cells*, 23(6), 842-851. <https://doi.org/10.1634/stemcells.2004-0120>
- Orelia, C., Harvey, K. N., Miles, C., Oostendorp, R. A., van der Horn, K., & Dzierzak, E. (2004, Jun 1). The role of apoptosis in the development of AGM hematopoietic stem cells revealed by Bcl-2 overexpression. *Blood*, 103(11), 4084-4092. <https://doi.org/10.1182/blood-2003-06-1827>
- Orford, K. W., & Scadden, D. T. (2008, Feb). Deconstructing stem cell self-renewal: genetic insights into cell-cycle regulation. *Nat Rev Genet*, 9(2), 115-128. <https://doi.org/10.1038/nrg2269>
- Orkin, S. H., & Zon, L. I. (2008, Feb 22). Hematopoiesis: an evolving paradigm for stem cell biology. *Cell*, 132(4), 631-644. <https://doi.org/10.1016/j.cell.2008.01.025>
- Osawa, M., Hanada, K., Hamada, H., & Nakauchi, H. (1996, Jul 12). Long-term lymphohematopoietic reconstitution by a single CD34-low/negative hematopoietic stem cell. *Science*, 273(5272), 242-245. <https://doi.org/10.1126/science.273.5272.242>
- Oswald, J., Boxberger, S., Jørgensen, B., Feldmann, S., Ehninger, G., Bornhäuser, M., & Werner, C. (2004). Mesenchymal stem cells can be differentiated into endothelial cells in vitro. *Stem Cells*, 22(3), 377-384. <https://doi.org/10.1634/stemcells.22-3-377>
- Ottersbach, K., & Dzierzak, E. (2005, Mar). The murine placenta contains hematopoietic stem cells within the vascular labyrinth region. *Dev Cell*, 8(3), 377-387. <https://doi.org/10.1016/j.devcel.2005.02.001>
- <Palis and Yoder 2001.pdf>
- Papayannopoulou, T., Craddock, C., Nakamoto, B., Priestley, G. V., & Wolf, N. S. (1995, Oct 10). The VLA4/VCAM-1 adhesion pathway defines contrasting mechanisms of lodgement of transplanted murine hemopoietic progenitors between bone marrow and spleen. *Proc Natl Acad Sci U S A*, 92(21), 9647-9651. <https://doi.org/10.1073/pnas.92.21.9647>
- Papayannopoulou, T., & Nakamoto, B. (1993, Oct 15). Peripheralization of hemopoietic progenitors in primates treated with anti-VLA4 integrin. *Proc Natl Acad Sci U S A*, 90(20), 9374-9378. <https://doi.org/10.1073/pnas.90.20.9374>
- Paradis, V., Dargere, D., Vidaud, M., De Gouville, A. C., Huet, S., Martinez, V., Gauthier, J. M., Ba, N., Sobesky, R., Ratziu, V., & Bedossa, P. (1999, Oct). Expression of connective tissue growth factor in experimental rat and human liver fibrosis. *Hepatology*, 30(4), 968-976. <https://doi.org/10.1002/hep.510300425>

- Park, H. S., Jung, H. Y., Park, E. Y., Kim, J., Lee, W. J., & Bae, Y. S. (2004, Sep 15). Cutting edge: direct interaction of TLR4 with NAD(P)H oxidase 4 isozyme is essential for lipopolysaccharide-induced production of reactive oxygen species and activation of NF-kappa B. *J Immunol*, *173*(6), 3589-3593.
<https://doi.org/10.4049/jimmunol.173.6.3589>
- Passegué, E., Wagers, A. J., Giuriato, S., Anderson, W. C., & Weissman, I. L. (2005, Dec 5). Global analysis of proliferation and cell cycle gene expression in the regulation of hematopoietic stem and progenitor cell fates. *J Exp Med*, *202*(11), 1599-1611.
<https://doi.org/10.1084/jem.20050967>
- Paul, S. R., Bennett, F., Calvetti, J. A., Kelleher, K., Wood, C. R., O'Hara, R. M., Jr., Leary, A. C., Sibley, B., Clark, S. C., Williams, D. A., & et al. (1990, Oct). Molecular cloning of a cDNA encoding interleukin 11, a stromal cell-derived lymphopoietic and hematopoietic cytokine. *Proc Natl Acad Sci U S A*, *87*(19), 7512-7516.
<https://doi.org/10.1073/pnas.87.19.7512>
- Pearl-Yafe, M., Mizrahi, K., Stein, J., Yolcu, E. S., Kaplan, O., Shirwan, H., Yaniv, I., & Askenasy, N. (2010, Jul). Tumor necrosis factor receptors support murine hematopoietic progenitor function in the early stages of engraftment. *Stem Cells*, *28*(7), 1270-1280.
<https://doi.org/10.1002/stem.448>
- Peidl, A., Perbal, B., & Leask, A. (2019). Yin/Yang expression of CCN family members: Transforming growth factor beta 1, via ALK5/FAK/MEK, induces CCN1 and CCN2, yet suppresses CCN3, expression in human dermal fibroblasts. *PLoS One*, *14*(6), e0218178. <https://doi.org/10.1371/journal.pone.0218178>
- Pennica, D., Swanson, T. A., Welsh, J. W., Roy, M. A., Lawrence, D. A., Lee, J., Brush, J., Taneyhill, L. A., Deuel, B., Lew, M., Watanabe, C., Cohen, R. L., Melhem, M. F., Finley, G. G., Quirke, P., Goddard, A. D., Hillan, K. J., Gurney, A. L., Botstein, D., & Levine, A. J. (1998, Dec 8). WISP genes are members of the connective tissue growth factor family that are up-regulated in wnt-1-transformed cells and aberrantly expressed in human colon tumors. *Proc Natl Acad Sci U S A*, *95*(25), 14717-14722.
<https://doi.org/10.1073/pnas.95.25.14717>
- Perbal, B. (2004, 2004/01/03/). CCN proteins: multifunctional signalling regulators. *The Lancet*, *363*(9402), 62-64. [https://doi.org/https://doi.org/10.1016/S0140-6736\(03\)15172-0](https://doi.org/https://doi.org/10.1016/S0140-6736(03)15172-0)
- Perbal, B., & Takigawa, M. (2005). *CCN proteins: A new family of cell growth and differentiation regulators*.
- Peters, M., Schirmacher, P., Goldschmitt, J., Odenthal, M., Peschel, C., Fattori, E., Ciliberto, G., Dienes, H. P., Meyer zum Büschenfelde, K. H., & Rose-John, S. (1997, Feb 17). Extramedullary expansion of hematopoietic progenitor cells in interleukin (IL)-6-sIL-

- 6R double transgenic mice. *J Exp Med*, 185(4), 755-766.
<https://doi.org/10.1084/jem.185.4.755>
- Pi, L., Ding, X., Jorgensen, M., Pan, J. J., Oh, S. H., Pintilie, D., Brown, A., Song, W. Y., & Petersen, B. E. (2008, Mar). Connective tissue growth factor with a novel fibronectin binding site promotes cell adhesion and migration during rat oval cell activation. *Hepatology*, 47(3), 996-1004. <https://doi.org/10.1002/hep.22079>
- Pinder, J. B., Attwood, K. M., & Dellaire, G. (2013). Reading, writing, and repair: the role of ubiquitin and the ubiquitin-like proteins in DNA damage signaling and repair. *Front Genet*, 4, 45. <https://doi.org/10.3389/fgene.2013.00045>
- Pinho, S., & Frenette, P. S. (2019). Haematopoietic stem cell activity and interactions with the niche. *Nature reviews. Molecular cell biology*, 20(5), 303-320.
<https://doi.org/10.1038/s41580-019-0103-9>
- Pittenger, M. F., Mackay, A. M., Beck, S. C., Jaiswal, R. K., Douglas, R., Mosca, J. D., Moorman, M. A., Simonetti, D. W., Craig, S., & Marshak, D. R. (1999, Apr 2). Multilineage potential of adult human mesenchymal stem cells. *Science*, 284(5411), 143-147. <https://doi.org/10.1126/science.284.5411.143>
- Placzek, W. J., Wei, J., Kitada, S., Zhai, D., Reed, J. C., & Pellicchia, M. (2010, May 6). A survey of the anti-apoptotic Bcl-2 subfamily expression in cancer types provides a platform to predict the efficacy of Bcl-2 antagonists in cancer therapy. *Cell Death Dis*, 1(5), e40. <https://doi.org/10.1038/cddis.2010.18>
- Planque, N., & Perbal, B. (2003, Aug 22). A structural approach to the role of CCN (CYR61/CTGF/NOV) proteins in tumourigenesis. *Cancer Cell Int*, 3(1), 15.
<https://doi.org/10.1186/1475-2867-3-15>
- Poltorak, A., He, X., Smirnova, I., Liu, M. Y., Van Huffel, C., Du, X., Birdwell, D., Alejos, E., Silva, M., Galanos, C., Freudenberg, M., Ricciardi-Castagnoli, P., Layton, B., & Beutler, B. (1998, Dec 11). Defective LPS signaling in C3H/HeJ and C57BL/10ScCr mice: mutations in Tlr4 gene. *Science*, 282(5396), 2085-2088.
<https://doi.org/10.1126/science.282.5396.2085>
- Ponomaryov, T., Peled, A., Petit, I., Taichman, R. S., Habler, L., Sandbank, J., Arenzana-Seisdedos, F., Magerus, A., Caruz, A., Fujii, N., Nagler, A., Lahav, M., Szyper-Kravitz, M., Zipori, D., & Lapidot, T. (2000, Dec). Induction of the chemokine stromal-derived factor-1 following DNA damage improves human stem cell function. *The Journal of clinical investigation*, 106(11), 1331-1339. <https://doi.org/10.1172/jci10329>
- Ponticos, M. (2013, 2013/03/01/). Connective tissue growth factor (CCN2) in blood vessels. *Vascular Pharmacology*, 58(3), 189-193.
<https://doi.org/https://doi.org/10.1016/j.vph.2013.01.004>

- Ponticos, M. (2013, Mar). Connective tissue growth factor (CCN2) in blood vessels. *Vascul Pharmacol*, 58(3), 189-193. <https://doi.org/10.1016/j.vph.2013.01.004>
- Poulos, M. G., Guo, P., Kofler, N. M., Pinho, S., Gutkin, M. C., Tikhonova, A., Aifantis, I., Frenette, P. S., Kitajewski, J., Rafii, S., & Butler, J. M. (2013, Sep 12). Endothelial Jagged-1 is necessary for homeostatic and regenerative hematopoiesis. *Cell Rep*, 4(5), 1022-1034. <https://doi.org/10.1016/j.celrep.2013.07.048>
- Poulos, M. G., Ramalingam, P., Gutkin, M. C., Kleppe, M., Ginsberg, M., Crowley, M. J. P., Elemento, O., Levine, R. L., Rafii, S., Kitajewski, J., Greenblatt, M. B., Shim, J. H., & Butler, J. M. (2016, Dec 21). Endothelial-specific inhibition of NF- κ B enhances functional haematopoiesis. *Nat Commun*, 7, 13829. <https://doi.org/10.1038/ncomms13829>
- Prockop, D. J. (1997, Apr 4). Marrow stromal cells as stem cells for nonhematopoietic tissues. *Science*, 276(5309), 71-74. <https://doi.org/10.1126/science.276.5309.71>
- Qureshi, S. T., Larivière, L., Leveque, G., Clermont, S., Moore, K. J., Gros, P., & Malo, D. (1999, Feb 15). Endotoxin-tolerant mice have mutations in Toll-like receptor 4 (Tlr4). *J Exp Med*, 189(4), 615-625. <https://doi.org/10.1084/jem.189.4.615>
- Raaijmakers, M. H., Mukherjee, S., Guo, S., Zhang, S., Kobayashi, T., Schoonmaker, J. A., Ebert, B. L., Al-Shahrour, F., Hasserjian, R. P., Scadden, E. O., Aung, Z., Matza, M., Merckenschlager, M., Lin, C., Rommens, J. M., & Scadden, D. T. (2010, Apr 8). Bone progenitor dysfunction induces myelodysplasia and secondary leukaemia. *Nature*, 464(7290), 852-857. <https://doi.org/10.1038/nature08851>
- Rafii, S., Mohle, R., Shapiro, F., Frey, B. M., & Moore, M. A. (1997, Nov). Regulation of hematopoiesis by microvascular endothelium. *Leuk Lymphoma*, 27(5-6), 375-386. <https://doi.org/10.3109/10428199709058305>
- Raicevic, G., Najar, M., Pieters, K., De Bruyn, C., Meuleman, N., Bron, D., Toungouz, M., & Lagneaux, L. (2012, Jul). Inflammation and Toll-like receptor ligation differentially affect the osteogenic potential of human mesenchymal stromal cells depending on their tissue origin. *Tissue Eng Part A*, 18(13-14), 1410-1418. <https://doi.org/10.1089/ten.TEA.2011.0434>
- Raicevic, G., Rouas, R., Najar, M., Stordeur, P., Boufker, H. I., Bron, D., Martiat, P., Goldman, M., Nevessignsky, M. T., & Lagneaux, L. (2010, Mar). Inflammation modifies the pattern and the function of Toll-like receptors expressed by human mesenchymal stromal cells. *Hum Immunol*, 71(3), 235-244. <https://doi.org/10.1016/j.humimm.2009.12.005>
- Ramirez, P., Rettig, M. P., Uy, G. L., Deych, E., Holt, M. S., Ritchey, J. K., & DiPersio, J. F. (2009, Aug 13). BIO5192, a small molecule inhibitor of VLA-4, mobilizes

- hematopoietic stem and progenitor cells. *Blood*, 114(7), 1340-1343.
<https://doi.org/10.1182/blood-2008-10-184721>
- Raposo, G., & Stahl, P. D. (2019, 2019/09/01). Extracellular vesicles: a new communication paradigm? *Nature Reviews Molecular Cell Biology*, 20(9), 509-510.
<https://doi.org/10.1038/s41580-019-0158-7>
- Rattazzi, M., Puato, M., Faggin, E., Bertipaglia, B., Zambon, A., & Pualetto, P. (2003, Oct). C-reactive protein and interleukin-6 in vascular disease: culprits or passive bystanders? *J Hypertens*, 21(10), 1787-1803. <https://doi.org/10.1097/00004872-200310000-00002>
- Reagan, M. R., & Rosen, C. J. (2016, Mar). Navigating the bone marrow niche: translational insights and cancer-driven dysfunction. *Nat Rev Rheumatol*, 12(3), 154-168.
<https://doi.org/10.1038/nrrheum.2015.160>
- Rekhtman, N., Radparvar, F., Evans, T., & Skoultchi, A. I. (1999, Jun 1). Direct interaction of hematopoietic transcription factors PU.1 and GATA-1: functional antagonism in erythroid cells. *Genes Dev*, 13(11), 1398-1411.
<https://doi.org/10.1101/gad.13.11.1398>
- Ren, G., Zhao, X., Wang, Y., Zhang, X., Chen, X., Xu, C., Yuan, Z. R., Roberts, A. I., Zhang, L., Zheng, B., Wen, T., Han, Y., Rabson, A. B., Tischfield, J. A., Shao, C., & Shi, Y. (2012, Dec 7). CCR2-dependent recruitment of macrophages by tumor-educated mesenchymal stromal cells promotes tumor development and is mimicked by TNF α . *Cell Stem Cell*, 11(6), 812-824. <https://doi.org/10.1016/j.stem.2012.08.013>
- Renström, J., Istvanffy, R., Gauthier, K., Shimono, A., Mages, J., Jardon-Alvarez, A., Kröger, M., Schiemann, M., Busch, D. H., Esposito, I., Lang, R., Peschel, C., & Oostendorp, R. A. (2009, Aug 7). Secreted frizzled-related protein 1 extrinsically regulates cycling activity and maintenance of hematopoietic stem cells. *Cell Stem Cell*, 5(2), 157-167.
<https://doi.org/10.1016/j.stem.2009.05.020>
- Reya, T., Duncan, A. W., Ailles, L., Domen, J., Scherer, D. C., Willert, K., Hintz, L., Nusse, R., & Weissman, I. L. (2003, May 22). A role for Wnt signalling in self-renewal of haematopoietic stem cells. *Nature*, 423(6938), 409-414.
<https://doi.org/10.1038/nature01593>
- Riser, B. L., Denichilo, M., Cortes, P., Baker, C., Grondin, J. M., Yee, J., & Narins, R. G. (2000, Jan). Regulation of connective tissue growth factor activity in cultured rat mesangial cells and its expression in experimental diabetic glomerulosclerosis. *J Am Soc Nephrol*, 11(1), 25-38. <https://doi.org/10.1681/asn.V11125>
- Riser, B. L., Najmabadi, F., Perbal, B., Peterson, D. R., Rambow, J. A., Riser, M. L., Sukowski, E., Yeger, H., & Riser, S. C. (2009, May). CCN3 (NOV) is a negative regulator of CCN2 (CTGF) and a novel endogenous inhibitor of the fibrotic pathway in an in vitro model

- of renal disease. *Am J Pathol*, 174(5), 1725-1734.
<https://doi.org/10.2353/ajpath.2009.080241>
- Roca, H., Varsos, Z. S., Sud, S., Craig, M. J., Ying, C., & Pienta, K. J. (2009, Dec 4). CCL2 and interleukin-6 promote survival of human CD11b+ peripheral blood mononuclear cells and induce M2-type macrophage polarization. *J Biol Chem*, 284(49), 34342-34354.
<https://doi.org/10.1074/jbc.M109.042671>
- Rodriguez, S., Chora, A., Goumnerov, B., Mumaw, C., Goebel, W. S., Fernandez, L., Baydoun, H., HogenEsch, H., Dombkowski, D. M., Karlewicz, C. A., Rice, S., Rahme, L. G., & Carlesso, N. (2009, Nov 5). Dysfunctional expansion of hematopoietic stem cells and block of myeloid differentiation in lethal sepsis. *Blood*, 114(19), 4064-4076.
<https://doi.org/10.1182/blood-2009-04-214916>
- Romero Marquez, S., Hettler, F., Hausinger, R., Schreck, C., Landspersky, T., Henkel, L., Angerpointner, C., Demir, I. E., Schiemann, M., Bassermann, F., Götze, K. S., Istvánffy, R., & Oostendorp, R. A. J. (2021, Oct 1). Secreted factors from mouse embryonic fibroblasts maintain repopulating function of single cultured hematopoietic stem cells. *Haematologica*, 106(10), 2633-2640.
<https://doi.org/10.3324/haematol.2020.249102>
- Rooney, B., O'Donovan, H., Gaffney, A., Browne, M., Faherty, N., Curran, S. P., Sadlier, D., Godson, C., Brazil, D. P., & Crean, J. (2011, Feb 4). CTGF/CCN2 activates canonical Wnt signalling in mesangial cells through LRP6: implications for the pathogenesis of diabetic nephropathy. *FEBS Lett*, 585(3), 531-538.
<https://doi.org/10.1016/j.febslet.2011.01.004>
- Rossi, D. J., Bryder, D., Seita, J., Nussenzweig, A., Hoeijmakers, J., & Weissman, I. L. (2007, Jun 7). Deficiencies in DNA damage repair limit the function of haematopoietic stem cells with age. *Nature*, 447(7145), 725-729. <https://doi.org/10.1038/nature05862>
- Rossi, D. J., Bryder, D., Zahn, J. M., Ahlenius, H., Sonu, R., Wagers, A. J., & Weissman, I. L. (2005, Jun 28). Cell intrinsic alterations underlie hematopoietic stem cell aging. *Proc Natl Acad Sci U S A*, 102(26), 9194-9199. <https://doi.org/10.1073/pnas.0503280102>
- Ruf, F., Schreck, C., Wagner, A., Grziwok, S., Pagel, C., Romero, S., Kieslinger, M., Shiono, A., Peschel, C., Götze, K. S., Istvanffy, R., & Oostendorp, R. A. (2016, Sep). Loss of Sfrp2 in the Niche Amplifies Stress-Induced Cellular Responses, and Impairs the In Vivo Regeneration of the Hematopoietic Stem Cell Pool. *Stem Cells*, 34(9), 2381-2392.
<https://doi.org/10.1002/stem.2416>
- Rufer, N., Brümmendorf, T. H., Kolvraa, S., Bischoff, C., Christensen, K., Wadsworth, L., Schulzer, M., & Lansdorp, P. M. (1999, Jul 19). Telomere fluorescence measurements in granulocytes and T lymphocyte subsets point to a high turnover of hematopoietic stem cells and memory T cells in early childhood. *J Exp Med*, 190(2), 157-167.
<https://doi.org/10.1084/jem.190.2.157>

- Rupec, R. A., Jundt, F., Rebholz, B., Eckelt, B., Weindl, G., Herzinger, T., Flaig, M. J., Moosmann, S., Plewig, G., Dörken, B., Förster, I., Huss, R., & Pfeffer, K. (2005, Apr). Stroma-mediated dysregulation of myelopoiesis in mice lacking I kappa B alpha. *Immunity*, 22(4), 479-491. <https://doi.org/10.1016/j.immuni.2005.02.009>
- Ryseck, R. P., Macdonald-Bravo, H., Mattéi, M. G., & Bravo, R. (1991, May). Structure, mapping, and expression of fisp-12, a growth factor-inducible gene encoding a secreted cysteine-rich protein. *Cell Growth Differ*, 2(5), 225-233.
- Safadi, F. F., Xu, J., Smock, S. L., Kanaan, R. A., Selim, A. H., Odgren, P. R., Marks, S. C., Jr., Owen, T. A., & Popoff, S. N. (2003, Jul). Expression of connective tissue growth factor in bone: its role in osteoblast proliferation and differentiation in vitro and bone formation in vivo. *J Cell Physiol*, 196(1), 51-62. <https://doi.org/10.1002/jcp.10319>
- Sala-Torra, O., Gundacker, H. M., Stirewalt, D. L., Ladne, P. A., Pogossova-Agadjanyan, E. L., Slovak, M. L., Willman, C. L., Heimfeld, S., Boldt, D. H., & Radich, J. P. (2007, Apr 1). Connective tissue growth factor (CTGF) expression and outcome in adult patients with acute lymphoblastic leukemia. *Blood*, 109(7), 3080-3083. <https://doi.org/10.1182/blood-2006-06-031096>
- Scandura, J. M., Bocconi, P., Massagué, J., & Nimer, S. D. (2004, Oct 19). Transforming growth factor beta-induced cell cycle arrest of human hematopoietic cells requires p57KIP2 up-regulation. *Proc Natl Acad Sci U S A*, 101(42), 15231-15236. <https://doi.org/10.1073/pnas.0406771101>
- Schober, J. M., Chen, N., Grzeszkiewicz, T. M., Jovanovic, I., Emeson, E. E., Ugarova, T. P., Ye, R. D., Lau, L. F., & Lam, S. C. (2002, Jun 15). Identification of integrin alpha(M)beta(2) as an adhesion receptor on peripheral blood monocytes for Cyr61 (CCN1) and connective tissue growth factor (CCN2): immediate-early gene products expressed in atherosclerotic lesions. *Blood*, 99(12), 4457-4465. <https://doi.org/10.1182/blood.v99.12.4457>
- Schofield, R. (1978). The relationship between the spleen colony-forming cell and the haemopoietic stem cell. *Blood Cells*, 4(1-2), 7-25.
- Schönberger, K., Obier, N., Romero-Mulero, M. C., Cauchy, P., Mess, J., Pavlovich, P. V., Zhang, Y. W., Mitterer, M., Rettkowski, J., Lalioti, M. E., Jäcklein, K., Curtis, J. D., Féret, B., Sommerkamp, P., Morganti, C., Ito, K., Ghyselinck, N. B., Trompouki, E., Buescher, J. M., Pearce, E. L., & Cabezas-Wallscheid, N. (2022, Jan 6). Multilayer omics analysis reveals a non-classical retinoic acid signaling axis that regulates hematopoietic stem cell identity. *Cell Stem Cell*, 29(1), 131-148.e110. <https://doi.org/10.1016/j.stem.2021.10.002>

- Schreck, C., Bock, F., Grziwok, S., Oostendorp, R. A., & Istvánffy, R. (2014, Mar). Regulation of hematopoiesis by activators and inhibitors of Wnt signaling from the niche. *Ann N Y Acad Sci*, 1310, 32-43. <https://doi.org/10.1111/nyas.12384>
- Schuettpelez, L. G., & Link, D. C. (2013). Regulation of hematopoietic stem cell activity by inflammation. *Front Immunol*, 4, 204. <https://doi.org/10.3389/fimmu.2013.00204>
- Schutze, N., Noth, U., Schneidereit, J., Hendrich, C., & Jakob, F. (2005, 2005/03/17). Differential expression of CCN-family members in primary human bone marrow-derived mesenchymal stem cells during osteogenic, chondrogenic and adipogenic differentiation. *Cell Communication and Signaling*, 3(1), 5. <https://doi.org/10.1186/1478-811X-3-5>
- Seita, J., & Weissman, I. L. (2010, Nov-Dec). Hematopoietic stem cell: self-renewal versus differentiation. *Wiley Interdiscip Rev Syst Biol Med*, 2(6), 640-653. <https://doi.org/10.1002/wsbm.86>
- Serbina, N. V., & Pamer, E. G. (2006, Mar). Monocyte emigration from bone marrow during bacterial infection requires signals mediated by chemokine receptor CCR2. *Nat Immunol*, 7(3), 311-317. <https://doi.org/10.1038/ni1309>
- Sesler, C. L., & Zayzafoon, M. (2013). NFAT signaling in osteoblasts regulates the hematopoietic niche in the bone microenvironment. *Clin Dev Immunol*, 2013, 107321. <https://doi.org/10.1155/2013/107321>
- Severe, N., Karabacak, N. M., Gustafsson, K., Baryawno, N., Courties, G., Kfoury, Y., Kokkaliaris, K. D., Rhee, C., Lee, D., Scadden, E. W., Garcia-Robledo, J. E., Brouse, T., Nahrendorf, M., Toner, M., & Scadden, D. T. (2019, 2019/10/03/). Stress-Induced Changes in Bone Marrow Stromal Cell Populations Revealed through Single-Cell Protein Expression Mapping. *Cell Stem Cell*, 25(4), 570-583.e577. <https://doi.org/https://doi.org/10.1016/j.stem.2019.06.003>
- Shao, L., Feng, W., Li, H., Gardner, D., Luo, Y., Wang, Y., Liu, L., Meng, A., Sharpless, N. E., & Zhou, D. (2014, May 15). Total body irradiation causes long-term mouse BM injury via induction of HSC premature senescence in an Ink4a- and Arf-independent manner. *Blood*, 123(20), 3105-3115. <https://doi.org/10.1182/blood-2013-07-515619>
- Shen, M. M., Skoda, R. C., Cardiff, R. D., Campos-Torres, J., Leder, P., & Ornitz, D. M. (1994, Mar 15). Expression of LIF in transgenic mice results in altered thymic epithelium and apparent interconversion of thymic and lymph node morphologies. *Embo j*, 13(6), 1375-1385.
- Shi, C., Jia, T., Mendez-Ferrer, S., Hohl, T. M., Serbina, N. V., Lipuma, L., Leiner, I., Li, M. O., Frenette, P. S., & Pamer, E. G. (2011, Apr 22). Bone marrow mesenchymal stem and progenitor cells induce monocyte emigration in response to circulating toll-like

- receptor ligands. *Immunity*, 34(4), 590-601.
<https://doi.org/10.1016/j.immuni.2011.02.016>
- Shi-Wen, X., Leask, A., & Abraham, D. (2008, Apr). Regulation and function of connective tissue growth factor/CCN2 in tissue repair, scarring and fibrosis. *Cytokine Growth Factor Rev*, 19(2), 133-144. <https://doi.org/10.1016/j.cytogfr.2008.01.002>
- Shimo, T., Nakanishi, T., Nishida, T., Asano, M., Sasaki, A., Kanyama, M., Kuboki, T., Matsumura, T., & Takigawa, M. (2001). Involvement of CTGF, a hypertrophic chondrocyte-specific gene product, in tumor angiogenesis. *Oncology*, 61(4), 315-322.
<https://doi.org/10.1159/000055339>
- Shizuru, J. A., Negrin, R. S., & Weissman, I. L. (2005). Hematopoietic stem and progenitor cells: clinical and preclinical regeneration of the hematolymphoid system. *Annu Rev Med*, 56, 509-538. <https://doi.org/10.1146/annurev.med.54.101601.152334>
- Si, Y., Tsou, C.-L., Croft, K., & Charo, I. F. (2010). CCR2 mediates hematopoietic stem and progenitor cell trafficking to sites of inflammation in mice. *The Journal of clinical investigation*, 120(4), 1192-1203. <https://doi.org/10.1172/JCI40310>
- Si, Y., Tsou, C. L., Croft, K., & Charo, I. F. (2010, Apr). CCR2 mediates hematopoietic stem and progenitor cell trafficking to sites of inflammation in mice. *The Journal of clinical investigation*, 120(4), 1192-1203. <https://doi.org/10.1172/jci40310>
- Silver, J. S., & Hunter, C. A. (2010, Dec). gp130 at the nexus of inflammation, autoimmunity, and cancer. *J Leukoc Biol*, 88(6), 1145-1156. <https://doi.org/10.1189/jlb.0410217>
- Sipkins, D. A., Wei, X., Wu, J. W., Runnels, J. M., Côté, D., Means, T. K., Luster, A. D., Scadden, D. T., & Lin, C. P. (2005, Jun 16). In vivo imaging of specialized bone marrow endothelial microdomains for tumour engraftment. *Nature*, 435(7044), 969-973.
<https://doi.org/10.1038/nature03703>
- Spangrude, G. J., Heimfeld, S., & Weissman, I. L. (1988, Jul 1). Purification and characterization of mouse hematopoietic stem cells. *Science*, 241(4861), 58-62.
<https://doi.org/10.1126/science.2898810>
- Standiford, T. J., Kunkel, S. L., Phan, S. H., Rollins, B. J., & Strieter, R. M. (1991, May 25). Alveolar macrophage-derived cytokines induce monocyte chemoattractant protein-1 expression from human pulmonary type II-like epithelial cells. *J Biol Chem*, 266(15), 9912-9918.
- Stier, S., Ko, Y., Forkert, R., Lutz, C., Neuhaus, T., Grünewald, E., Cheng, T., Dombkowski, D., Calvi, L. M., Rittling, S. R., & Scadden, D. T. (2005, Jun 6). Osteopontin is a hematopoietic stem cell niche component that negatively regulates stem cell pool size. *J Exp Med*, 201(11), 1781-1791. <https://doi.org/10.1084/jem.20041992>

- Strieter, R. M., Wiggins, R., Phan, S. H., Wharram, B. L., Showell, H. J., Remick, D. G., Chensue, S. W., & Kunkel, S. L. (1989, Jul 31). Monocyte chemotactic protein gene expression by cytokine-treated human fibroblasts and endothelial cells. *Biochem Biophys Res Commun*, *162*(2), 694-700. [https://doi.org/10.1016/0006-291x\(89\)92366-8](https://doi.org/10.1016/0006-291x(89)92366-8)
- Sugiyama, T., Kohara, H., Noda, M., & Nagasawa, T. (2006, Dec). Maintenance of the hematopoietic stem cell pool by CXCL12-CXCR4 chemokine signaling in bone marrow stromal cell niches. *Immunity*, *25*(6), 977-988. <https://doi.org/10.1016/j.immuni.2006.10.016>
- Sumiyoshi, K., Kubota, S., Furuta, R. A., Yasui, K., Aoyama, E., Kawaki, H., Kawata, K., Ohgawara, T., Yamashiro, T., & Takigawa, M. (2010, Mar). Thrombopoietic-mesenchymal interaction that may facilitate both endochondral ossification and platelet maturation via CCN2. *Journal of cell communication and signaling*, *4*(1), 5-14. <https://doi.org/10.1007/s12079-009-0067-1>
- Summers, C., Rankin, S. M., Condliffe, A. M., Singh, N., Peters, A. M., & Chilvers, E. R. (2010, Aug). Neutrophil kinetics in health and disease. *Trends Immunol*, *31*(8), 318-324. <https://doi.org/10.1016/j.it.2010.05.006>
- Sun, S.-C. (2017, 2017/09/01). The non-canonical NF- κ B pathway in immunity and inflammation. *Nature Reviews Immunology*, *17*(9), 545-558. <https://doi.org/10.1038/nri.2017.52>
- Sweet, M. J., & Hume, D. A. (1996, Jul). Endotoxin signal transduction in macrophages. *J Leukoc Biol*, *60*(1), 8-26. <https://doi.org/10.1002/jlb.60.1.8>
- Tachibana, K., Hirota, S., Iizasa, H., Yoshida, H., Kawabata, K., Kataoka, Y., Kitamura, Y., Matsushima, K., Yoshida, N., Nishikawa, S., Kishimoto, T., & Nagasawa, T. (1998, Jun 11). The chemokine receptor CXCR4 is essential for vascularization of the gastrointestinal tract. *Nature*, *393*(6685), 591-594. <https://doi.org/10.1038/31261>
- Taichman, R. S., & Emerson, S. G. (1994, May 1). Human osteoblasts support hematopoiesis through the production of granulocyte colony-stimulating factor. *J Exp Med*, *179*(5), 1677-1682. <https://doi.org/10.1084/jem.179.5.1677>
- Taichman, R. S., Reilly, M. J., & Emerson, S. G. (1996, Jan 15). Human osteoblasts support human hematopoietic progenitor cells in vitro bone marrow cultures. *Blood*, *87*(2), 518-524.
- Takigawa, M. (2018). An early history of CCN2/CTGF research: the road to CCN2 via hcs24, ctgf, ecogenin, and regenerin. *Journal of cell communication and signaling*, *12*(1), 253-264. <https://doi.org/10.1007/s12079-017-0414-6>

- Takizawa, H., Fritsch, K., Kovtonyuk, L. V., Saito, Y., Yakkala, C., Jacobs, K., Ahuja, A. K., Lopes, M., Hausmann, A., Hardt, W. D., Gomariz, Á., Nombela-Arrieta, C., & Manz, M. G. (2017, Aug 3). Pathogen-Induced TLR4-TRIF Innate Immune Signaling in Hematopoietic Stem Cells Promotes Proliferation but Reduces Competitive Fitness. *Cell Stem Cell*, 21(2), 225-240.e225. <https://doi.org/10.1016/j.stem.2017.06.013>
- Takizawa, H., Regoes, R. R., Boddupalli, C. S., Bonhoeffer, S., & Manz, M. G. (2011, Feb 14). Dynamic variation in cycling of hematopoietic stem cells in steady state and inflammation. *J Exp Med*, 208(2), 273-284. <https://doi.org/10.1084/jem.20101643>
- Tanaka, T., Narazaki, M., & Kishimoto, T. (2018, Aug 1). Interleukin (IL-6) Immunotherapy. *Cold Spring Harb Perspect Biol*, 10(8). <https://doi.org/10.1101/cshperspect.a028456>
- Tanum, G. (1984, Apr). The megakaryocyte DNA content and platelet formation after the sublethal whole body irradiation of rats. *Blood*, 63(4), 917-920.
- Tikhonova, A. N., Dolgalev, I., Hu, H., Sivaraj, K. K., Hoxha, E., Cuesta-Domínguez, Á., Pinho, S., Akhmetzyanova, I., Gao, J., Witkowski, M., Guillaumot, M., Gutkin, M. C., Zhang, Y., Marier, C., Diefenbach, C., Kousteni, S., Heguy, A., Zhong, H., Fooksman, D. R., Butler, J. M., Economides, A., Frenette, P. S., Adams, R. H., Satija, R., Tsirigos, A., & Aifantis, I. (2019, 2019/05/01). The bone marrow microenvironment at single-cell resolution. *Nature*, 569(7755), 222-228. <https://doi.org/10.1038/s41586-019-1104-8>
- Tothova, Z., Kollipara, R., Huntly, B. J., Lee, B. H., Castrillon, D. H., Cullen, D. E., McDowell, E. P., Lazo-Kallanian, S., Williams, I. R., Sears, C., Armstrong, S. A., Passegué, E., DePinho, R. A., & Gilliland, D. G. (2007, Jan 26). FoxOs are critical mediators of hematopoietic stem cell resistance to physiologic oxidative stress. *Cell*, 128(2), 325-339. <https://doi.org/10.1016/j.cell.2007.01.003>
- Trumpp, A., Essers, M., & Wilson, A. (2010, Mar). Awakening dormant haematopoietic stem cells. *Nat Rev Immunol*, 10(3), 201-209. <https://doi.org/10.1038/nri2726>
- Tsou, C. L., Peters, W., Si, Y., Slaymaker, S., Aslanian, A. M., Weisberg, S. P., Mack, M., & Charo, I. F. (2007, Apr). Critical roles for CCR2 and MCP-3 in monocyte mobilization from bone marrow and recruitment to inflammatory sites. *The Journal of clinical investigation*, 117(4), 902-909. <https://doi.org/10.1172/jci29919>
- Uchida, N., & Weissman, I. L. (1992, Jan 1). Searching for hematopoietic stem cells: evidence that Thy-1.1^{lo} Lin⁻ Sca-1⁺ cells are the only stem cells in C57BL/Ka-Thy-1.1 bone marrow. *J Exp Med*, 175(1), 175-184. <https://doi.org/10.1084/jem.175.1.175>
- Valle-Tenney, R., Rebolledo, D. L., Lipson, K. E., & Brandan, E. (2020, May). Role of hypoxia in skeletal muscle fibrosis: Synergism between hypoxia and TGF- β signaling upregulates CCN2/CTGF expression specifically in muscle fibers. *Matrix Biol*, 87, 48-65. <https://doi.org/10.1016/j.matbio.2019.09.003>

- van Deursen, J. M. (2014, May 22). The role of senescent cells in ageing. *Nature*, *509*(7501), 439-446. <https://doi.org/10.1038/nature13193>
- Vandoorne, K., Rohde, D., Kim, H. Y., Courties, G., Wojtkiewicz, G., Honold, L., Hoyer, F. F., Frodermann, V., Nayar, R., Herisson, F., Jung, Y., Désogère, P. A., Vinegoni, C., Caravan, P., Weissleder, R., Sosnovik, D. E., Lin, C. P., Swirski, F. K., & Nahrendorf, M. (2018, Aug 3). Imaging the Vascular Bone Marrow Niche During Inflammatory Stress. *Circ Res*, *123*(4), 415-427. <https://doi.org/10.1161/circresaha.118.313302>
- Visnjic, D., Kalajzic, Z., Rowe, D. W., Katavic, V., Lorenzo, J., & Aguila, H. L. (2004, May 1). Hematopoiesis is severely altered in mice with an induced osteoblast deficiency. *Blood*, *103*(9), 3258-3264. <https://doi.org/10.1182/blood-2003-11-4011>
- Vorwerk, P., Wex, H., Hohmann, B., Oh, Y., Rosenfeld, R. G., & Mittler, U. (2000, Sep). CTGF (IGFBP-rP2) is specifically expressed in malignant lymphoblasts of patients with acute lymphoblastic leukaemia (ALL). *Br J Cancer*, *83*(6), 756-760. <https://doi.org/10.1054/bjoc.2000.1364>
- Wang, L., Shi, M., Tong, L., Wang, J., Ji, S., Bi, J., Chen, C., Jiang, J., Bai, C., Zhou, J., & Song, Y. (2019, Feb). Lung-Resident Mesenchymal Stem Cells Promote Repair of LPS-Induced Acute Lung Injury via Regulating the Balance of Regulatory T cells and Th17 cells. *Inflammation*, *42*(1), 199-210. <https://doi.org/10.1007/s10753-018-0884-6>
- Wang, L. D., & Wagers, A. J. (2011). Dynamic niches in the origination and differentiation of haematopoietic stem cells. *Nature reviews. Molecular cell biology*, *12*(10), 643-655. <https://doi.org/10.1038/nrm3184>
- Wang, M., Crisostomo, P. R., Herring, C., Meldrum, K. K., & Meldrum, D. R. (2006, Oct). Human progenitor cells from bone marrow or adipose tissue produce VEGF, HGF, and IGF-I in response to TNF by a p38 MAPK-dependent mechanism. *Am J Physiol Regul Integr Comp Physiol*, *291*(4), R880-884. <https://doi.org/10.1152/ajpregu.00280.2006>
- Wang, W., Strecker, S., Liu, Y., Wang, L., Assanah, F., Smith, S., & Maye, P. (2015). Connective Tissue Growth Factor reporter mice label a subpopulation of mesenchymal progenitor cells that reside in the trabecular bone region. *Bone*, *71*, 76-88. <https://doi.org/10.1016/j.bone.2014.10.005>
- Wang, Y., Schulte, B. A., LaRue, A. C., Ogawa, M., & Zhou, D. (2006, Jan 1). Total body irradiation selectively induces murine hematopoietic stem cell senescence. *Blood*, *107*(1), 358-366. <https://doi.org/10.1182/blood-2005-04-1418>
- Wang, Z. J., Zhang, F. M., Wang, L. S., Yao, Y. W., Zhao, Q., & Gao, X. (2009, Jun). Lipopolysaccharides can protect mesenchymal stem cells (MSCs) from oxidative stress-induced apoptosis and enhance proliferation of MSCs via Toll-like receptor(TLR)-4 and PI3K/Akt. *Cell Biol Int*, *33*(6), 665-674. <https://doi.org/10.1016/j.cellbi.2009.03.006>

- Waskow, C., Madan, V., Bartels, S., Costa, C., Blasig, R., & Rodewald, H.-R. (2009, 2009/04/01). Hematopoietic stem cell transplantation without irradiation. *Nature Methods*, 6(4), 267-269. <https://doi.org/10.1038/nmeth.1309>
- Waskow, C., Paul, S., Haller, C., Gassmann, M., & Rodewald, H. R. (2002, Sep). Viable c-Kit(W/W) mutants reveal pivotal role for c-kit in the maintenance of lymphopoiesis. *Immunity*, 17(3), 277-288. [https://doi.org/10.1016/s1074-7613\(02\)00386-2](https://doi.org/10.1016/s1074-7613(02)00386-2)
- Weih, F., Carrasco, D., Durham, S. K., Barton, D. S., Rizzo, C. A., Ryseck, R. P., Lira, S. A., & Bravo, R. (1995, Jan 27). Multiorgan inflammation and hematopoietic abnormalities in mice with a targeted disruption of RelB, a member of the NF-kappa B/Rel family. *Cell*, 80(2), 331-340. [https://doi.org/10.1016/0092-8674\(95\)90416-6](https://doi.org/10.1016/0092-8674(95)90416-6)
- Weissman, I. L., Anderson, D. J., & Gage, F. (2001). Stem and progenitor cells: origins, phenotypes, lineage commitments, and transdifferentiations. *Annu Rev Cell Dev Biol*, 17, 387-403. <https://doi.org/10.1146/annurev.cellbio.17.1.387>
- Welch, M. D., Howlett, M., Halse, H. M., Greene, W. K., & Kees, U. R. (2015, Aug). Novel CT domain-encoding splice forms of CTGF/CCN2 are expressed in B-lineage acute lymphoblastic leukaemia. *Leuk Res*, 39(8), 913-920. <https://doi.org/10.1016/j.leukres.2015.05.008>
- Wells, J. E., Howlett, M., Halse, H. M., Heng, J., Ford, J., Cheung, L. C., Samuels, A. L., Crook, M., Charles, A. K., Cole, C. H., & Kees, U. R. (2016, Sep 1). High expression of connective tissue growth factor accelerates dissemination of leukaemia. *Oncogene*, 35(35), 4591-4600. <https://doi.org/10.1038/onc.2015.525>
- Wilson, A., Laurenti, E., Oser, G., van der Wath, R. C., Blanco-Bose, W., Jaworski, M., Offner, S., Dunant, C. F., Eshkind, L., Bockamp, E., Lió, P., Macdonald, H. R., & Trumpp, A. (2008, Dec 12). Hematopoietic stem cells reversibly switch from dormancy to self-renewal during homeostasis and repair. *Cell*, 135(6), 1118-1129. <https://doi.org/10.1016/j.cell.2008.10.048>
- Wilson, A., Murphy, M. J., Oskarsson, T., Kaloulis, K., Bettess, M. D., Oser, G. M., Pasche, A. C., Knabenhans, C., Macdonald, H. R., & Trumpp, A. (2004, Nov 15). c-Myc controls the balance between hematopoietic stem cell self-renewal and differentiation. *Genes Dev*, 18(22), 2747-2763. <https://doi.org/10.1101/gad.313104>
- Winkler, I. G., Barbier, V., Nowlan, B., Jacobsen, R. N., Forristal, C. E., Patton, J. T., Magnani, J. L., & Lévesque, J. P. (2012, Nov). Vascular niche E-selectin regulates hematopoietic stem cell dormancy, self renewal and chemoresistance. *Nat Med*, 18(11), 1651-1657. <https://doi.org/10.1038/nm.2969>
- Winkler, I. G., Barbier, V., Wadley, R., Zannettino, A. C., Williams, S., & Lévesque, J. P. (2010, Jul 22). Positioning of bone marrow hematopoietic and stromal cells relative to blood

- flow in vivo: serially reconstituting hematopoietic stem cells reside in distinct nonperfused niches. *Blood*, 116(3), 375-385. <https://doi.org/10.1182/blood-2009-07-233437>
- Wohrer, S., Knapp, D. J., Copley, M. R., Benz, C., Kent, D. G., Rowe, K., Babovic, S., Mader, H., Oostendorp, R. A., & Eaves, C. J. (2014, Jun 26). Distinct stromal cell factor combinations can separately control hematopoietic stem cell survival, proliferation, and self-renewal. *Cell Rep*, 7(6), 1956-1967. <https://doi.org/10.1016/j.celrep.2014.05.014>
- Wolock, S. L., Krishnan, I., Tenen, D. E., Matkins, V., Camacho, V., Patel, S., Agarwal, P., Bhatia, R., Tenen, D. G., Klein, A. M., & Welner, R. S. (2019, Jul 9). Mapping Distinct Bone Marrow Niche Populations and Their Differentiation Paths. *Cell Rep*, 28(2), 302-311.e305. <https://doi.org/10.1016/j.celrep.2019.06.031>
- Wright, S. D. (1999, Feb 15). Toll, a new piece in the puzzle of innate immunity. *J Exp Med*, 189(4), 605-609. <https://doi.org/10.1084/jem.189.4.605>
- Wu, X., & Karin, M. (2015, Jul). Emerging roles of Lys63-linked polyubiquitylation in immune responses. *Immunol Rev*, 266(1), 161-174. <https://doi.org/10.1111/imr.12310>
- Wu, X., Yamamoto, M., Akira, S., & Sun, S. C. (2009, Dec 8). Regulation of hematopoiesis by the K63-specific ubiquitin-conjugating enzyme Ubc13. *Proc Natl Acad Sci U S A*, 106(49), 20836-20841. <https://doi.org/10.1073/pnas.0906547106>
- Wu, Z., Andersen, P. L., Moraes, T., McKenna, S. A., Zhang, Y., Zhang, W., Ellison, M. J., & Xiao, W. (2020, Oct). Uev1A amino terminus stimulates poly-ubiquitin chain assembly and is required for NF- κ B activation. *Cell Signal*, 74, 109712. <https://doi.org/10.1016/j.cellsig.2020.109712>
- Xiao, C., & Ghosh, S. (2005). NF-kappaB, an evolutionarily conserved mediator of immune and inflammatory responses. *Adv Exp Med Biol*, 560, 41-45. https://doi.org/10.1007/0-387-24180-9_5
- Xie, Y., Yin, T., Wiegraebe, W., He, X. C., Miller, D., Stark, D., Perko, K., Alexander, R., Schwartz, J., Grindley, J. C., Park, J., Haug, J. S., Wunderlich, J. P., Li, H., Zhang, S., Johnson, T., Feldman, R. A., & Li, L. (2009, Jan 1). Detection of functional haematopoietic stem cell niche using real-time imaging. *Nature*, 457(7225), 97-101. <https://doi.org/10.1038/nature07639>
- Xu, C., Gao, X., Wei, Q., Nakahara, F., Zimmerman, S. E., Mar, J., & Frenette, P. S. (2018, Jun 22). Stem cell factor is selectively secreted by arterial endothelial cells in bone marrow. *Nat Commun*, 9(1), 2449. <https://doi.org/10.1038/s41467-018-04726-3>
- Xu, J., Smock, S. L., Safadi, F. F., Rosenzweig, A. B., Odgren, P. R., Marks, S. C., Jr., Owen, T. A., & Popoff, S. N. (2000, Feb). Cloning the full-length cDNA for rat connective tissue

- growth factor: implications for skeletal development. *J Cell Biochem*, 77(1), 103-115. [https://doi.org/10.1002/\(sici\)1097-4644\(20000401\)77:1<103::aid-jcb11>3.0.co;2-g](https://doi.org/10.1002/(sici)1097-4644(20000401)77:1<103::aid-jcb11>3.0.co;2-g)
- Xue, Y., Lim, S., Yang, Y., Wang, Z., Jensen, L. D., Hedlund, E. M., Andersson, P., Sasahara, M., Larsson, O., Galter, D., Cao, R., Hosaka, K., & Cao, Y. (2011, Dec 4). PDGF-BB modulates hematopoiesis and tumor angiogenesis by inducing erythropoietin production in stromal cells. *Nat Med*, 18(1), 100-110. <https://doi.org/10.1038/nm.2575>
- Yamane, T., Kunisada, T., Tsukamoto, H., Yamazaki, H., Niwa, H., Takada, S., & Hayashi, S. I. (2001, Jul 15). Wnt signaling regulates hemopoiesis through stromal cells. *J Immunol*, 167(2), 765-772. <https://doi.org/10.4049/jimmunol.167.2.765>
- Yamashita, M., Fatyol, K., Jin, C., Wang, X., Liu, Z., & Zhang, Y. E. (2008, Sep 26). TRAF6 mediates Smad-independent activation of JNK and p38 by TGF-beta. *Mol Cell*, 31(6), 918-924. <https://doi.org/10.1016/j.molcel.2008.09.002>
- Yamazaki, S., Ema, H., Karlsson, G., Yamaguchi, T., Miyoshi, H., Shioda, S., Taketo, M. M., Karlsson, S., Iwama, A., & Nakauchi, H. (2011, Nov 23). Nonmyelinating Schwann cells maintain hematopoietic stem cell hibernation in the bone marrow niche. *Cell*, 147(5), 1146-1158. <https://doi.org/10.1016/j.cell.2011.09.053>
- Yang, P., Troncione, L., Augur, Z. M., Kim, S. S. J., McNeil, M. E., & Yu, P. B. (2020, Dec). The role of bone morphogenetic protein signaling in vascular calcification. *Bone*, 141, 115542. <https://doi.org/10.1016/j.bone.2020.115542>
- Yano, H., Hamanaka, R., Zhang, J. J., Yano, M., Hida, M., Matsuo, N., & Yoshioka, H. (2021, Aug). MicroRNA-26 regulates the expression of CTGF after exposure to ionizing radiation. *Radiat Environ Biophys*, 60(3), 411-419. <https://doi.org/10.1007/s00411-021-00915-9>
- Yonemura, Y., Ku, H., Lyman, S. D., & Ogawa, M. (1997, Mar 15). In vitro expansion of hematopoietic progenitors and maintenance of stem cells: comparison between FLT3/FLK-2 ligand and KIT ligand. *Blood*, 89(6), 1915-1921.
- Yoshida, K., Taga, T., Saito, M., Suematsu, S., Kumanogoh, A., Tanaka, T., Fujiwara, H., Hirata, M., Yamagami, T., Nakahata, T., Hirabayashi, T., Yoneda, Y., Tanaka, K., Wang, W. Z., Mori, C., Shiota, K., Yoshida, N., & Kishimoto, T. (1996, Jan 9). Targeted disruption of gp130, a common signal transducer for the interleukin 6 family of cytokines, leads to myocardial and hematological disorders. *Proc Natl Acad Sci U S A*, 93(1), 407-411. <https://doi.org/10.1073/pnas.93.1.407>
- Yoshimura, T., Galligan, C., Takahashi, M., Chen, K., Liu, M., Tessarollo, L., & Wang, J. M. (2014, Jan 7). Non-Myeloid Cells are Major Contributors to Innate Immune Responses via Production of Monocyte Chemoattractant Protein-1/CCL2. *Front Immunol*, 4, 482. <https://doi.org/10.3389/fimmu.2013.00482>

- Zandstra, P. W., Conneally, E., Petzer, A. L., Piret, J. M., & Eaves, C. J. (1997, Apr 29). Cytokine manipulation of primitive human hematopoietic cell self-renewal. *Proc Natl Acad Sci U S A*, *94*(9), 4698-4703. <https://doi.org/10.1073/pnas.94.9.4698>
- <Zhang et al. 2018.pdf>. <https://doi.org/10.1073/pnas.1713889115>
- Zhang, H., Hu, H., Greeley, N., Jin, J., Matthews, A. J., Ohashi, E., Caetano, M. S., Li, H. S., Wu, X., Mandal, P. K., McMurray, J. S., Moghaddam, S. J., Sun, S. C., & Watowich, S. S. (2014, Dec 15). STAT3 restrains RANK- and TLR4-mediated signalling by suppressing expression of the E2 ubiquitin-conjugating enzyme Ubc13. *Nat Commun*, *5*, 5798. <https://doi.org/10.1038/ncomms6798>
- Zhang, H., Li, H. S., Hillmer, E. J., Zhao, Y., Chrisikos, T. T., Hu, H., Wu, X., Thompson, E. J., Clise-Dwyer, K., Millerchip, K. A., Wei, Y., Puebla-Osorio, N., Kaushik, S., Santos, M. A., Wang, B., Garcia-Manero, G., Wang, J., Sun, S. C., & Watowich, S. S. (2018, Mar 6). Genetic rescue of lineage-balanced blood cell production reveals a crucial role for STAT3 antiinflammatory activity in hematopoiesis. *Proc Natl Acad Sci U S A*, *115*(10), E2311-e2319. <https://doi.org/10.1073/pnas.1713889115>
- Zhang, H., Nguyen-Jackson, H., Panopoulos, A. D., Li, H. S., Murray, P. J., & Watowich, S. S. (2010, Oct 7). STAT3 controls myeloid progenitor growth during emergency granulopoiesis. *Blood*, *116*(14), 2462-2471. <https://doi.org/10.1182/blood-2009-12-259630>
- Zhang, H., Rodriguez, S., Wang, L., Wang, S., Serezani, H., Kapur, R., Cardoso, A. A., & Carlesso, N. (2016, Jun 14). Sepsis Induces Hematopoietic Stem Cell Exhaustion and Myelosuppression through Distinct Contributions of TRIF and MYD88. *Stem cell reports*, *6*(6), 940-956. <https://doi.org/10.1016/j.stemcr.2016.05.002>
- Zhang, J., Niu, C., Ye, L., Huang, H., He, X., Tong, W. G., Ross, J., Haug, J., Johnson, T., Feng, J. Q., Harris, S., Wiedemann, L. M., Mishina, Y., & Li, L. (2003, Oct 23). Identification of the haematopoietic stem cell niche and control of the niche size. *Nature*, *425*(6960), 836-841. <https://doi.org/10.1038/nature02041>
- Zhang, P., Behre, G., Pan, J., Iwama, A., Wara-Aswapati, N., Radomska, H. S., Auron, P. E., Tenen, D. G., & Sun, Z. (1999, Jul 20). Negative cross-talk between hematopoietic regulators: GATA proteins repress PU.1. *Proc Natl Acad Sci U S A*, *96*(15), 8705-8710. <https://doi.org/10.1073/pnas.96.15.8705>
- Zhang, Q. H., Ye, M., Wu, X. Y., Ren, S. X., Zhao, M., Zhao, C. J., Fu, G., Shen, Y., Fan, H. Y., Lu, G., Zhong, M., Xu, X. R., Han, Z. G., Zhang, J. W., Tao, J., Huang, Q. H., Zhou, J., Hu, G. X., Gu, J., Chen, S. J., & Chen, Z. (2000, Oct). Cloning and functional analysis of cDNAs with open reading frames for 300 previously undefined genes expressed in CD34+ hematopoietic stem/progenitor cells. *Genome Res*, *10*(10), 1546-1560. <https://doi.org/10.1101/gr.140200>

- Zhang, X., Chen, X., Liu, J., Dong, X., Jin, Y., Tian, Y., Xue, Y., Chen, L., Chang, Y., Liu, Y., & Wang, J. (2015). Knockdown of WISP1 inhibit proliferation and induce apoptosis in ALL Jurkat cells. *Int J Clin Exp Pathol*, *8*(11), 15489-15496.
- Zhao, C., Xiu, Y., Ashton, J., Xing, L., Morita, Y., Jordan, C. T., & Boyce, B. F. (2012, Apr). Noncanonical NF- κ B signaling regulates hematopoietic stem cell self-renewal and microenvironment interactions. *Stem Cells*, *30*(4), 709-718. <https://doi.org/10.1002/stem.1050>
- Zhao, M., & Li, L. (2015, Dec). Regulation of hematopoietic stem cells in the niche. *Sci China Life Sci*, *58*(12), 1209-1215. <https://doi.org/10.1007/s11427-015-4960-y>
- Zhao, M., Perry, J. M., Marshall, H., Venkatraman, A., Qian, P., He, X. C., Ahamed, J., & Li, L. (2014, Nov). Megakaryocytes maintain homeostatic quiescence and promote post-injury regeneration of hematopoietic stem cells. *Nat Med*, *20*(11), 1321-1326. <https://doi.org/10.1038/nm.3706>
- Zhao, M., Ross, J. T., Itkin, T., Perry, J. M., Venkatraman, A., Haug, J. S., Hembree, M. J., Deng, C. X., Lapidot, T., He, X. C., & Li, L. (2012, Aug 30). FGF signaling facilitates postinjury recovery of mouse hematopoietic system. *Blood*, *120*(9), 1831-1842. <https://doi.org/10.1182/blood-2011-11-393991>
- Zhao, Y., Ling, F., Wang, H. C., & Sun, X. H. (2013). Chronic TLR signaling impairs the long-term repopulating potential of hematopoietic stem cells of wild type but not Id1 deficient mice. *PLoS One*, *8*(2), e55552. <https://doi.org/10.1371/journal.pone.0055552>
- Zhong, L., Yao, L., Tower, R. J., Wei, Y., Miao, Z., Park, J., Shrestha, R., Wang, L., Yu, W., Holdreith, N., Huang, X., Zhang, Y., Tong, W., Gong, Y., Ahn, J., Susztak, K., Dymant, N., Li, M., Long, F., Chen, C., Seale, P., & Qin, L. (2020, Apr 14). Single cell transcriptomics identifies a unique adipose lineage cell population that regulates bone marrow environment. *Elife*, *9*. <https://doi.org/10.7554/eLife.54695>
- Zhou, B. O., Ding, L., & Morrison, S. J. (2015, Mar 30). Hematopoietic stem and progenitor cells regulate the regeneration of their niche by secreting Angiopoietin-1. *Elife*, *4*, e05521. <https://doi.org/10.7554/eLife.05521>
- Zou, Y. R., Kottmann, A. H., Kuroda, M., Taniuchi, I., & Littman, D. R. (1998, Jun 11). Function of the chemokine receptor CXCR4 in haematopoiesis and in cerebellar development. *Nature*, *393*(6685), 595-599. <https://doi.org/10.1038/31269>

